Avian Borna Virus in Psittacine Birds

Viral distribution, tropism and immune response

Basim Ibrahim Hasan Al-Ibadi

INAUGURAL DISSERTATION
submitted to the Faculty of Medicine
in partial fulfilment of the requirements
for the PhD-degree
of the Faculties of Veterinary Medicine and Medicine
of the Justus Liebig University Giessen, Germany

édition scientifique
VVB LAUFERSWEILER VERLAG

1. Auflage 2015

1st Edition 2015

Printed in Germany

édition scientifique
VVB LAUFERSWEILER VERLAG

STAUFENBERGRING 15, D-35396 GIESSEN
Tel: 0641-5599888 Fax: 0641-5599890
email: redaktion@doktorverlag.de

www.doktorverlag.de

Avian borna virus in psittacine birds;

Viral distribution, tropism and immune response

INAUGURAL DISSERTATION

submitted to the

Faculty of Veterinary Medicine

in partial fulfilment of the requirements

for the **PhD-Degree (Doctor of Philosophy)**

of Faculties of Veterinary Medicine and Medicine

of the Justus Liebig University Giessen

by

Basim Ibrahim Hasan AL-Ibadi

of Baghdad, Iraq

Giessen 2015

From the Institute of Veterinary Pathology
of the Faculty of Veterinary Medicine of the
Justus-Liebig-University Giessen

Director: Prof. Dr. habil. Christiane Herden

Assessor and Member of the Examination Committee:
Prof. Dr. habil. Christiane Herden
Assessor and Member of the Examination Committee:
Prof. Dr. rer. nat. Georg Herrler
Member and Chairman of the Examination Committee:
Prof. Dr. Norbert Weißmann
Examiner:
Prof. Dr. Dieter Glebe

Date of the Doctoral Defence: 22nd December 2015

Declaration

I declare that I have completed this dissertation single-handedly without the unauthorized help of a second party and only with the assistance acknowledged therein. I have appropriately acknowledged and referenced all text passages that are derived literally from or are based on the content of published or unpublished work of others, and all information that relates to verbal communications. I have abided by the principles of good scientific conduct laid down in the charter of the Justus Liebig University of Giessen in carrying out the investigations described in the dissertation.

Basim Ibrahim Hasan AL-Ibadi

Tables of contents

Index of Figures

Index of Figures

Index of Tables

Index of Tables

Abbreviations

7-AAD	7-Aminoactinomycin D
ABC	Avidin biotin complex
ABV	Avian borna virus
ABV-2	Avian borna virus 2
ABV-4	Avian borna virus 4
ABV-2-N	Avian borna virus 2 nucleoprotein
ABV-4-N	Avian borna virus 4 nucleoprotein
ANCOVA	Analysis of covariance
APC	Allophycocyanin
APCs	Antigen presenting cells
bp	Base pair
BC cells	Buffy coat
BCIP	Bromo-4-chloro-3-indolyl-phosphate
BoDV	Borna disease virus
BLAST	Basic local alignment search tool
BrdU	Bromodeoxyuridine
BSA	Bovine serum albumin
BSA/TBS	Bovine serum albumin/tris buffered saline
ºC	Celsius or centigrade
CD3	Cluster of differentiation 3 (Pan T cells)
CD4	Cluster of differentiation 4
CD8a	Cluster of differentiation 8 alpha
cDNA	Complementary DNA
CEC32	Quail fibroblast cell line
CNS	Central nervous system
Cy3	Cyanine 3 dye
DAB	Diaminobenzidine
DAPI	4', 6-diamidino-2-phenylindole
DEPC	Diethylpyrocarbonate
DIG	Digoxigenin
DMF	Dimethylformamide
DNA	Deoxyribonucleic acid
DNase	Deoxyribonuclease
dpi	Day post infection

EDTA	Ethylenediaminetetraacetate
F	Forward
FC	Flow cytometry
Fig	Figure
FL2	Fluorescent light 2
FL4	Fluorescent light 4
FPD	Feather picking disorder
G	Gravity force
g	Gram
GIT	Gastrointestinal tract
HCL	Hydrochloric acid
H and E	Haematoxylin and Eosin
H+L antibody	Heavy and light chain antibody
ic	Intracerebral
ID_{50}	Infectious dose
IgG	Immunoglobulin G
IgY	Immunoglobulin Y
IHC	Immunohistochemistry
IIF	Indirect immunofluorescence
IFN-γ	Interferon gamma
ISH	In situ hybridization
iv	Intravenous
IU	International unit
kb	Kilo bas pair
kDa	Kilo Dalton
l	Liter
M13	M13 vector
MDCK cell lines	Madine Darby Canine Kidney Cell lines
mg	Milligram
ml	Mililiter
µm	Micrometer
µM	Micro mole
MNC	Mononuclear cells
mRNA	Messenger ribonucleic acid

MUM-1	Multiple myeloma oncogene-1
MW	Molecular weight
N	Molar
n	Number
ng/µl	Nanogram per microliter
NBT	Nitroblueteterazolium
NES	Nuclear export signal
NK	Natural killer cells
NLS	Nuclear localization signal
NNS	Non-segmented negative strand
NSAIDs	None steroidal anti-inflammatory drugs
NSS	Neutral sheep serum
NTP mix	Nucleoside 5´-triphosphates mixture
Oligo	Oligonucleotides
ORF	Open reading frames
p	Phosphoprotein
PAP	Peroxidase anti peroxidase
PBS	Phosphate buffered saline
PCR	Polymerase chain reaction
PDD	Proventriculus dilatation Disease
PE	Phycoerythrin
PES	Prostaglandin endoperoxide synthetase
PFA	Paraformaldehyde
PGK1	Phosphoglycerate kinase 1 gene
PHA-M	Phytohemagglutinin A mitogen
P value	Probability value
R	Reverse
®	Registered trademark
RBC	Red blood cells
RNA	Ribonucleic acid
RNAse	Ribonuclease
RNP	Ribonucleoprotein complex
rpm	Revolution per minute
r	Regression

r_s	Spearman rank Correlation Coefficient
RT	Reverse Transcriptase
RT-PCR	Real time- Polymerase chain reaction
ssDNA	Sodium salt deoxyribonucleic acid
SSC	Saline-sodium citrate
St. Dev	Standard deviation
TA cloning	Adenine and Thymine cloning
TBS	Tris-buffered saline
$TCID_{50}$	Tissue culture infectious dose 50
TEA	Tris-acetate-EDTA buffer
TM	Trademark
U/µl	Unit per microliter
UV	Ultraviolet
V	Voltage
WB	Washing Buffer

1. Introduction

Proventricular dilatation disease (PDD) is a chronic and fatal disease affecting mainly psittacine birds such as macaws, amazon or African grey parrots, conures, cockatoos, and cockatiels. PDD was identified in the late of 1970s and was originally known as "macaw wasting syndrome" (Graham, 1991; Hughes, 1984; Clark, 1984). PDD is characterized by ganglioneuritis in the enteric nervous system and encephalomyelitis (Berhane et al., 2001). Clinically, birds with PDD are presenting gastrointestinal tract dysfunction (diarrhea, dysphagia, regurgitation, and passage of undigested food in the droppings), and/or neurological symptoms (ataxia, abnormal gait, incoordination), or both (Mannl et al., 1987; Vice, 1992; Gregory et al., 1994). Avian borna virus (ABV) is a newly discovered member of the family Bornaviridae that has been identified as the etiological agent of PDD (Honkavuori et al., 2008, Kistler et al., 2008). Subsequent studies confirmed an association between ABV and PDD (Lierz et al., 2009; Villanueva et al., 2009; Gancz et al., 2009; Gray et al., 2010; Kistler et al., 2010; Raghav et al., 2010; Piepenbring et al., 2012). Until now, fourteen ABV genotypes have been detected in psittacine and non psittacine birds (Kuhn et al., 2015). The most successful route of infection for a widespread ABV distribution within the central and peripheral nervous system and association of antiviral immune response is yet unknown and needs to be investigated. In addition, host factors such as immunocompetence, individual constitution and genetic factors as well as virulence of the respective ABV genotype and time course of the infection most likely play an important role for the outcome of the disease. Therefore, the study aimed to characterize the distribution pattern of different ABV genotypes and inflammatory lesions combined with analysis of the invading immune cell populations after ABV-2 and after ABV-4 infection in cockatiels. This can essentially contribute to enlarge the knowledge on neurotropic virus infections that are able to cause neurological and gastrointestinal dysfunctions. Experimental ABV infections allow to analyse defined conditions, e.g. route of infection, time course of infection or pathogenicity of ABV genotype. To address the route of infection, animals were infected intracerebrally and intravenously and potential ABV infection of cockatiel blood cells was performed additionally. For this purpose, isolation, culturing, and infection of cockatiel blood cells was established in the current study. Moreover, subpopulations of the immune cells of the cockatiel blood were further characterized. Infection of cockatiel blood cells with ABV-4 was tried without and after stimulation with phytohaemagglutinin (PHA-M) mitogen in vitro. To sum up, differences in pathogenicity between ABV-2 and ABV-4 were identified after experimental infection with ABV-2 or ABV-4 in cockatiels as seen by differences in the

organ tropism and histological lesions. ABV-2 has a more pronounced tropism for the GIT and peripheral organs while ABV-4 was mainly found in the CNS and peripheral organs. The study also indicates that CD3-positive cells were found in the inflammatory lesions after experimental infection with ABV-2 and ABV-4 in cockatiels. Moreover, this study provides evidence that at least *in vitro* under the applied conditions ABV-4 infection of cockatiel blood cells is not possible. Whether the haematological route might play a role for viral dissemination after ABV infection has to be addressed in the future.

2. Literature review

2.1. Psittacine proventricular dilatation (PDD)

2.1.1. Definition

Psittacine proventricular dilatation (PDD) is a progressive, variably contagious and often fatal disease affecting predominantly psittacine birds worldwide. Typical clinical signs such as gastrointestinal dysfunction and associated wasting with or without neurological symptoms are caused by non purulent inflammation in the enteric, autonomic and central nervous system. PDD is characterized by encephalomyelitis and ganglioneuritis (Berhane et al., 2001; Gregory et al., 1994). Ganglia of the crop, proventriculus, gizzard and small intestine are most frequently affected resulting in motility disorders and dilatation of the proventriculus. PDD is affecting not only psittacine birds (parrots) but also non psittacine birds such as waterfowl (Daoust et al., 1991; Guo et al., 2014), canary (*Serinus canaria*), greenfinch (*Carduelis chloris*), a long-wattled umbrella bird (*Cephalopterus penduliger*), and a bearded barbet (*Lybius dubius*) (Perpiñán et al., 2007). Raptors such as red-tailed hawk (*Buteo jamancensis*), peregrine falcon (*Falco peregrinus*) and bald eagle (*Haliaeetus leucocephalus*) could also be infected with PDD (Shivaprasad, 2005; Hoppes et al., 2013).

2.1.2. History of psittacine proventricular dilatation

PDD was firstly identified in macaws imported into the United States and Germany from Bolivia (Ridgway et al., 1983; Mannl et al., 1987; Gerlach, 1991; Gregory et al., 1994; Gregory et al., 1995) and in Canada (Berhane et al., 2004). At that time, PDD was also described as “macaw wasting or fading syndrome”, “macaw wasting syndrome”, and “gastric distension of macaws” in 1979 because initially, the disease seemed to occur only in macaws (Gregory et al., 1994). Since then, the causative agent of this disease remained unclear. When it became apparent that the disease occurred also in psittacines other than macaws, more general terms were used to describe the syndrome including proventricular dilatation, proventricular dilatation syndrome, psittacine proventricular dilatation syndrome (Graham et al., 1991). Additionally, other lesions than proventricular dilatation, such as myocarditis, and non purulent encephalitis have also been reported (Hughes, 1984; Gerlach, 1991). Recently, PDD has been identified in more than 80 species of psittaciformes including members of the *Cacatuidae* families (i.e., cockatoos and cockatiels) and *Psittacidae* (i.e., lovebirds, macaws, parakeets, parrots, Amazon parrots, and conures) (Gregory et al., 1994; Mannl et al., 1987; Weissenböck et al., 2009a; Shivaprasad et al., 2010).

2.1.3. Clinical signs of PDD

Clinical signs of PDD consist of gastrointestinal and/or neurological clinical signs. Both sexes suffered from PDD and birds of any age can be affected with PDD (Graham et al., 1991; Gregory et al., 1994; Kistler et al., 2010). Two forms of PDD have been identified; the classical form (gastrointestinal form) and the nervous form. Affected birds mostly develop gastrointestinal clinical signs such as depression, weight loss (with or without decreased appetite), constant or intermittent regurgitation, and/or passage of undigested seeds in the faeces indicating a malabsorptive or maldigestive disorder. Passing of nutrients and undigested feed in the faeces occurs due to inflammation of the enteric nervous system (Gregory et al., 1994). The affected birds may also exhibit neurological clinical symptoms such as abnormal gait, ataxia and propioceptive defect, tremors and occasionally seizures (Gregory et al., 1994). Some birds are displaying both gastrointestinal and neurological signs (Mannl et al., 1987; Vice 1992). Clinical signs of PDD can appear suddenly or progress slowly.

Horie and colleagues (2012) detected avian borna virus (ABV-5) RNA in parrots *Eclectus roratus* with feather picking disorder (FPD) in Japan. Birds had no clinical signs of PDD. It remains unknown whether ABV-5 is associated with FPD. Feather picking disorder (FPD) is a destructive behaviour pattern of birds commonly seen in captive birds and commercial poultry which chew or bite their own feathers with their beak, resulting in damage to the feathers and occasionally the skin of the neck, chest, flank, inner thigh and ventral wing.

2.1.4. Occurrence and geographical distribution of PDD

Acute outbreaks of PDD with high mortality have been reported in psittacine birds (Lublin et al., 2006; Kistler et al., 2010). PDD outbreaks most frequently occur in crowded indoor aviaries (Gancz et al., 2010). PDD occurs worldwide,e.g. in the United States (Woerpel et al., 1984), in Australia (Sullivan et al., 1997; Doneley et al., 2007), Middle East (Lublin et al., 2006; Kistler et al., 2008; Wyss et al., 2009), South America (Marietto-Goncalves et al., 2009), South Africa (Gancz et al., 2010; Last et al.,2012) and Japan (Ogawa et al.,2011). Birds trading and smuggling could have contributed to the global dissemination of PDD among continents (Gregory et al., 1997; Doneley et al., 2007; Honkavuori et al. 2008; Staeheli et al., 2010).

2.1.5. PDD in psittacine birds

PDD is threatening the aviculture of psittacine birds. PDD has been observed in more than 80 species of psittacine birds (Clark et al., 1984; Mannl et al., 1987; Weissenböck et al., 2009a; Shivaprasad et al., 2010). Certain species, such as African grey parrots (*Psittacus erithacus*),

blue and gold macaws (*Ara ararauna*), cockatoos, and Amazon parrots, seem to be most frequently affected (Schmidt et al., 2003) whereas other species, such as budgerigars (*Melopsittacus undulatus*), appear to be more resistant to the disease (Graham et al., 1991; Reavill et al., 2007). It is noteworthy that Spix's macaw is an endangered species in the wild in Brazil and it is undoubtedly affected by PDD (Wyss et al., 2009; Enderlein et al., 2011).

2.1.6. PDD in non psittacine birds

A PDD-like disease was identified in wild Canada geese (*Branta canadensis*) which showed emaciation, severe proventricular food impaction, nonsuppurative encephalomyelitis and ganglioneuritis typical to PDD in psittacine birds (Daoust et al., 1991). PDD-like disease has also been described in many raptors such as red-tailed hawk (*Buteo jamancensis*), peregrine falcon (*Falco peregrinus*) (Shivaprasad 2005). Perpiñán and colleagues (2007) identified PDD in canaries (*Serinus canaria*), a long-wattled umbrella bird (*Cephalopterus penduliger*), a bearded barbet (*Lybius dubius*), honey creeper, and weaver finch with clinical and pathologic findings compatible with PDD.

2.1.7. Aetiology

Since the description of PDD in the late 1970's in Macaws which had been imported into the United States and Germany (Graham, 1984; Hughes, 1984; Gerlach, 1991), a viral agent was believed as a cause of the disease (Gregory1995; Gregory et al., 1998a). Several viruses have been supposed as cause, e.g. adeno-like virus, herpes virus (Pacheco's disease virus), polyomavirus, avian encephalomyelitis virus, and paramyxo-like virus (Gregory et al., 1998b; Grund, et al., 2002) and the cause remained unknown for approximately 40 years. In 2008, independent researchers detected a novel avian borna virus (ABV) in birds suffering from PDD and claimed it is as the etiological agent for PDD (Honkavuori et al., 2008; Kistler et al., 2008).

2.2. Discovery of avian borna viruses (ABV)

ABV was firstly identified from psittacines suffering from PDD (Kistler et al., 2008; Hounkavouri et al., 2008). In one of the first studies, RNA extracted from parrots with PDD in the United States was hybridized to a panviral microarray. This screening yielded a discovery of a Borna disease virus (BoDV-1-like virus) in birds with PDD, which was confirmed by high-throughput sequencing (Kistler et al., 2008). In a second independent study, RNA extracted from tissues of parrots with PDD in Israel was reversely transcribed and also directly subjected to high throughput sequencing followed by searches for sequence

similarities to known viruses. Again, genetic material with similarity to BoDV-1 was identified (Hounkavouri et al., 2008).

2.3. Avian borna virus (ABV)

2.3.1. Taxonomy

Avian borna viruses (ABV) belong to the order *Mononegavirales*, family *Bornaviridae*, genus Borna virus and was discovered in psittaciform birds with proventricular dilatation disease (PDD) in 2008 (Kistler et al., 2008; Hounkavouri et al., 2008). At that time, it was designated to five distinct ABV genetic subgroups or genotypes (ABV-1, ABV-2, ABV-3, ABV-4, and ABV-5, Kistler et al., 2008). Until now, a total of 14 ABV genotypes have been identified in psittacine and non-psittacine birds (Weissenböck et al., 2009; Delnatte et al., 2011; Horie et al., 2010; Horie et al., 2013; Kuhn et al., 2015). Seven ABV genotypes (ABV-1, ABV-2, ABV-3, ABV-4, ABV-5, ABV-6, and ABV-7) have mainly been identified in psittacine birds (Honkavuori et al., 2008; Gancz et al., 2010; Kuhn et al., 2015). Moreover, seven additional ABV genotypes have also been detected in non psittacine birds (Kuhn et al., 2015), in canaries (*Serinus canaria*) from Germany named as ABV-C1, ABV-C2, and ABV-C3 (Weissenböck et al., 2009b; Rinder et al., 2012), in Canada geese (*Branta canadensis*) designated as (ABV-CG) genotype (Delnatte et al., 2011), in mallards (*Anas platyrhynchos*) and in wood ducks (*Aix sponsa*) (Guo et al., 2014), in a Bengalese finch (*Lonchura striata*) (Rubbenstroth et al., 2013), in trumpeter swans (*Cygnus buccinator*) and feral mute swans (*Cygnus olor*) in North America (Guo et al., 2012; Delnatte et al., 2013). ABV-2 and ABV-4 genotypes are the most common genotypes in psittacine birds in Europe and North America. The genetic variability of ABV is much greater than the variability observed among the mammalian borna viruses (Dürrwald et al., 2007; Weissenböck et al., 2009; Kuhn et al., 2015). For ABV, there is conservation in genomic nucleotide sequence is around 91–100% within one ABV genotype, and 68-85% between ABV genotypes, and 60-69% when compared to BoDV isolates (Kistler et al., 2008; Payne et al., 2011). For mammalian borna viruses, a highly homology in genomic nucleotide sequence (95%) have been detected in all mammalian borna viruses isolates (Staeheli et al., 2000; Dürrwald et al., 2006; Dürrwald et al., 2014; Kuhn et al., 2015). Borna disease virus 2 (BoDV-2) (No/98 isolate) showed diversity in genomic nucleotide sequence (15%) when compared to BoDV-1 (Nowotny et al., 2000; Kuhn et al., 2015). Recent study revealed that an additional genotype of borna virus were discovered in a Loveridge's garter snake (*Elapsoidea loveridgei*) from Tanzania (Stenglein et al., 2014), and an unclassified bornavirus was detected in reptiles (Fujino et al., 2012). Due to sequence comparisons of bornavirus genomes, alignments comparison of

genomic and protein sequences, phylogenetic analyses and known biological characteristics of bornaviruses, Kuhn and colleagues, (2015) reorganized species classification of the genus Bornavirus, family name *Bornaviridae* in an proposed updated taxonomy for ABV as given in table 1.

Table 1: Proposed classification of bornaviruses (Kuhn et al., 2015)

Order	Family	Genus	Species	Virus
Mononegavirals	Bornaviridae	Borna virus	Mammalian 1 bornavirus	Borna disease virus 1 (BoDV-1)
				Borna disease virus 2 (BoDV-2)
			Psittaciform 1 bornavirus	parrot bornavirus 1 (PaBV-1) parrot bornavirus 2 (PaBV-2) parrot bornavirus 3 (PaBV-3) parrot bornavirus 4 (PaBV-4) parrot bornavirus 7 (PaBV-7)
			Passeriform 1 bornavirus	canary bornavirus 1 (CnBV-1) canary bornavirus 2 (CnBV-2) canary bornavirus 3 (CnBV-3) munia bornavirus 1 (MuBV-1)
			Waterbird 1 bornavirus	aquatic bird bornavirus 1 (ABBV-1)
			Passeriform 2 bornavirus	estrildid finch bornavirus 1(EsBV1)
		unassigned bornaviruses	Elapid 1 bornavirus	Loveridge's garter snake virus1(LGSV1)
		tentative, unclassified bornaviruses		avian bornavirus MALL (ABVMALL) Gaboon viper virus 1 (GaVV-1) parrot bornavirus 5 (PaBV-5) parrot bornavirus 6 (PaBV-6)

2.3.2. Virion morphology and physical characteristics

ABV shares similarities to the mammalian borna virus regarding the genome organization and morphology. ABV viral particles were 83 to 104 nanometer (nm) in diameter with lipid envelope (Hopes et al., 2010; reviewed in Herden et al., 2013).

2.3.3. ABV genome

Avian borna viruses are negative-sense, single-stranded, none segmented enveloped RNA viruses (Kistler et al., 2008). ABV has six open reading frames (ORF) with a typical 3' to 5' genome organization as known for *Mononegavirales* (reviewed in Herden et al., 2013). The first predicted transcription unit encodes for the viral nucleoprotein (N), the second predicted transcription unit for the regulatory protein (X) and the viral phosphoprotein (P), and the third transcription unit is predicted to code for the viral matrix protein (M), the viral glycoprotein (G) and the RNA-dependent-RNA- polymerase (L) (Kistler et al., 2008). Similarly to BoDV-1 genome organization, ABV X and P are encoded from overlapping reading frames and the primary transcript of the third transcription unit is likely formed by splicing (Kistler et al., 2008). Three transcription units (I, II, III) have been determined in the genomic organization of BoDV-1 with three transcription initiation signals (S1–S3) and four transcription termination signals (T1-T4) which harbour at least six open reading frames (ORFs) (Carbone et al., 1994, Schneemann et al., 1995, de la Torre 2002, Tomonaga 2002, reviewed in Herden et al., 2013). BoDV replicates and transcribes in the nucleus of the host cells. A 21-22 nucleotide (nt) deletion in the region between the N and X gene have been identified in parrot bornavirus 1 (PaBV-1), parrot bornavirus 2 (PaBV-2), parrot bornavirus 3 (PaBV-3), parrot bornavirus 4 (PaBV-4), parrot bornavirus 5 (PaBV-5), parrot bornavirus 7 (PaBV-7), ABV-Canada geese (ABV-CG), and reptile bornavirus (Kistler et al., 2008; Rinder et al., 2009; Payne et al., 2011a; Fujino et al., 2012; Mirhosseini et al., 2012; Rubbenstroth et al., 2012; Horie et al., 2012). These fragments might have regulatory function for the control of expression of the viral proteins X and P (Rinder et al., 2009). The loss of these elements in ABV suggests that regulation of the X protein expression may be carried out by other means in ABV-infected cells (Kistler et al., 2008; Rinder et al., 2009; Staeheli et al., 2010).

2.3.4. ABV proteins

2.3.4.1. ABV nucleoprotein (N)

The BoDV-N gene is encoded by the first transcription unit (Cubitt et al., 1994; Schneemann et al., 1995; Kobayashi et al., 2001). BoDV-N interacts with the viral RNA and accumulates in the nucleus during the life cycle of the virus (Briesa et al., 1992). During the viral replication cycle, BoDV-1-N is synthesized like other proteins within the cytoplasm and then enters the nucleus, where it participates in the transcription and replication process (Schwemmie et al., 1999; reviewed in Herden et al., 2013). There are two different isoforms of BoDV-1-N (p38 (38 kDa) and p40 (40 kDa) (Briese et al., 1996; Kobayashi et al., 2001). Both isoforms (p38 and p40) are differed in presence or absence in the amino acids terminal basic sequence that mediates the nuclear localization. The p40 is primarily located within the nucleus while p38 is mainly expressed in the cytoplasm (Pyper and Gartner, 1997). In comparison to ABV-N, until now, there is no evidence that ABV have different isoforms as it was found for classical BoDV-1 (Gray et al., 2010; Villanueva et al., 2010). So far, ABV-N was detected *in vivo* in the nucleus of neurons with or without weaker immunoreactivity in the cytoplasm. *In vivo*, Ouyang and colleagues (2009) searched for ABV-N in the CNS of 13 psittacines with confirmed PDD. ABV-N was present intranuclearly in glial cells of the cerebrum, and Purkinje neurons of the cerebellum in all 13 PDD birds. These findings were confirmed by investigations by Weissenböck et al., 2009a. In a subsequent study, Wünschmann and colleagues, (2011) detected ABV-N in neurons, astroglial cells, Bergmann glial cells, ependymal cells, ganglia of the myenteric plexus in the gastrointestinal tract, cardiomyocytes, tubular epithelial cells of the kidney, epithelial cells of the GIT organs, photoreceptors, smooth muscle cells of the lamina muscularis of the GIT organs, arteries in the heart in tissues of 7 psittacines with PDD and 8 psittacines without PDD. *In vitro*, Gray and colleagues, (2010) injected forebrain from a yellow-collared macaw with confirmed proventricular dilatation disease (M24) into primary duck embryonic fibroblasts (DEFs). Three days later, nuclear and cytoplasmic signals for ABV-N were detected in DEFs by immunofluorescence assay.

2.3.4.2. ABV phosphoprotein (P)

BoDV-P is encoded by the second transcription unit (Cubitt et al., 1994; Schneemann et al., 1995). The 5'-end of the P protein ORF overlaps with the 3'-end of the regulatory X protein. The function of BoDV-P is a cofactor for the RNA-dependent RNA polymerase. Moreover, BoDV-P may also be responsible for binding to other viral proteins and served as a regulatory cofactor in persistently infected cell. *In vivo*, ABV-P was present in the neurons and nerve

fibers of the brain, enteric ganglia of the upper digestive tract, nerve fibers and smooth muscle fibers of the upper digestive tract as well as in myocytes and fibers of the conductive system of the heart in tissues of 31 psittacine birds with PDD (Weissenböck et al., 2009a). Weissenböck and colleagues (2009a) also referred that staining pattern of ABV-P was variable; they found ABV-P in neuronal nuclei only or also in the cytoplasm and vice versa. ABV-P was also detected in the nuclei and cell bodies of enteric ganglia as well as nerve fibers in 31 psittacine birds with PDD (Weissenböck et al., 2009a). In another study, ABV-P was present in the cytoplasm and nuclei of infected cells of the lamina propria, epithelial cells in the gastrointestinal tract (GIT), myocytes and hepatocytes in 30 captive European parrots with clinical and/or histopathological signs of PDD (Rinder et al., 2009). Due to detection of ABV-P in both the cytoplasm and nucleus of infected cells, nuclear replication of ABV was suggested as known for BoDV-1 (Rinder et al., 2009). ABV-P was also detected in the central nervous system and gastrointestinal tract in 10 psittacine birds with PDD indicating that ABV has a broad distribution pattern and tissue tropism in psittacine birds with PDD (Kistler et al., 2009). Recently, Payne et al., (2011a) showed that ABV-P was present in the nucleus and/or cytoplasm in the cells of various organs such as glial cells and neurons of the brain and spinal cord, enteric nervous tissues, cells in the lamina propria of the GIT, cells of the retina, tubular epithelial cells of the kidneys, seminiferous tubules, islet cells of the pancreas and smooth muscle cells of blood vessels in the heart of 14 apparently healthy cockatiels. Until now, there are no *in vitro* studies on expression patterns of ABV-P.

2.3.4.3. ABV- X Protein (X)

Mammalian borna virus-X is encoded by the second transcription unit (Wehner et al., 1997). In naturally and experimentally infected animals, BoDV-X is localized mainly in the cytoplasm (Wehner et al., 1997; Herden et al., 1999). The function of the small non-structural X protein in viral pathogenesis is not completely understood. Recently it was proved that ABV-X (1322 strain isolated from a psittacine bird with PDD) and BoDV-X (He/80 and No/98 strains isolated from horses) interfered with the type I IFN system and have type I IFN-inhibiting properties (Wensman et al., 2013). It has been proposed that the function of the 10 kDa BoDV-X is to be a regulatory component for the viral polymerase complex (Schneider et al., 2003; Poenisch et al., 2009). For ABV, ABV-X is the smallest non structural protein of ABV. ABV-X is not a part of the viral RNP in all ABV genotypes. The ABV-X protein is non structural protein and it was shown to be present in both nucleus and cytoplasm of the ABV-infected cells *in vivo* (Mirhosseini et al., 2011). Until now, there are no *in vitro* studies on the expression pattern of ABV-X.

2.3.4.4. ABV matrix protein (M)

A 16-kDa (M) non glycosylated BoDV-M is encoded by the third transcription unit (Cubitt et al., 1994; Schneemann et al., 1995). BoDV-M has been co-purified with N and colocalized with other nucleocapsid proteins, including P, suggesting the association of M with viral RNPs. The function of BoDV-M is binding to RNPs and other viral proteins without blocking the viral polymerase to release mature viral particles during the process of assembly and budding (Chase et al., 2007). Until now, there are no *in vitro* or *in vivo* studies on ABV-M expression patterns.

2.3.4.5. ABV glycoprotein (G)

For BoDV-1, a 56-kDa (G) glycoprotein is encoded by the third transcription unit (Cubitt et al., 1994; Schneemann et al., 1995). Posttranslationally, a modification by N-glycosylation with high-mannose oligosaccharides increase mass of the G precursor to a mass of 84 to 94 kDa (gp94) Richt et al., 1998; Perez et al., 2001). Cleavage by the cellular protease furin yields GP-1 and GP-2 that correspond to the N- and C-terminal regions, respectively, of gp94 (Richt et al., 1998). The GP-1 product is transported to the plasma membrane where it is anchored through its C-terminal transmembrane domain (Richt et al., 1998; Lipkin and Briese, 2007; Clemente and de la Torre, 2007). The function of GP–N is necessary for virus receptor recognition and cell entry (Perez et al., 2001) while function of GP–C transported to the cell surface has a central role in the fusion of the viral envelope with the cell membrane of the host (Kiermayer et al., 2002; Eickmann et al., 2005). BoDV-1-G accumulates in cytoplasim of infected cells (Eickmann et al., 2005). There were additional predicted potential N-linked glycosylation sites in ABV-G sequences, suggesting that in ABV-G may be even more highly glycosylated than BoDV-1-G (Mirhosseini, 2011). Presence of glycosylation sites might allow the virus to attach to many epitopes on the host cells, which could explain the multitropism of ABV. For ABV-G, *in vivo* and *in vitro* studies for analyses of its expression pattern are lacking so far.

2.3.4.6. ABV RNA-dependent RNA polymerase (L)

For BoDV-1-L, a 190 kDa protein is encoded by the third transcription unit (Cubitt et al., 1994; Schneemann et al., 1995). BoDV-1-L is localized in the nucleus of the infected cells (Walker et al., 2000). For ABV-L, there are no *in vivo* and *in vitro* studies for analyses of its expression pattern so far.

2.4. Infection cycle of ABV

As ABV was firstly identified in psittacines suffered from PDD in 2008, there are no published data on the molecular mechanism of ABV replication and transcription. As ABV is homologous (60-70%) to the classical BoDV, similarities to the replication cycle of classical BoDV-1 seem to be likely. BoDV-1 attached to cell surface receptors of the host cells via receptor-mediated endocytosis (Gonzalez-Dunia et al., 1998). Entry of an enveloped virus into host cells usually requires membrane-fusing activity of viral surface glycoproteins, thus BoDV-1 glycoprotein has an important role in receptor recognition and cell entry (Gonzalez-Dunia et al., 1998; Richt et al., 1998; Clemente and de la Torre, 2007). BoDV-1-G binds to one or more (still unidentified) cell surface receptors of the host cells. BoDV-1-G is sufficient for virus receptor recognition and cell entry (Perez et al., 2001) as well as mediates the pH dependent fusion event (Gonzalez-Dunia et al., 1998). As the virus fuses to host membrane, its ribonucleoprotein RNP is released into the cytoplasm of infected cells (de la Torre, 2006; Clemente and de la Torre, 2009). Then, the viral ribonucleoprotein RNP is imported into the nucleus, where both RNA replication and transcription occur (Cubitt et al., 1994). BoDV has unique properties in replication and transcription of its genome (Pringle et al., 1996; reviewed in Herden 2013). BoDV replicates and transcribes in the nucleus of the host infected cells (Briese et al., 1992; De la Torre, 1994; Schneeman et al., 1995). Therefore, nuclear import and export of the viral genome are critical for the viral life cycle. It has been shown that the nucleolus could be the site for BoDV replication and/or transcription (Pyper et al., 1998). For transcription of BoDV**,** BoDV has also unusual transcriptional strategy. The genome is transcribed into six primary transcripts, two of which are modified posttranslationally by splicing to yield two additional mRNAs. The BoDV polymerase uses three transcriptional initiation sites and four transcriptional termination sites for the transcription of the viral genome (Briese et al., 1994; Cubitt et al., 1994). Among six different proteins of BoDV, only N is translated from a monocistronic mRNA, while transcripts of other viral proteins are polycistronic. The BoDV polymerase produces a 1.2-kb mRNA that codes for the N protein in the first transcription unit. Moreover, the BoDV polymerase produces a bicistronic 0.8-kb mRNA that codes for X and P in the second transcription unit. In the third transcription unit, the BoDV polymerase produces either short or long transcripts at the transcription termination sites T3 or T4. These transcripts contain introns which may or may not be removed by splicing. The resulting mature transcripts are synthesize the viral proteins M, G, and L (Briese et al., 1992; de la Torre., 2002; Schneemann et al., 1994; reviewed in Herden et al., 2013). BoDV employs the RNA splicing machinery for gene expression and the genome contains

three introns: intron I, intron II, and a proposed intron III (Cubitt et al., 1994; Cubitt et al., 2001; Tomonaga et al., 2000). Transcripts that retain intron I serve as messages for expression of the M protein of BoDV, and those that retain intron II serve as messages for expression of the envelope glycoprotein. Transcripts that lack both introns serve as messages for expression of the polymerase protein of BoDV. Once the BoDV replication and transcription occur, the viral ribonucleoprotein RNP is subsequently transport to the cytoplasm. Recent studies have suggested that nuclear localization signal (NLS) and/or nuclear export signal (NES) are expressed by the major viral antigens such as N and P are imported to travel between the cytoplasm and nucleus through the nuclear pore complex (Kobayashi et al., 1998; Kobayashi et al., 2001). BoDV employs a switch mechanism that changes the direction of nuclear transport of the viral RNPs dependent on the viral life cycle in infected cells. BoDV-N and BoDV-P in the nucleus may play a key role for determining the direction of BoDV-RNP movement (Kobayashi et al., 2001). Increased levels of P could mediate retention of the viral RNPs in the nucleus by the masking of the NES of N during the nuclear replication stage (Cubitt et al., 1994; Malik et al., 1999; Kobayashi et al., 2001). On the other hand, a decreased level of P in the nucleus can increase free NES, mediating nuclear export of N-containing RNP complexes (Kobayashi et al., 2001). It is possible that the nuclear export activity of BoDV-N is blocked by direct binding of P to the NES of N (Kobayashi et al., 2001). Assembly and release of BoDV are poorly understood (Compans et al., 1994). Budding of BoDV particles is only observed at the cell surface of BoDV-infected MDCK cells after treatment with *n*-butyrate. Whether this reflects the natural pathway for the exit of BoDV remains to be determined (Kohno et al., 1999).

2.5. Cultivation of ABV

In vitro, ABV is well adapted to avian cells tissue culture such as quail fibroblast cell line (CEC32), the quail skeletal muscle cell line (QM7) and duck embryonic fibroblast (DEF) (Rinder et al., 2009). Results of a recent study (Rinder et al., 2009) showed that ABV-2 and ABV-4 genotypes caused persistent, noncytolytic infections in quail and chicken cell lines but they did not replicate in cultured mammalian cells used for classical BoDV infection. This was also proved in a subsequent study (Staeheli et al., 2010). In contrast, mammalian borna viruses grow efficiently in both mammalian and avian cell lines (Rinder et al., 2009; Staeheli et al., 2010; Rubbenstroth et al., 2012; Rubbenstroth et al., 2013; Rubbenstroth et al., 2014). Data of other studies revealed that ABV has low affinity to adapt and cultivate in mammalian cell lines such as Vero cells or Madin-Darby canine kidney (MDCK) cell line (Gray et al.,

2010; Herzog et al., 2010). Piepenbring and colleagues (2012) isolated ABV from the brain of a scarlet macaw (*Ara macao*) that died from PDD successfully in the quail cell line CEC-32.

2.6. Natural ABV infection in psittacines

Many ABV infected birds do not develop obvious clinical symptoms after ABV infection and remain healthy as carriers for long time in captivity (Payne et al., 2011a, Heffels-Redmann et al., 2011; Heffels-Redmann et al., 2102). Heffels-Redmann and colleagues (2011) analyzed presence of ABV infection in 1515 birds of 54 different genera of the order *Psittaciformes* and 5 genera of non-psittacine birds. Findings of the study showed variability in the course of ABV infection in Europe. Thirty seven out of 73 birds had histotpathological lesion typical for PDD, ABV antigen and ABV RNA was found in 26 out of 37 birds, and the ABV isolation from brain and retina was successful in 37 out of 73 birds. Moreover, 36 out of 73 birds had no histopathological lesion, had no ABV antigen and ABV RNA in 29 out of 73 birds and the ABV isolation from brain and retina was not successful in 15/ 36 birds. These birds were seropositive probably indicating an inapparent infection with a low pathogenic ABV strain or an early stage of infection.

Heffels-Redmann and colleagues (2102) detected different courses of natural ABV infection in 63 psittacines in an investigation period of one year. The course of ABV infection showed variability in ABV shedding, serum antibody production, occurrence of clinical signs typical for PDD, and histopathological findings in psittacines as follows: Group 1 (acute ABV infection) consist of six out of the 63 psittacines had various courses of acute ABV infection and forms of clinical PDD. Group 2 (inapparent ABV infection) consist of thirteen out of the 63 psittacines that were consistently or inconsistently ABV positive by PCR and serology. Group 3 (subclinical ABV infections) consist of thirteen out of the 63 psittacines exhibiting only anti-ABV antibodies. Group 4 (Intermittent ABV infection) consist of eight out of the 63 psittacines that had positive ABV-RNA detection in crop and cloaca, but did not develop anti-ABV specific antibodies. Group 5 (Abortive ABV infection) consist of twenty-three out of the 63 psittacines that had negative ABV-RNA detection or anti-ABV antibodies over the whole observation period.

Lierz and colleagues (2009) tested 61 psittacine birds for the presence of ABV infection. One out of 61 birds had classical symptoms, gross lesions and histological alterations of PDD. One out of 61 birds had gross lesions, but no histological alterations or clinical signs consistent with PDD. The remaining 59 birds did not develop PDD signs. Finding of this study revealed that nineteen out of 59 parrots had ABV RNA in their cloacal swabs by quantitative real-time reverse transcription-PCR, indicating that ABV infection may occur without clinical evidence

of PDD. Moreover, ABV was also detected in clinically healthy parrots, cockatiels, and macaw (Lierz et al., 2009; Kloet Dorrestein, 2009; Payne et al., 2011).

Until now, seven genotypes (ABV-1, ABV-2, ABV-3, ABV-4, ABV-5, ABV-6, and ABV-7) of avian borna viruses (ABV) have been identified in psittacine birds (Honkavuori et al., 2008; Gancz et al., 2010). So far, avian borna viruses were detected in over 80 species of psittacine and non psittacine birds (Kuhn et al., 2015). In more recent study, avian Borna virus was identified in 40 out 86 wild parrots in Brazil (Encinas-Nagel et al., 2014). For instance, ABV infection with clinical PDD was detected in Australia in sulphur-crested cockatoo (*Cacatua galareta*), palm cockatoo (*Probosciger atterimus*), red-tailed black cockatoo (*Calyptorhynchus magnificus*), galah (*Eolophus roseicapillus*), gang gang (*Callocephalon fimbriatum*), cockatiel (*Nymphicus hollandicus*), red-capped parrot (*Purpureicephalus spurius*), eclectus parrot (*Eclectus roratus*) and spix macaw (*Cyanopsitta spixii*) (Wyss et al., 2009; Enderlein et al., 2011; Heffels-Redmann et al., 2011).

Encinas-Nagel and colleagues (2014) detected mononuclear infiltrates in the ganglia of the proventriculus or crop, which were diagnosed as suspected PDD and also in the brain of 50 out of 86 free-ranging wild psittacine birds. By real-time reverse transcription PCR (rRT-PCR), ABV-4 RNA was detected in brain, eye, crop, proventriculus, gizzard, adrenal gland, and heart in 86 out of 86 free-ranging psittacine birds (Encinas-Nagel et al., 2014).

2.7. Natural ABV infection in non psittacines

Up to now, seven ABV genotypes have been detected in non psittacine birds (Weissenböck et al., 2009b ; Delnatte et al., 2011; Rinder et al., 2012 ; Guo et al., 2012; Delnatte et al., 2013 ; Rubbenstroth et al., 2013; Guo et al., 2014). ABV-4 was present at a high prevalence in North American geese, swans, and ducks (Hoppes et al., 2013).

In canaries, three genotypes of ABV were discovered and designated as ABV-C1, ABV-C2, and ABV-C3 (Kuhn et al., 2015). Weissenböck and colleagues (2009) detected ABV-C1 in a canary (*Serinus canaria*) from Germany. The animal showed nonsuppurative ganglioneuritis of the proventriculus and gizzard and encephalitis, lesions comparable to proventricular dilatation disease (PDD) of psittacine birds. A wide distribution of ABV was also detected in captive canary birds in Germany (Rubbenstroth et al. 2013). Rubbenstroth and colleagues, (2014a) inoculated domestic canaries (*Serinus canaria* forma domestica) and cockatiels (*Nymphicus hollandicus*) with ABV. Findings of this study showed that ABV-infected canaries did not exhibit PDD-like symptoms. Moreover, ABV RNA in cloacal swabs and organ samples or ABV-specific antibodies were not detected after ABV infection in

cockatiels and canaries which could indicate that horizontal transmission of ABV is inefficient in immunocompetent fully fledged domestic canaries and cockatiels.

In finches, a new genotype of ABV was discovered in captive estrildid finches (*Estrildidae*) in Saxony in Germany called ABV-EF for estrildid finch (Rubbenstroth et al., 2014b). ABV-EF genotype is differ markedly from the genotypes present in psittacine birds. ABV infection was also detected in a Bengalese finch (*Lonchura striata*) (Rubbenstroth et al. 2013).

In geese, it has also been shown that healthy Canada geese (*Branta canadensis*) could harbour ABV-CG without clinical signs of PDD (Payne et al., 2011; Payne et al., 2013). Avian borna virus of Canada geese (ABV-CG) was also found in the brain of bald eagles (*Haliaeetus leucocephalus*) that died with characteristic pathological findings (encephalitis) of PDD (Hoppes et al., 2013). ABV-CG was also found in the Mississippi kite (*Ictinia mississippiensis*), trumpeter swans (*Cygnus buccinator*), feral mute swans (*Cygnus olor*) (Smith et al., 2010; Payne et al., 2012b ; Guo et al. 2012 ; Delnatte et al. 2013). Delnatte and colleagues, (2011) detected ABV-N and ABV-RNA in wild Canada geese and trumpeter swans (*Cygnus buccinators*). Findings of the study (Delnatte et al., 2011) showed that the ABV antigen and ABV-RNA were detected in 11/12 wild goose brains and 2/2 swans brains. By analyzing the sequences of the amplified gene, a unique new genotype designated as (ABV-CG) genotype was discovered. Recent studies revealed that ABV-CG was also detected in snow geese (*Chen caerulescens*) and Ross's geese (*Chen rossii*) (Payne et al. 2012a, Payne et al. 2012b). ABV-CG and viral RNA were also isolated from Pekin duck eggs from commercial sources (Payne et al. 2012b). ABV-CG RNA was also detected in three species of gulls in North American, herring gull (*Larus argentatu*) ring-billed gull (*Larus delawarensi*) and laughing gull (*Larus atricilla*) (Payne et al. 2012b). ABV-CG infection was also found in toucan (*Rhamphastos sp*.), in mallards (*Anas platyrhynchos*) and in wood ducks (*Aix sponsa*) (Guo et al. 2014).

2.8. Experimental ABV infection in psittacines

Initial studies of experimental infections in birds fulfilled Henle-Koch postulates by using small numbers of animals. Gancz and colleagues (2009) inoculated 3 cockatiels (*Nymphicus hollandicus*) by multiple routes (intramuscular, intraocular, intranasal, and oral) with brain homogenate containing ABV-4. Sixty-six days post infection, PDD-associated signs, characteristic histopathologic lesions in the CNS and myenteric ganglia occurred in 2 out of the 3 birds, and test results were positive for ABV-4. ABV-N and ABV-4 RNA were detected in the CNS, GIT, and peripheral organs in cockatiels (*Nymphicus hollandicus*) after experimental infection with brain homogenate containing ABV-4 via multiple routes (Gancz

et al., 2009). However, brain homogenate also contained sequences with partial analogy to viruses of the family *Astroviridae* and family *Retroviridae*. Gray and colleagues (2010) inoculated 2 adult Patagonian conures (*Cyanoliseus patagonis*) with ABV-4, strain M24 originally isolated from a yellow-collared macaw. The conures were known to be chronic carriers of psittacine herpesvirus, but they appeared to be healthy. Antibodies against ABV were detected 33 dpi, and shedding of viral RNA was detected 62 dpi. Clinical PDD developed in both birds, after which 1 bird died and the other was euthanized. Histopathologic analysis showed typical PDD lesions in the gastrointestinal tract organs, adrenal gland, and heart. It was not determined whether the herpesvirus infection was a potentiating factor for ABV infection (Gancz et al., 2009; Gray et al., 2010). Piepenbring and colleagues (2015) inoculated 19 cockatiels (*Nymphicus hollandicus*) with ABV-4 and 18 cockatiels ABV-2 via intracerebral and intravenous route of infection. Twelve birds exhibited clinical signs typical for PDD from day 22 onward after ABV-2 infection while five birds exhibited clinical signs typical for PDD from day 33 onward after ABV-4 infection. These findings could indicate effect of the ABV genotype on the outcome of disease after ABV infection.

2.9. Epidemiology of ABV

ABV infection does not spread quickly among birds except in crowded aviaries and nurseries (Lierz et al., 2009; Rubbenstroth et al., 2014). Mode of ABV transmission is still unknown. Recent epidemiological data indicate that ABV infection occurs in psittacine and non-psittacine birds worldwide e.g. in Israel, USA, Australia, Canada and Brazil (Kistler et al., 2008; Honkavuori et al., 2008; Weissenböck et al., 2009; Raghav et al., 2010; Encinas-Nagel et al., 2014), Spain, Italy, United Kingdom, Denmark, Germany (Enderlein et al., 2009; Lierz et al., 2009; Rinder et al., 2009), Austria, Switzerland and Hungary (Weissenböck et al., 2009a). There are many factors that complicate analysis of the epidemiology of ABV infection in parrots such as apparently healthy carriers, presence of many ABV genotypes, and extent of incubation period (Payne et al. 2011).

2.10. Pathogenesis

The incubation period of ABV after natural infection is unknown. The incubation period of ABV in experimental infections ranged between 11 days (Gregory et al., 1997), or 2 to 4 weeks (Kistler et al., 2010), 20 to 60 days, up to 200 days (reviewed in Herden et al., 2013), months to years (Gregory et al., 1995, Gancz et al., 2009, Gray et al., 2010). ABV-specific serum antibodies have been detected already at 6 days post infection in experimentally ABV-2 and ABV-4 infected cockatiels (Piepenbring et al., 2015, Lierz et al., 2012). ABV-specific serum antibodies could be present between 7 and 60 days after ABV infection (reviewed in

Herden et al., 2013). Many recent studies have elucidated that these ABV antibodies are non-neutralizing antibodies and raised against the phosphoprotein, nucleoprotein, matrix protein and X protein (de Kloet et al., 2009; Villanueva et al., 2010; de Kloet et al., 2011; Heffels-Redmann et al., 2011). Neutralizing antibodies against mammalian BoDV also do not occur, if ever only late after infection and are potentially directed against viral glycoprotein (Stitz et al., 1998). Heffels-Redmann and colleagues (2012) reported that the anti-ABV serum antibodies did not protect birds from development of disease and onset of lesions, similarly as /or BoDV-infected immune competent mammals (Narayan et al., 1983, Herden et al., 1999). Payne and colleagues (2011a) observed a massive lymphocytic infiltration and lymphoid nodule formation within and around the ganglia throughout the gastrointestinal tract in apparently healthy cockatiels shedding ABV-4 and seropositive, suggesting that presence of ABV antibodies in sera of asymptomatic cockatiels do not induce efficient humoral immune response. It has been shown that birds displaying high serum antibody titers are rather prone to develop clinical PDD (Heffels-Redmann et al., 2012). In swabs, ABV-RNA was detected between 20 and 72 days post infection (dpi) depending on the inoculation route of ABV (intracerebral, intravenous, intramuscular). Piepenbring and colleagues (2012) detected the presence of ABV-RNA earlier after intracerebral infection in cockatiels than after intravenous infection. Recent study (Heffels-Redmann et al., 2012) referred that birds with high viral RNA load more likely develop PDD symptoms. ABV-infected birds could also shed the virus without showing clinical signs which may contribute to ABV transmission (reviewed in Herden et al., 2013). The characteristic gross finding of ABV infection and PDD is dilatation of the proventriculus. Lymphoplasmacytic infiltrates within autonomic nerves and ganglia in the digestive tract is the characteristic histopathologic lesion of PDD (Gregory, 1995). Moreover, nonpurulent encephalitis, myelitis and/or ganglioradiculitis of spinal nerves have also been detected (Greogry et al., 1994; Ouyang et al., 2009; Hopes et al., 2010; Kistler et al., 2010; Raghav et al., 2010; Wünschmann et al., 2011; Piepenbring et al., 2012). Peripheral neuritis, inflammation of the myocardium, cardiac muscle cells and conducting fibers, adrenal glands and eye may also occur (reviewed in Herden et al., 2013). It has been shown that ABV has high tropism not only to the central nervous tissues but also to peripheral organs. ABV antigen or ABV RNA was detected most frequently in the brain, spinal cord, gastrointestinal tract (reviewed in Herden et al., 2013). ABV antigen or ABV-RNA could also be present in many other organs such as heart, liver, kidney, spleen, pancreas, lung, gonads, thyroid, and skin (reviewed in Herden et al., 2013). Weissenböck and colleagues (2010) detected hybridization signals in the brain, in the vegetative nerve system, glandular epithelia and

smooth muscle cells of the intestinal tract and in cardiomyocytes in naturally PDD affected birds. Whether a comparable immunopathogenesis as known for mammalian Bornavirus infections occur requires further investigations.

2.11. Comparison of ABV and BoDV-tropism

BoDV exhibit a high preference for the CNS in naturally or experimentally infected animals whereas ABV can have a broad distribution patterns in PDD positive birds but also in psittacines without clinical signs (Rinder et al., 2009; Ouyang et al., 2009; Heffels-Redmann et al., 2011; Weissenböck et al., 2009a, Gray et al., 2010, Wünschmann et al., 2011, Piepenbring et al., 2012). Distribution patterns of ABV in naturally PDD affected birds has been characterized in many studies but a detailed kinetic analyses of organ distribution as it is possible in experimental trials was lacking. Distribution patterns of ABV in organs of naturally PDD affected birds has been described by demonstrating either viral antigen by immunohistochemistry (IHC) or Western blotting (WB), or detection of viral RNA by reverse transcription polymerase chain reaction (RT-PCR) or in situ hybridization (Honkavuori et al., 2008; Gancz et al., 2009; Kistler et al.,2010; Lierz et al., 2009; Ouyang et al.,2009; Weissenböck et al.,2009a; Weissenböck et al., 2009b; Lierz et al.,2010; Raghav et al.,2010; Reßmeyer et al., 2010; Wünschmann et al.,2011; Rubbenstroth et al.,2013). Results of Piepenbring et al., (2012) showed that ABV-RNA was detected in numerous tissues after experimental infection ABV-4 in cockatiels. Rinder and colleagues (2009) detected ABV-N in the brain, crop, liver, kidney, heart, and lung. Ouyang and colleagues (2009) detected ABV-N mainly in the cerebrum, cerebellum and spinal cord of PDD infected birds. Raghav and colleagues (2010) detected ABV-N in the brain, spinal cord, adrenal gland, pancreas, and kidney in psittacine birds with histopathologic evidence of PDD. Ouyang and colleagues (2009) detected ABV-N in neurons of the cerebral cortex, Purkinje cells and Bergmann glial cells in the cerebellum and ependymal cells of the central nervous system. Rinder and colleagues (2009) detected ABV-N and ABV-P in the intestinal mucosa, epithelial cells, lamina propria cells, liver cells and myocytes supporting the conclusion that ABV can productively infect non-neuronal cells. Weissenböck and colleagues (2010) detected ABV-2 and ABV-4 RNA in the vegetative nerve system, glandular epithelia and smooth muscle cells of the intestinal tract and cardiomyocytes in naturally PDD affected birds by in situ hybridization.

2.12. Routes of ABV transmission

2.12.1. Horizontal route of transmission

Many studies described the intermittent ABV shedding in urine and faeces of ABV-infected birds (Raghav et al., 2010; Villanueva et al., 2010; Payne et al., 2011a, Heffels Redmann et al., 2011). Based on these findings, the oral-faecal route of infection was assumed as the most common mode of transmission of ABV. Other authors proposed that ABV shedding via urine is the main way of viral release and more important than via faeces of ABV infected birds suffering from PDD (Heffels-Redmann et al., 2011; Piepenbring et al., 2012; Heatley and Villalobos, 2012). Piepenbring and colleagues (2012) demonstrated sucessul experimental infection with ABV-4 via intravenous and intracerebral routes of infection in cockatiels. Findings of Piepenbring and colleagues showed that ABV-RNA was not only found in the central nervous system but also in gastrointestinal organs and skin. ABV was found in fecal particles passing from one host and introduced into the oral cavity of another host. This indicates that the orofecal route might be the main way of horizontal ABV transmission (Piepenbring et al., 2012). In another study experimental infection of cockatiels via the oral-nasal route only was not successful. Orofecal transmission after hatch could also be a mode of transmission as described in a recent study (Kerski et al. 2012). Heffel-Redmann and colleagues (2011) detected the ABV RNA in 86 of 347 crop swabs and 99 of 381 cloacal swabs in captive psittacines with PDD by real time RT–PCR which supports possible orofeacal transmission. Findings of the study (Rubbenstroth et al., 2014) suggested that direct contact transmission of ABV was not successful in domestic canaries (*Serinus canaria forma domestica*) and cockatiels (*Nymphicus hollandicus*).

2.12.2. Vertical route of transmission

A previous study already showed that ABV antigen was detected in testes and ovaries of infected parrots (Raghav et al., 2010). Lierz and colleagues, (2011) detected ABV-RNA in 2 out of 30 dead-in-shell embryos of various psittacines that originated from ABV-infected flocks with a history of PDD. These findings indicated that ABV might be transmitted vertically from ABV-infected parents to offspring. Findings of subsequent studies showed that ABV RNA was detected in eggs, embryos, and hatchlings of different psittacine species and canaries (Kerski et al., 2012; Monaco et al., 2012; Rubbenstroth et al., 2013). These data might argue for a vertical transmission, however, productive viral replication has so far not been shown. It was assumed that ABV reach eggs either from penetration of the shell after egg contamination, or contamination of oviduct secretions or ABV infection of ova or sperm (Monaco et al., 2012). Findings of the study by Payne et al., 2012 showed that ABV grow in

the fibroblasts derived from commercial duck eggs suggesting that the vertical transmission may be possible. Kerski and colleagues (2012) detected anti-ABV antibodies and ABV-2 RNA in egg yolks of embryos obtained from infected sun conures (*Aratinga solstitialis*), supporting that vertical transmission might occur.

2.13. Diagnosis

2.13.1. Intra vitam diagnosis

Visualization of dilatation of the proventriculus can be carried out by diagnostic imaging techniques/radiography. Detection of anti-ABV antibodies and ABV-RNA are the best diagnostic approach for intra vitam diagnosis of ABV. Serological tests can be used to diagnose anti-ABV antibodies such as western blot assay (De Kloet & Dorrestein, 2009; Lierz et al., 2009; Villanueva et al., 2009), enzyme linked immunosorbent assay (ELISA) technique (de Kloet et al., 2011) and indirect immunofluorescence (IIF) assay (Gray et al., 2010; Herzog et al., 2010). IIF assay is an appropriate serological technique with high sensitivity and specifity for detection of ABV-specific serum antibodies (Herzog et al., 2010). Another suitable method is to test the presence of ABV-RNA in faeces, swabs of crop and cloaca by using RT-PCR, (Rinder et al., 2009; Lierz et al., 2009; Enderlein et al., 2009; Gray et al., 2010; Kistler et al., 2010; Piepenbring et al., 2012).

In some birds only the detection of anti-ABV serum antibodies succeeded, in others ABV-RNA was undetectable, while still others in both tests reacted positively (Herzog et al., 2010; Enderlein et al., 2010, Heffels-Redmann et al., 2011, 2012). Thus, diagnosis of ABV infection requires a combination of serological investigation and genome detection (Gough et al., 1996; Herzog et al., 2010; Enderlein et al., 2010, Lierz et al., 2010; Heffels-Redmann et al., 2011, 2012).

2.13.2. Post mortem diagnosis

Histopathology, ABV isolation, ABV antigen and ABV-RNA detection are the best methods for the post mortem diagnosis of ABV. Identification of the lymphoplasmacytic infiltrates in the GIT and CNS in biopsy sample is typical and comprise the characteristic histopathological lesion. Detection of ABV-RNA by in situ hybridization (ISH) and RT-PCR in tissues was also used. Detection of viral genomic and mRNA of ABV-2 and ABV-4 by in situ hybridization (ISH) procedure using digoxigenin-labeled RNA probes in tissues of birds with PDD has been described by Weissenböck et al. (2010). Many studies used RT-PCR to demonstrated the presence of ABV RNA in biopsies of psittacine birds with PDD, in feather calami, in eggs, embryos, and hatchlings obtained from infected sun conures (*Aratinga*

solstitialis), and in the brain of apparently healthy macaws (de Kloet et al., 2009 ; de Kloet et al., 2011; Heffels-Redmann et al., 2012; Kerski et al., 2012). Immunohistochemistry (IHC) has been performed to study the tissue distribution and localization of ABV antigen in psittacines (Gancz et al., 2009; Weissenböck et al., 2009a; Rinder, et al., 2009; Ouyang et al., 2009; Herzog et al., 2010; Raghav et al., 2010, Wünschmann et al., 2010) by applying either cross reactive anti-BoDV-1 antibodies against viral N, P, X protein or ABV specific antibodies against ABV N (reviewed in Herden et al., 2013). It has been shown that the monoclonal anti-BoDV-1 N antibody Bo18 is not good marker for detection of ABV antigen by IHC (reviewed in Herden et al., 2013). Isolation of ABV is also a good diagnostic procedure. ABV has been isolated successfully in the quail fibroblast cell lines CEC-32, the quail skeletal muscle cell line QM7 (Rinder et al., 2009, Herzog et al., 2010, Piepenbring et al., 2012), and duck embryo fibroblasts (Gray et al., 2010).

2.14. Differential diagnoses

Many diseases may have the same clinical symptoms as in PDD such as megabacteriosis (infection with *Ornithogaster macrorhabdos*). Other diseases which have to be differentiated from PDD are clostridial enteritis, fungal and yeast infections, heavy metal toxicosis, intestinal obstruction, neoplasia and parasitism, pyloric dysfunction and pancreatitis (Bond et al., 1993; Taylor et al., 1997; Antinoff et al., 2001; Hoppes et al., 2010).

2.15. Prevention and control

It is quite advisable to examine birds for presence of the ABV infection periodically and then separate the positively tested birds (Lierz et al., 2010).

2.15.1. Vaccination

A recent study (Heffels-Redmann et al., 2012) suggested that serum antibodies are not protective and that ABV might escape recognition by the innate immune system (Staeheli et al., 2010). This might indicate that induction of an immune response may actually increase the severity of the disease, so vaccination may be contraindicated. Serological examination should be performed continuously and suspected birds should be removed from flocks and incoming birds should be tested again and quarantined. Sanitation, disinfection, isolation of ABV-infected birds, control of the illegal trading are also useful for good management and control of the infection. Counseling the owner, as well as establishing a long-term management plan, are also important aspects of veterinary care.

2.15.2. Therapeutics

There is no curative therapy for PDD infected birds or ABV infection (Staeheli et al., 2010, Lierz et al., 2010). Supportive care of the PDD affected birds such as providing easily digested food to diseased birds, prevention secondary infections, symptomatic therapy by the use of anti-inflammatory medication to diminish the amount of inflammatory nerve injury in PDD affected birds (Levine and Practice,2003; Gancz et al.,2010; Hoppes et al.,2010, Hoppes et al.,2012). The supportive therapy may maintain the survival of PDD affected birds for months up to years (Suedmeyer, 1992; Gerlach, 1994; Gregory et al., 1997). Many affected birds respond favourably to none steroidal anti-inflammatory drugs (NSAIDs). Birds under treatment should be housed separately from any susceptible birds. Another study suggested that PDD affected birds which displayed severe gastro-intestinal and neurological signs were successfully treated after taking amantadine hydrochloride (Clubb et al., 2009; Gancz et al., 2010).

3. Materials and Methods

The study was governmentally approved according to the guide for the care and use of animals (Registration number: GI 18/9 – NR.02/210). All clinical data, demonstration of ABV RNA data and ABV-specific antibodies data were part of the doctoral thesis of Anne Piepenbring. In the current Ph.D thesis, inflammatory lesions, distribution patterns of ABV antigen, ABV-2 RNA and ABV-4 RNA were characterized in the central nervous system (CNS) as well as in the peripheral organs of the experimentally infected cockatiels over the investigation period of 33 weeks.

3.1. Animals

Ten females and nine males of cockatiels *Nymphicus hollandicus* were infected with ABV-2. Eleven females and seven males of cockatiels *Nymphicus hollandicus* were also infected with ABV-4. All birds were investigated over a period of 231 days post infection (dpi) after ABV-2 infection and 230 dpi after ABV-4 infection (table 2 and table 3).

3.2. Experimental infection of cockatiels with ABV-2

For the experimental infection of cockatiels with ABV-2, nineteen cockatiels were divided into 2 groups (intracerebral (ic) and intravenous (iv) inoculation), each composed of 9 birds. One bird remained untreated and served as sentinel bird in group ic. Two birds were inoculated ic and two birds were inoculated iv with mock cell suspension without ABV-2 and served as control group (table 2). Birds of the mock group were separated from the ABV-2 infected birds.

3.3. Experimental infection of cockatiels with ABV-4

Eighteen cockatiels were randomly divided into 2 groups (group ic and group iv), each composed of 9 birds and were inoculated either intracerebrally or intravenously with ABV-4. One bird did not receive any treatment and served as sentinel bird in group ic. For details, see table 3).

Table 2: list of experimentally ABV-2 infected cockatiels

Bird ID	Gender	Age (days)	Inoculation route
N 32	female	196	iv
N 25	female	212	iv
N 34	female	203	iv
N 45	male	175	iv
N 19	male	235	iv
N 48	female	133	iv
N 33	male	202	iv
N 42	male	161	iv
N 29	male	169	iv
N 24	female	216	ic
N39	female	168	ic
N 47	male	164	ic
N 27	female	212	ic
N 30	female	196	ic
N 22	male	233	ic
N 40	female	182	ic
N 46	female	175	ic
N 49	male	106	ic
N 28	male	196	sentinel
N 60			mock
N 61			mock
N 63			mock
N 69			mock

(iv) intravenous, (ic) intracereberal

Table 3: list of experimentally ABV-4 infected cockatiels

Bird ID	Gender	Age (days)	Inoculation route
N15	female	121	ic
N 21	male	137	ic
N 19	female	137	ic
N 26	female	137	ic
N 16	female	137	ic
N 13	male	137	iv
N 18	male	137	iv
N 25	male	137	iv
N 12	female	137	iv
N 11	female	137	ic
N 10	female	137	iv
N 22	female	121	iv
N 23	female	121	iv
N 27	male	137	iv
N 29	female	44	iv
N 20	female	121	ic
N 24	male	137	ic
N 30	male	44	ic
N 14	male	137	sentinel

(iv) intravenous, (ic) intracereberal
sentinel was reared in group ic

3.4. Animals housing

The cockatiels were obtained from the flock from Clinic for Birds, Reptiles, Amphibians and Fishes, Justus-Liebig-University-Giessen. The cockatiels were reared by their parents. The flock was kept in aviaries with nesting boxes and a seed diet without sunflower seeds (Versele-Laga, Germany).

3.5. Virus preparation and isolation

ABV-2 and ABV-4 genotypes were isolated by Sibylle Herzog, Institute of Virology, Faculty of Veterinary Medicine, Justus-Liebig-University-Giessen. The ABV-2 genotype was isolated from the brain of a cockatiel suffering from PDD. The ABV-4 genotype was isolated from the brain of a scarlet macaw (*Ara macao*) that died from PDD. Tissue samples were homogenized, clarified, 10-fold diluted in culture medium, and used for infection. The persistently ABV-infected CEC-32 cells were incubated for 6 days at 37°C (Herzog et al., 2010). By using polyclonal serum from rats experimentally infected with BoDV, indirect immunofluorescence was used (Herzog et al., 2010).

3.6. Inoculation of the virus

For inoculations, the supernatant of the virus was used for infection. The infectivity titer of ABV-4 was 1×10^4 $TCID_{50}$/mL. The infectivity titer of ABV-2 was 3×10^3 ID_{50}/ml. For the experimental infection, 0.1 mL of the inoculum of each genotype was inoculated.

3.7. Clinical examination

All birds were examined daily until 231 days after ABV-2 infection, 230 days after ABV-4 infection as part of the doctoral thesis of Anne Piepenbring to determine the health status of the infected cockatiels. Blood and swabs samples were collected weekly.

3.8. Euthanization

If the experimentally ABV-2 or ABV-4 infected birds exhibited clinical signs typical for PDD (table 4 and 5), they were euthanized immediately. After ABV-2 infection, 12/18 experimentally ABV-2 infected birds exhibited clinical sign (six birds were died at 32, 46, 50, 84, 86, and 137 dpi, and six birds were euthanized at 68, 76, 88, 120, 172 and 231 dpi (table 4). Six out of 18 experimentally ABV-2 infected birds did not display clinical signs and were euthanized at the end of the experiment at day 231 dpi (table 4). After ABV-4 infection, 5/18 experimentally ABV-4 infected birds exhibited clinical sign and were euthanized at 60, 116, 206, 229, and 229 dpi. Moreover, 11/18 experimentally ABV-2 infected birds did not display clinical signs and were euthanized at 115 dpi (3 birds), 116 dpi (2 birds), 229 dpi (3 birds) and 230 dpi (3 birds) (table 5). Two out of 18 experimentally ABV-4 infected birds did not exhibit clinical sign and died suddenly at 66 and 120 dpi (table 5).

Table 4: List of cockatiels which showed clinical signs after ABV-2 infection

Bird ID	gender	Route of infection	Birds with clinical signs			
			gastrointestinal signs	neurological signs	death	euthanasia
			days p.i	days p.i	dpi	dpi
N39	female	ic	22		32	
N 32	female	iv	45		46	
N 25	female	iv	46		50	
N 24	female	ic	40	32		68
N 34	female	iv	57			76
N 47	male	ic	83		84	
N 27	female	ic	71	85	86	
N 45	male	iv	78			88
N 19	male	iv	104			120
N 48	female	iv	121		137	
N 30	female	ic	139			172
N 46	female	ic	86			231
N 22	male	ic				231
N 40	female	ic				231
N 33	male	iv				231
N 42	male	iv				231
N 29	male	iv				231
N 49	male	ic				231
N28	male	sentinel				231

(iv) intravenous, (ic) intracereberal, (dpi) days post infection. ABV-2 infection, early time points (32-86) dpi, mid time points (87-172) dpi, and late time points (173-231) dpi.

Table 5: List of cockatiels which showed clinical signs after ABV-4 infection

Bird ID	gender	Route of infection	Birds with clinical signs			
			gastrointestinal signs	neurological signs	death	euthanasia
			days p.i	days p.i	dpi	dpi
N15	female	ic	37	41		60
N 21	male	ic			66	
N 19	female	ic				115
N 26	female	ic				115
N 16	female	ic				115
N 13	male	iv	116			116
N 18	male	iv				116
N 25	male	iv				116
N 12	female	iv			120	
N 11	female	ic		199		206
N 10	female	iv	126			229
N 22	female	iv		159		229
N 23	female	iv				229
N 27	male	iv				229
N 29	female	iv				229
N 20	female	ic				230
N 24	male	ic				230
N 30	male	ic				230
N 14	male	sentinel				230

(iv) intravenous, (ic) intracereberal, (dpi) days post infection. ABV-4 infection, early time points (37-66) dpi, mid time points (67-126) dpi, and late time points (127-230) dpi.

3.9. Organ sampling

Swab samples from the crop and cloaca were collected weekly. Blood samples were also collected. Tissue samples from brain, spinal cord, sciatic nerve, eye, heart, liver, kidney, liver, spleen, pancreas, crop, proventriculus, gizzard, intestine, skin and skeletal muscles were also collected.

3.10. Re-isolation of ABV-2 and ABV-4

Infectious virus was re-isolated by using samples from brain and retina as described (Herzog et al., 2010).

3.11. Histological examination of tissue sections

3.11.1. Fixation of tissue sections of ABV infected cockatiels

Organ samples were fixed in 10% formalin, then embedded into embedding plastic cassettes.

3.11.2. Preparation of formalin-fixed tissue sections

Organs samples were processed in an automatic Tissue Tek VIP® machine (Sakura, Germany). Tissues were dehydrated through using different concentrations of alcohols at 37° C (50% ethanol for 30 minutes, 70% ethanol for 60 minutes, 80% ethanol for 60 minutes, 96% ethanol for 30 minutes, 100% isopropanol two times for 60 minutes each), and cleared by xylene at 40° C three times for 90 minutes each and then infiltrated with Roti-plast paraffin (Roth, Germany) at 60° C three times for one hour each to enable sectioning. After embedding the biopsies into paraffin by Tissue-Tek® TEC ™ (Sakura, Germany), biopsies were sectioned at 5µm using Leica RM2255 rotary microtome (Leica, Germany) and then placed on Superfrost plus® slides (R.Langenbrinck, Germany). Slides were routinely stained by an automatic HMS740 Microm robot-stainer (Microm GmbH, Germany) with heamatoxylin and eosin (H&E). The HE staining protocol was performed according to the protocol provided by the manufacturer of the machine (Microm GmbH, Germany). Slides were mounted with Tissue-Tek® coverslipping films (Sakura, Germany) in an automated coverslipper machine (Vogel, Germany).

3.12. Evaluation of inflammatory lesions

For evaluation of inflammatory lesions after ABV-2 and ABV-4 infection, respective semiquantitative scores were established for assessing the severity of lesions as mild, moderate and severe by 200 magnification power as given in table 6.

Table 6: Scores of inflammatory lesions

Organs	Scores		
	Mild	**Moderate**	**Severe**
CNS	**A-** Perivascular infiltration of mononuclear cells as a monolayer. **B-** Infiltration of 1-15 mononuclear cells perivascularly per field.	**A-** Perivascular infiltration of mononuclear cells as bilayer. **B-** Infiltration of 15-30 cells perivascularly per field.	**A-** Perivascular infiltration of mononuclear cells as three layers or more. **B-** Infiltration of more than 30 cells perivascularly per field.
GIT	**A-** Infiltration of mononuclear cells in the intestinal mucosa, lamina muscularis, submucosa, connective tissue in the GIT and/or perineural/ periganglionic infiltration.		
	B- Infiltration of 10-30 cells per field.	**B-** Infiltration of 30-50 cells per field.	**B-** Infiltration of more than 50 cells per field.
Peripheral organs	**A-** Infiltration of mononuclear cells either as perivascular/ perineural/ periganglionic or follicular-shape like aggregations. **B-** Perivascular/ periganglionic or perineural infiltration of mononuclear cells as a monolayer. **C-** Infiltration of 1-15 mononuclear cells per field.	**A-** Infiltration of mononuclear cells either as perivascular/ perineural/ periganglionic or follicular-shape like. **B-** Perivascular/ periganglionic or perineural infiltration of mononuclear cells as abilayer or triple layer. **C-** Infiltration of 15-30 cells per field.	**A-** Infiltration of mononuclear cells either as perivascular/ perineural/ periganglionic or follicular-shape like. **B-** Perivascular/ periganglionic or perineural infiltration of mononuclear cells more than three layers. **C-** Infiltration of more than 30 mononuclear cells per field.

(CNS) central nervous system, (GIT) gastrointestinal tract, 200 magnification power

3.13. Immunohistochemistry (IHC)

For demonstration of the presence of ABV antigen in all ABV-2 and ABV-4 infected animals, a polyclonal rabbit anti Borna disease virus antibody was used. The anti BoDV antibody had been proven to be cross reactive antibody with ABV by (Herzog et al., 2010).

3.13.1. BoDV-antibody

The antibody directed against BoDV phosphoprotein (BoDV-P) was provided by Professor Dr. Juergen Richt, Kansas State University. The anti-BoDV antibody (p24) was diluted 1:2000 with 20% pig serum/tris buffered saline (TBS) and 100µl of the diluted primary antibody was applied on each slide.

3.13.2. Secondary antibody

A biotinylated pig anti-rabbit IgG (Vector laboratories Inc, USA) served as secondary antibody. The secondary antibody was diluted with 20% pig serum/TBS and 100µl of the diluted secondary antibody was applied on each slide.

3.13.3. Block serum

20% pig serum (PAA Laboratories GmbH, Germany) in TBS was applied and 100µl of the diluted serum was applied on each slide. Slides were incubated with the blocking solution for 15 minutes at room temperature.

3.13.4. Control

A brain and GIT tissue sections from ABV-2 experimentally infected cockatiel were used as a positive control. In parallel, a serum (Sigma-Aldrich, Germany) of healthy rabbit served as a negative control for the polyclonal anti-BDV antibody without adding the primary antibody.

3.13.5. Evaluation the positive signals

Presence of intranuclear or intracytoplasmic immunostaining was considered as positive immunohistchemical reaction for staining of the ABV antigen.

3.13.6. IHC protocol

1. Deparaffinization of the slides was performed by immersing slides with xylene (3x5 minutes), isopropanol (2x3 minutes), 96% ethanol (3 minutes), and 80% ethanol (3 minutes).
3. Inhibition of the endogenous peroxidase (H_2O_2) was performed by adding 197ml of methanol and 3ml 30% hydrogen peroxidase (H_2O_2) for 30 minutes at room temperature.
4. Washing three times with TBS, five minutes each.

5. Citrate pretreatment pH= 6.5 as antigen retrieval method was used. Slides were placed in heated water bath and incubated with citrate buffer solution at 95 °C for 25 minutes. Slides were left to cool for 10 minutes at room temperature.

6. For blocking, 100µl 20% pig serum in TBS was applied for 15 minutes at room temperature.

7. A 100µl of the primary antibody and the rabbit serum diluted 1:2000 in 20% pig serum/TBS were applied and subsequently incubated in the refrigerator at 4 °C overnight.

8. Tissue sections were washed in TBS/buffer three times, 5 minutes each.

9. A 100µl of the secondary antibody diluted 1:100 in 1% bovine serum albumin (BSA) /TBS was applied on each slide and were incubated with the secondary antibody for 30 minutes at room temperature.

10. Tissue sections were washed in TBS/buffer three times, 5 minutes each.

11. Tissue sections were incubated with 100µl avidin biotin complex (ABC) Vectastain kit® (Vector laboratories Inc, USA). The ABC kit was diluted 1:100 in 1% BSA/TBS before applying to each slide.

12. Tissue sections were washed in TBS/buffer three times, 5 minutes each.

13.Tissue sections were incubated with 3, 3 diaminobenzdine-teterahydrochloride (DAB) solution for 10 minutes at room temperature.

14. Tissue sections were washed in TBS/buffer three times, 5 minutes each, followed by washing in distilled water once for 5 minutes at room temperature.

15. Tissue sections were immersed in Kardasewitsch stain for 5 minutes at room temperature.

16. Tissue sections were washed in TBS/buffer twice, 5 minutes each.

17. Tissue sections were stained with Papanicolaou for 30 seconds at room temperature.

18. Tissue sections were washed in tap water twice, 5 minutes each followed by washing in distilled water once for 5 minutes at room temperature.

19.Dehydration of tissue sections was carried out by immersing them in different concentrations of alcohols (50% ethanol, 70% ethanol, 80% ethanol, 96% ethanol, and in 2 changes of 100% isoproponal), 3 minutes each.

20. Tissue sections were immersed in 2 changes of xylene, 3 minutes each.

21. Slides were mounted with Tissue-Tek® coverslipping films (Sakura, Germany) in an automated coverslipper machine (Vogel, Germany).

3.14. Evaluation of ABV distribution pattern

For evaluating the distribution of the ABV antigen, semi quantitative scores were established (score 1, score 2 and score 3) by 200 magnification power as shown in table 7.

Table 7: Scores of ABV antigen detection

Organs	Scores		
	Score 1	Score 2	Score 3
CNS	presence of 1-15 positive cells in the field.	presence of 15-30 positive cells in the field	presence of more than 30 positive cells in the field
GIT	presence of 1-10 positive cells in the field	presence of 10-30 positive cells in the field	presence of more than 30 positive cells in the field
Peripheral organs	presence of 1-15 positive cells in the field	presence of 15-40 positive cells in the field	presence of more than 40 positive cells in the field

(CNS) central nervous system, (GIT) gastrointestinal tract, 200 magnification power

3.15. Characterization of the immune cells

Characterization of the immune cells was done by IHC to characterize B lymphocytes, T lymphocytes and macrophages in all organs after ABV-2 and ABV-4 infection. Due to the lack of the specific antibodies that recognise T cells (table 8), macrophages (table 9) and B cells (table 10) of cockatiels, cross reactivity of different cell surface markers from other species of mammals was tested in advance.

3.15.1. Preparation of tissue sections

The same formalin-fixed and paraffin-embedded tissues that were used for demonstration of ABV antigen were applied.

3.15.2. Controls

Formalin-fixed and paraffin-embedded tissue sections of feline B-cell lymphoma and feline T-cell lymphoma were used as positive control. Moreover, formalin-fixed and paraffin-embedded normal chicken spleen, normal chicken bursa, feline lymph node were also used. For monoclonal antibodies, mouse anti-chicken T cells (T1) (Hirschberger et al., 1987) was applied. Serum of healthy rabbit was centrifuged at 1500 g for 10 minutes and served as negative control for polyclonal antibodies.

3.15.3. Primary antibodies, secondary antibodies, and blocking procedures

They are listed in table 8, 9 and 10.

3.15.4. Antigen retrieval

Citrate buffer, proteinase, and target retrieval methods were applied as in table (8, 9, and 10).

Table 8: List of tested T cell markers

Primary antibodies		Secondary antibodies		Substrate	Antigen retrieval	Blocking
Description	**Dilution**	**Description**	**Dilution**	**Antibody**		
Rabbit-anti-human CD3 Dako, Germany	1:100 in 20 % pig serum/TBS	Pig anti-Rabbit IgG, Dako, Germany	1:100 in 20 % pig serum/TBS	Rabbit peroxidase anti-peroxidase (PAP) Dianova, Germany	target retrieval pH 9 Dako, Germany	20 % pig serum in TBS, Sigma Aldrich, Germany
Rat anti-human CD3 Biorad, Germany	1:100 in 20% pig serum/TBS	Pig anti-Rabbit IgG, Dako, Germany	1:100 in 20 % pig serum/TBS	Avidin biotin complex (ABC) Kit Vector,USA	citrate buffer pH 6.5	20 % pig serum in TBS, Sigma Aldrich, Germany

(ABC) avidin biotin complex, (PAP) peroxidase anti peroxidase. Target retrieval at 97 °C for 25 minutes, citrate buffer at 95 °C for 25 minutes.

Table 9: List of tested macrophage markers

Primary antibodies		Secondary antibodies		Substrate	Antigen retrieval	Blocking
Description	**Dilution**	**Description**	**Dilution**	**Antibody**		
Myeloid histiocyte antigen, clone MAC 378, Dako, Germany	1:1000 in 1% BSA/TBS Sigma Aldrich , Germany	Rat anti-mouse IgG, Dianova, USA	1:100 in 1% BSA/TBS	Mouse PAP Dianova, USA	proteinase pH 7.4 Sigma Aldrich , Germany	10 % rat serum in TBS, Sigma Aldrich , Germany
Rabbit anti human lysosome, Dako, Germany	1:600 in 20 % pig serum / TBS	Pig anti-rabbit IgG, Dako, Germany	1:100 in 20 % pig serum/TBS	Rabbit PAP Dianova, USA	proteinase pH 7.4 Sigma Aldrich , Germany	20 % pig serum in TBS, Sigma Aldrich, Germany
Mouse anti-chicken monocytes, KUL01, Biorad , Germany	1:200 in 1% BSA/TBS	Pig anti-rabbit IgG, Dako, Germany	1:100 in 20 % pig serum/TBS	Elite ABC complex, Vector, USA	citrate buffer pH 6.5	20 % pig serum in TBS, Sigma Aldrich, Germany

(ABC) avidin biotin complex, (PAP) peroxidase anti peroxidase. Proteinase (type XXIV) at 37 °C for 5 minutes, citrate buffer at 95 °C for 25 minutes

Table 10: List of tested B cell markers

Primary antibodies		Secondary antibodies		Substrate	Antigen retrieval	Blocking
Description	Dilution	Description	Dilution			
Mouse anti-duck IgY , Biorad, Germany	1:100 in TBS	Biotinlynated goat anti-mouse IgG, Vector, USA	1:100 in 1% BSA/TBS	Mouse peroxidise anti-peroxidise (PAP) Dianova, USA	citrate buffer pH 6.5	20 % goat serum in TBS
Mouse anti-human CD20, DCS ImmunoLine, Germany	1:100 in 1% BSA/TBS	Biotinlynated horse anti-mouse IgG Vector, USA	1:100 in 1% BSA/TBS	Mouse PAP Dianova, USA	citrate buffer pH 6.5	10 % rat serum in TBS
Rat anti-feline CD45, clone B220 Cedarlane,USA	1:1000 in 1% BSA/TBS	Biotinlynated rabbit anti-rat IgG (H+L) Vector, USA	1:100 in 1% BSA/TBS	ABC Kit, Vector, USA.	citrate buffer pH 6.5	horse serum Dako, Germany
Mouse anti-dog IgG, Dianova, USA	1:600 in 20% pig Serum in TBS	Pig anti rabbit IgG1 Dako, Germany	1:100 in 20% pig serum in TBS	Rabbit PAP Dianova, USA	proteinase pH 7.4 Sigma, Germany	20 % pig serum in TBS,
Mouse anti-human MUM1 protein, Dako, Germany	1:100 in 1% BSA/TBS	Pig anti rabbit-IgG1, Dako, Germany	1:100 in 20% pig serum in TBS	Mouse PAP Dianova, USA	citrate buffer pH 6.5	20 % pig serum in TBS, Dako, Germany
Mouse anti-CD79α , clone JBC117 Dako, Germany	1:50 in 1% BSA/TBS	Biotinlynated horse anti-mouse IgG, Vector, USA	1:100 in 1% BSA/TBS	ABC complex Vector, USA	target retrieval Dako, Germany	undiluted horse serum
Mouse anti CD79a cy, clone HM 57, Acris,Germany	1:100 in 1% BSA/TBS	Biotinlynated horse anti-mouse IgG, Vector, USA	1:100 in 1% BSA/TBS	ABC complex	citrate buffer pH 6.5	undiluted horse serum

(H+L) heavy and light chain antibody, (MUM-1 protein) multiple myeloma oncogene 1. (ABC) avidin biotin complex, (PAP) peroxidase anti peroxidase. Proteinase (type XXIV) at 37 °C for 5 minutes, citrate buffer at 95 °C for 25 minutes, target retrieval at 97 °C for 25 minutes

2.15.5. IHC protocol for characterization of the immune cells in cockatiels after ABV-2 and ABV-4 infection

IHC protocol was applied as mentioned in paragraph (3.14.5) except of the following different steps.

1. Antigen retrieval was performed as given in table 8, 9, and 10 at 95 °C for 25 minutes followed by cooling for 10 minutes at room temperature.
2. For blocking, 100µl diluted blocking solution was applied onto each slide (see table 8, 9, and 10).
3. A 100µl diluted primary antibodies were applied (table 8, 9, and 10). Tissue sections were subsequently incubated in the refrigerator at 4 °C overnight.
4. A 100µl diluted secondary antibody was applied (table 8, 9, and 10). Tissue sections were subsequently incubated for 30 minutes at room temperature.
5. Avidin biotin complex (ABC) and peroxidise anti peroxidise (PAP) methods were used as listed in table 8, 9, and 10 and 100µl of ABC Vectastain kit® (Vector laboratories Inc, USA), diluted 1:100 in 1% BSA/TBS was applied.

3.16. Generating the ABV-2 and ABV-4 RNA specific probes for the ISH

3.16.1. Generating the ABV-2 specific oligonucleotide probes

In order to design hybridization probes specific for ABV-2 N gene, ABV-2 N gene sequence (accession number at Genbank: GQ850506.1) was used. Using primer-BLAST, we designed primers suitable for amplification of a fragment 230 bases in length (table 11). The exact location of the primers in the sequence chosen are 706 to 726 (forward primer) and 915 to 935 (reverse primer). The sequence from position 706 to position 935 was used for the design of two oligonucleotides (accession number: GQ850501.1) as shown in (**Fig. 1).** The sequence of oligonucleotides 1 is identical to 706-826 bases (table 12). Oligonucleotides 2 are homologous to 800-935 bp of the ABV-2 N but oligonucleotides 2 have the reverse complementary sequence (table 12). Both oligos overlap by 20 bases. A PCR was performed (tables 13 and 14). In the first cycle, oligo1 and oligo2 annealed at the overlapping region and the polymerase extended both oligos producing a double stranded template. This template was subsequently amplified using the forward and reverse primers. This amplicon was subsequently ligated into PCR 4.0 TOPO vector (Invitrogen, Germany). After ligation, amplification of the ligated DNA was performed by PCR. After amplification of the ligated DNA, the obtained PCR products were used as template for producing sense probe (**Fig. 2**) and antisense probe (**Fig. 3**) by in vitro transcription. Because of the location of the promoter for T7 polymerase between the annealing sites for primer M13-F and the annealing site for primer ABV-2 N-R, the sense RNA transcript was produced transcripts by T7 polymerase (**Fig. 2**). Because of the location of the promoter for T7 polymerase between the annealing sites for primer M13-F and the annealing site for primer ABV-2 N-F, the antisense RNA transcript was generated transcripts by T7 polymerase (**Fig. 3**).

Fig. 1: Oligonucleotides used for generation of the ABV-2 specific probes

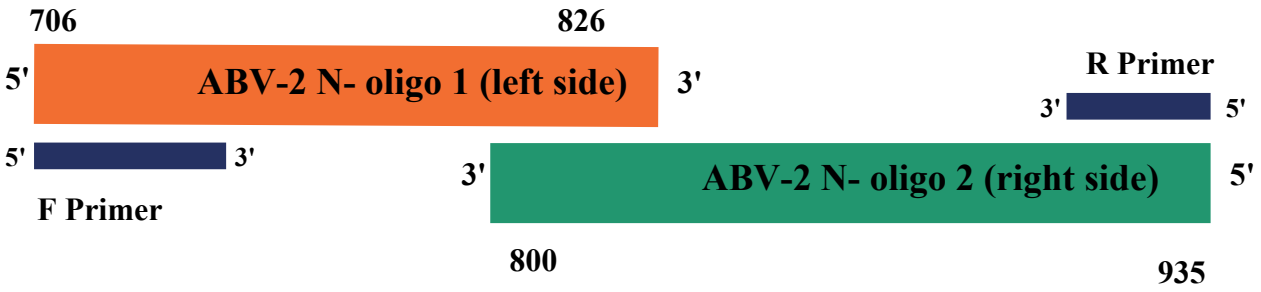

The amplification reaction of the ABV-2 N oligonucleotides is listed in table 17. PCR conditions are demonstrated in the table 18. PCR was applied in PTC-200 peltier thermal cycler (Biozyme, Germany).

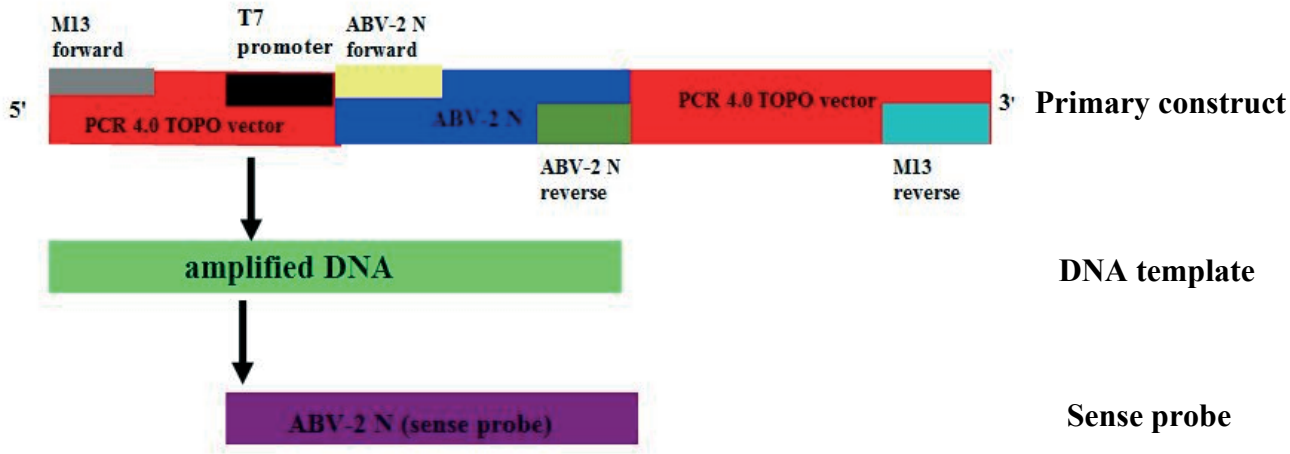

Fig. 2: Schematic diagram of generating of the ABV-2 N sense probe. PCR products containing ABV-2 N segments (primary construct) were used. From the primary construct (see above), amplified DNA was generated (green row) and used as a DNA template for in vitro transcription. From the template, the ABV-2 N sense probe was generated starting from T7 promoter till ABV-2 N reverse priming sites (violet row).

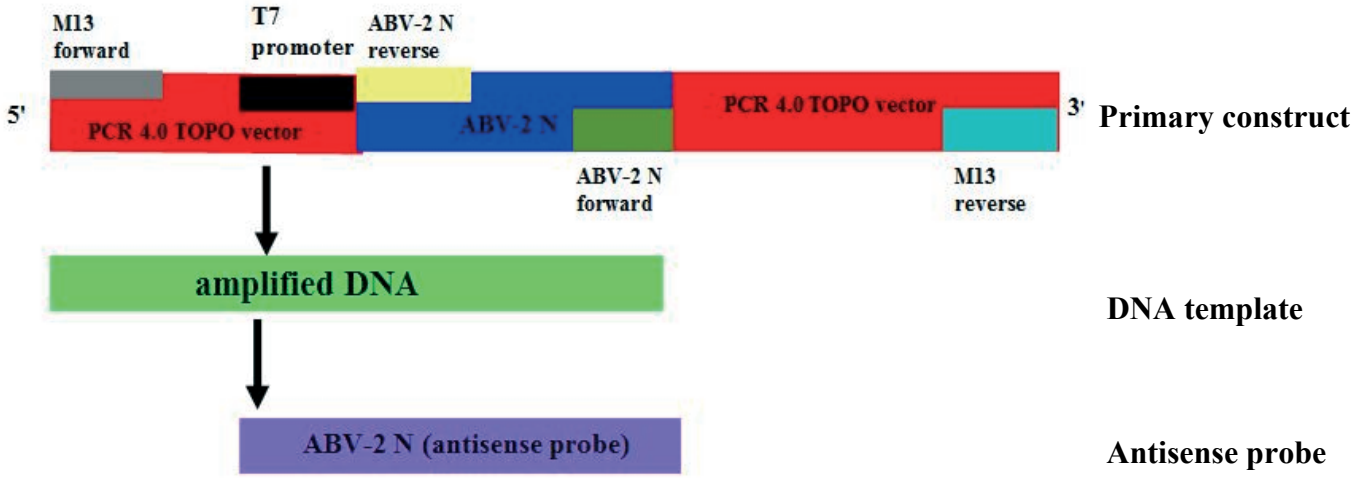

Fig. 3: Schematic diagram of generating of the ABV-2 N antisense probe. PCR products containing ABV-2 N segments (primary construct) were used. From the primary construct (see above), amplified DNA was generated (green row) and used as a DNA template for in vitro transcription. From the template, the ABV-2 N antisense probe was generated starting from T7 promoter till ABV-2 N forward priming sites (violet row).

Table 11: Sequences and orientation of the specific ABV-2 N gene primers

Primers	Sequence (5'->3')	Length (bases)
ABV-2-N-F	5′-ATGCCACACTGACAATCCCG-3′	20
ABV-2-N-R	5′-TAGCCGGCCATTGTTGGATT -3′	20

F= forward, R= reverse

Table 12: Sequences of the ABV-2-N oligonucleotides

Oligonucleotides of ABV-2 N	Sequence (5'->3')
Oligo 1 (left side)	acattgacaatcccggccgtagcacttgaaattaaggagttcctagatgtaactacaaagctaaagg cagagcatggggacatgtttaaatatcttggtgctattcgtcattccgacgcga
Oligo 2 (right side)	tgaaagccctggcaaagagtttatggatcagatcaaattagtggcagggtttgcacaaatgaccac atacacaacaatcaaagagtatctcaacgagtgtatggatgccacattgacaatcccggccgta

ABV-2-N oligonucleotides (designed using the accession number: GQ850501.1)

Table 13: Composition of the PCR-reaction for amplification of the ABV-2 N oligonucleotides

Reagent	Amount µl	Concentration
Sterile H_2O	13.4 µl	
Buffer containing $MgCl_2$ (complete buffer)	2.4 µl	10X concentrated
ABV-2-N-R	0.8 µl	10µM
ABV-2-N-F	0.8 µl	10µM
dNTP	0.4 µl	0.2 mM
BioTherm™ DNA-Polymease (Thermo Scientific, Germany)	0.2 µl	5U/µl
Oligo 1- ABV-2 N- left side (DNA) (Biomers, Germany)	1µl	10µM
Oligo 2-ABV-2 N-right side (DNA) (Biomers, Germany)	1 µl	10µM
Total volume per reaction	20 µl	

F= forward, R= reverse, µM= micromolar, U/µl= unit per microliter, mM= millimolar

Table 14: Conditions of the PCR-reaction using ABV-2 N oligonucleotides

Reaction	Time	Temperature in °C	Cycles
Initial denaturation	120 seconds	94 °C	
Denaturation	15 seconds	94 °C	35 cycles
Annealing	30 seconds	50 °C	
Extension	60 seconds.	72 °C	
Final extension	10 minutes	72 °C	
Cooling	∞	4°C	

3.16.1.1. Visualization of PCR products by gel electrophoresis

PCR products were analyzed by gel electrophoresis. 2% agarose (Biozyme, Germany) in 0.5x tris base, boric acid and ethylenediaminetetraacetic acid (TBE) buffer was used. Gel electrophoresis protocol was carried out as follows:

1. Weigh 0.6 g agarose powder (Biozym, Germany) and add it to beaker.
2. Add 30 ml (0.5x) TBE buffer to the flask.
3. Melt the agarose on hot plate until the solution becomes clear. Heat the solution from 150°C up to 200°C until it boils.
4. Add 1µl Midori-green dye (Nippon Genetics Europe GmbH, Germany), diluted 1:10 to the agarose solution.
5. Pour the melted agarose solution into the casting tray and let cool until it becomes solid.
6. Let the solution cool at room temperature for 30 minutes or in refrigerator for 15 minutes.
7. Add enough 0.5x TBE buffer over the gel.
8. Add 1µl of 6X orange DNA loading dye (Thermo Scientific, Germany) to each 5µl PCR-reaction.
9. In a separate well, add 3.5µl pUC Mix Marker, 8 (MBI Fermentas, Germany).
10. Carefully pipette mixture of each sample into separate wells in the gel.
11. Turn on the power supply 6 volt/cm electrodes distance for one hour.
12. Observe the PCR products through UV light with a transilluminator (Bachhofer Laboratories, Germany) with 254 nm wave length.

3.16.1.2. Purification of DNA

Amicon Ultra Centrifugal filters (Merck, Germany) were used to purify PCR products. The purification protocol was performed according to the manufacturer. Concentration of the DNA was measured by Nanodrop®2000 spectrophotometer (Thermo scientific GmbH, Germany). The purified DNA was stored in a centrifuge tube at -20°C.

3.16.1.3. Ligation of PCR products into PCR TOPO 4 TA® Vector

The TOPO TA cloning kit (Life Technologies, Germany) was used to ligate two DNA fragments. The first DNA is the amplified DNA strand which has identity to the ABV-2 N gene sequences. The second DNA is the PCR 4.0 TOPO vector. PCR 4.0 TOPO vector contains the M13-F and M13-R priming sites. The components of the ligation reaction are listed in table 15.

Table 15: Composition of the TOPO® ligation reaction

Reagent	amount in µl	Concentration
Fresh PCR product	3 µl	112 ng/µl
5X T4 DNA ligase reaction buffer	1 µl	
Sterile H_2O	2 µl	
PCR 4.0 TOPO® vector	1 µl	25 ng/µl
Final volume	7 µl	

PCR products (amplified ABV-2-N segments), ng/µl= nanogram per microliter, µl= microliter

The protocol of the TA ligation reaction was performed according to the instructions of the manufacturer. The TA TOPO® reaction was placed on ice for 2 minutes and then stored at -20 °C.

3.16.1.4. Polymerase chain Reaction (PCR)

We used QIAGEN Multiplex PCR Kit (Qiagen, Germany) to generate the template for the ABV-2 N probes. Insert-specific primers (ABV-2-N primers) were commercially produced by (Biomers, Germany). The PCR was carried out in PTC-200 Peltier thermal cycler (MJ Research, Canada). The composition of the PCR reaction is stated in table 16 and the conditions of the PCR are listed in table 17.

Table 16: Composition of the PCR-reaction

Reagent	Amount µl	Concentration
Sterile H_2O	13.2 µl	
Multiplex-master mix (MM) (Qiagen®, Germany)	15 µl	2 X concentrated
M13-F + ABV-2-N-R **OR**	0.8 µl	10µM
M13-F+ ABV-2-N-F	0.8 µl	10µM
Ligated DNA containing ABV-2-N gene fragments	1 µl	10µM
Total volume per reaction	30 µl	

F= forward, R= reverse, µM= micromolar, µl= microliter

Table 17: Conditions of the PCR-reaction

Reaction	Time	Temperature in °C	Cycles
Initial denaturation	120 seconds	94 °C	
Denaturation	15 seconds	94 °C	35 cycles
Annealing	30 seconds	55 °C	
Extension	60 seconds.	72 °C	
Final extension	10 minutes	72 °C	
Cooling	∞	4°C	

3.16.1.5. Purification of PCR products

PCR products were cleaned by Amicon Ultra Centrifugal filters (Merck, Germany) and protocol of the purification was performed according to the instructions of the manufacturer.

3.16.1.6. In vitro transcription

DIG-RNA labeling kit (Roche, Germany) was used for this purpose. For initiation of in vitro transcription, T7 RNA polymerase was added to generate the sense and anti sense orientated ABV-2 RNA probes (table 18). For generating the sense probe, the T7 RNA polymerase was added to PCR products (DNA template) and the transcription started from T7 promoter until ABV-2 N-R priming sites (**Fig. 2**). For synthesis of the antisense RNA probe, the T7 RNA polymerase was added to PCR products (DNA template) and the transcription started from T7 promoter until ABV-2 N-F priming sites (**Fig. 3**). The sense orientated probe is detecting ABV-2 genome while antisense probe is targeting ABV-2 mRNA. After producing of the probes, probes were kept at -80 °C until use. In vitro transcription reaction was prepared as given in table 22. For generating of the ABV-2 probes, we employed the same protocol for the in vitro transcription as mentioned (**3.16.1.5.1.**). The components of the in vitro transcription reaction are listed in table 18.

Table 18: In vitro transcription reaction for generating the ABV-2 probes

Components	Amount in µl	Concentration
Sterile H_2O	12 µl	
10x transcription buffer	3 µl	10 times concentrated
10x NTP Labelling Mix	2 µl	10 times concentrated and containing (10 mM ATP,10 mM CTP,10mM GTP,6.5 mM UTP,3.5 mM DIG-11-UTP)
Ribolock RNase inhibitor (Fermentas, Germany)	1 µl	40 U/µl
PCR product (ABV-2-N)	10 µl	85 ng/µl
T7 RNA polymerase	2 µl	20 U/µl
Total	30 µl	

NTP= nucleotides triphosphate, µl= microliter, ng/µl= nanogram per microliter, U/µl= units per microliter, mM= millimolar

3.16.1.7. In vitro transcription protocol

1. Add the components of the in vitro transcription (table 14) in order to 500 µl microfuge tube on ice.
2. Mix the reagents of the in vitro transcription gently and spin down.
3. Incubate the mixture on Accu Block™ Mini heat block (Labnet International, Germany) at 37°C for 2 hours.
4. Add 2µl DNAse I (10 units/µl). Vortex, centrifuge, and incubate for 15 minutes at 37°C on heat block.
5. Add 2µl of (0.2M) ethylenediaminetetraacetate (EDTA), vortex and spin down.
6. Add 2.5µl of 4M lithium chloride, vortex and spin down.
7. Add 75µl of 98% ethanol, vortex and spin down. Then store it at -20 °C overnight.
8. At the second day, centrifuge the mixture at 14,000 g for 15 minutes.
9. Remove supernatant and wash the pellet with aliquots of 50µl of 70% ethanol, vortex and spin down.
10. Centrifuge the mixture 14,000 g at 4 °C for 5 minutes.
11. Remove supernatant and let the pellet to dry for 10 minutes.
12. Add 100 µl of bi-distilled DEPC treated water, then mix, vortex and spin down.

13. Add 1 µl of RNase inhibitor to the mixture and mix it.

14. Aliquot the 100 µl into eppendorfs (10µl pro eppendorf) and store it at -80°C freezer until use.

3.16.2. Generation of ABV-4 specific riboprobes

3.16.2.1. Sequencing of the DNA plasmid carrying the ABV-4 N segment

Cloned DNA carrying the ABV-4 N gene sequences had been generated by a former doctoral study (Saskia Ressmeyer) using the PCR4® TOPO vector (Invitrogen, Germany). The cloned DNA was commercially sequenced by GATC (Biotech AG, Germany) and analyzed by Blast (Zhang et al., 2000; Morgulis et al., 2008). The inserted sequence was complimentary to the ABV-4 N segment (isolate 16) (accession number: GQ496360.1) with a homology of 100% for the respective ABV-4 N segments and therefore suitable for generating the ABV-4 riboprobes (**Fig. 4 and 5**).

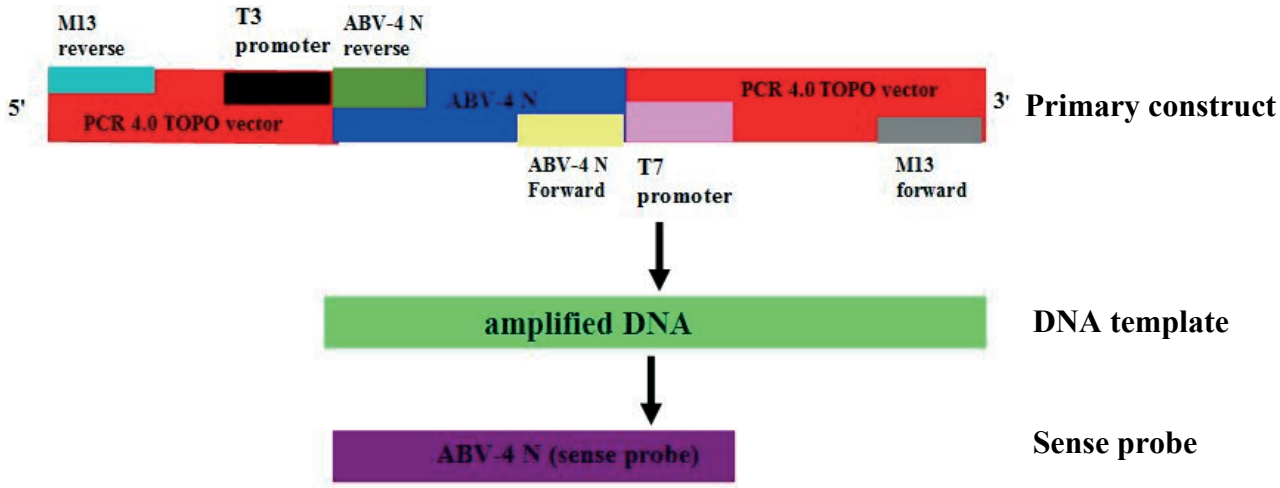

Fig. 4: Schematic diagram of generating of the ABV-4 N sense probe. From the primary construct (see above), amplified DNA was generated (green row) and used as a DNA template for in vitro transcription. From the template, the ABV-4 N sense probe was generated starting from T7 promoter till ABV-4 N reverse priming sites (violet row).

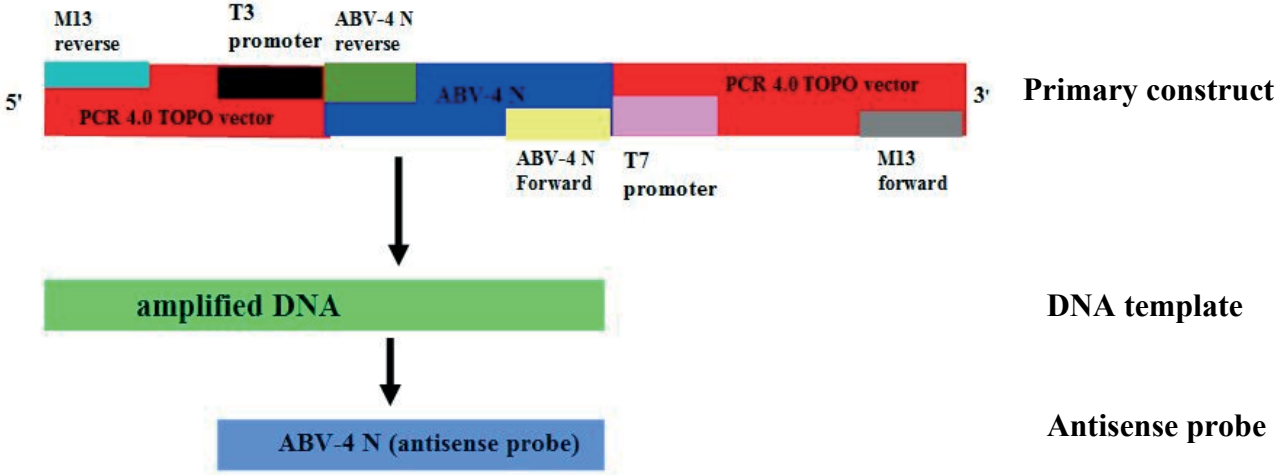

Fig. 5: Schematic diagram of generating of the ABV-4 N antisense probe. From the primary construct (see above), amplified DNA was generated (green row) and used as a DNA template for in vitro transcription. From the template, the ABV-4 N antisense probe was generated starting from T3 promoter till ABV-4 N forward priming sites (blue row).

3.16.2.2. Amplification of the plasmid DNA carrying the ABV-4 N segment by PCR

The PCR 4.0 TOPO vector primers (M13 primers) were commercially synthesized by Invitrogen GmbH, Germany while insert-specific primers (ABV-4 N primers) were commercially produced by Metabion International GmbH AG, Germany. PCR was carried out in a PTC-200 peltier thermal cycler (MJ research, Canada). The primers sequences, orientation and sizes are given in table 19. Composition and conditions of the PCR reaction are stated in table 20 and 21.

Table 19: Sequences and orientation of the insert-specific and vector primers

Primer	Base sequences	Length (Bases)
ABV-4-N-F	5'-CATGAGGCTATWGATTGGATTA- 3'	20
ABV-4-N-R	5'-TAGCCNGCCMKTGTWGGRTTYT-3'	25
M13-F	5' -TGTAAAACGACGGCCAGT-3'	20
M13-R	5' -CAGGAAACAGCTATGACC-3'	20

F= forward, R= reverse

Table 20: Composition of the PCR-reaction

Reagent	Amount µl	Concentration
Sterile H_2O	18.7 µl	
Buffer containing $MgCl_2$ (complete buffer)	2.5 µl	10X concentrated
M13-F+ ABV-4-N-R **OR**	2 µl	10µM
M13-R+ ABV-4-N-F	2 µl	
dNTP	0.5 µl	10µM
BioTherm™ DNA-polymease (Thermo Scientific, Germany)	0.3 µl	5U/µl
cloned DNA	1 µl	140 ng/µl
Total volume per reaction	25 µl	

F= forward, R=reverse, µl= microliter, µM= micromolar, U/µl= unit per microliter, ng/µl= nanogram per microliter

Table 21: Conditions of the PCR-reaction

Reaction	Time	Temperature in °C	Cycles
Initial denaturation	120 seconds	94 °C	
Denaturation	15 seconds	94 °C	35 cycles
Annealing	30 seconds	55 °C	
Extension	45 seconds	72 °C	
Final extension	10 minutes	72 °C	
Cooling	∞	4°C	

3.16.2.3. Visualization of PCR products by gel electrophoresis

The same gel electrophoresis protocol for visualization was used as shown previously **(3.16.1.1.)** with pUC Mix, 8 (MBI Fermentas, Germany) as marker.

3.16.2.4. Purification of DNA

Amicon Ultra Centrifugal filters (Merck, Germany) were applied to clean PCR products. The purification protocol was performed according to the instructions of the manufacturer.

3.16.2.5. In vitro transcription

For in vitro transcription, PCR products generated by the standard plasmid-specific primers M13 forward and M13 reverse in conjunction with one insert specific primer each were used. The amplificates contain promoters for the binding sites for the T7 and T3 RNA polymerase. Digoxigenin (DIG) RNA labeling kit (Roche, Germany) was used to produce DIG–labeled ABV-4 riboprobes. For initiation of the in vitro transcription, T7 or T3 RNA polymerase were added (table 22). For generating the sense orientated RNA probe, the T7 RNA polymerase was added to PCR products (DNA template) and the transcription started from T7 promoter until ABV-4 N-R priming sites (**Fig. 4**). For synthesis of the antisense RNA probe, the T3 RNA polymerase was added to PCR products (DNA template) and the transcription started from T3 promoter until ABV-4 N-F priming sites (**Fig. 5**). The sense orientated probe is detecting ABV-4 genome while antisense probe is targeting ABV-4 mRNA. After producing of the probes, probes were kept at -80 °C until use. The components of the in vitro transcription reaction are listed in table 22.

Table 22: The in vitro transcription reaction for generating the ABV-4 probes

Components	Amount in µl	Concentration
Sterile H_2O	12 µl	
10x transcription buffer	3 µl	10 times concentrated
10x NTP Labelling mix	2 µl	10 times concentrated and containing (10 mM ATP,10 mM CTP,10 mM GTP, 6.5 mM UTP,3.5 mM DIG-11-UTP)
Ribolock RNase inhibitor (Fermenta, USA)	1 µl	40 U/µl
PCR product	10 µl	60 ng/µl
T7 RNA polymerase **OR**	2 µl	20 U/µl
T3 RNA polymerase	2 µl	20 U/µl
Total	30 µl	

µl= microliter, U/µl= unit per microliter, ng/µl= nanogram per microliter, mM= millimolar

3.16.2.6. In vitro transcription protocol

We used the same in vitro transcription protocol that applied to generate ABV-2 probes as mentioned in **(3.16.1.7.)**.

3.17. Determination of digoxigenin labeling of the probes

Spot test was applied to quantify and estimate the efficiency of the labeling of the ISH riboprobe with digoxigenin (DIG). Serial dilutions of the respective riboprobes were applied on positive charged Zeta-Probe GT membrane (Biorad, Germany). Labeled control RNA (100ng/µl, 760 base pairs, it contains 10µg DIG) was used as a standard for comparison with sense and antisense riboprobes. Labeled control RNA was provided with the in vitro transcription kit (Roche, Germany). Quantification of the labeling of the respective probe was performed as follows:

1. Apply 2µl of eight different dilutions in DEPC-H_2O of the DIG-labeled probe and labeled control to Zeta-Probe GT membranes (Biorad, Germany).
2. Dry the membrane at room temperature, fix nucleic acid to the membrane by cross linking with UV light at 125 millijoules for 1 minute.
3. Incubate membrane 1 minute in 1xPBS at room temperature.

4. Background blocking: per 1.2 ml sterile neutral sheep serum and 1.8 ml of 10 % triton-X 100 (Sigma Aldrich, Germany), add 57 ml of buffer 1. Afterwards, incubate the membrane in the mixture for 30 minutes at room temperature.

5. For the immunological detection, incubate the membrane with the alkaline phosphatase (AP) conjugated anti-digoxigenin (Fab fragments) antibody (Roche, Germany) for two hours in a dark chamber. The antibody was diluted 1:300 in DEPC-H_2O.

6. Membrane washing: for 2x5 minutes in sterile 1xPBS.

7. For the colorimetric detection of the AP activity, dissolve 15 mg of levamisole in 50 ml buffer 3 and then add 250µl of Nitroblueteterazolium (NBT) (Sigma Aldrich, Germany), 200µl of 5-bromo-4-chloro-3-indolyl-phosphate X-Phosphate (BCIP) (Sigma Aldrich, Germany) to the solution respectively. Incubate the membrane in the staining solution for 30 minutes at room temperature.

8. The working concentration of NBT was 75mg/ml while the working concentration of BCIP was 50mg/ml. NBT was diluted in 70% dimethylformamide while BCIP was diluted in 100% dimethylformamide.

9. Membrane washing was performed for 2 x 5 minutes in sterile 1xPBS.

10. The intensity of the colour reaction of the labeled control RNA was compared with the DIG-labeled probe in different dilutions.

3.18. In situ hybridization (ISH)

ISH was used to detect the ABV-2 and ABV-4 RNA in paraffin embedded tissue sections of all experimentally ABV-2 and ABV-4 infected birds.

3.18.1. Controls

A brain and GIT tissue sections from ABV-2 experimentally infected cockatiel were used as a positive control. In parallel, we prepared a negative control for each slide where the ABV-2 or ABV-4 riboprobes were not added but only hybridization mix.

3.18.2. Evaluation the positive signals for ISH probes

Presence of intranuclear hybridization signals are considered as positive reaction for the genomic RNA while intranuclear and/or intracytoplasmic hybridization signals are considered as positive reaction for the mRNA of the virus.

3.18.3. DIG-labeled riboprobes

We used ABV-2 and ABV-4 probes for the ISH as presented in Fig 1, 3 and 4. Each 5µl of each DIT-labeled riboprobes was diluted in 100µl hybridization mix. Concentration of the

ABV-2 and ABV-4 riboprobes was measured by Nanodrop®2000 spectrophotometer (Thermo scientific GmbH, Germany). The 40µl diluted probe was added onto each slide.

3.18.4. Preparation of paraffinized tissue sections

Tissue sections were cut into 5µm by microtom, mounted on positively charged Super Frost Plus slides (Thermo Scientific, Germany) and adhered to the slide by baking at 60°C for approximately 30 minutes. Tissue sections were not employed for in situ hybridization technique before drying at room temperature for at least 24 hour to ensure that the tissue was well adhered to the slide and to avoid loss of tissue during the hybridization process.

3.18.5 Evaluation of ABV-2 and ABV-4 RNA distribution pattern

For evaluating the distribution of the ABV-2 RNA and ABV-4 RNA, we used the same semi quantitative scores which were shown in table 7.

3.18.6. ISH protocol

1. Deparaffinizing tissue sections was carried out by immersing them in xylene (3 times changes, 5 minutes each).
2. Dehydration of tissue sections was carried out by immersing through series of alcohol concentrations: 98% isopropanol, 96% ethanol, 70% ethanol (once, 5 minutes each), followed by washing in bi-distilled DEPC treated water (2 times, for 5 minutes), and in sterile 1xPBS (once, for 5 minutes).
3. To obtain better penetration of the probe in tissue sections, tissue sections were washed in 2M HCl for 20 minutes at room temperature.
4. Washing in 2 x standard saline citrate (SSC) +5 mM EDTA-Na_2 (see annex) at 50 °C for 30 minutes twice.
5. For proteolysis, tissue sections were incubated with RNase free Proteinase K (Carl Roth GmbH, Germany) at 37 °C for one hour. Proteinase solution composed of (1ml 1M tris, pH8; 1ml 0.1M $CaCl_2$, and 60ml bi-distilled water treated with DEPC) for each glass cuvette. A 6µl of RNase free Proteinase K (5µg/ml) was added to 60 ml the proteinase solution in each glass cuvette. The working concentration of proteinase K was 10 mg/ml.
6. To stop the reaction, tissue sections were incubated with 0.2 % glycine-PBS for 5 minutes at room temperature.
7. Post-fixation was carried out in 4% paraformaldehyde (PFA) / 1xPBS for 4 minutes at room temperature.
8. Tissue sections were washed in 1xPBS for 1 minute twice and subsequently washed in 1xPBS+5 mM $MgCl_2$ for 15 minutes at room temperature.

9. Acetylation of tissue sections in 0.25% acetanhydride in 0.1M triethanolamine-DEPC-H_2O, pH 7.5 for 10 minutes at room temperature.

10. Tissue sections were washed in 1xPBS for 1 minute twice and then washed in 1xPBS for 15 minutes once at room temperature.

11. Prehybridization step was carried out by incubation of tissue sections with prehybridization mix (PHB-Mix) for at least one hour at 52 °C (see annex of preparation of PHB-Mix). For each 49,5ml prehybridization mix (PHB-Mix), 0.5ml sodium salts DNA (ssDNA) from calf liver type IV (Sigma Aldrich, Germany), and 1.25ml RNA stocks solution (Sigma Aldrich, Germany) was added (see annex).

12. Hybridization was performed by adding 40µl of the DIG-labeled probed on each slide. Slides were covered with Gel Bond® Film (Biozym, Germany), sealed with Fix-o-gum ® glue (Marabau, Germany). Slides were transferred to a humid chamber and were incubated at 52 °C in the oven overnight.

13. After removing the Gel Bond® Film and Fix-o-gum ® glue from slides, post hybridization was carried out by washing tissue sections in 6xSSC+45 % formamide at 42 °C for 15 minutes twice and in 2xSSC for 5 minutes at room temperature twice.

14. Tissue sections were incubated with RNAse solution (see annex) for 30 minutes at 37 °C

15. Washing of tissue sections in 2xSSC twice for 5 minutes at room temperature followed by second washing in 0.2 x SSC for 15 minutes at 45 °C twice.

16. Washing in buffer 1 (see annex) for 1 minutes once at room temperature.

17. Washing in buffer 2 (blocking solution) (see annex) for 30 minutes at room temperature.

18. Tissue sections were incubated with anti-DIG antibody (Roche GmbH, Germany) solution for 2 hours in a humified champer at RT in the dark. Two parallel lines were encircled around area of the tissue on each slide by PAP-Pen (Dako, Germany). A 300µl anti-DIG antibody solution was added to each slide.

19. Washing in buffer 1 (see annex) for 15 minutes twice at room temperature.

20. Washing in buffer 3 (see annex) for 2 minutes once at room temperature.

21. Tissue sections were incubated with NBT/BCIP staining solution (see annex) in humified and dark environment for 18 hours at room temperature.

22. The reaction of staining solution was stopped by washing of tissue sections in buffer 4 for 10 minutes at room temperature in dark twice.

23. Tissue sections were washed with bi-distilled water for 2 minutes twice followed by washing in tap water for 2 minutes at room temperature twice.

24. Tissue sections were mounted with Kaiser glycergel mounting medium (Merck, Germany) and then cleaned for examination under light microscope (Nikon, Germany).

3.19. Cultivation of cockatiel blood cells

3.19.1. Collection of blood samples

Blood samples from the right jugular vein of healthy cockatiel were collected to demonstrate the isolation procedure. According to the permission number (499-M), blood samples were obtained directly after euthanization. Insulin syringe 0.5ml with 30 gauge needle (Braun, Germany) and heparinized micro tubes containing of 35 I.U lithium heparin/ml blood (Sarsted, Germany) were used to collect blood samples.

3.19.2. Isolation of buffy coat (BC) cells from healthy cockatiels

BC cells are white blood cells and thrombocytes. BC cells were prepared by centrifugation of the diluted blood at 3000 rpm for 15 minutes at room temperature. After that, we obtained three distinct layers, a layer of plasma lying in the top, a layer of red blood cells (RBC) located in the bottom, and a thin layer in between which represents the BC. BC cells contains of most of white blood cells and thrombocytes.

3.19.2.1. Protocol of isolation of BC cells from whole blood

The isolation the BC cells from the cockatiel blood was performed as follows:

1. A 0.5ml blood sample was diluted in 2ml sterile 1xPBS and placed into sterile conical glass test tube.
2. Heparinised blood samples were centrifuged by Rotina 48RC (Hettich,Germany) at 3000 rpm for 15 minutes between 18-20°C.
3. After 15 minutes, BC were gently collected and transferred to a new conical sterile glass test tube.
4. BC cells then washed in 9 ml sterile 1xPBS and centrifuged at 2500 rpm for 10 minutes twice in order to remove RBCs contamination.
5. BC cells were suspended in 3ml RPMI-1640 medium (PAA, Germany) and mixed by pipetting.
6. Resuspended BC cells were propagated in RPMI-1640 medium in 6 wells cell culture plate (Nunclon brand ^{TM} Surface, Germany).
7. A 50µl of cells were counted by using trypan blue assay under IX70 S8F inverted microscope (Olympus, USA).
8. RPMI-1640 culture medium for BC cells had to be changed every four days.

3.19.3. Isolation of mononuclear cells (MNC) from healthy chicken

Peripheral blood MNC are blood cells with a round shaped nucleus, such as monocytes, B-lymphocytes, T-lymphocytes and NK cells. Isolation of MNC from whole blood was performed through using density gradient Ficoll-Paque™ Premium (GE Healthcare, Germany) with a density 1.077g/ml. For characterization of the cockatiels immune cells by indirect immunofluorescence and by flow cytometry, chicken MNC served as positive control.

3.19.3.1. Protocol of separation of chicken MNC

Isolation of MNC was achieved as follows:

1. Sterile conical glass test tubes were prepared and 3.5ml Ficoll®Paque ™ premium was added into sterile conical glass test tubes.
3. A 2 ml blood sample was diluted into 2.5ml of sterile 1xPBS.
4. The diluted blood was carefully layered over Ficoll-Paque™ Premium.
5. Centrifuge at 3100 rpm for 15 minutes between 18-20°C.
6. After centrifugation, three layers were obtained, an upper layer (plasma), a lower layer in the bottom (erythrocytes), and an intermediate layer located represents the mononuclear cells.
7. MNC were pulled by sterile pipette and transferred to a clean glass test tube containing of 8 ml sterile 1xPBS.
8. Centrifuge at 2500 rpm for 15 minutes between 18-20°C to wash them twice to remove as much as possible of the contaminated RBC.
9. MNC pellets were suspended in sterile RPMI-1640 culture medium (PAA, Germany) containing 1% penicillin/streptomycin (PAA, Germany), gentamycine (PAA, Germany) and fetal calve serum (PAA, Germany).
10. Resuspended cells were propagated into 6 well tissue culture well plate (Sarsted Inc, USA) containing of 3 ml RPMI-1640 culture medium in each well.
11. A 50µl of MNC were counted by using trypan blue assay under IX70 S8F inverted microscope (Olympus, USA).
12. RPMI-1640 culture medium for MNC had to be changed every four days.

3.20. Characterization of the immune cells in BC cells of cockatiel

We employed two different methods to characterize the BC cells as follows:

1. Indirect immunofluorescence (IIF)
2. Flow cytometry (FC)

3.20.1. Characterization of cockatiels immune cells by (IIF)

After successful isolation of BC cells, it was important to recognize B lymphocytes, T lymphocytes, monocytes, thrombocytes, CD4 and CD8 cells sub populations in BC cells. Due to the lack of specific antibodies that recognize the immune cells in cockatiel, we tested the cross reactivity of the antibodies from other species of animals (table 23). Moreover, we tested antibodies generated specific for human, chicken, and duck immune cells (table 24). Respective positive controls were also used for each cell surface marker. Feline gastrointestinal tract tissue sections of feline B-cell lymphoma, feline T-cell lymphoma cell line, feline lymph node, normal chicken bursa, and normal chicken spleen were used as positive control.

3.20.1.1. Preparation and fixation of BC cells

After isolation the BC cells, we smeared 150µl BC cells on poly-L-lysine coated slides (R.Langenbrinck, Germany). Each smear contains at least 1000 cells. Smear was air dried for 20 minutes at room temperature. BC cells were fixed with ice cold 3% PFA for 15 minutes. PFA was diluted in sterile 1xPBS. An amount 100µl 3% PFA was added on each smear.

3.20.1.2. Blocking

We used 5% goat serum (Sigma-Aldrich, Germany), diluted in sterile 1xPBS.

3.20.1.3. Control

Chicken MNC served as positive control for recognizing CD4, CD8a, CD3 cells, B cells, monocytes and thrombocytes as given in table 24. Moreover, we prepared a negative control for each marker in which the primary antibody was not added.

3.20.1.4. Evaluation of the positive signals

We considered any cell having a collar-like staining around it as positive cell.

3.20.1.5. Primary and secondary antibodies

Primary and secondary antibodies are listed in table 23 and 24.

Table 23: List of antibodies tested for cross reactivity with cockatiels by IIF

Primary antibodies	Dilutions in 1xPBS	Secondary antibodies	Dilutions in 1xPBS	Blocking
Rabbit anti-human CD3, Dako, Germany	1:100 1:300 1:500	Cy3 conjugate goat anti-rabbit IgG (H+L) Dianaova, USA	1:50, 1:100, 1:200, 1:300	5% goat serum, diluted in 1xPBS
Mouse anti-human CD3, clone PC3, Dako, Germany	1:100 1:300 1:500	Cy3 conjugate goat anti-mouse IgG (H+L) Dianaova, USA	1:50, 1:100, 1:200, 1:300	5% goat serum, diluted in 1xPBS
Mouse anti-human CD3, clone F7.2.38, Dako, Germany	1:100 1:300 1:500 1:1000	Cy3 conjugate goat anti-mouse IgG (H+L) Dianaova, USA	1:50, 1:100, 1:200, 1:300	5% goat serum, diluted in 1xPBS
Rat anti-human CD45R, clone B220, Dako, Germany	1:100 1:300 1:500 1:1000	Cy3 conjugate goat anti-rat IgG (H+L), Dianaova, USA	1:50, 1:100, 1:200, 1:300	5% goat serum, diluted in 1xPBS
Rabbit anti-dog IgG2a, Dako, Germany	1:100 1:200 1:300 1:500 1:1000	Cy3 conjugate goat anti-rabbit IgG (H+L) Dianaova, USA	1:50, 1:100, 1:200, 1:300	5% goat serum, diluted in 1xPBS
Mouse anti-human CD79α cy, clone, HM 57, Dako, Germany	1:100 1:300 1:500 1:1000	Cy3 conjugate goat anti-mouse IgG (H+L) Dianaova, USA	1:50, 1:100, 1:200, 1:300	5% goat serum, diluted in 1xPBS
Mouse anti-human CD79α cy, clone, JBB117, Dako, Germany	1:100 1:300 1:500 1:1000	Cy3 conjugate goat anti-mouse IgG (H+L) Dianaova, USA	1:50, 1:100, 1:200, 1:300	5% goat serum, diluted in 1xPBS

(MNC) mononuclear cells, (PBS) phosphate buffer saline, (Cy3) cyanine 3 fluorescent conjugates dyes, maximal excitation wavelength of Cy3 dye (550 nanometer), maximal emission wavelength of Cy3 dye (570 nanometer), (H+L) heavy and light chain antibody.

Table 24: List of antibodies that applied to characterize the immune cells in cockatiel BC

Primary antibody	Dilution	Secondary antibody	Dilution	Blocking	Positive control
Rat anti-human CD3, clone CD3-12, Biorad, Germany	1:100 in sterile 1xPBS	Cy3 conjugate goat anti-rat IgG (H+L), Dianaova, USA	1:50 in sterile 1xPBS	5% goat serum, diluted in 1xPBS	chicken MNC
Mouse anti-chicken CD4, clone2-35, Biorad, Germany	1:100 in sterile 1xPBS	Cy3 conjugate goat anti-mouse IgG (H+L), Dianaova, USA	1:50 in sterile 1xPBS	5% goat serum, diluted in 1xPBS	chicken MNC
Mouse anti-chicken CD8a, clone 11-39, Biorad, Germany	1:100 in sterile 1xPBS	Cy3 conjugate goat anti-mouse IgG (H+L), Dianaova, USA	1:50 in sterile 1xPBS	5% goat serum, diluted in 1xPBS	chicken MNC
Mouse anti-duck IgY, clone14A3, Biorad, Germany	1:50 in sterile 1xPBS	Cy3 conjugate goat anti-mouse IgG (H+L), Dianaova, US	1:50 in sterile 1xPBS	5% goat serum, diluted in 1xPBS	chicken MNC
Mouse anti-chicken thrombocytes, clone 11C3, Biorad, Germany	1:200 in sterile 1xPBS	Cy3 conjugate goat anti-mouse IgG (H+L), Dianaova, USA	1:50 in sterile 1xPBS	5% goat serum, diluted in 1xPBS	chicken MNC
Mouse anti-chicken monocytes, clone KUL01, Biorad, Germany	1:50 in sterile 1xPBS	Cy3 conjugate goat anti-mouse IgG (H+L), Dianaova, USA	1:50 in sterile 1xPBS	5% goat serum, diluted in 1xPBS	chicken MNC

(MNC) mononuclear cells, (PBS) phosphate buffer saline, (Cy3) cyanine 3 fluorescent conjugates dyes, maximal excitation wavelength of Cy3 dye (550 nanometer), maximal emission wavelength of Cy3 dye (570 nanometer), (H+L) heavy and light chain antibody.

3.20.1.6. General protocol for detection of CD3, CD4, CD8a, B cells, monocytes, and thrombocytes

1. Cell pellets were prepared as a smear by placing 150µl BC cells on poly-lysine coated slides (R.Langenbrinck, Germany).
2. BC cells were air dried for 20 minutes then fixed in ice cold 3% PFA.

3. BC cells were washed in ice cold sterile 1xPBS twice.

4. BC cells were incubated with 5% goat serum (Sigma Aldrich, Germany) in sterile 1xPBS for 30 minutes at room temperature.

5. BC cells were incubated with the primary antibodies (listed in table 24), for one hour at RT.

6. BC cells were washed with sterile ice cold 1xPBS twice.

7. BC cells were incubated with the secondary antibodies (listed in table 24), in a humidified chamber for 1 hr at room temperature in the dark.

8. BC cells were washed in ice cold sterile 1xPBS twice in the dark.

9. BC cells were incubated with 1µg diamidino-2-phenylindole (DAPI) (Thermo Scientific, Germany) per 1ml 1xPBS for 10 minutes at room temperature in the dark.

10. BC cells were washed in ice cold sterile 1xPBS twice in the dark.

11. BC cells were rinsed in sterile distilled water once in the dark.

12. BC cells were mounted with few drops of Entallen mounting medium (Merck, Germany) and then coated with coverslip (Roth, Germany).

13. Slides were stored at 4°C in dark and examined under Nikon fluorescence microscope (Nikon, Germany).

3.20.2. Characterization of the cockatiel immune cells in BC by flow cytometry (FC)

To substantiate IIF results flow cytometry (FC) was also used to characterize cockatiel BC cells. We performed FC at the same day of isolation of BC cells. Flow cytometry experiments were performed in collaboration with Professor Carsten Staszyk, Institute of Veterinary Anatomy, Histology and Embryology, Justus-Liebig University-Giessen. Samples were analyzed by Acurri C6 Flow cytometer machine (BD Biosciences, Germany) immediately.

3.20.2.1. Preparation of cells

We prepared cell pellets from BC cells by centrifugation at 1500 rpm at room temperature. A 100µl 1xPBS was added to the cell pellet and mixed gently. Then, we added 100µl of BC cells suspension in each well of the 96 well plate (cell star®, Germany). Each 100µl cells suspension contains of 1×10^4 cells as assessed by trypan blue assay. Cell pellets were washed with 1xPBS twice to remove the culture medium followed by washing with washing buffer (WB) once. BC cells were not fixed with any fixative agents for the FC. We used live BC cells and we performed all steps of the FC experiment on ice.

3.20.2.2. Blocking

We used 5% goat serum (PAA, Germany), diluted in 1xPBS.

3.20.2.3. Washing

A 15 ml washing buffer (WB) was prepared to wash cells pellet.

3.20.2.4. Primary antibodies

The same primary antibodies that were applied in IIF (listed in table 24). For the FC protocol, the primary antibodies were diluted with sterile 1xPBS and 50µl diluted primary antibody was added to each well in the well plate as given in table 25.

Table 25: List of the primary antibodies

Primary antibody	Dilution
Rat anti-human CD3, clone CD3-12 , Biorad, Germany	1:100 in sterile WB
Mouse anti chicken CD4, clone2-35, Biorad, Germany	1:300 in sterile WB
Mouse anti chicken CD8a, clone 11-39, Biorad, Germany	1:200 in sterile WB
Mouse anti duck IgY, clone14 A3, Biorad, Germany	1:400 in sterile WB
Mouse anti chicken thrombocytes, clone 11C3, Biorad, Germany	1:600 in sterile WB
Mouse anti chicken monocytes, clone KUL01, Biorad, Germany	1:500 in sterile WB

(IgY) is a marker for B cells, (WB) washing buffer.

3.20.2.5. Secondary antibodies

We used allophycocyanin (APC) conjugated goat anti-rat IgG1 (BD Bioscience, Germany) as secondary antibody for anti-CD3 antibody, diluted 1:400 in sterile washing buffer. We employed polyclonal phycoerythrin (PE) conjugated goat anti-mouse (BD Bioscience, Germany) as a secondary antibody for the mouse derived antibodies, diluted 1: 600 in sterile washing buffer. A 50µl diluted secondary antibody was added to each well in the well plate.

3.20.2.6. Controls

Chicken MNC were used as a positive control for CD3, CD4, CD8a, B cells, monocyte and thrombocyte markers. We employed three different negative controls (negative control for the primary antibody where only the primary antibody was added to the BC cells, negative control for the secondary antibody where only the secondary antibody was added to the BC cells, and negative control for BC cells where no antibodies added). For discriminating between live and dead BC cells, we incubated BC cells with 7-aminoactinomycin D (7-AAD) dye (Biosciences, Germany) in one well of the 96 well plate. The 7-AAD will mark the non-viable cells by binding to the nuclei of dead cells. Before measurement, we added 2µl 7-AAD dye to the well containing BC cells only, mixed well, incubated for 10 minutes and then analysed.

3.20.2.7. Flow cytometry protocol

1. BC cells were propagated in 96 well plate (cell star®, Germany) and centrifuged by a universal 32 centrifuge (Hettich, Germany) at 1600 rpm at 4 °C for 5 minutes.
2. All samples were washed in sterile washing buffer WB and then centrifuged at 1600 rpm for 5 minutes at 4 °C.
3. Supernatant was discarded and BC cells were washed in sterile WB and then centrifuged 1600 rpm for 5 minutes at 4 °C.
4. Supernatant was discarded and an amount of 100µl of 5% goat serum was added in each well. BC cells were incubated with 5%goat serum/1xPBS for 20 minutes at 4°C in refrigerator.
5. Supernatant was then discarded and primary antibodies (see table 25) were added to each well. BC cells were incubated for 40 minutes in refrigerator at 4 °C.
6. BC cells are washed with sterile WB twice and then centrifuged at 1600 rpm for 5 minutes at 4 °C.
7. BC cells were washed with sterile WB three times and then centrifuged at 1600 rpm for 5 minutes at 4 °C.
8. Supernatant was discarded and then secondary antibodies (see table 25) were added. The well plate was incubated for 40 minutes at 4 °C.
9. Conical and round-bottom special tubes (BD Bioscience, Germany) were prepared and BC cells were suspended with 50µl sterile 1xPBS into FACS tubes.
10. FC measurement was performed by Acurri C6 software, threshold 10,000 events, BD flow cytometer machine (BD Bioscience, Germany).

3.21. Experimental infection of BC cells with ABV-4 one day post isolation

3.21.1. Preparation of BC cells

We isolated BC cells from healthy cockatiel. After isolation of BC cells, we counted BC cells by trypan blue assay. We centrifuged the BC cells at 2500 rpm for 5 minutes to obtain a cell pellet.

3.21.2. Infection with ABV-4

We used ABV-4 to infect BC cells. ABV-4 was provided by Dr. Sybille Herzog from the Institute of Veterinary Virology, Faculty of Veterinary Medicine, Justus-Liebig-University-Giessen and was obtained from infected quail fibroblast cell lines (CEC32) by Dr. Sybille Herzog. The titer of ABV-4 was 2×10^6 ID_{50}/ml. Different dilutions of the cellular supernatant of ABV-4 suspension 1:100, 1:500 and 1:1000 with RPMI-1640 culture medium were applied. Before the infection, BC cells were counted by trypan blue assay. We added 2ml of the diluted

ABV-4 suspension for each 1.5×10^5cells/ml. We infected BC cells with ABV-4 one day post isolation. The experimental infection of BC was implemented as follows:

1. BC cells were prepared by centrifugation at 2500 rpm for 5 minutes.
2. BC cells were added into well plate, then gently mixed and incubated with 2 ml diluted ABV-4 suspension in the incubator at 37°C for one hour.
3. ABV-4 infected BC cells were transferred to sterile glass conical test tubes for centrifugation at 2500 rpm for five minutes.
4. The supernatant was discarded and cells were washed with RPMI-1640 culture medium once.
5. BC cells were centrifuged at 2500 rpm for 5 minutes.
6. The supernatant was discarded and cells were suspended in 2ml RPMI-1640 medium and propagated into Nunclon brand^{TM}Surface 6 well plate (Sigma Aldrich, Germany).
7. RPMI-1640 culture medium of infected cells was replaced every three days.
8. BC cells were observed for 15 days post infection respectively and viability of BC cells was recorded by trypan blue every day.

3.22. Demonstration of ABV antigen in BC cells by IIF

We investigated the presence of ABV antigen in the BC cells at 3, 5, 9, and 15 days post infection (dpi) after ABV-4 infection.

3.22.1. Preparation of BC cells

Two mililiter of culture medium containing BC cells were collected and pull out into glass test tubes. BC cells were centrifuged at 1500 for 5 minutes. After obtaining cells pellet, 50µl cell pellet were subsequently smeared onto poly-lysine coated slides (R.Langenbrinck, Germany). BC cells were counted by trypan blue assay. Each smear contains of 1.5×10^3 cells. The smear was dried at room temperature for 20 minutes.

3.22.2. Fixation

BC cells were fixed in ice cold 70% methanol for 15 minutes at room temperature.

3.22.3. Blocking

For blocking, 100µl 5% goat serum (Sigma Aldrich, Germany) diluted in sterile 1xPBS was used for each slide. BC cells were incubated with the blocking serum for 30 minutes at room temperature.

3.22.4. Primary antibody

We used polyclonal anti-Borna disease virus (BoDV) rat serum to investigate the presence of ABV in BC cells after ABV-4 infection. Polyclonal anti-borna disease virus (BoDV) rat serum

was proved to be cross reactive to detect ABV antigen (Herzog et al., 2010). The antibody was diluted 1:100 in 1xPBS. We added 50µl diluted rat serum onto each BC cells smear. BC cells were incubated with the primary antibody for 1 hr at room temperature.

3.22.5. Secondary antibody

We used Cy3 conjugate goat anti-rat (Dianova, USA) as a secondary antibody, diluted 1:50 in 1xPBS. We added 50µl diluted goat anti rat onto each BC cells smear. BC cells were incubated with the secondary antibody in a humidified chamber for one hour in the dark at room temperature.

3.22.6. Controls

BoDV infected-MDCK cell line were used as positive control. None infected BC cells were incubated with the primary and secondary antibodies for comparison with infected BC cells. Moreover, infected BC cells were incubated with the secondary antibody only.

3.22.7. IIF protocol for demonstration of ABV antigen

The protocol was accomplished as follows:

1. After preparation the BC cells smear, the end of the smear was marked with a circle by pap pen (Dako, Germany) to define the area of interest.
2. BC cells were washed in ice cold sterile 1xPBS once.
3. BC cells were incubated with 5% goat serum (Sigma Aldrich, Germany) in sterile 1xPBS for 30 minutes at room temperature.
4. BC cells were incubated with the polyclonal anti-BoDV rat serum for one hour at room temperature.
5. BC cells were washed with sterile ice cold 1xPBS twice.
6. BC cells smear was incubated with cy3 conjugate goat anti-rat (Dianova, USA) in a humidified chamber for one hour at room temperature in the dark.
7. BC cells were washed in ice cold sterile 1xPBS twice in the dark.
8. BC cells were incubated with 1µg/ml DAPI for 10 minutes in the dark at room temperature.
9. BC cells were washed in ice cold sterile 1xPBS twice in the dark.
10. BC cells were rinsed in sterile distilled water once in the dark.
11. BC cells were mounted with few drops of Fluroshield mounting medium (Serva, USA) and then sealed with coverslip (Roth, Germany).
12. Slides were stored at 4°C in the dark and examined under Nikon fluorescence microscope (Nikon, Germany).

3.23. Demonstration of ABV-4 RNA in BC cells

For investigation of ABV-4 RNA in BC cells after ABV-4 infection, RNA from the isolated BC cells as well as from the ABV-4 suspension was isolated by specific kits for each. Then, the total RNA was reversely transcribed using random primers and cDNA applied to PCR.

3.23.1. RNA extraction from BC cells

We used the RNasey Mini kit (Qiagen, Germany) to isolate the total RNA from BC cells after ABV-4 infection. We also isolated the total RNA from the negative control (non infected BC cells) for comparison. Total RNA was extracted by the trizol-chloroform method using trizol (Ambion, Life Technologies, Germany). Isolation of total RNA from infected BC cells was performed according to the instructions of the manufacturer. After isolation, the concentration of RNA was measured by Nanodrop®2000 spectrophotometer (Thermo scientific GmbH, Germany). The RNA pellet was stored at - 80 °C until use.

3.23.2. RNA extraction from ABV-4 suspension

The Qiamp viral RNA mini kit (Qiagen, Germany) was used to isolate total RNA from the ABV-4 suspension. Isolation of ABV-4 RNA was carried out according to the instructions of the manufacturer. Concentration of total RNA was subsequently measured by Nanodrop®2000 spectrophotometer. Total RNA was stored at - 80 °C until use.

3.24. Reverse transcription reaction (RT)

RNA extracted from BC cells and from ABV-4 suspension were washed with (7X) wipe out buffer for effective elimination of genomic DNA contamination from RNA samples. Reagents were gently mixed, subsequently incubated for 2 minutes at 42°C, followed by transferring immediately to ice box. Then, RNA extracted from BC cells and from ABV-4 suspension were reversely transcribed into cDNA by reverse transcriptase using QuantiTect Reverse Transcription kit (Qiagen, Germany) as given in table 26.

Table 26: Reverse transcription reaction

Component	Volume µl	Final concentration
Quantiscript RT buffer	4 µl	five times concentrated (5X)
Quantitect reverse transcriptase	2 µl	
RT primer mixture	2 µl	0.7µM
RNA template	12 µl	300 ng/µl
Total volume	20 µl	

ng/µl= nanogram per microliter, µM= micromolar

Reagents were gently mixed and subsequently incubated in a PTC-200 Peltier thermal cycler (Biozyme, Germany). RT programme was run for 15 minutes at 42 °C, 3 minutes 95°C and at 4°C. Afterwards, the cDNA was subsequently stored at -20°C.

3.25. PCR for amplification of the ABV-4 RNA

We amplified the cDNAs which are generated from total RNA extracted from BC cells and from ABV-4 suspension. ABV-4-forward and ABV-4-reverse primers were used. PCR was achieved in a thermocycler PTC-200 (Biozyme, Germany). For visualisation of the cDNA fragments, 2% agarose gel electrophoresis technique was subsequently performed. The power was set to 7 volt/cm electrodes distance for one hour. PCR was performed as given in tables 27 and 28.

Table 27: Composition of the PCR-reaction

Reagent	Amount µl	Concentration
Sterile H_2O	16.7 µl	
Buffer containing $MgCl_2$ (complete buffer)	2.5 µl	10X concentrated
ABV-4-N-R	2 µl	10µM
ABV-4-N-F	2 µl	10µM
dNTP	0.5 µl	10µM
BioTherm™ DNA-polymease	0.3 µl	5U/µl
cDNA	1 µl	
Total volume per reaction	25 µl	

F= forward, R= reverse, µl= microliter, µM= micromolar, cDNA= complementary DNA

Table 28: Conditions of the PCR-reaction

Reaction	Time	Temperature in °C	Cycles
Initial denaturation	120 seconds	94 °C	
Denaturation	15 seconds	94 °C	35 cycles
Annealing	30 seconds	55 °C	
Extension	45 seconds	72 °C	
Final extension	10 minutes	72 °C	
Cooling	∞	4°C	

3.26. Demonstration of house keeping gene

To confirm that the cDNA amplification was successful, amplification of the PGK1 (phosphoglycerate kinase 1) gene was used. PGK1 gene was used as reference house keeping gene (accession number at the Genbank: NM_204985) for cockatiels by (Olias et al., 2014). PGK1-F and PGK1-R primers (Biomers, Germany) were used (table 29). PCR was achieved in a thermocycler PTC-200 (Biozyme, Germany). For visualisation of the amplicons, 2% agarose gel electrophoresis technique was subsequently performed. The power was set to 7 volt/cm electrodes distance for 90 minutes. PCR was performed as given in tables 30 and 31.

Table 29: Sequences and orientation of PGK1 gene primers

Primers	Sequence (5'->3')	Length (bases)
PGK1-F	5′- AAAGTTCAGGATAAGATCCAGCTG -3′	24
PGK1-R	5′- GCCATCAGGTCCTTGACAAT-3′	20

PGK1= Phosphoglycerate kinase 1, F= forward, R= reverse

Table 30: Composition of the PCR-reaction

Reagent	Amount µl	Concentration
Sterile H_2O	13.7 µl	
Buffer containing $MgCl_2$ (complete buffer)	2.5 µl	10X concentrated
PGK1-R	1 µl	10µM
PGK1-F	1 µl	10µM
dNTP	0.5 µl	10µM
BioTherm™ DNA-polymease	0.3 µl	5U/µl
cDNA of infected BC cells	1 µl	
Total volume per reaction	20 µl	

F= forward, R= reverse, µl= microliter, µM= micromolar, cDNA= complementary DNA

Table 31: Conditions of the PCR-reaction

Reaction	Time	Temperature in °C	Cycles
Initial denaturation	120 seconds	94 °C	
Denaturation	15 seconds	94 °C	35 cycles
Annealing	30 seconds	55 °C	
Extension	45 seconds	72 °C	
Final extension	10 minutes	72 °C	
Cooling	∞	4°C	

3.27. Stimulation of BC cells with PHA-M mitogen

BC cells were stimulated by phytohemagglutinin (PHA-M) (Sigma Aldrich, Germany) *in vitro*. PHA-M is a lectin extract from the red kidney bean (p*haseolus vulgaris*) contain potent, cell agglutinating and mitogenic activities. The main steps for stimulation of BC cells *in vitro* were accomplished as follows:

3.27.1 Preparation of PHA-M mitogen

PHA-M mitogen (5mg) was reconstituted with 5ml sterile 1xPBS and divided into 5 aliquots (1ml each) as stocks and then stored frozen in -20 °C until use. The reconstituted product was further diluted 1:100 in RPMI-1640 culture medium and then stored frozen in -20 °C until use. A 100µl of diluted PHA-M mitogen was added to each 1ml RPMI-1640 culture medium containing BC cells in each well of the Nunclon brand^{TM}Surface 6 well plate (Sigma Aldrich, Germany), gently shaked and then buffy coat cells were incubated for 5 days at 37°C.

3.27.2 Stimulation of cockatiels BC cells *in vitro*

We applied a final concentration 10µg/ml of PHA-M in RPMI-1640 culture medium. BC cells were stimulated at the same day of isolation. Stimulated BC cells were observed under IX70 S8F inverted microscope (Olympus, USA) for 5 days successively after stimulation with PHA-M. In parallel, we prepared none stimulated BC cells similarly in order to count total number of cells by trypan blue assay for comparison with total count number of stimulating BC cells.

3.28. Assessment of proliferating

We applied two methods to investigate the stimulation of BC cells *in vitro*. Firstly, the total count number of stimulated BC cells by trypan blue assay was compared to the cells count of unstimulated BC cells. The second method was investigation of the bromodeoxyuridine (BrdU) incorporation in the proliferative BC cells by IIF. In the cells smear, we counted 400 stimulated BC cells and 400 unstimulated BC cells daily up to 5 days post stimulation. We investigated BrdU incorporation in the stimulated BC cells from 2 hours up to 12 days post stimulation by IIF. Results of both methods were compared.

3.28.1. Trypan blue assay

We investigated the total count number of BC cells by counting the stimulated BC cells under light microscope (Nikon, Germany). Shortly, we counted the total number of stimulated BC cells (400 cells per field) and compare it with total number of none stimulated BC cells (400 cells per field) daily for 5 days respectively.

3.28.2. Detection of the Bromodeoxyuridine (BrdU) incorporation by IIF

3.28.2.1. Preparation of BrdU

BrdU (Sigma Aldrich, Germany) was used. BrdU was dissolved in sterile water at a concentration of 10 mg/ml as stocks. Each stock contained of BrdU 10µg/µl and was kept in the dark in -80°C until use. To reach a 10µM of Bromodeoxyuridine as a final treatment concentration, 6µl BrdU stock was added to 20ml RPMI-1640 medium containing stimulated BC cells in the well plate. BC cells were incubated for 6 hours in the dark at 37°C.

3.28.2.2. Preparation of BC cells

A 100µl stimulated BC cells was smeared onto poly-lysine coated slide (R.Langenbrinck, Germany), air dried for 20 minutes at room temperature followed by marking a circle around the dried smear by pap pen (Dako,Germany).

3.28.2.3. Blocking

5%goat serum (PAA, Germany) diluted in 1xPBS was used and 50µl was applied on the smear. Cells smear was incubated with the blocking solution for one hour at 37°C.

3.28.2.4. Primary antibody

Mouse anti-BrdU antibody (Santa Cruz Biotechnology, Germany) was used. The primary antibody was diluted 1:50 in 1xPBS/BSA and incubated overnight at 4°C and 50µl of the diluted primary antibody was added to each well of the plate.

3.28.2.5. Secondary antibody

Cy3 conjugated goat anti-mouse (Dianova, USA) was diluted 1:50 in 1xPBS/BSA and applied on the smear and incubated in a humidified chamber at 37°C in the incubator for one hour in the dark. A 50µl of the diluted secondary antibody was added to each well of the plate.

3.28.2.6. DAPI staining

BC ells were stained with DAPI. Concentration of DAPI was 1µg/ml. DAPI was diluted 1:1000 in 1xPBS and 150µl diluted DAPI was added to the smear. BC cells were incubated with DAPI for 10 minutes at room temperature in the dark.

3.28.2.7. Control

The primary antibody was not added to the stimulated or the non stimulated BC cells as negative control.

3.28.2.8. Assessment the positive signals

Nuclear staining of stimulated BC cells with anti-BrdU antibody indicated to the positive results of this assay.

3.28.2.9. Indirect immunofluorescence for detection of BrdU

1. A 6µl BrdU (10mg/ml) stock solution was added to 20ml RPMI-1640 medium and incubated with 10,000 stimulating BC cells at 37°C in the incubator for 6 hours in the dark.
2. RPMI-1640 medium was pipetted out and cells were washed with sterile 1xPBS three times.
3. BC cells were fixed with 70% ethanol for 30 minutes at room temperature.
4. BC cells were washed with sterile 1xPBS three times.
5. BC cells were permeabilized with 50 µl 0.3% triton X-100 (Serva GmbH, Germany) for 15 minutes at room temperature. Triton X-100 was diluted in 1xPBS.
6. For denaturation, 100µl 2M HCl was added to the cells smear followed by incubation of the slides for one hour at 37°C in the incubator.
7. For neutralization of the acid, BC cells were neutralized with 100µl 0.1M sodium borate (Na_2B4O7, pH 8.5) to the smear for 5 minutes at room temperature.
8. BC cells were washed with sterile 1xPBS followed by washing with PBS Tween 20® (Sigma Aldrich, Germany)/1xPBS for 5 minutes three times at room temperature.
9. BC cells were blocked with 5% goat serum/PBS at 37°C in the incubator for one hour.
10. BC cells were incubated with the primary antibody at 4°C overnight.
11. BC cells were washed with sterile 1xPBS for 5 minutes at room temperature.
12. BC cells were incubated with secondary antibody at 37°C in the incubator for one hour.
13. BC cells were washed in sterile 1xPBS three times, 5 minutes each. Then DAPI was added to the cells in the final wash to stain the DNA.
14. BC cells were mounted with Fluroshield mounting medium (Serva, USA) and then sealed with coverslip (Roth, Germany).
15. Slides were stored at 4°C in the dark and examined under Nikon fluorescence microscope (Nikon, Germany).

3.29. Experimental infection of stimulated BC cells at the same day of isolation

BC cells were stimulated with PHA-M and then infected with ABV-4 at the same day of isolation (**Fig. 6**). In parallel, we prepared non stimulated BC cells and infected them with ABV-4 as a control.

3.29.1. Demonstration of BrdU in stimulated BC cells

By IIF, we investigated the stimulation through detecting BrdU in proliferating BC cells for up to 5 days post stimulation and post infection respectively as shown in **Fig. 6**.

3.29.2. Demonstration of ABV antigen in stimulated BC cells

Presence of ABV-4 antigen in stimulated BC cells was investigated from day 0 until 5 dpi by IIF shown in **Fig. 6**. Polyclonal serum from rats experimentally infected with BoDV was used.

3.29.3. Demonstration of ABV-4 RNA in stimulated BC cells

By RT-PCR, total RNA extracted from stimulated BC cells was detected from day 0 until day 5 dpi respectively (see **Fig. 6**). At day 0, we investigated the stimulation and the ABV-4 RNA in the stimulated BC cells 10 hours post stimulation and post infection. For comparison, we also investigated the stimulation and presence of ABV-4 RNA in the non stimulated BC cells.

3.30. Experimental infection of stimulated BC cells at day 3 post stimulation

BC cells were isolated and stimulated with PHA-M at day 1, then, infected with ABV-4 at day 3 post isolation and stimulation as shown in **Fig. 7**. BrdU incorporation and presence of ABV-4 RNA were analyzed in the stimulated BC cells at day 4, 6, 8, 10, 12, and 14 post stimulation respectively. For comparison, we also investigated the presence of ABV-4 RNA in the negative control (non stimulated BC cells) at days 4, 6, 8, 10, 12 and 14 post stimulation.

Fig. 6: Schematic diagram for the experimental infection of stimulated BC cells at day 1 post stimulation.

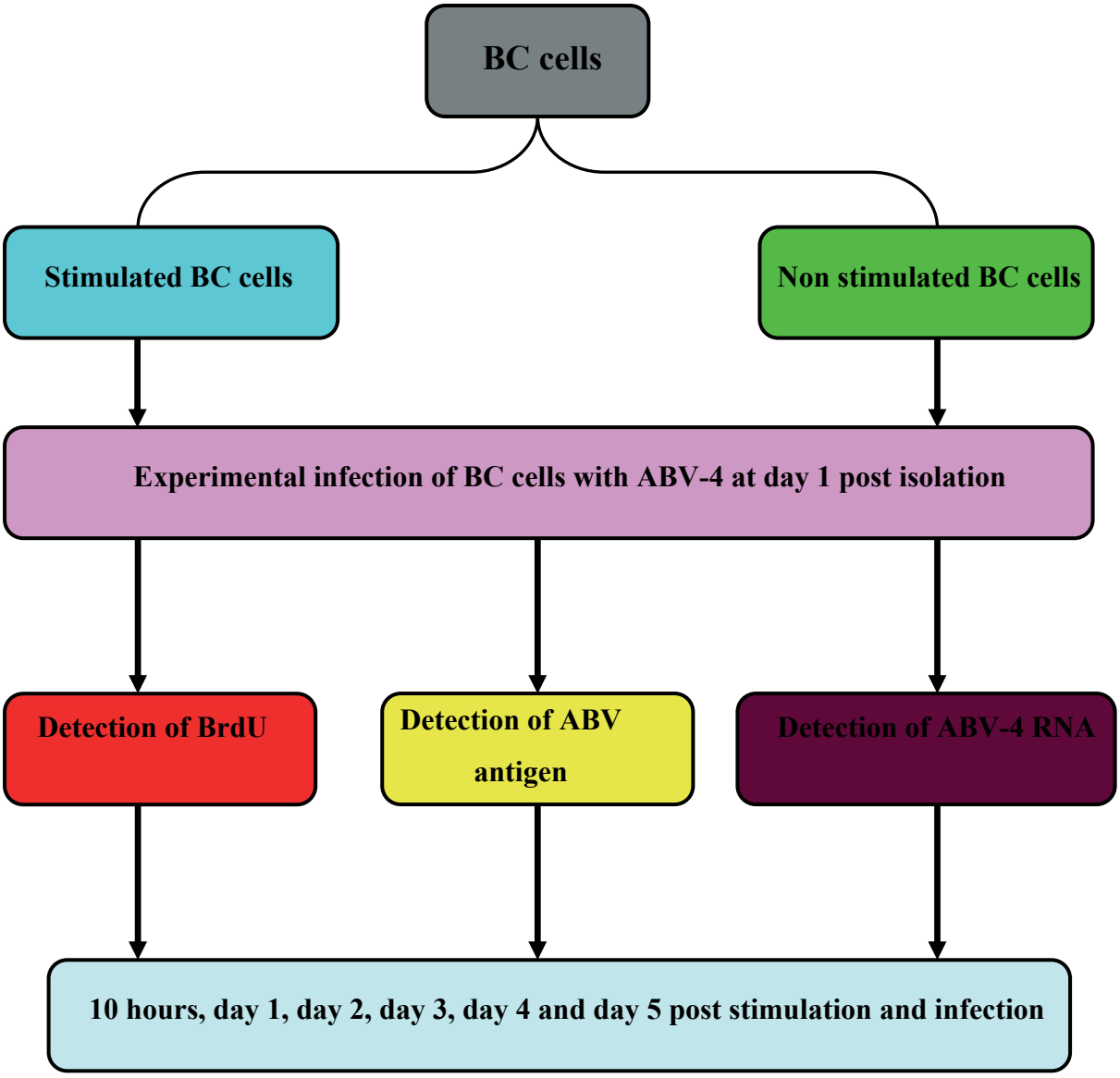

Fig. 7: Schematic diagram for the experimental infection of stimulated BC cells at day 3 post stimulation.

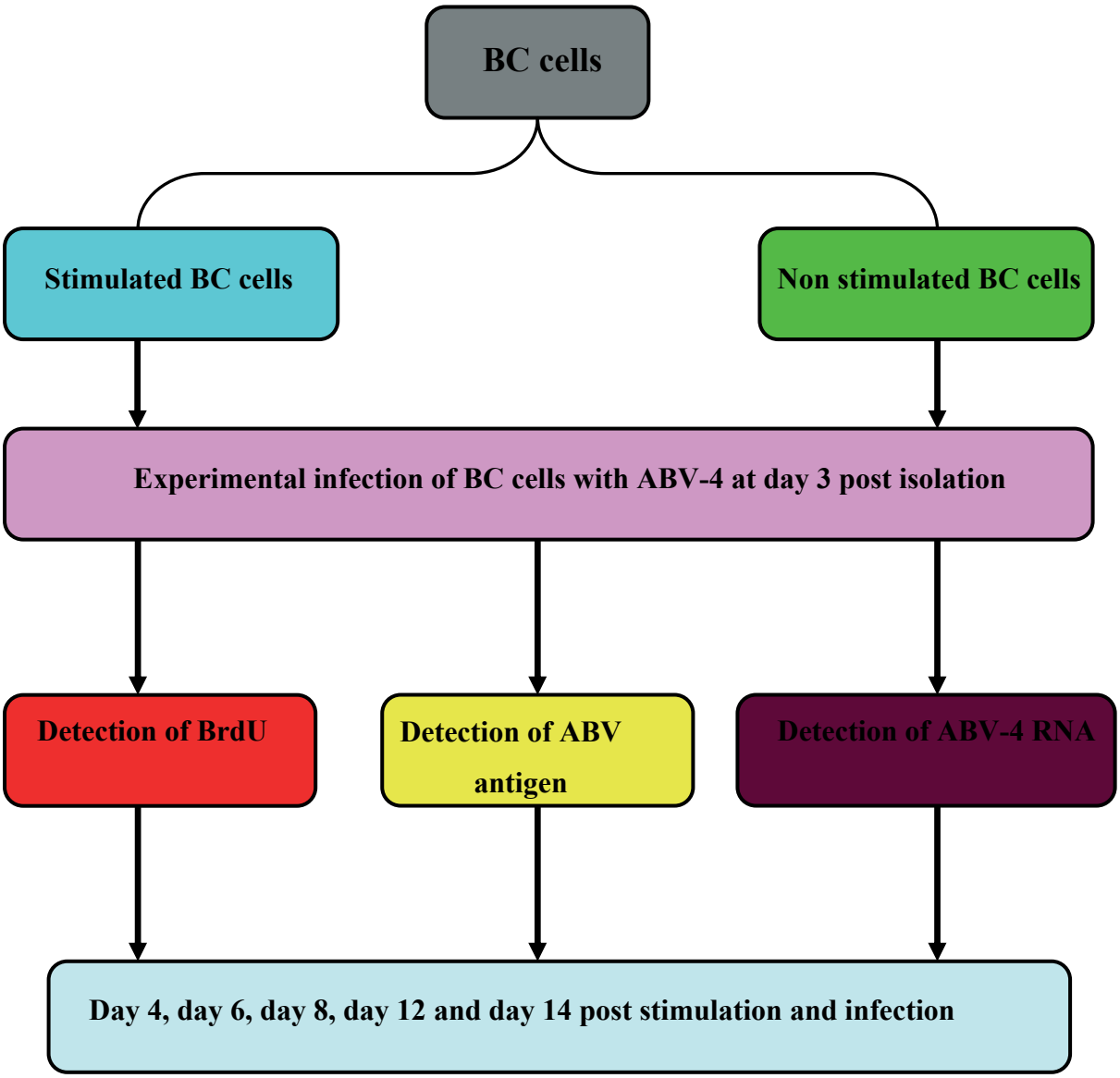

3.31. Description of the statistical analysis of the data

The statistical analysis was carried out by Dr. Failling, Institute of Biomathematics, Faculty of Veterinary Medicine, Justus-Liebig-University-Giessen. Mostly, the computations were made by means of the statistical software package BMDP/Dynamic, Release 8.1, (DIXON 1993). Furthermore the program package StatXact, Cytel Studio Vers. 9.0.0 (2010) was used for exact statistical calculation methods. For the description of quantitative, approximately normal distributed data, the arithmetic mean ($\bar{x}$), standard deviation (s), minimum (x_{min}), maximum (x_{max}) and sample size (n) were calculated. To test the differences between the infection with ABV-2 and ABV-4 genotypes, the infection routes within the organ systems regarding the day post infection as a covariate, a two-way analysis of covariance (ANCOVA) was calculated using the program BMDP2V. For the investigation of the relationship between the severity of inflammation and the distribution of viral antigen a correlation analysis was done by the use of the program BMDP6D, also this program was used for the estimation of the regression line for each group between the score values of the organ systems and time post infection. For the correlation analysis of graded variables the Spearman's correlation test with the program "StatXact" (Cytel software corporation, USA) was calculated. At all analyses a statistical significance level of $\alpha = 0.05$ was used and results with p-values ≤ 0.05 were regarded to indicate statistical significance.

4. Results

4.1. Clinical signs

All data of clinical signs were obtained and recorded by Anne Piepenbring, Clinic for Birds, Reptiles, Amphibians and Fishes, Justus Liebig University Giessen as a part of her doctoral thesis dealing with the clinical signs and diagnostics of ABV infections (Piepenbring et al., in revision). If a bird displayed clinical signs typical for PDD (emaciation, undigested seed in the faeces, neurologic signs) and if its general condition was reduced, it was euthanized.

4.1.1. Clinical signs after ABV-2 infection

First symptoms occurred on day 22 after ABV-2 infection (Piepenbring et al., in revision). In total, 12/18 inoculated birds exhibited clinical signs (10 birds exhibited gastrointestinal, 2 birds exhibited gastrointestinal and neurological clinical signs) as shown in table 32. Gastrointestinal clinical signs consisted of reduced general condition, diarrhea, emaciation, and undigested seed in the faeces while neurological clinical sign were mainly ataxia. Moreover, 4/18 inoculated birds remained clinically healthy until end of the experiment at 231 dpi. Also, 2/18 inoculated birds died suddenly without exhibiting clinical signs.

Table 32: List of cockatiels which showed clinical signs after ABV-2 infection

Bird ID	Gender	Route of infection	Birds with clinical signs			
			gastrointestinal signs	neurological signs	Death	Euthanasia
			days p.i	days p.i	dpi	dpi
N39	female	ic	22		32	
N 32	female	iv	45		46	
N 25	female	iv	46		50	
N 24	female	ic	40	32		68
N 34	female	iv	57			76
N 47	male	ic	83		84	
N 27	female	ic	71	85	86	
N 45	male	iv	78			88
N 19	male	iv	104			120
N 48	female	iv	121		137	
N 30	female	ic	139			172
N 46	female	ic	86			231

(iv) intravenous, (ic) intracereberal, (dpi) days post infection. ABV-2 infection, early time points (32-86) dpi, mid time points (87-172) dpi, and late time points (173-231) dpi.

4.1.2. Clinical signs after ABV-4 infection

First symptoms occurred on day 33 after ABV-4 infection (Piepenbring et al., 2012). In total, 5/18 inoculated birds displayed clinical signs (2 birds exhibited neurological, 2 birds exhibited gastrointestinal signs, and one bird displayed neurological and gastrointestinal clinical signs) as shown in table 33. Moreover, 11/18 inoculated birds remained healthy during the whole investigation period until the end of the experiment at 230 dpi. Also, 2/18 inoculated birds died suddenly without exhibiting clinical signs.

Table 33: List of cockatiels which showed clinical signs after ABV-4 infection

Bird ID	Gender	Route of infection	Birds with clinical signs			
			gastrointestinal signs	neurological signs	Death	Euthanasia
			days p.i	days p.i	dpi	dpi
N15	female	ic	37	41		60
N 13	male	iv	116			116
N 11	female	ic		199		206
N 10	female	iv	126			229
N 22	female	iv		159		229

(iv) intravenous, (ic) intracereberal, (dpi) days post infection. ABV-4 infection, early time points (37-66) dpi, mid time points (67-126) dpi, and late time points (127-230) dpi.

4.1.3. Comparison of the clinical observation

Five birds of the ABV-4 infected groups exhibited symptoms consistent with PDD, of which the five birds showed neurological signs. In contrast after ABV-2 infection, 12 birds displayed clinical signs typical for PDD. Within the ABV-2 infected groups, clinical signs consisted of mostly gastrointestinal clinical signs.

4.2. Gross lesions

4.2.1. Gross lesions after ABV-2 infection

Necropsy revealed a dilatation of proventriculus in 10/18 birds with severe dilatation in five birds, moderate dilatation in four birds and mild dilatation in one bird after ABV-2 infection (**Fig. 8)**.

4.2.2. Gross lesions after ABV-4 infection

Proventriculi were dilated in 7/18 birds, with severe dilatation in one bird, moderate dilatation in four birds and mild dilatation in two birds after ABV-4 infection (Piepenbring et al., 2012).

4.2.3. Comparison of gross lesions

Proventriculi were enlarged in 10/18 birds after ABV-2 infection and in 7/18 birds after ABV-4 infection. In the ABV-2 group, 5 birds had a severely dilated proventriculus in contrast to one bird in the ABV-4 group (**Fig. 8)**. After ABV-2 or ABV-4 infection, the correlation between clinical signs and gross lesions could be divided as follows:

1) The ABV-2 or ABV-4 infected birds that exhibited gastrointestinal and/or neurological clinical signs, also displayed moderate to severe dilatation of proventriculus.

2) The ABV-2 or ABV-4 infected birds that did not exhibit clinical signs, also did not display dilatation of proventriculus.

However, one ABV-2 infected bird exhibited gastrointestinal and neurological clinical signs but dilatation of proventriculus was not found. Moreover, one ABV-2 infected bird did not exhibit clinical signs but it displayed a mild dilatation of proventriculus. One ABV-4 infected bird exhibited neurological clinical signs but dilatation of proventriculus was not found. Two ABV-4 infected birds did not exhibit clinical signs but it displayed a mild dilatation of proventriculus. Severity of gross lesions associated with clinical signs but in mild cases it could vary.

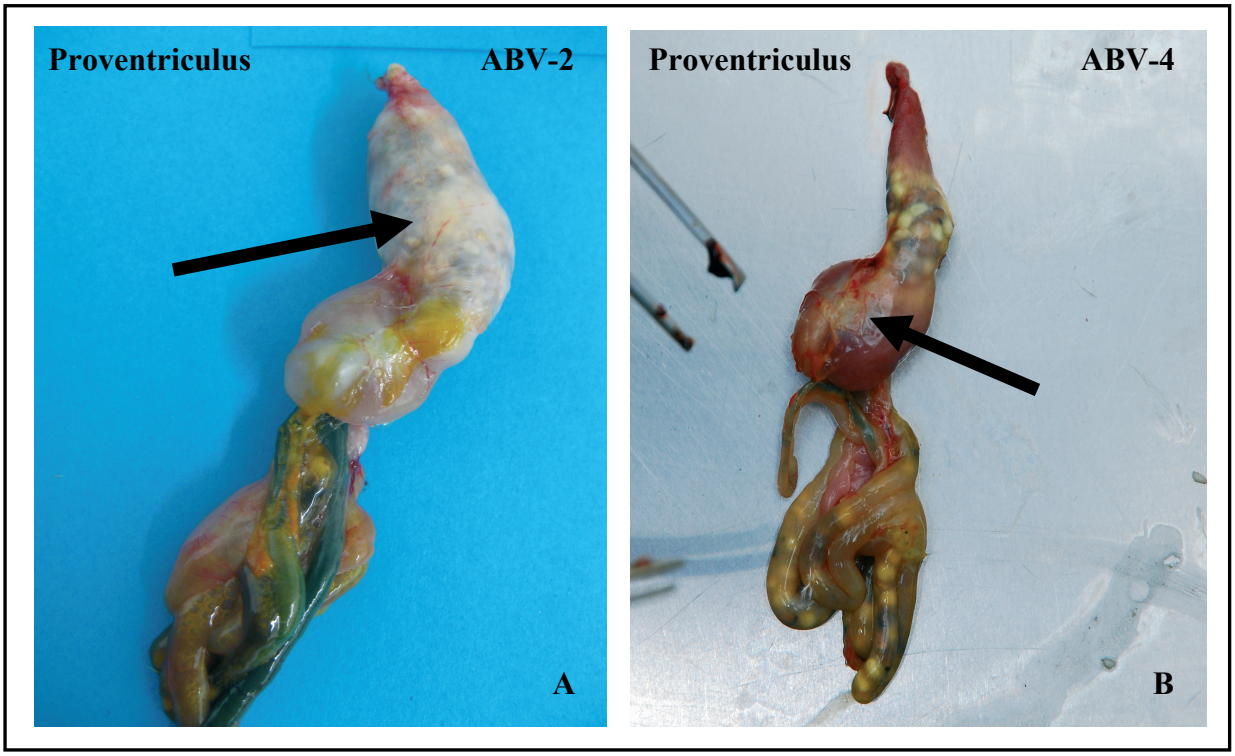

Fig. 8: Typical gross lesions with dilatation of proventriculus in cockatiels after ABV-2 and ABV-4 infection. (A) Proventriculus, severe dilatation of proventriculus (arrow), after ABV-2 infection, 68 dpi. (B) Proventriculus, severe dilatation of proventriculus (arrow), after ABV-4 infection, 60 dpi.

4.3. Histological findings

4.3.1. Histological lesions after ABV-2 infection

In the CNS, gliosis was detected in the brain in 13/18 experimentally ABV-2 infected birds. Gliosis was not found in the brain in 5/18 birds but mild gliosis was detected in it in 11/18 birds, and moderate gliosis in 2/18 experimentally ABV-2 infected birds. No obvious inflammatory infiltrates were found in the brain in 18/18 experimental ABV-2 infected animals (**Fig. 9**). No inflammatory lesions were found in the spinal cord in 7/18 birds but mild inflammatory lesions were detected in it in 5/18 experimentally ABV-2 infected birds. Spinal cord was not present in 6/18 experimentally ABV-2 infected birds (table 34). Inflammatory lesions were detected in the eye in 3/18 experimentally ABV-2 infected birds. Inflammatory lesion were not detected in the eye in 14/18 birds but mild inflammatory lesions were detected in it in 2/18 birds, and moderate lesions in 1/18 experimentally ABV-2 infected birds (table 34). The eye was autolytic in 1/18 birds. Inflammatory lesions were detected at the first time point investigated in the CNS at 46 dpi until the end of the investigation period.

The kinetic of gliosis generally revealed that gliosis was mild or moderate at early time points (32-84 dpi), then decreased to only mild from mid time points (86-172 dpi) until late time points 231 dpi in the 13/18 experimentally ABV-2 infected birds. Nevertheless, there was variability in the kinetic of gliosis. At early time points (32-84 dpi), one bird had no gliosis (bird ID: 47) and one additional bird had no inflammatory lesion in the spinal cord (bird ID: 25) at early time points. At mid time points (86-172 dpi), two birds had no gliosis (bird ID: 27 and 30) and two additional birds had no inflammatory lesion in the spinal cord (bird ID: 45 and 30) at mid time points. At late time points 231 dpi, two birds had no gliosis (bird ID: 49 and 29) and no inflammatory lesions in the spinal cord at late time points.

In the GIT, inflammatory lesions were detected in all comparable GIT organs but mainly in the intestine and proventriculus. Inflammatory lesions in the GIT consisted of mononuclear cells infiltrates in the intestinal mucosa and /or submucosa, lamina muscularis as well as around nerves and ganglia or in the ganglia and nerve fibers of gizzard, proventriculus, intestine and crop (**Fig. 10**).

Inflammatory lesions were not detected in the crop in 3/18 birds but mild inflammatory lesions were detected in it in 14/18 birds (table 34). The crop was autolytic in 1/18 birds. Inflammatory lesions were not detected in the gizzard in 2/18 birds but mild inflammatory lesions were detected in it in 11/18 birds, moderate lesions in 4/18 experimentally ABV-2 infected birds. The gizzard was autolytic in 1/18 birds. Inflammatory lesions were not detected in the proventriculus in 4/18 birds but mild inflammatory lesions were detected in it

in 7/18 birds, moderate in 4/18 birds, and severe in 2/18 birds (table 34). The proventriculus was autolytic in 1/18 birds. Inflammatory lesions were not detected in the intestine in 2/18 birds but mild inflammatory lesions were found in it in 11/18 birds, moderate in 2/18 birds, and severe in 1/18 birds (table 34). The intestine was autolytic in 2/18 birds.

The kinetic of inflammatory lesions in the GIT was variable. In the crop, inflammatory lesions were mild from early time points at 32-86 dpi until late time points at 231 dpi in the 14/18 experimentally ABV-2 infected birds (table 34). In the gizzard, inflammatory lesions were mild or moderate from early time points at 32-86 dpi until late time points at 231 dpi in the 15/18 experimentally ABV-2 infected birds (table 34). In the proventriculus, inflammatory lesions were mild and moderate at early time points at 32-86 dpi. However, inflammatory lesions were severe in the proventriculus in only 1/18 birds at early time points. At mid time points 88-172 dpi, inflammatory lesions decreased in the proventriculus to mild only. At late time points, inflammatory lesions were mild, moderate and severe at 231 dpi. In the intestine, inflammatory lesions were variable in severity during the whole investigation period.

In the peripheral organs, inflammatory lesions were mainly found in the kidney, liver, spleen and skin. Inflammatory lesions in the peripheral organs were found as infiltration of mononuclear cells, sometimes with follicular shape-like appearance. Periganglionitis and/or perineuritis were also detected in the peripheral organs. Infiltration of mononuclear cells in the heart was always detected in the adjacent ganglia but not in the heart itself. Infiltrations of mononuclear cells in the liver were found as follicular shape-like aggregations around the central veins or bile ducts. Infiltrations of mononuclear cells in the kidney were detected around ganglia, or as follicular shape-like aggregations around blood vessels. Infiltrations of mononuclear cells in the pancreas were found as follicular shape-like aggregations around blood vessels, interlobular ducts, acini and islets. Infiltrations of mononuclear cells in the skin were detected around feather follicles (**Fig. 11**).

Inflammatory lesions were not detected in the heart in 4/18 birds but mild inflammatory lesions were detected in it in 11/18 birds, and moderate in 2/18 birds. The heart was autolytic in 1/18 birds. Inflammatory lesions were not detected in the liver in 4/18 birds but mild inflammatory lesions were detected in it in 9/18 birds, and moderate in 4/18 birds (table 34). The liver was autolytic in 1/18 birds. Inflammatory lesions were not detected in the kidney in 1/18 birds but mild inflammatory lesions were detected in it in 7/18 birds, moderate in 5/18 birds, and severe in 4/18 birds. The kidney was autolytic in 1/18 birds. Inflammatory lesions were not detected in the spleen in 1/18 birds but mild inflammatory lesions were detected in it in 4/18 birds, moderate in 7/18 birds, and severe in 1/18 birds. The spleen was not present in

5/18 birds. Inflammatory lesions were not detected in the pancreas in 10/18 birds but mild inflammatory lesions were detected in it in 6/18 birds. The pancreas was not found in 2/18 birds. Inflammatory lesions were not detected in the adrenal gland in 1/18 birds but mild inflammatory lesions were detected in it in 2/18 birds, moderate in 1/18 birds, and severe in 2/18 birds. The adrenal gland was not found in 12/18 birds. Inflammatory lesions were not detected in the skin in 6/18 birds but mild inflammatory lesions were detected in it in 5/18 birds, and moderate in 4/18 birds (table 34). The skin was not found in 3/18 birds. Inflammatory lesions were not detected in the muscles in 18/18 experimentally ABV-2 infected birds.

The kinetic of inflammatory lesion in the peripheral organs revealed that inflammatory lesions neither decreased nor increased in all the peripheral organs from early time points until late time points at 231 dpi and could be of variable in severity.

In the sentinel group, mild gliosis was detected in the brain. Moreover, follicular shape-like infiltrates were detected in the GIT and in some of the peripheral organs in the sentinel bird. Inflammatory lesions in the sentinel group were not found in or around the nerves or in the ganglia of the GIT and peripheral organs.

In the mock group, no gliosis was found in the brain. Moreover, mild follicular shape-like aggregations were detected in the GIT but not in the nerves or ganglia in only 1/4 birds. Mild follicular shape-like aggregations were also detected in some of the peripheral organs of the mock group but not in the nerves or ganglia.

Interestingly, the follicular shape-like infiltrates in the GIT and in some of the peripheral organs in the sentinel bird and mock group were smaller in size than in the infected birds.

4.3.2. Histological lesions after ABV-4 infection

In the CNS, inflammatory lesions in the CNS consisted of perivascular infiltration of mononuclear cells as well as gliosis in 17/17 experimentally ABV-4 infected birds (**Fig. 9**). Inflammatory lesions were detected in the brain in 17/17 birds. The brain was not available in 1/18 birds. Inflammatory lesions were detected in the spinal cord in 11/18 experimentally ABV-4 infected birds. Inflammatory lesions were found in the eye in 9/18 experimentally ABV-4 infected birds. Inflammatory lesions were detected in the CNS at the first time point investigated at 60 dpi until the end of the investigation period.

Mild inflammatory lesions were detected in the brain in 9/18 birds, moderate in 7/18, and severe in 1/18 bird. Mild inflammatory lesions were detected in the spinal cord in 9/18 birds, and moderate in 2/18 birds. Spinal cord was not available in 6/18 experimentally ABV-4 infected birds (table 35). Inflammatory lesions were not detected in the eye in 7/18 birds but

mild inflammatory lesions were detected in it in 4/18 birds, and moderate in 5/18 birds (table 35).

The kinetic of inflammatory lesions in the CNS was variable in severity. In the brain, inflammatory lesions were mild and moderate from early time points until 230 dpi. In the spinal cord, inflammatory lesions were mild at early time points and mid time points in most majority of birds but then increased to moderate at late time points in only 2 birds. In the eye, inflammatory lesions were mild and moderate at early and mid time points in most majority of birds but inflammatory lesions were not detected at late time points also in most majority of birds. However, two birds had mild inflammatory lesions in the eye at 229 dpi.

In the GIT, inflammatory lesions were detected in all comparable GIT organs but mainly in the proventriculus. Inflammatory lesions in the GIT consisted of mononuclear cells infiltrates in the intestinal mucosa and /or submucosa, lamina muscularis as well as around nerves and ganglia or in the ganglia and nerve fibers of gizzard, proventriculus, intestine and crop (**Fig. 10**).

Inflammatory lesions were not detected in the crop in 5/18 birds but mild inflammatory lesions were detected in it in 7/18 birds, and moderate in 3/18 birds (table 35). The crop was not available in 3/18 birds. Inflammatory lesions were not detected in the gizzard in 10/18 birds but mild inflammatory lesions were detected in it in 2/18 birds, and moderate in 1/18 experimentally ABV-4 infected bird (table 35). The gizzard was not available in 3/18 birds. The gizzard was autolytic in 2/18 birds. Inflammatory lesions were not detected in the proventriculus in 4/18 birds but mild inflammatory lesions were detected in it in 6/18 birds, moderate in 2/18 birds, and severe in 2/18 birds (table 35). The proventriculus was not available in 2/18 birds. Inflammatory lesions were not detected in the intestine in 5/18 birds but mild inflammatory lesions were detected in it in 4/18 birds, moderate in 3/18 birds, and severe in 4/18 birds (table 35). The intestine was not available in 1/18 birds. The intestine was autotyic in 1/18 birds.

The kinetic of inflammatory lesions in the GIT revealed that inflammatory lesions decreased in all GIT organs at 230 dpi in most majority of experimentally ABV-4 infected birds.

In the peripheral organs, inflammatory lesions were mainly found in the liver, kidney, heart, pancreas, and skin. Inflammatory lesions in the peripheral organs were found as infiltration of mononuclear cells, sometimes with follicular shape-like aggregations. Periganglionitis and/or perineuritis were also detected in the peripheral organs (**Fig. 11**). Infiltration of mononuclear cells in the heart was detected in the myocardium and in the pericardial ganglia. Infiltrations of mononuclear cells were also detected as follicular shape-like aggregations in the liver,

kidney, and pancreas. Infiltrations of mononuclear cells were detected around feather follicles in the skin.

Inflammatory lesions were not detected in the heart in 7/18 birds but mild inflammatory lesions were detected in it in 8/18 birds, moderate in 1/18, and severe in 1/18 experimentally ABV-4 infected birds (table 35). The heart was not available in 1/18 birds. Inflammatory lesions were not detected in the liver in 5/18 birds but mild inflammatory lesions were detected in it in 8/18 birds, moderate in 2/18 birds, and severe in 3/18 birds (table 35). Inflammatory lesions were not detected in the kidney in 2/18 birds but mild inflammatory lesions were detected in it in 5/18 birds, moderate in 5/18 birds, and severe in 5/18 birds. The kidney was not available in 1/18 bird (table 35). Mild inflammatory lesions were detected in the spleen in 2/18 birds, moderate in 7/18 birds, and severe in 4/18 birds. The spleen was not available in 5/18 birds. Inflammatory lesions were not detected in the pancreas in 5/18 birds but mild inflammatory lesions were detected in 7/18 birds, moderate in 2/18 birds, and severe in 1/18 birds. The pancreas was not available in 3/18 birds. Mild inflammatory lesions were detected in the adrenal gland in 2/18 birds. The adrenal gland was not available in 16/18 birds. Inflammatory lesions were not detected in the skin in 6/18 birds but mild inflammatory lesions were detected in 6/18 birds, moderate in 4/18 birds, and severe in 2/18 birds (table 35). Inflammatory lesions were not detected in the muscles in 16/18 birds but mild inflammatory lesions were detected only in 1/18 birds. The muscles were not available in 1/18 bird.

The kinetic of inflammatory lesion in the peripheral organs was variable in severity among the peripheral organs in most majority of birds. Inflammatory lesions could be mild in the heart, moderate in the pancreas, and severe in the kidney at early time points (60 and 66 dpi). At mid time points, inflammatory lesions were mild and severe in the heart, moderate and severe in the liver, mild, moderate, and severe in the kidney and spleen. At late time points 230 dpi, mild, moderate, and severe inflammatory lesions were detected in the kidney, spleen, liver and skin. Inflammatory lesions were not detected in the skin at early time points (60 and 66 dpi) but inflammatory lesions increased as mild and moderate at mid time points at 88-137 dpi and then as mild, moderate and severe at late time points at 230 dpi in the 18/18 experimentally ABV-4 infected birds (table 35).

In the sentinel group, mild gliosis was detected in the brain. Mild follicular shape-like aggregations were also detected in some of the GIT organs but not in the nerves or around ganglia. Moreover, moderate and severe follicular shape-like aggregations were found in the peripheral organs of the sentinel group but not in the nerves or around ganglia.

4.3.3. Comparison of histological lesions after ABV-2 and ABV-4 infection

In the CNS, gliosis was detected but no obvious perivascular cuffing in the brain at the first time point investigated at 46 dpi in 13/18 experimentally **ABV-2** infected birds. Gliosis was detected as mild and moderate in 13/18 experimentally **ABV-2** infected birds. Mild inflammatory lesions were detected in the spinal cord in 5/18 experimentally **ABV-2** infected birds. Mild inflammatory lesions were detected in the eye in 2/18 birds, and moderate in 1/18 experimentally **ABV-2** infected birds (table 34). There was a correlation between clinical signs, gross lesions, and gliosis at early time points (32-84 dpi) and mid time points (86-172 dpi) but not at late time points at 231 dpi **after ABV-2 infection**. If birds exhibited gastrointestinal and/or neurological signs, and had moderate to severe dilatation of proventriculus, they also had mild to moderate gliosis **after ABV-2 infection** and that occurred at early time points (32-84 dpi) and mid time points (86-172 dpi). However, one bird displayed gastrointestinal and neurological signs but it had no dilatation of proventriculus and had no gliosis at early time points (32-84 dpi). If birds did not exhibit clinical signs, and had no dilatation of proventriculus, they also had only mild gliosis **after ABV-2 infection** and that occurred at late time points at 231 dpi **after ABV-2 infection**.

After ABV-4 infection, perivascular cuffings of mononuclear cells were detected in the brain at the first time points investigated at 60 dpi in 2/18 experimentally **ABV-4** infected birds. Inflammatory lesions and gliosis were detected in the brain as mild, moderate, and severe in the 17/18 experimentally **ABV-4** infected birds. Mild inflammatory lesions were detected in the spinal cord in 9/18 birds, and moderate in 2/18 experimentally **ABV-4** infected birds. Mild inflammatory lesions were detected in the eye in 4/18 birds, and moderate in 5/18 experimentally **ABV-4** infected birds (table 35). The correlation between clinical signs, gross lesions, and inflammatory lesions in the brain **after ABV-4 infection** was somehow variable. If birds exhibited gastrointestinal and/or neurological signs, and had moderate to severe dilatation of proventriculus, they also had mild to moderate inflammatory lesions in the brain **after ABV-4 infection** and that occurred at early time points 60 and 66 dpi and mid time points 115, 116, and 120 dpi. However, one bird exhibited gastrointestinal and neurological signs, and had severe dilatation of proventriculus but it had only mild inflammatory lesions in the brain at early time points (60 and 66 dpi). Another bird at the same time points did not exhibit clinical signs, and had no dilatation of proventriculus but it had moderate inflammatory lesions in the brain. If birds did not exhibit clinical signs, and had no dilatation of proventriculus, they also had mild inflammatory lesions in it after **ABV-4** infection and that occurred at late time points at 230 dpi **after ABV-4 infection**. However, two birds did not

exhibit clinical signs, and had mild dilatation of proventriculus but they had moderate or severe inflammatory lesions in the brain respectively.

By comparison between kinetic of inflammatory lesions in the CNS, we found that there was variability in the kinetic of gliosis from early time points (32-84 dpi) until late time points 231 dpi in the 13/18 experimentally **ABV-2** infected birds. Mild and moderate gliosis was detected at early time points (32-84 dpi). However, one bird had no gliosis at early time points (32-84 dpi). At mid time points (86-172 dpi), only mild gliosis was detected. However, two birds had no gliosis at mid time points (86-172 dpi). At late time points at 230 dpi, only mild gliosis was also detected. However, two birds had no gliosis at 230 dpi. **After ABV-4 infection,** the kinetic of inflammatory lesions in the brain was mild and moderate in the 17/18 birds during the whole investigation period. However, one bird had severe inflammatory lesions in the brain at 116 dpi.

In the GIT, inflammatory lesions were detected in the crop as mild in 14/18 experimentally **ABV-2** infected birds. **After ABV-4 infection**, inflammatory lesions were detected in the crop as mild and moderate in 9/18 experimentally **ABV-4** infected birds. Inflammatory lesions were detected in the gizzard as mild and moderate in 15/18 experimentally **ABV-2** infected birds. Inflammatory lesions were detected in the gizzard as mild in 2/18, and moderate in 1/18 experimentally **ABV-4** infected birds. Inflammatory lesions were detected in the proventriculus in 13/18 experimentally **ABV-2** infected birds. Inflammatory lesions were detected in the proventriculus in 10/18 experimentally **ABV-4** infected birds. Inflammatory lesions were detected in the intestine in 14/18 experimentally **ABV-2** infected birds. Inflammatory lesions were detected in the intestine in 11/18 experimentally **ABV-4** infected birds.

After ABV-2 infection, there was variable correlation in severity between clinical signs and gross lesions with inflammatory lesions in the GIT. If birds exhibited clinical signs, and had dilatation of proventriculus, they also had inflammatory lesions in all GIT organs **after ABV-2 infection.** Moreover, if birds did not exhibit clinical signs, and did not display dilatation of proventriculus, they could also have inflammatory lesions in all GIT organs **after ABV-2 infection.**

After ABV-4 infection, the correlation between clinical signs and gross lesions with inflammatory lesions in the GIT was variable. If birds exhibited clinical signs, and had dilatation of proventriculus, they could also have inflammatory lesions in all GIT organs **after ABV-4 infection.** However, one bird had inflammatory lesions in some but not all GIT organs. Moreover, if birds did not exhibit clinical signs, and did not display dilatation of

proventriculus, they could also have inflammatory lesions in some of the GIT organs but not all **after ABV-4 infection**. However, one bird had no clinical signs, and exhibited dilatation of proventriculus and inflammatory lesions were detected only in the crop and proventriculus in this bird.

By comparison between kinetic of inflammatory lesions in the GIT, we found that inflammatory lesions in the GIT **after ABV-2 infection** were variable. Mild inflammatory lesions were detected in the crop, mild and moderate in the gizzard during the whole investigation period. Moreover, mild, moderate, and severe inflammatory lesions were detected in the proventriculus during the whole investigation period. Mild, moderate, and severe inflammatory lesions were detected in the intestine at early and mid time points 88-137 dpi but then decreased to mild inflammatory lesions in it at late time points at 231 dpi. **After ABV-4 infection**, we found that inflammatory lesions in the GIT were variable in severity at early and mid time points but then decreased at late time points 230 dpi in experimentally **ABV-4** infected birds (table 35).

In the peripheral organs, inflammatory lesions were predominantly detected in the liver, kidney, spleen and skin **after ABV-2 infection** (table 34) while inflammatory lesions were mainly detected in the, liver, kidney, heart, pancreas, and skin **after ABV-4 infection** (table 35). Inflammatory lesions were detected in neurons of the adjacent ganglia of the heart but not in the heart itself in 11/18 experimentally **ABV-2** infected birds. Inflammatory lesions were not only detected in neurons of the pericardial ganglia but also in the myocardium in 10/18 experimentally **ABV-4** infected birds. Inflammatory lesions were detected in the heart as mild and moderate in 13/18 experimentally **ABV-2** infected birds. Inflammatory lesions were detected in the heart as mild, moderate, and severe in 10/18 experimentally **ABV-4** infected birds. Inflammatory lesions were detected in the liver as mild and moderate in 14/18 experimentally **ABV-2** infected birds. Inflammatory lesions were detected in the liver as mild, moderate and severe in 13/18 experimentally **ABV-4** infected birds. Inflammatory lesions in the kidney and spleen did show the same severity **after ABV-2 infection** as in the kidney and spleen **after ABV-4 infection**. Inflammatory lesions were detected in the pancreas as mild in 5/18 experimentally **ABV-2** infected birds. Inflammatory lesions were detected in the pancreas as mild, moderate and severe in 10/18 experimentally **ABV-4** infected birds. Inflammatory lesions were detected in the skin as mild and moderate in 9/18 experimentally **ABV-2** infected birds. Inflammatory lesions were detected in the skin as mild, moderate and severe in 12/18 experimentally **ABV-4** infected birds.

There was variable correlation in severity between clinical signs and gross lesions with inflammatory lesions in the peripheral organs **after ABV-2 infection** and **after ABV-4 infection**. If birds exhibited clinical signs, and had dilatation of proventriculus, they could also have inflammatory lesions in the peripheral organs **after ABV-2 infection** and **after ABV-4 infection**. Moreover, if birds did not exhibit clinical signs, and did not display dilatation of proventriculus, they could also have inflammatory lesions in peripheral organs **after ABV-2 infection** and **after ABV-4 infection**. Nevertheless there were some exceptions, one bird (bird ID: 16) did not exhibit clinical signs, and displayed mild dilatation of proventriculus but inflammatory lesions were not detected in all the peripheral organs except in the kidney of this bird **after ABV-4 infection**. Another interesting finding, one bird (bird ID: 30) did not exhibit clinical signs, and did not display dilatation of proventriculus and severe inflammatory lesions were detected in the liver, kidney, pancreas, and skin of this bird **after ABV-4 infection**.

The kinetic of inflammatory lesion in the peripheral organs revealed that inflammatory lesions neither decreased nor increased in the heart, liver, spleen from early time points until late time points at 231 dpi **after ABV-2 infection**. Inflammatory lesions increased in the kidney at mid time point and at late time point **after ABV-2 infection**.

After ABV-4 infection, the kinetic of inflammatory lesion was variable in severity in the peripheral organs. For example in the heart, mild inflammatory lesions were detected in the heart at early time points **after ABV-4 infection**. However, inflammatory lesions were not found in the heart in one bird at early time points **after ABV-4 infection**. Mild inflammatory lesions were detected in the heart at mid time point **after ABV-4 infection**. However, inflammatory lesion were not found in the heart in two birds at mid time point **after ABV-4 infection**. Moreover, severe inflammatory lesion were detected in the heart in one bird at mid time point **after ABV-4 infection**. We also found the same variability in the kinetic of inflammatory lesions in the peripheral organs **after ABV-4 infection**.

Table 34: Scores of inflammatory lesions after ABV-2 infection

dpi	bird ID	CNS			Gastrointestinal organs				Peripheral organs							
		brain	s.cord	eye	crop	gizzard	prov.	intestine	heart	liver	kidney	spleen	pancreas	adrenal .g	skin	muscles
32	39	2	N.A	0	1	1	1	A	1	0	1	N.A	1	N.A	N.A	0
46	32	1	N.A	0	1	1	3	1	1	1	2	2	0	N.A	2	0
50	25	1	0	0	0	0	1	3	1	1	1	2	0	0	0	0
68	24	2	1	0	1	2	1	1	1	1	2	N.A	0	3	1	0
76	34	1	1	1	1	2	2	1	1	1	0	1	N.A	N.A	0	0
84	47	0	1	2	1	1	2	2	2	2	2	2	1	N.A	2	0
86	27	0	1	1	1	1	0	1	0	1	3	1	0	N.A	N.A	0
88	45	1	0	0	1	2	1	2	0	2	1	1	0	3	0	0
120	19	1	1	0	1	1	1	0	2	1	3	1	1	2	1	0
137	48	1	N.A	0	1	1	0	0	1	0	2	2	0	N.A	0	0
172	30	0	0	0	1	1	2	1	1	0	1	3	0	1	2	0
231	22	1	N.A	0	1	1	2	1	1	2	3	2	0	N.A	1	0
231	40	1	0	0	0	2	3	1	1	0	3	2	1	N.A	2	0
231	49	0	0	0	0	0	1	1	0	2	1	2	0	N.A	1	0
231	33	1	0	0	1	1	0	1	0	1	1	N.A	1	N.A	N.A	0
231	42	1	0	0	1	1	1	1	1	1	1	N.A	0	1	0	0
231	29	0	N.A	A	A	A	A	A	A	A	A	N.A	N.A	N.A	1	0
231	46	1	N.A	0	1	1	0	1	1	1	2	0	1	N.A	0	0

CNS= central nervous system, s.cord= spinal cord, N.A= not available, Prov.= proventriculus, dpi= days post infection, A= autolytic organ, = CNS, = GIT, = peripheral organs

Table 35: Scores of inflammatory lesions after ABV-4 infection

dpi	bird ID	CNS			Gastrointestinal organs				Peripheral organs							
		brain	s.cord	eye	crop	gizzard	prov.	intestine	heart	liver	kidney	spleen	pancreas	adrenal .g	skin	muscles
60	15	1	1	N.A	1	1	3	3	1	3	3	N.A	2	N.A	0	0
66	21	2	N.A	0	1	0	1	2	0	0	1	2	0	N.A	0	0
115	16	2	0	2	1	0	2	0	0	0	1	N.A	0	N.A	0	0
115	19	1	1	2	0	0	2	3	3	2	N.A	2	1	N.A	2	0
115	26	1	1	2	0	1	1	1	0	1	3	1	1	1	1	0
116	13	2	N.A	2	1	2	1	2	0	1	0	1	N.A	N.A	2	1
116	18	3	N.A	1	2	A	A	2	1	3	2	3	1	N.A	1	0
116	25	1	1	2	2	0	1	0	1	1	3	2	1	N.A	1	0
120	12	1	N.A	0	N.A	N.A	0	1	1	0	0	3	0	1	0	0
206	11	2	N.A	1	1	0	0	1	1	1	1	2	2	N.A	0	0
229	10	2	2	1	N.A	N.A	N.A	N.A	1	1	2	2	0	N.A	1	0
229	22	1	1	0	1	A	3	3	1	1	2	2	N.A	N.A	3	0
229	23	1	2	0	0	0	A	A	2	1	1	N.A	1	N.A	1	0
229	27	1	1	0	0	0	0	1	0	0	1	2	1	N.A	2	0
229	29	2	1	1	1	0	1	0	1	2	2	N.A	N.A	N.A	1	0
230	20	1	1	0	0	0	1	0	0	1	2	3	0	N.A	2	0
230	24	N.A	1	0	N.A	0	0	0	0	0	3	3	1	N.A	0	0
230	30	2	N.A	N.A	2	N.A	N.A	3	N.A	3	3	N.A	3	N.A	3	N.A

CNS= central nervous system, s.cord= spinal cord, N.A= not available, Prov.= proventriculus, dpi= days post infection, = CNS, = GIT, = peripheral organs

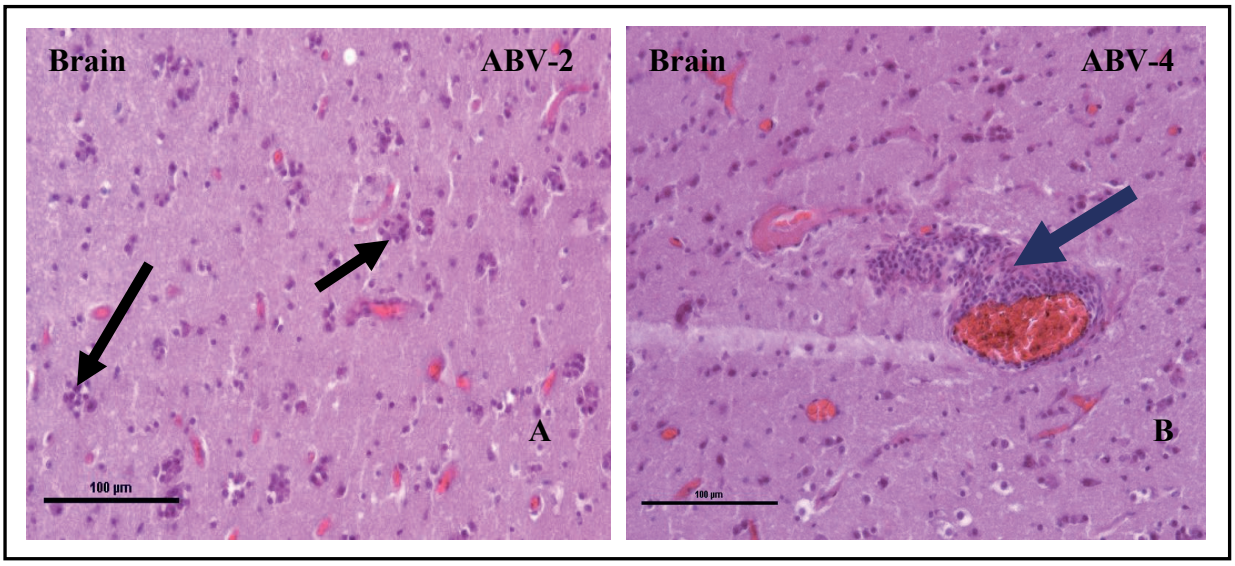

Fig. 9: Inflammatory lesions in the brain after experimental infection with ABV-2 and ABV-4 in cockatiels. (A) Gliosis, after ABV-2 infection (black arrow), 68 dpi. (B) Perivascular infiltrates in the brain after ABV-4 infection (blue arrow), 60 dpi. H & E staining. Scale bar 100µm.

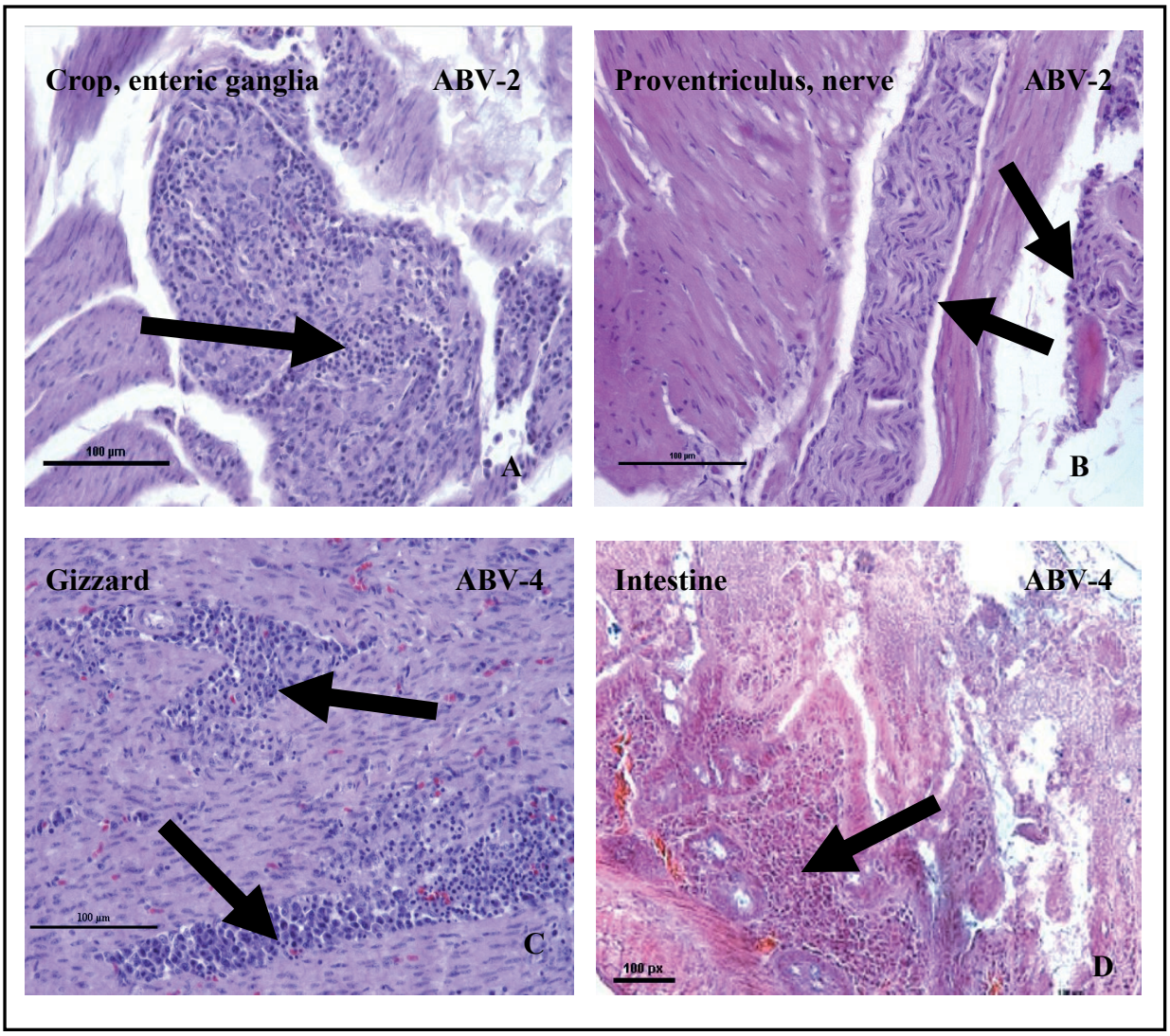

Fig. 10: Inflammatory lesions in the GIT organs after experimental infection with ABV-2 and ABV-4 in cockatiels. (A) Periganglionic infiltration of mononuclear cells in the enteric ganglia of the crop after ABV-2 infection (arrow), 86 dpi. (B) Perineural infiltration of mononuclear cells in the nerve of proventriculus after ABV-2 infection (arrow), 172 dpi. (C) Gizzard, infiltration of mononuclear cells in lamina muscularis after ABV-4 infection (arrow), 116 dpi. (D) Intestine, follicular shape-like aggregation of immune cells in the intestinal mucosa after ABV-4 infection (arrow), 115 dpi. H & E staining. Scale bar 100µm.

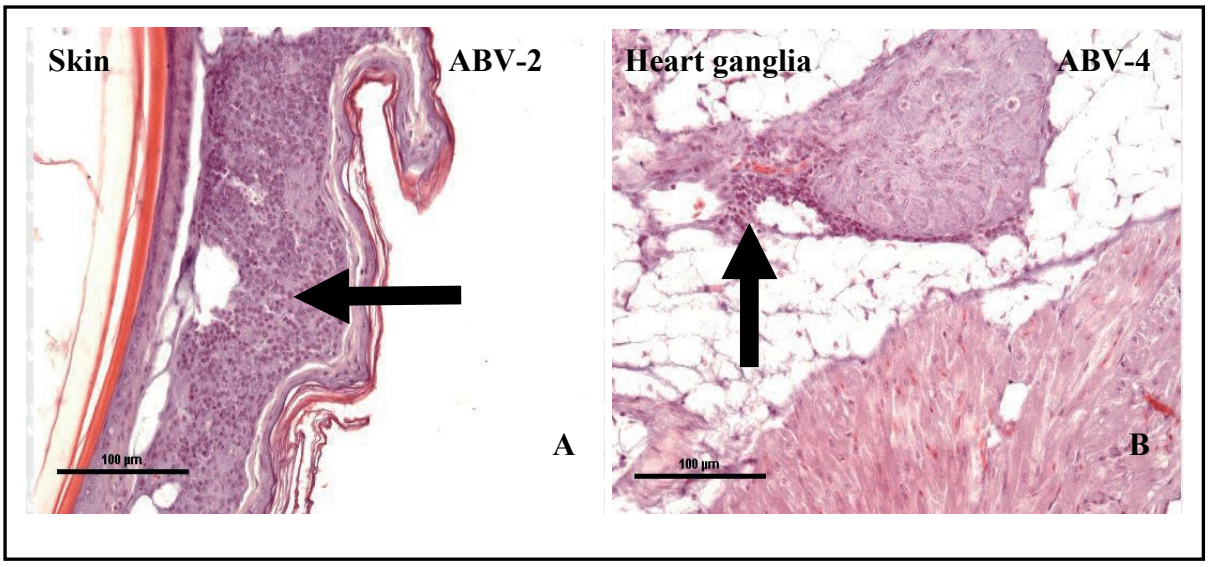

Fig. 11: Inflammatory lesions in the peripheral organs after experimental infection with ABV-2 and ABV-4 in cockatiels. (A) Skin, infiltration of mononuclear cells around feather follicles after ABV-2 infection (arrow), 231 dpi. (B) Heart ganglia, infiltration of mononuclear cells around heart ganglia after ABV-4 infection (arrow), 229 dpi. H & E staining. Scale bar 100µm.

4.4. Characterization of the infiltrating immune cells after ABV infection

By IHC, we characterized the immune cell infiltration in all organs after ABV-2 and ABV-4 infection. We detected CD3-positive cells in the GIT and peripheral organs but not in the CNS after ABV-2 infection (**Fig. 12**). Moreover, we detected CD3-positive cells in the CNS, GIT and peripheral organs after ABV-4 infection (**Fig. 12**). We detected infiltrations of CD3-positive cells in the brain after ABV-4 infection as well as in gizzard, proventriculus and intestine after ABV-2 and ABV-4 infection and in kidney, liver and skin after ABV-2 and ABV-4 infection (**Fig. 12**). The identification of cockatiel B cells and macrophage was not successful because B cells and macrophage markers did not cross react with cockatiel immune cells by immunohistochemistry.

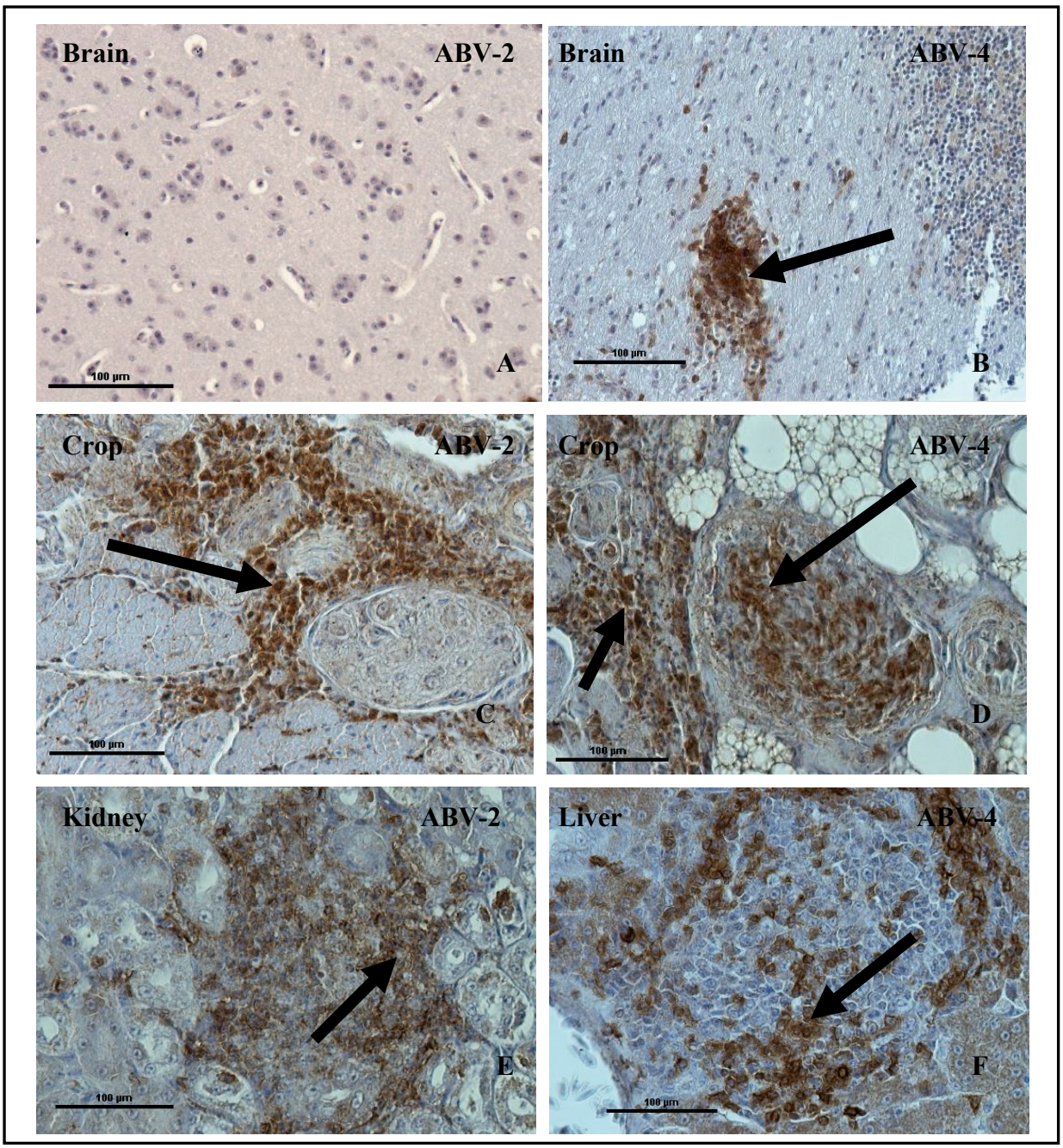

Fig. 12: Demonstration of CD3-positive cells in the brain, GIT and peripheral organs of experimentally ABV-2 and ABV-4 infected birds by IHC. (A) Brain, CD3-positive cells were not found after ABV-2 infection, 137 dpi. (B) Brain, CD3-positive cells found in the perivascular cuffing in it, ABV-4 infection, 116 dpi. (C) Crop, CD3-positive cells found around ganglia in the lamina muscularis, ABV-2 infection (arrow), 172 dpi. (D) Crop, CD3-positive cells found in / and around ganglia in the lamina muscularis, ABV-4 infection, 116 dpi. (E) Kidney, CD3-positive cells found in the follicular shape-like infiltrates, ABV-2 infection, 86 dpi. (F) Liver, CD3-positive cells found in the follicular shape-like infiltrates, ABV-4 infection (arrow), 230 dpi. Polyclonal rabbit anti-human CD3 antibody, DAB staining, Papanicolaou counterstaining, Scale bar 100µm.

4.5. Demonstration of ABV antigen

4.5.1. Distribution pattern of ABV antigen after ABV-2 infection

In the CNS, viral antigen was detected in the brain in 14/18, in the spinal cord in 3/18 birds and in the eye in 9/18 experimentally ABV-2 infected birds (table 36). Viral antigen was detected in the nucleus and/or cytoplasm of neurons (**Fig. 13**) as well as in nerve fibers or cellular processes of neurons of the cerebrum or cerebellum e.g. Purkinje cells and also glial cells (**Fig. 13**). Viral antigen was also detected in the neurons of retina and in the optic nerve in the eye (**Fig. 14**). ABV antigen was found at the first time points investigated at 46 dpi until the end of the investigation period.

Viral antigen was not detected in the brain in 4/18 birds but was detected as score 1 in 7/18 birds, score 2 in 6/18 birds and score 3 in 1/18 birds (table 36). Viral antigen was not detected in the spinal cord in 1/18 birds but was detected as score 1 in 2/18 birds, and score 3 in 1/18 birds (table 36). Spinal cord was not available in 14/18 experimentally ABV-2 infected birds (table 36). Viral antigen was not detected in the eye in 8/18 birds but was detected as score 1 in 5/18 birds, score 2 in 1/18 bird and score 3 in 3/18 birds (table 36). The eye was autolytic in 1/18 birds.

The kinetic of viral antigen detection in the CNS revealed variability (table 36). In the brain, viral antigen was detected as score 1 and score 2 during the whole investigation period. However, some variability in detection of viral antigen in the brain was also found. Viral antigen was not detected in the brain in two birds at early time points 46-86 dpi, in one bird at mid time points 88-137 dpi, and in one bird at late time points 231 dpi. The kinetic of viral antigen detection in the eye was also variable. It was not detected in the eye at early time points 46-86 dpi, then it was detected as score 1 up to score 3 at mid time points 88-137 dpi and at late time points 231 dpi. However, viral antigen was not detected in the eye in 2 birds at mid time points and in one bird at late time points. In the spinal cord, it was not possible to investigate the kinetic of viral antigen detection in it due to unavailability of spinal cord in 14/18 birds (table 36).

In the GIT, viral antigen was detected in all GIT organs mainly in gizzard and proventriculus. Nucleus and cytoplasm of neurons of the enteric ganglia in the lamina muscularis of gizzard (**Fig. 15**) and proventriculus and also nerve fibers mainly harbored viral antigen. Nucleus of the epithelium of the crop, the glandular epithelium of gizzard as well as of the proventriculus and smooth muscle fibers in the lamina muscularis of all GIT organs also showed positive immunostaining.

Viral antigen was not detected in the crop in 1/18 birds but was found as score 1 in 10/18 birds, score 2 in 5/18 birds and score 3 in 1/18 bird (table 36). The crop was autolytic in 1/18 birds. Viral antigen was detected in the gizzard as score 1 in 8/18 birds, score 2 in 6/18 birds and score 3 in 1/18 bird (table 36). The gizzard was autolytic in 1/18 birds. The gizzard was not available in 2/18 birds. Viral antigen was detected in the proventriculus as score 1 in 10/18 birds, score 2 in 5/18 birds and score 3 in 2/18 birds (table 36). The proventriculus was autolytic in 1/18 birds. Viral antigen was not detected in the intestine in 7/18 birds but was detected as score 1 in 6/18 birds, score 2 in 1/18 bird and score 3 in 2/18 birds (table 36). The intestine was autolytic in 2/18 birds.

The kinetic of viral antigen detection in the GIT revealed that viral antigen detection was detected as score 1 and score 2 in all GIT organs during the whole investigation period 231 dpi. However, some variability was also found in detection of viral antigen in the GIT organs. Viral antigen was not found in the crop in 1/18 bird at early time points (46-86 dpi). In another bird at late time points 231 dpi, viral antigen was detected in the crop as score 3 in 1/18 bird. Viral antigen was found in the gizzard as score 3 in 1/18 bird at 231 dpi. Viral antigen was found in the proventriculus as score 3 in 1/18 bird at mid time points (88-137 dpi) and as score 3 in 1/18 bird at late time points at 231 dpi.

In the peripheral organs, viral antigen was detected in the heart, liver, kidney, pancreas, and skin. Viral antigen detection was detected in liver cells, neurons of adjacent ganglia in the heart (**Fig. 16**) and nerve fibers, epithelium of renal tubules, epithelial cells of the pancreas, cells with features of red pulp macrophages in the spleen, epithelial cells around feather follicles in the skin, and muscle fibers and nuclei in the heart and muscle fibers in the skeletal muscles.

Viral antigen was not detected in the heart in 5/18 birds but it was detected as score 1 in 11/18 birds, and score 2 in 1/18 birds (table 36). The heart was autolytic in 1/18 birds. Viral antigen was not detected in the liver in 10/18 birds but was detected as score 1 in 6/18 birds, and score 2 in 1/18 birds (table 36). The liver was autolytic in 1/18 birds. Viral antigen was not detected in the kidney in 5/18 birds but it was detected as score 1 in 1/18 birds, score 2 in 7/18 birds and score 3 in 4/18 birds (table 36). The kidney was autolytic in 1/18 birds. Viral antigen was detected in the spleen as score 1 in 4/18 birds, and score 2 in 3/18 birds (table 36). The spleen was not available in 11/18 birds. Viral antigen was not detected in the pancreas in 1/18 birds but was detected as score 1 in 9/18 birds and score 2 in 6/18 birds (table 36). The pancreas was not available in 2/18 birds. Viral antigen was detected in the adrenal gland as score 2 in 2/18 birds, and score 3 in 1/18 bird. Adrenal gland was not available in 15/18 birds. Viral antigen was not detected in the skin in 6/18 birds but was detected as score 1 in 6/18 birds,

score 2 in 2/18 birds and score 3 in 1/18 birds (table 36). The skin was not available in 3/18 birds. Viral antigen was not detected in the skeletal muscles in 16/18 experimentally ABV-2 infected birds. Viral antigen was found in muscle fibers of the skeletal muscles as score 1 in 2/18 birds.

The kinetic of viral antigen detection in the peripheral organs revealed variability. Viral antigen increased in the liver and kidney at late time points 231 dpi. Moreover, it increased in the skin at only mid time points 88-137 dpi. It was detected in the heart as score 1, and in the pancreas as score 1 and score 2 during the whole investigation period. Viral antigen was detected in the heart as score 3 in 1/18 bird at late time points. Viral antigen was not detected in the liver at early time points 46-86 dpi but was detected as score 1 in only 1/18 bird at early time points.

In the sentinel group, viral antigen was not found in the CNS. Viral antigen was not detected in the nerves or enteric ganglia of all GIT organs in the sentinel bird. Viral antigen was not detected in the nerves or ganglia of the heart, kidney, skin as well as in the skeletal muscles in the sentinel.

In the mock group, viral antigen was not found in the CNS in all birds of the mock group. Viral antigen was not detected in the nerves or enteric ganglia of all GIT organs in the mock group. Moreover, viral antigen detection was not found in the nerves or ganglia in all peripheral organs in the mock group.

Unspecific background of the polyclonal anti-p24 antibody was also obtained in the intestinal epithelium and smooth muscle fibers only in 2/4 mock birds.

4.5.2. Distribution pattern of ABV antigen after ABV-4 infection

In the CNS, viral antigen was detected in the brain in 17/18, in the spinal cord in 11/18 and in the eye in 9/18 experimentally ABV-4 infected birds (table 37). Viral antigen was detected intranuclearly or intracytoplasmically in the neurons (**Fig.13**). It was also detected in nerve fibers and/or cellular processes of neurons of the cerebrum or cerebellum e.g. Purkinje cells, and glial cells (**Fig. 14**), in the neurons of retina and in the optic nerve in the eye (**Fig.14**). ABV antigen was found at the first time points investigated at 60 dpi until the end of the investigation period at 230 dpi.

Viral antigen was detected in the brain as score 1 in 9/18 birds, score 2 in 7/18 birds and score 3 in 1/18 experimentally ABV-4 infected birds (table 37). The brain was not available in 1/18 birds. Viral antigen was not detected in the spinal cord in 1/18 but was detected as score 1 in 9/18 birds, score 2 in 2/18 birds. Spinal cord was not available in 6/18 birds (table 37). Viral antigen was not detected in the eye in 7/18 birds but was detected as score 1 in 3/18 birds,

score 2 in 5/18 bird and score 3 in 1/18 birds. The eye was not available in 2/18 birds (table 37).

The kinetic of viral antigen detection in the CNS was variable. Viral antigen was detected in the brain as score 1 and score 2 during the whole investigation period. However, viral antigen detection was detected as score 3 in the brain in 1/18 birds at mid time points 116 dpi. In the spinal cord, viral antigen was detected as score 1 from early time points at 60 and 66 dpi until late time points at 230 dpi. However, viral antigen was detected as score 2 in the spinal cord in 2/18 birds at 229 dpi. The kinetic of viral antigen detection in the eye revealed as score 2 at early and mid time points, then decreased at late time points.

In the GIT, viral antigen was detected in all GIT organs mainly in intestine and proventriculus. Nucleus and cytoplasm of neurons of the enteric ganglia in the lamina muscularis of gizzard and proventriculus and also nerve fibers mainly harbored viral antigen. Nucleus of the epithelium of all GIT organs and smooth muscle fibers in the lamina muscularis of all GIT organs could also harbor viral antigen (**Fig. 15**).

Viral antigen was not detected in the crop in 5/18 birds but it was found as score 1 in 7/18 birds, score 2 in 3/18 birds (table 37). The crop was not available in 3/18 birds. Viral antigen was not detected in the gizzard in 9/18 birds but it was found as score 1 in 2/18 birds and score 2 in 2/18 birds. The gizzard was not available in 3/18 birds. The gizzard was autolytic in 1/18 birds. Viral antigen was not detected in the proventriculus in 3/18 birds but it was found as score 1 in 6/18 birds, score 2 in 3/18 birds, and score 3 in 2/18 birds (table 37). The proventriculus was not available in 2/18 birds. The proventriculus was autolytic in 2/18 birds. Viral antigen was not detected in the intestine in 5/18 birds but it was found as score 1 in 4/18 birds, score 2 in 3/18 birds, and score 3 in 4/18 birds (table 37). The intestine was not available in 1/18 birds. The intestine was autolytic in 1/18 birds.

The kinetic of viral antigen detection in the GIT revealed that viral antigen was decreased in all GIT organs at late time points at 230 dpi in most majority of birds or could be negative in experimentally ABV-4 infected birds.

In the peripheral organs, viral antigen was mainly detected in the heart, liver, kidney and spleen. Viral antigen detection was detected in liver cells, neurons of adjacent ganglia in the heart (**Fig. 16**) and nerve fibers, smooth muscle layer in the aorta, epithelium of renal tubules, epithelial cells of the pancreas, cells with features of red pulp macrophages in the spleen, epithelial cells around feather follicles in the skin, and muscle fibers and nuclei in the heart and muscle fibers in the skeletal muscles.

Viral antigen was not detected in the heart in 7/18 birds but it was found as score 1 in 8/18 birds, score 2 in 1/18 birds and score 3 in 1/18 birds (table 37). The heart was not available in 1/18 birds. Viral antigen was not detected in the liver in 5/18 birds but it was found as score 1 in 7/18 birds, score 2 in 2/18 birds and score 3 in 4/18 birds (table 37). Viral antigen was not detected in the kidney in 2/18 birds but it was found as score 1 in 4/18 birds, score 2 in 6/18 birds and score 3 in 5/18 birds (table 37). The kidney was not available in 1/18 birds. Viral antigen detection was detected in the spleen as a score 1 in 2/18 birds, score 2 in 7/18 birds and score 3 in 4/18 birds (table 37). The spleen was not available in 5/18 birds. Viral antigen was not detected in the pancreas in 5/18 birds but it was found as score 1 in 7/18 birds, score 2 in 1/18 birds and score 3 in 1/18 birds (table 37). The pancreas was not available in 4/18 birds. Viral antigen was detected in the adrenal gland as score 1 in 2/18 birds. Adrenal gland was not available in 16/18 birds. Viral antigen was not detected in the skin in 5/18 birds but it was found as score 1 in 7/18 birds, score 2 in 4/18 birds and score 3 in 2/18 birds (table 37). Viral antigen was not detected in the skeletal muscles in 15/18 birds. Viral antigen was only detected in muscle fibers in 2/18 experimentally ABV-4 infected birds. Skeletal muscles were not available in 1/18 birds.

The kinetic of viral antigen in the peripheral organs revealed variability. Viral antigen was detected in the liver, kidney, and spleen as score 1, score 2, and score 3 during the whole investigation period at 230 dpi. Viral antigen was detected in the pancreas as score 1 during the whole investigation period of 230 dpi in most of majority of birds. However, it was detected in the pancreas as score 2 in 1/18 birds at early time points and as score 3 at late time points. Viral antigen was not detected in the skin at early time points but was found as score 1 and score 2 at mid time points and then increased up to score 3 at late time points.

In the sentinel group, viral antigen was not found in the CNS. Viral antigen was not detected in the nerves or enteric ganglia of all GIT organs in the sentinel bird. Viral antigen was not detected in the nerves or ganglia of the heart, liver, kidney, skin as well as skeletal muscles in the sentinel.

4.5.3. Comparison of ABV antigen distribution after ABV-2 and ABV-4 infection

In the CNS, viral antigen detection was detected in the CNS at the first time point investigated at 46 dpi until the end of the investigation period at 231 dpi **after ABV-2 infection**. Viral antigen was not detected in the brain in 4/18 birds but viral antigen detection was detected as score 1 and score 2 in 13/18 birds and score 3 in 1/18 birds during the whole investigation period **after ABV-2 infection**.

Viral antigen was detected in the CNS at the first time point investigated at 60 dpi until the end of the investigation period at 230 dpi after ABV-4 infection. Viral antigen was detected in the brain as score 1 and score 2 in 16/18 birds and score 3 in 1/18 birds during the whole investigation period **after ABV-4 infection**. The brain was not available in 1/18 birds **after ABV-4 infection**.

The distribution of viral antigen detection in the CNS was the same and also intracellular localization was the same **after ABV-2 infection** and **after ABV-4 infection**. Viral antigen was distributed and detected in neurons, glial cells, Purkinje cells in the cerebrum or cerebellum as well as in neurons of retina and in the optic nerve in the eye **after ABV-2 infection** and **after ABV-4 infection**.

The kinetic of viral antigen detection in the CNS revealed that viral antigen detection was detected as score 1 and score 2 during the whole investigation period after **ABV-2 infection** and **after ABV-4 infection**. Nevertheless, viral antigen was not detected in the brain in 2/18 birds at early time points 46-86 dpi, in 1/18 bird at mid time points 88-137 dpi, and in 1/18 bird at late time points 231 dpi **after ABV-2 infection**.

There was variable correlation between clinical signs, gross lesions with viral antigen detection in the CNS **after ABV-2 infection**. If birds exhibited gastrointestinal and/or neurological signs, and had moderate to severe dilatation of proventriculus, they could have viral antigen in the CNS **after ABV-2 infection**. However, 1/18 birds did not exhibit clinical signs, and had not dilatation of proventriculus but viral antigen was detected in the brain as score 3 at 231 dpi **after ABV-2 infection**. If birds did not exhibit clinical signs, and did not display dilatation of proventriculus, they could also have viral antigen in the CNS **after ABV-2 infection**.

After ABV-4 infection, there was variable correlation between clinical signs, gross lesions with viral antigen detection in the CNS. If birds exhibited gastrointestinal and/or neurological signs, and had dilatation of proventriculus, they could have viral antigen in the CNS after ABV-4 infection. If birds did not exhibit clinical signs, and did not display dilatation of proventriculus, they could also have viral antigen in the CNS after ABV-4 infection.

In the GIT, viral antigen was detected in all GIT organs mainly in gizzard and proventriculus **after ABV-2 infection**. Viral antigen was detected as score 1 and score 2 in all GIT organs during the whole investigation period in most majority of birds after ABV-2 infection. However, an exception in detection of viral antigen in the GIT was also found. For example in the intestine, viral antigen was detected in it as score 3 in 1/18 bird at early time points, and as score 3 in 2/18 birds at late time points after ABV-2 infection.

After ABV-4 infection, viral antigen was detected in all GIT organs mainly in intestine and proventriculus. Viral antigen was detected as score 1, score 2 in the crop and gizzard at early time points and mid time points after ABV-4 infection. Moreover, viral antigen was detected as score 1, score 2, and score 3 in the intestine and proventriculus at early time points and mid time points after ABV-4 infection. Viral antigen was not found in the gizzard at late time points 230 dpi after ABV-4 infection.

The distribution of viral antigen detection in the GIT was the same and also intracellular localization was the same **after ABV-2 infection** and **after ABV-4 infection**. Viral antigen was distributed and detected in neurons of the enteric ganglia of the GIT, nerve fibers and smooth muscle vessels, GIT epithelium, and smooth muscle fibers of the GIT.

The kinetic of viral antigen detection in the GIT revealed that viral antigen was detected as score 1 and score 2 during the whole investigation period **after ABV-2 infection**. **After ABV-4 infection**, viral antigen detection decreased in all GIT organs at late time points of 230 dpi in most majority of birds.

After ABV-2 infection, there was no clear correlation between clinical signs, gross lesions with viral antigen detection in the GIT. If birds exhibited gastrointestinal and/or neurological signs, and had moderate to severe dilatation of proventriculus, they could also viral antigen as score 1 and score 2 in the GIT after ABV-2 infection. However, 4/18 birds exhibit gastrointestinal and/or neurological signs, and had dilatation of proventriculus but viral antigen was detected in the GIT as score 3 after ABV-2 infection. If birds did not exhibit clinical signs, and did not display dilatation of proventriculus, they could also have viral antigen in the GIT after ABV-2 infection.

After ABV-4 infection, there was no clear correlation between clinical signs, gross lesions with viral antigen detection in the GIT. If birds exhibited gastrointestinal and/or neurological signs, and had moderate to severe dilatation of proventriculus, they could also viral antigen as score 1 and score 2 in the GIT after ABV-4 infection. If birds did not exhibit clinical signs, and did not display dilatation of proventriculus, they could also have viral antigen in some but

not all GIT organs after ABV-4 infection. However, viral antigen detection was detected as score 2 and score 3 in the GIT in 1/18 bird without exhibiting clinical and gross lesions.

In the peripheral organs, viral antigen was predominantly detected in the heart, liver, kidney, pancreas, spleen and skin **after ABV-2 infection** (table 36) while viral antigen was mainly detected in the heart, liver, kidney and spleen **after ABV-4 infection** (table 37). Viral antigen was detected in neurons of the adjacent ganglia but not in the heart itself in 12/18 birds **after ABV-2 infection**. **After ABV-4 infection**, viral antigen detection was not only found in neurons of the pericardial ganglia but also in muscle fibers and smooth muscle layer in the aorta, myocardial fibers and Purkinje fibers in 10/18 birds.

Viral antigen was detected in the liver at early time points and mid time points in only 1/18 bird and in 2/18 birds at mid time points **after ABV-2 infection**. Viral antigen was not detected in the liver in 10/18 birds **after ABV-2 infection**. **After ABV-4 infection**, viral antigen was detected in the liver as score 1, score 2, and score 3 during the whole investigation period 230 dpi in most majority of birds in 18/18 birds **after ABV-4 infection**.

By comparison between kinetic of viral antigen detection in the peripheral organs, we found that viral antigen detection decreased in all the peripheral organs at late time point 231dpi in most majority of birds **after ABV-2 infection**. **After ABV-4 infection**, viral antigen detection increased in all the peripheral organs at mid time points 88-137 dpi until late time points 231 dpi in most majority of experimentally **ABV-4** infected birds.

After ABV-2 infection, the correlation between clinical signs, gross lesions with viral antigen detection in the peripheral organs was variable. If birds exhibited gastrointestinal and/or neurological signs, and had moderate to severe dilatation of proventriculus, they could also have viral antigen in the heart, kidney, pancreas, skin but not in the liver at early time points. If birds did not exhibit clinical signs, and did not display dilatation of proventriculus, they could also have viral antigen in all the peripheral organs mainly in kidney, pancreas, and skin **after ABV-2 infection**.

After ABV-4 infection, the correlation between clinical signs, gross lesions with viral antigen detection in the peripheral organs was also variable. If birds exhibited gastrointestinal and/or neurological signs, and had moderate to severe dilatation of proventriculus, they could also have viral antigen in the heart, liver, kidney, spleen, and pancreas but not in the skin at early time points. If birds did not exhibit clinical signs, and did not display dilatation of proventriculus, they could also have viral antigen in all the peripheral organs mainly in kidney, liver, and spleen **after ABV-4 infection**.

Table 36: Scores of viral antigen detection after ABV-2 infection

dpi	bird ID	CNS			Gastrointestinal organs				Peripheral organs							
		brain	s.cord	eye	crop	gizzard	prov.	intestine	heart	liver	kidney	spleen	pancreas	adrenal .g	skin	muscles
32	39	1	N.A	0	0	1	1	A	1	0	0	N.A	1	N.A	N.A	0
46	32	0	1	0	1	1	1	0	1	0	2	N.A	1	N.A	1	0
50	25	1	1	0	1	N.A	1	0	0	0	0	2	N.A	N.A	0	0
68	24	2	0	0	2	2	1	1	0	0	2	N.A	1	N.A	1	0
76	34	0	N.A	1	1	2	1	1	1	0	0	N.A	0	N.A	0	0
84	47	2	N.A	0	1	2	2	0	0	1	0	2	2	N.A	0	0
86	27	1	N.A	3	2	1	2	3	1	0	3	N.A	2	N.A	N.A	0
88	45	0	N.A	0	2	1	3	0	1	1	0	1	1	N.A	0	0
120	19	2	N.A	1	1	2	1	1	1	1	2	N.A	2	3	1	0
137	48	2	N.A	0	1	1	1	0	1	0	1	N.A	2	N.A	0	0
172	30	1	N.A	3	2	1	1	3	0	0	2	1	1	2	1	0
231	22	2	N.A	1	1	2	2	1	1	0	3	1	1	N.A	2	1
231	40	1	N.A	2	2	2	2	1	1	1	3	2	2	N.A	3	1
231	49	3	N.A	0	1	1	1	0	1	0	2	N.A	1	N.A	1	0
231	33	1	N.A	1	1	N.A	2	0	0	1	2	N.A	1	N.A	N.A	0
231	42	2	3	1	1	1	1	1	1	1	2	N.A	1	2	0	0
231	29	0	N.A	A	A	A	A	A	A	A	A	N.A	N.A	N.A	1	0
231	46	1	N.A	3	3	3	3	2	2	2	3	1	2	N.A	2	0

CNS= central nervous system, s.cord= spinal cord, N.A= not available, Prov.= proventriculus, dpi= days post infection, A= autolytic organ, = CNS, = GIT, = peripheral organs

Table 37: Scores of viral antigen detection after ABV-4 infection

dpi	bird ID	CNS			Gastrointestinal organs				Peripheral organs							
		brain	s.cord	eye	crop	gizzard	prov.	intestine	heart	liver	kidney	spleen	pancreas	adrenal .g	skin	muscles
60	15	1	1	N.A	1	1	3	3	1	3	3	N.A	2	N.A	0	0
66	21	2	N.A	0	1	0	1	2	0	0	1	2	0	N.A	0	0
115	16	2	0	2	1	0	2	0	0	0	1	N.A	0	N.A	0	0
115	19	1	1	2	0	0	2	3	3	2	N.A	2	1	N.A	2	0
115	26	1	1	2	0	1	1	1	0	1	3	1	1	1	1	0
116	13	2	N.A	2	1	2	1	2	0	1	0	1	N.A	N.A	2	1
116	18	3	N.A	1	2	A	A	2	1	3	2	3	1	N.A	1	0
116	25	1	1	2	2	0	1	0	1	1	3	2	1	N.A	1	0
120	12	1	N.A	0	N.A	N.A	0	1	1	0	0	3	0	1	0	0
206	11	2	N.A	3	1	2	2	1	1	3	2	2	N.A	N.A	1	1
229	10	2	2	1	N.A	N.A	N.A	N.A	1	1	2	2	0	N.A	1	0
229	22	1	1	0	1	A	3	3	1	1	2	2	N.A	N.A	3	0
229	23	1	2	0	0	0	A	A	2	1	1	N.A	1	N.A	1	0
229	27	1	1	0	0	0	0	1	0	0	1	2	1	N.A	2	0
229	29	2	1	1	1	0	1	0	1	2	2	N.A	N.A	N.A	1	0
230	20	1	1	0	0	0	1	0	0	1	2	3	0	N.A	2	0
230	24	N.A	1	0	N.A	0	0	0	0	0	3	3	1	N.A	0	0
230	30	2	N.A	N.A	2	N.A	N.A	3	N.A	3	3	N.A	3	N.A	3	N.A

CNS= central nervous system, s.cord= spinal cord, N.A= not available, Prov.= proventriculus, dpi= days post infection, A= autolytic organ, = CNS, = GIT, = peripheral organs

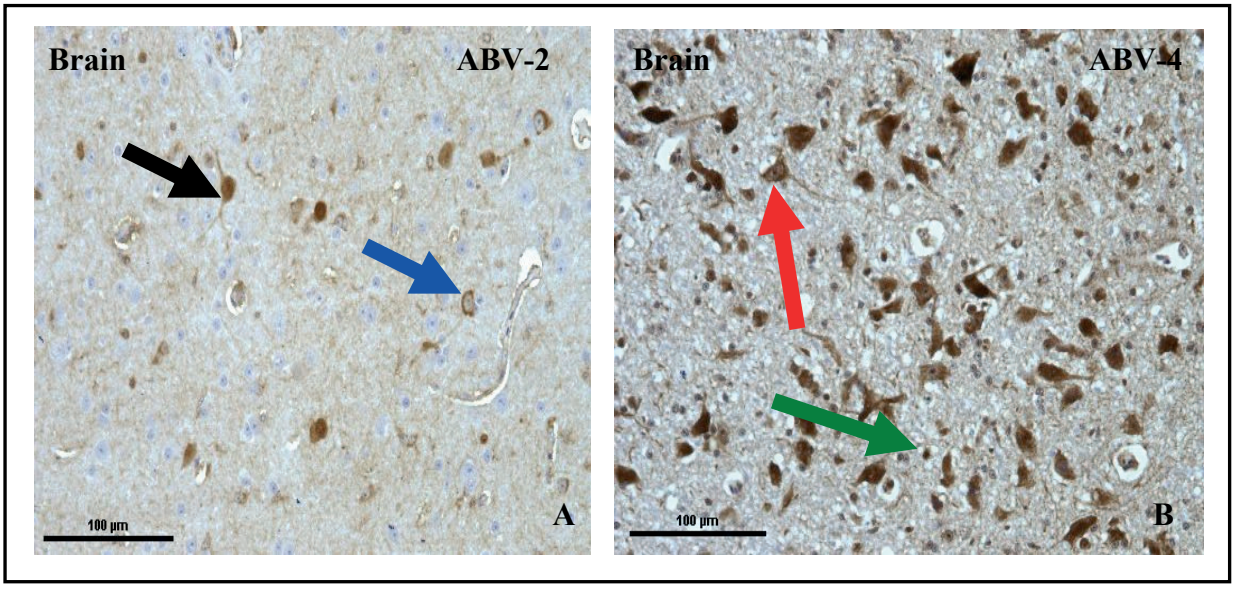

Fig. 13: Demonstration of ABV antigen in the brain by IHC. (A) Cerebrum, viral antigen was found in the nucleus (black arrow) and cytoplasm (blue arrow) of neurons after ABV-2 infection, 84 dpi. (B) Cerebrum, viral antigen found in the nucleus of neurons (red arrow) and in glial cells (green arrow) after ABV-4 infection, 60 dpi. Polyclonal rabbit anti-BoDV-P (p24) antibody, DAB staining, Papanicolaou counterstaining. Scale bar 100µm.

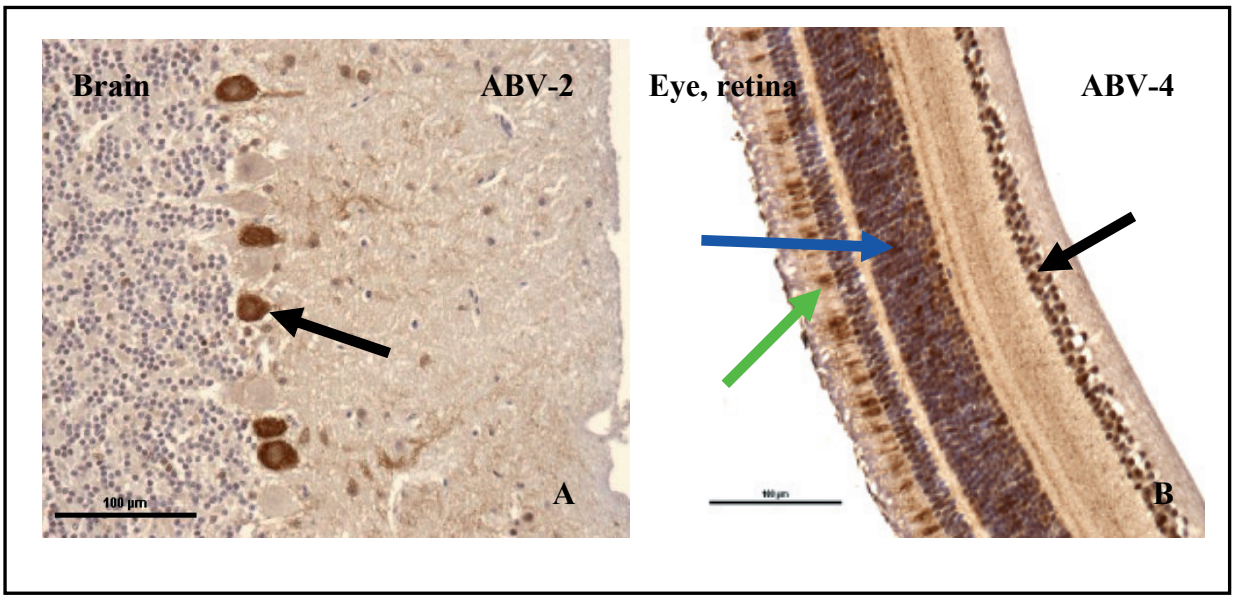

Fig. 14: Demonstration of ABV antigen in the CNS by IHC. (A) Cerebellum, viral antigen was found in Purkinje neurons after ABV-2 infection (arrow), 120 dpi. (B) Eye, retina, viral antigen found in neurons of retina in different layers, in nerve fiber layer (green arrow), photoreceptors (black arrow), and in the neurons located in the outer nuclear layers of the retina (blue arrow), 115 dpi. Polyclonal rabbit anti-BoDV-P (p24) antibody, DAB staining, Papanicolaou counterstaining. Scale bar 100µm.

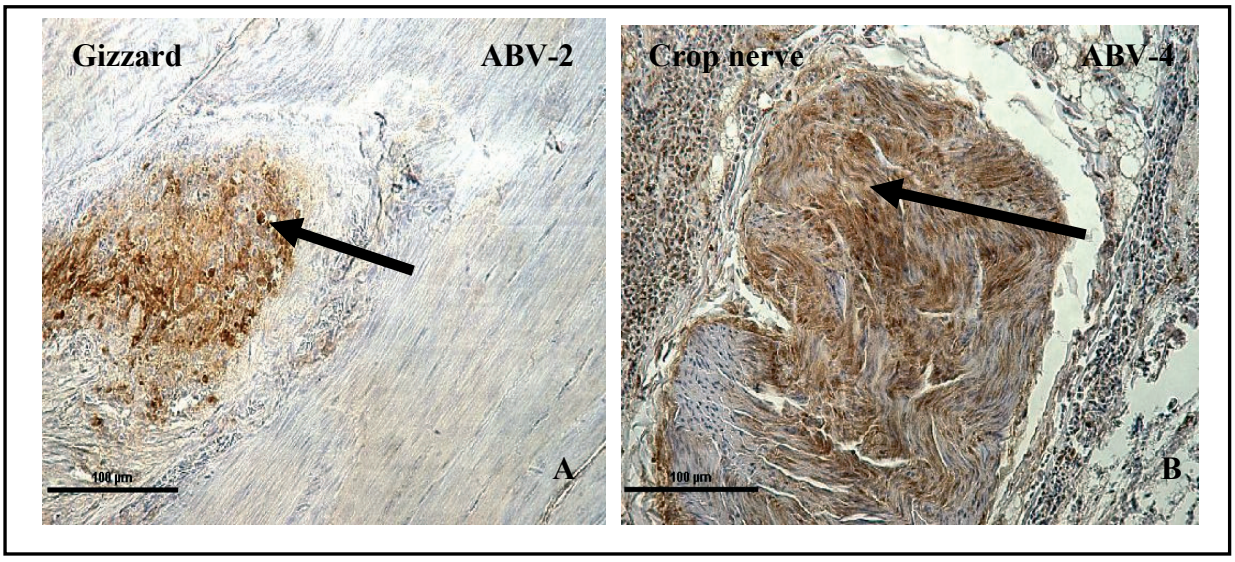

Fig. 15: Demonstration of ABV antigen in the GIT by IHC. (A) Gizzard, viral antigen was found in neurons of enteric ganglia after ABV-2 infection (arrow), 137 dpi. (B) Crop nerve, viral antigen found in the nerve of the crop after ABV-4 infection (arrow), 116 dpi. Polyclonal rabbit anti-BoDV-P (p24) antibody, DAB staining, Papanicolaou counterstaining. Scale bar 100µm.

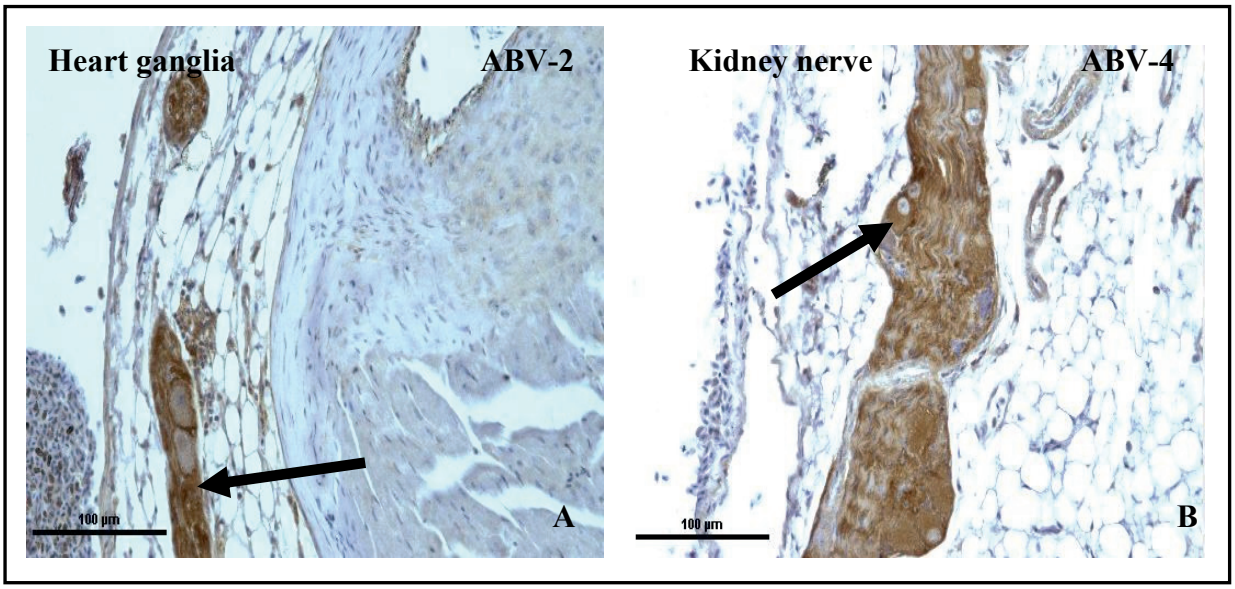

Fig. 16: Demonstration of ABV antigen in the peripheral organs by IHC. (A) Heart ganglia, viral antigen found in neurons of it (arrow), 231 dpi. (B) Kidney nerve, viral antigen was found in the nerve fibers and neurons (arrow), 230 dpi. Polyclonal rabbit anti-BoDV-P (p24) antibody, DAB staining, Papanicolaou counterstaining. Scale bar 100µm.

4.6. Generation of ABV-2 specific probes for the ISH

4.6.1. Amplification of the oligonucleotides of ABV-2 N region fragments

After performing the PCR to obtain the DNA template from two oligonucleotides of the ABV-2-N region, a fragment of 230 bp in length was expected (**Fig. 17**).

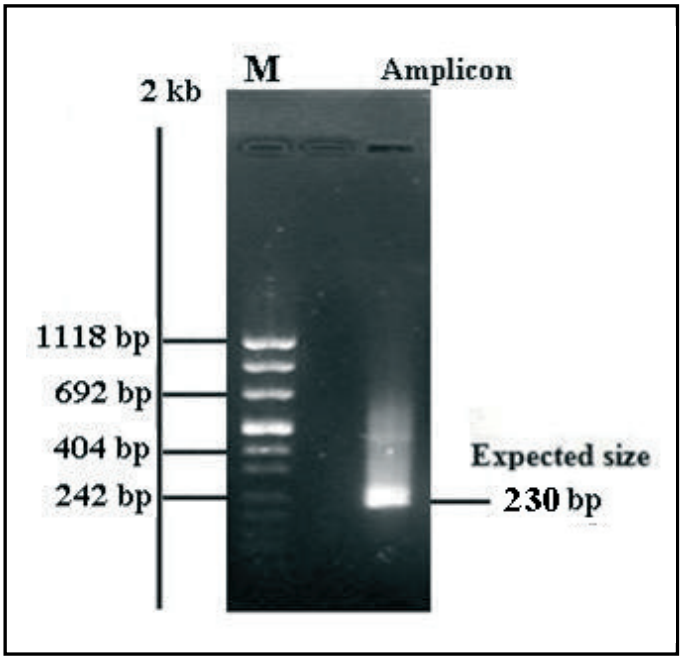

Fig. 17: Amplification of the ABV-2 N oligonucleotides. (M) pUC Mix marker, 8 as a DNA size marker. 2% agarose, 6 volt/cm electrodes distance, one hour.

4.6.2. Amplification of ligated DNA

After ligation of the amplicon of the ABV-2 N region into the TOPO vector, the ligated DNA was amplified. PCR products containing ABV-2 N segments were used as template to generate the ABV-2-N sense and antisense probes for *in vitro* transcription. From T7 promotor until ABV-2-N reverse priming site, the ABV-2 N sense probe was generated. From T7 promotor until ABV-2-N forward priming site, the ABV-2 N antisense probe was synthesized (**Fig. 18**). The expected size of sense and anti sense of ABV-2 templates was 265 bp (**Fig. 18**).

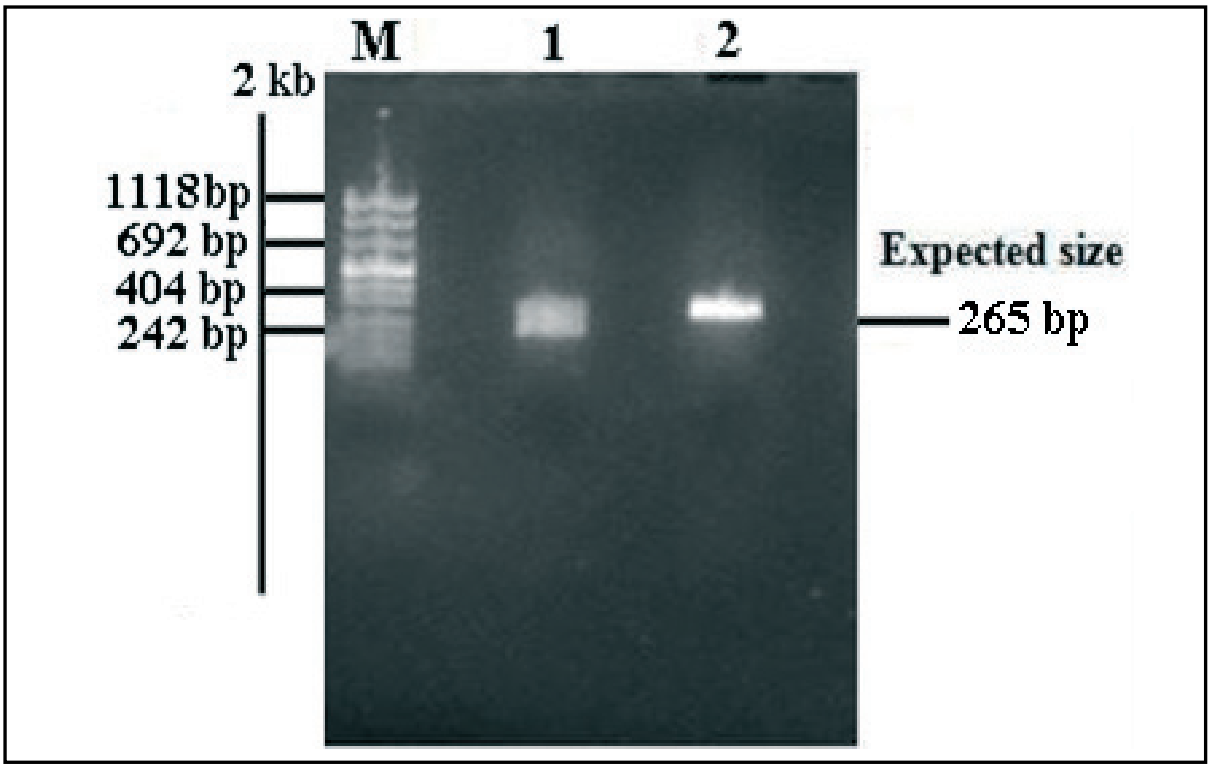

Fig. 18: Amplification of the ligated DNA. (M) pUC Mix Marker, 8 as a DNA size marker. Lane 1= Amplified DNA fragment for generation of the sense probe of ABV-2 N gene. Lane 2= Amplified DNA fragment for generation of the antisense probe of ABV-2 N gene. 2% agarose, 6 volt/cm electrodes distance, one hour.

4.7. Generation of ABV-4 specific probes for the ISH

4.7.1. Amplification of the cloned ABV-4-N-DNA

The cloned ABV-4-N-DNA was successfully amplified (**Fig. 19**). A combination of M13-F and ABV-4-N-R primers with the cloned ABV-4-N-DNA produced a template for the sense probe while combination of M13-R and ABV-4-N-F primers with the cloned ABV-4-N-DNA resulted in a template for the antisense probe. The expected size of sense and anti sense of ABV-4 templates was 478 bp (**Fig. 19**).

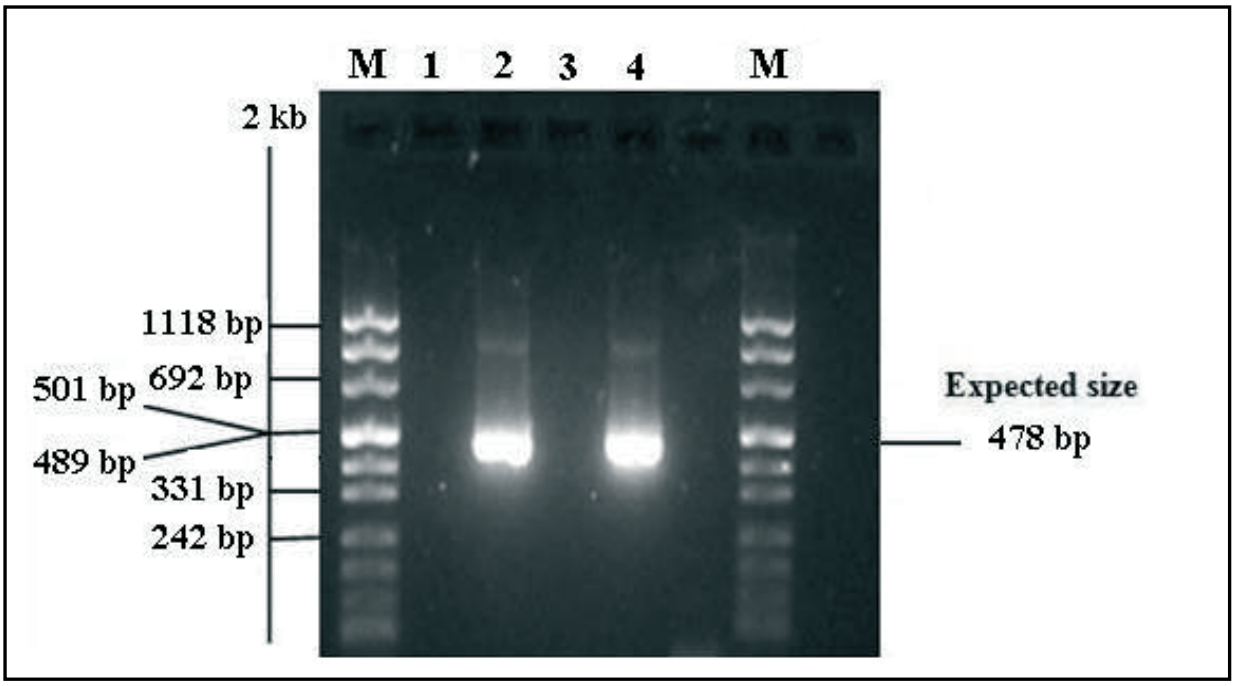

Fig. 19: Amplification of the fragments carrying the ABV-4 N gene. (M) pUC Mix Marker, 8. Lane 1 and 3= no fragment control. Lane 2= DNA amplicon (PCR products) which was utilized to generate the sense probe. Lane 4= DNA amplicon (PCR products) which were employed to generate the antisense probe. 2% agarose, 6 volt/cm electrodes distance, one hour.

4.8. Determination of labelling of ABV-2 and ABV-4 specific probes

A spot test was used to quantify the labelling of the ISH probes with digoxigenin. Results showed that ABV-2 and ABV-4 probes were succefully labelled with digoxigenin.

4.9. Demonstration of ABV RNA

4.9.1. Distribution pattern of the ABV-2 RNA after ABV-2 infection

In the CNS, in some birds, ABV-2 genome but not ABV-2 mRNA was detected in the CNS. In other birds, ABV-2 mRNA but not ABV-2 genome was detected in the CNS. ABV-2 genome was detected in the brain in 12/18 birds. Moreover, ABV-2 mRNA was detected in the brain in 10/18 birds. However, ABV-2 genome and ABV-2 mRNA were detected simultaneously in many other birds in 4/18 birds after ABV-2 infection.

ABV-2 genome and ABV-2 mRNA were detected only in neurons and glial cells in the brain, nerve fibers and neurons of retina and in the optic nerve in the eye. ABV-2 genome was only detected intranuclearly within affected cells. ABV-2 mRNA was detected intranuclearly and intracytoplasmically within affected cells (**Fig. 20**).

ABV-2 genome was not detected in the brain in 6/18 birds but it was detected as score 1 in 10/18 birds, and score 2 in 2/18 birds (table 38). ABV-2 mRNA was not detected in the brain in 8/18 birds but it was detected as score 1 in 9/18 birds, and score 3 in 1/18 birds (table 39). ABV-2 genome was not detected in the spinal cord in 2/18 birds but it was detected as score 1 in 1/18 bird, and score 2 in 1/18 bird (table 38). ABV-2 mRNA was not detected in the spinal cord in 1/18 birds but it was detected as score 1 in 3/18 birds (table 39). Spinal cord was not available in 14/18 birds. ABV-2 genome was not detected in the eye in 2/18 birds but it was detected as score 1 in 6/18 birds, and score 2 in 2/18 birds, and score 3 in 5/18 birds (table 38). ABV-2 mRNA was not detected in the eye in 10/18 birds but it was detected as score 1 in 5/18 birds (table 39). The eye was not available in 12/18 birds. The eye was autolytic in 1/18 birds.

The kinetic of ABV-2 RNA detection in the brain revealed that ABV-2 genome and ABV-2 mRNA were detected mainly as score 1 during the whole investigation period (table 38 and 39). However, some variability in detection of ABV-2 genome was found. ABV-2 genome was detected in the brain as score 2 in only 1/18 bird at early time points 46-86 dpi and also as score 2 only in 1/18 bird at late time points 231 dpi. Moreover, ABV-2 genome was not found in the brain only in 1/18 birds at early time points 46-86 dpi, in 2/18 birds at mid time points 88-172 dpi, and in 2/18 birds at late time points 231 dpi. Variability in detection of ABV-2 mRNA was also found. ABV-2 mRNA was not found in the brain in 3/18 birds at early time point, in 2/18 birds at mid time point, and in 2/18 birds at late time point. Moreover, ABV-2 mRNA was detected as score 3 in 1/18 birds at early time points.

In the GIT, ABV-2 genome was detected in all GIT organs during the whole investigation period of 231 dpi in 17/18 birds. ABV-2 genome was also detected in all GIT organs during the whole investigation period of 231 dpi in 17/18 birds. The GIT organs were autolytic in 1/18 birds.

ABV-2 genome and ABV-2 mRNA were detected in the glandular epithelium of gizzard and proventriculus, muscle fibers and nuclei in the lamina muscularis in crop, intestine, gizzard and proventriculus in 17/18 birds. Neurons of the enteric ganglia in the lamina muscularis of gizzard and proventriculus, nerve fibers, epithelial cells mainly harbor ABV-2 genome and viral mRNA in the nucleus or in the nucleus and cytoplasm respectively (**Fig. 21**).

ABV-2 genome was not found in the crop in 1/18 birds but it was detected as score 1 in 13/18 birds, and score 2 in 3/18 birds (table 38). ABV-2 mRNA was not found in the crop in 1/18 birds but it was detected as score 1 in 7/18 birds, score 2 in 5/18 birds, and score 3 in 4/18 birds (table 39). The crop was autolytic in 1/18 birds. ABV-2 genome was detected in the gizzard as score 1 in 9/18 birds, and score 2 in 8/18 birds (table 38). ABV-2 mRNA was not found in the gizzard in 1/18 birds but it was detected as score 1 in 1/18 birds, score 2 in 11/18 birds, and score 3 in 4/18 birds (table 39). The gizzard was autolytic in 1/18 birds. ABV-2 genome was detected in the proventriculus as score 1 in 10/18 birds, score 2 in 4/18 birds, and score 3 in 3/18 birds (table 38). ABV-2 mRNA was detected in the proventriculus as score 1 in 5/18 birds, score 2 in 7/18 birds, and score 3 in 5/18 birds (table 39). The proventriculus was autolytic in 1/18 birds. ABV-2 genome was detected in the intestine as score 1 in 14/18 birds, and score 2 in 2/18 birds (table 38). ABV-2 mRNA was detected in the intestine as score 1 in 7/18 birds, score 2 in 7/18 birds, and score 3 in 2/18 birds (table 39). The intestine was autolytic in 2/18 birds.

The kinetic of ABV-2 RNA detection in the GIT revealed that ABV-2 genome was detected in the crop, gizzard, and proventriculus as score 1, score 2 or rarely score 3 during the whole investigation period of 231 dpi. However, variability in detection of ABV-2 genome in the crop and proventriculus was found. ABV-2 genome was not found in the crop in 1/18 birds at early time points 46-86 dpi. Moreover, ABV-2 genome was detected in the proventriclus as score 3 in 3/18 birds at late time points. The kinetic of ABV-2 mRNA was also variable in the GIT. ABV-2 mRNA was detected in the crop as score 1 and score 2 at early and mid time points but increased up to score 3 at late time points. ABV-2 mRNA was detected in the gizzard and proventriculus and intestine as score 1, score 2 and score 3 during the whole investigation period of 231 dpi.

In the peripheral organs, ABV-2 genome and ABV-2 mRNA were detected in most of the peripheral organs in 18/18 experimentally ABV-2 infected birds. ABV-2 genome was detected as score 1, score 2, and score 3 in all the peripheral organs during the whole investigation period of 231 dpi. ABV-2 mRNA was detected as score 1, score 2 and score 3 in heart and liver, and it was detected in the kidney and skin as score 1 during the whole investigation period 231 dpi.

ABV-2 genome and viral mRNA were detected in liver cells, neurons of the pericardial ganglia, smooth muscle layer in the aorta, cardiomyocytes, nerve fibers, epithelial cells of renal tubules, epithelial cells of the pancreas, cells with features of red pulp macrophages in the spleen, epithelial cells around feather follicles in the skin, and smooth muscle fibers and nuclei in the heart and muscle fibers in the skeletal muscles (**Fig. 22**).

ABV-2 genome was not found in the heart in 3/18 birds but it was detected as score 1 in 1/18 bird, score 2 in 9/18 birds, and score 3 in 4/18 birds (table 38). ABV-2 mRNA was not found in the heart in 3/18 birds but it was detected as score 1 in 2/18 birds, score 2 in 5/18 birds, and score 3 in 7/18 birds (table 39). ABV-2 genome and ABV-2 mRNA were detected in the heart simultaneously in 14/18 birds. The heart was autolytic in 1/18 birds. ABV-2 genome was not found in the liver in 2/18 birds but it was detected as score 1 in 7/18 birds and score 2 in 8/18 birds (table 38). ABV-2 mRNA was not found in the liver in 2/18 birds but it was detected as score 1 in 2/18 birds, score 2 in 8/18 birds, and score 3 in 5/18 birds (table 39). ABV-2 genome and ABV-2 mRNA were detected in the liver simultaneously in 15/18 birds. The liver was autolytic in 1/18 birds. ABV-2 genome was not found in the kidney in 4/18 birds but it was detected as score 1 in 3/18 birds, score 2 in 4/18 birds, and score 3 in 6/18 birds (table 38). ABV-2 mRNA was not found in the kidney in 10/18 birds but it was detected as score 1 in 6/18 birds and score 2 in 1/18 birds (table 39). ABV-2 genome and ABV-2 mRNA were detected in the kidney simultaneously in 8/18 birds. The kidney was autolytic in 1/18 bird. ABV-2 genome was not found in the spleen in 3/18 birds but it was detected as score 1 in 2/18 birds and score 2 in 2/18 birds (table 38). ABV-2 mRNA was not found in the spleen in 7/18 birds (table 39). The spleen was not available in 11/18 birds. ABV-2 genome was not found in the pancreas in 1/18 bird but it was detected as score 1 in 6/18 birds, score 2 in 7/18 birds and score 3 in 2/18 birds (table 38). ABV-2 mRNA was not found in the pancreas in 13/18 birds but it was detected as score 1 in 2/18 birds, and score 3 in 1/18 bird (table 39). ABV-2 genome and ABV-2 mRNA were detected in the pancreas simultaneously in 3/18 birds. The pancreas was not available in 2/18 birds. ABV-2 genome was detected in the adrenal gland as score 2 in 2/18 birds and score 3 in 1/18 birds (table 38). ABV-2 mRNA was

not found in the adrenal gland in 1/18 birds but it was detected as score 1 in 2/18 birds (table 39). ABV-2 genome and ABV-2 mRNA were detected in the adrenal gland simultaneously in 2/18 birds. The adrenal gland was not available in 15/18 birds. ABV-2 genome was not found in the skin in 1/18 bird but it was detected as score 1 in 7/18 birds, score 2 in 6/18 birds and score 3 in 1/18 birds (table 38). ABV-2 mRNA was not found in the skin in 7/18 birds but it was detected as score 1 in 8/18 birds (table 39). ABV-2 genome and ABV-2 mRNA were detected in the skin simultaneously in 7/18 birds. The skin was not available in 3/18 birds. ABV-2 genome was not found in the skeletal muscles in 16/18 birds but it was detected in muscle fibers as score 1 in 2/18 birds (table 38). ABV-2 mRNA was not found in the skeletal muscles in 16/18 birds but it was detected in muscle fibers as score 1 in 2/18 birds (table 39). ABV-2 genome and ABV-2 mRNA were detected in the skeletal muscles simultaneously in 2/18 birds.

The kinetic of ABV-2 RNA in the peripheral organs revealed that detection of ABV-2 genome was variable. ABV-2 genome neither decreased nor increased in the heart, liver, kidney in most majority of birds and was detected as score 1, score 2 and score 3 during the whole investigation period of 231 dpi. ABV-2 genome increased in the pancreas at late time points 231 dpi while it increased in the skin at only mid time points 88-172 dpi. Likewise, the kinetic of ABV-2 mRNA neither decreased nor increased in the heart and kidney during the whole investigation period of 231 dpi. However, some variability in detection of ABV-2 mRNA in the heart and kidney was also found. ABV-2 mRNA was not detected in the heart and kidney in 2/18 birds at early time points 46-86 dpi. The kinetic of ABV-2 mRNA in the liver, pancreas, and skin decreased at late time points (231 dpi).

ABV-2 genome and ABV-2 mRNA were not found in the CNS, GIT, and peripheral organs in the sentinel bird. In the mock group, ABV-2 genome and ABV-2 mRNA were also not found in all organs in 4/4 birds.

4.9.2. Distribution pattern of the ABV-4 RNA after ABV-4 infection

In the CNS, ABV-4 genome and ABV-4 mRNA were detected in the CNS in experimentally ABV-4 infected birds. ABV-4 genome and ABV-4 mRNA were detected in the brain in 18/18 birds. ABV-4 genome and ABV-4 mRNA were also detected in the spinal cord in 12/18 birds. The spinal cord was not available in 6/18 birds.

ABV-4 genome and ABV-4 mRNA were detected in the cerebrum and cerebellum. Neurons, glial cells, nerve fibers, neurons of retina and in the optic nerve in the eye, Purkinje neurons could harbour ABV-4 genome and ABV-4 mRNA. ABV-4 genome was only detected

intranuclearly while ABV-4 mRNA was detected intranuclearly and intracytoplasmically within affected cells (**Fig. 20**).

ABV-4 genome was detected in the brain as score 1 in 12/18 birds and score 2 in 6/18 birds (table 40). ABV-4 mRNA was detected in the brain as score 2 in 6/18 birds and score 3 in 12/18 birds (table 41). ABV-4 genome was detected in the spinal cord as score 1 in 11/18 birds and score 2 in 1/18 birds (table 40). ABV-4 mRNA was detected in the spinal cord as score 2 in 9/18 birds and score 3 in 3/18 birds (table 41). The spinal cord was not available in 6/18 birds. ABV-4 genome was not found in the eye in 7/18 birds but it was detected as score 1 in 5/18 birds and score 2 in 4/18 birds (table 40). ABV-4 mRNA was not found in the eye in 16/18 birds (table 41). The eye was not available in 2/18 birds.

The kinetic of ABV-4 RNA in the CNS revealed that ABV-4 genome neither increased nor decreased in the brain and was detected as score 1 and score 2 during the whole investigation period 230 dpi. Moreover, ABV-4 mRNA neither increased nor decreased in the brain and was detected as score 2 and score 3 during the whole investigation period 230 dpi. The kinetic of ABV-4 genome in the spinal cord was detected mainly as score 1 during the whole investigation period 230 dpi. However, it was detected in the spinal cord as score 2 in only 1/18 birds at mid time points 115 dpi. ABV-4 mRNA in the spinal cord was detected as score 2 and score 3 during the whole investigation period of 230 dpi.

In the GIT, ABV-4 genome and ABV-4 mRNA were detected in all GIT organs in 14/18 experimentally ABV-4 infected birds. ABV-4 genome and ABV-4 mRNA were detected in the nuclei of glandular epithelium of gizzard and proventriculus, muscle fibers and nuclei in the lamina muscularis in the crop, intestine, gizzard and proventriculus. Neurons of the enteric ganglia in the lamina muscularis of gizzard and proventriculus, and nerve fibers mainly harbor ABV-4 genome and ABV-4 mRNA (**Fig. 21**). ABV-4 genome was detected in all GIT organs as score 1, score 2 and score 3 while ABV-4 mRNA was detected in the GIT organs as only score 1 and score 2 during the whole investigation period in experimentally ABV-4 infected birds.

ABV-4 genome was not found in the crop in 5/18 birds but it was detected as score 1 in 7/18 birds, score 2 in 2/18 birds and score 3 in 1/18 birds (table 40). ABV-4 mRNA was not found in the crop in 6/18 birds but it was detected as score 1 in 8/18 birds and score 2 in 1/18 birds (table 41). The crop was not available in 3/18 birds. ABV-4 genome and ABV-4 mRNA were detected in the crop simultaneously in 10/18 birds. ABV-4 genome was not found in the gizzard in 9/18 birds but it was detected as score 1 in 2/18 birds and score 2 in 2/18 birds (table 40). ABV-4 mRNA was not found in the gizzard in 10/18 birds but it was detected as

score 1 in 3/18 birds (table 41). ABV-4 genome and ABV-4 mRNA were detected in the gizzard simultaneously in 3/18 birds. The gizzard was not available in 3/18 birds. The gizzard was autolytic in 2/18 birds. ABV-4 genome was not found in the proventriculus in 3/18 birds but it was detected as score 1 in 3/18 birds, score 2 in 4/18 birds and score 3 in 4/18 birds (table 40). ABV-4 mRNA was not found in the proventriculus in 6/18 birds but it was detected as score 1 in 7/18 birds, score 2 in 1/18 birds (table 41). ABV-4 genome and ABV-4 mRNA were detected in the proventriculus simultaneously in 7/18 birds. The proventriculus was not available in 2/18 birds. The proventriculus was autolytic in 2/18 birds. ABV-4 genome was not found in the intestine in 5/18 birds but it was detected as score 1 in 3/18 birds, score 2 in 7/18 birds and score 3 in 1/18 birds (table 40). ABV-4 mRNA was not found in the intestine in 10/18 birds but it was detected as score 1 in 6/18 birds (table 41). ABV-4 genome and ABV-4 mRNA were detected in the intestine simultaneously in 6/18 birds. The intestine was not available in 1/18 birds. The intestine was autolytic in 1/18 birds.

The kinetic of ABV-4 RNA in the GIT revealed that ABV-4 genome and ABV-4 mRNA decreased in all GIT organs at late time points (230 dpi).

In the peripheral organs, ABV-4 genome was detected in all the peripheral organs in experimentally ABV-4 infected birds. ABV-4 mRNA was found but in some of the peripheral organs. ABV-4 genome and ABV-4 mRNA were detected in liver cells, nucleus of neurons of the pericardial ganglia, smooth muscle layer in the aorta, cardiomyocytes, nerve fibers, epithelial cells of renal tubules, epithelial cells of the pancreas, cells with features of red pulp macrophages in the spleen, epithelial cells around feather follicles in the skin, and smooth muscle fibers and nuclei in the heart and muscle fibers in the skeletal muscles (**Fig. 22**).

ABV-4 genome was not found in the heart in 7/18 birds but it was detected as score 1 in 3/18 birds, score 2 in 4/18 birds and score 3 in 3/18 birds (table 40). ABV-4 mRNA was not found in the heart in 13/18 birds but it was detected as score 1 in 4/18 birds (table 41). ABV-4 genome and ABV-4 mRNA were detected in the heart simultaneously in 4/18 birds. The heart was not available in 1/18 birds. ABV-4 genome was not found in the liver in 5/18 birds but it was detected as score 1 in 5/18 birds, score 2 in 5/18 birds and score 3 in 3/18 birds (table 40). ABV-4 mRNA was not found in the liver in 13/18 birds but it was detected as score 1 in 5/18 birds (table 41). ABV-4 genome and ABV-4 mRNA were detected in the liver simultaneously in 5/18 birds. ABV-4 genome was not found in the kidney in 2/18 birds but it was detected as score 1 in 8/18 birds, score 2 in 4/18 birds and score 3 in 3/18 birds (table 40). ABV-4 mRNA was not found in the kidney in 1/18 birds but it was detected as score 1 in 16/18 birds (table 41). ABV-4 genome and ABV-4 mRNA were detected in the kidney simultaneously in 15/18

birds. The kidney was not available in 1/18 bird. ABV-4 genome was detected in the spleen as score 1 in 13/18 birds (table 40). ABV-4 mRNA was detected in the spleen as score 1 in 9/18 birds and score 2 in 4/18 birds (table 41). ABV-4 genome and ABV-4 mRNA were detected in the spleen simultaneously in 13/18 birds. The spleen was not available in 5/18 birds. ABV-4 genome was not found in the pancreas in 7/18 birds but it was detected as score 1 in 7/18 birds (table 40). ABV-4 mRNA was not found in the pancreas in 6/18 birds but it was detected as score 1 in 8/18 birds (table 41). ABV-4 genome and ABV-4 mRNA were detected in the pancreas simultaneously in 7/18 birds. The pancreas was not available in 4/18 birds. ABV-4 genome was detected in the adrenal gland as score 1 in 1/18 birds and score 2 in 1/18 birds (table 40). ABV-4 mRNA was detected in the adrenal gland as score 1 in 1/18 birds and score 2 in 1/18 birds (table 41). ABV-4 genome and ABV-4 mRNA were detected in the adrenal gland simultaneously in 2/18 birds. The adrenal gland was not available in 16/18 birds. ABV-4 genome was not found in the skin in 5/18 birds but it was detected as score 1 in 7/18 birds, score 2 in 4/18 birds and score 3 in 2/18 birds (table 40). ABV-4 mRNA was not found in the skin in 4/18 birds but it was detected as score 1 in 13/18 birds and score 2 in 1/18 birds (table 40). ABV-4 genome and ABV-4 mRNA were detected in the skin simultaneously in 13/18 birds. ABV-4 genome was not found in the skeletal muscles in 14/18 birds but it was detected as score 1 in 1/18 birds, score 2 in 1/18 birds and score 3 in 1/18 birds (table 40). ABV-4 mRNA was not found in the skeletal muscles in 16/18 birds but it was detected as score 1 in 1/18 birds (table 40). ABV-4 genome and ABV-4 mRNA were detected in the skeletal muscles simultaneously in 1/18 birds. Skeletal muscles were not available in 1/18 birds.

The kinetic of ABV-4 RNA in the peripheral organs revealed that ABV-4 genome increased in the heart, liver, pancreas and skin at mid time points (115,116,120 dpi) until late time points at 230 dpi. ABV-4 genome in the kidney was detected as score 1, score 2 and score 3 during the whole investigation period of 230 dpi. The kinetic of ABV-4 mRNA neither decreased nor increased in all peripheral organs after ABV-4 infection.

In the sentinel bird, ABV-4 genome and ABV-4 mRNA were not found in all organs of the sentinel bird.

4.9.3. Comparison of ABV RNA distribution after ABV-2 and ABV-4 infection

In the CNS after ABV-2 infection, ABV-2 genome and/or ABV-2 mRNA were detected in the brain simultaneously in 4/18 experimentally ABV-2 infected birds. ABV-2 genome and ABV-2 mRNA were detected in the cerebrum only. ABV-2 genome and ABV-2 mRNA were detected in neurons of the brain, glial cells, and neurons of retina and in the optic nerve in the eye.

The kinetic of ABV-2 genome was detected as score 1 and score 2 during the whole investigation period (table 38). However, ABV-2 genome was not found in the CNS in some birds at early time points, mid time points and late time points 231 dpi. The kinetic of ABV-2 mRNA was detected as score 1 during the whole investigation period (table 39). However, ABV-2 mRNA was detected in the CNS as score 3 in only 1/18 birds at early time point.

In the CNS after ABV-4 infection, ABV-4 genome and ABV-4 mRNA were detected in the brain simultaneously in 18/18 experimentally ABV-4 infected birds. ABV-4 genome and ABV-4 mRNA were detected in the cerebrum and cerebellum. ABV-4 genome and ABV-4 mRNA were detected in neurons of the brain, glial cells, neurons of retina and in the optic nerve in the eye, and Purkinje neurons.

The kinetic of ABV-4 genome in the CNS showed a consistency as score 1 and score 2 during the whole investigation period of 230 dpi (table 40). The kinetic of ABV-4 mRNA in the CNS showed a consistency as score 2 and score 3 during the whole investigation period 230 dpi (table 41).

Taking together, more positive cells that harbor viral mRNA than genomic RNA in the CNS in experimentally ABV-4 infected birds than experimentally ABV-2 infected birds.

In the GIT after ABV-2 infection, ABV-2 genome and ABV-2 mRNA were detected in all GIT organs during the whole investigation period of 231 dpi. However, ABV-2 mRNA was not found in the gizzard in only 1/18 birds.

The kinetic of ABV-2 RNA in the GIT was variable. In the crop and gizzard, the kinetic of ABV-2 genome showed a consistency as score 1 and score 2 during the whole investigation period of 231 dpi. In the proventriculus, ABV-2 genome increased at late time points 231 dpi but it decreased in the intestine at late time points 231 dpi. The kinetic of ABV-2 mRNA showed a consistency as score 1, score 2 and score 3 in the crop, gizzard and proventriculus during the whole investigation period of 231 dpi. In the intestine, ABV-2 mRNA decreased at mid time points until late time points 231 dpi.

In the GIT after ABV-4 infection, ABV-4 genome and ABV-4 mRNA were detected in the GIT organs but with some variability. ABV-4 genome was not found in the crop in 5/18 birds,

in the gizzard in 9/18 birds, in the proventriculus in 3/18 birds, and in the intestine in 5/18 birds after ABV-4 infection. Moreover, ABV-4 mRNA was not found in the crop in 6/18 birds, in the gizzard in 10/18 birds, in the proventriculus in 6/18 birds, and in the intestine in 10/18 birds after ABV-4 infection.

The kinetic of ABV-4 RNA in the GIT revealed that ABV-4 genome and ABV-4 mRNA decreased in all GIT organs at late time point 230 dpi.

Taking together, more positive cells that harbor genomic RNA in the GIT in experimentally ABV-2 infected birds than genomic RNA in experimentally ABV-4 infected birds. Moreover, more positive cells that harbor viral mRNA in the GIT in experimentally ABV-2 infected birds than viral mRNA in experimentally ABV-4 infected birds.

In the peripheral organs after ABV-2 infection, ABV-2 genome and ABV-2 mRNA were detected in all the peripheral organs in all birds.

ABV-2 genome was detected as score 1, score 2, and score 3 in all the peripheral organs during the whole investigation period of 231 dpi. ABV-2 mRNA was detected as score 1, score 2 and score 3 in heart and liver, and it was detected in the kidney and skin as score 1 during the whole investigation period of 231 dpi.

The kinetic of ABV-2 genome neither decreased nor increased in the heart, liver, kidney during the whole investigation period of 231 dpi while it increased in the pancreas at late time point 231 dpi and in the skin at only mid time points 88-172 dpi. The kinetic of ABV-2 mRNA neither decreased nor increased in the heart and kidney during the whole investigation period of 231 dpi while it decreased in the liver, pancreas, and skin at late time points 231 dpi.

In the peripheral organs after ABV-4 infection, ABV-4 genome and ABV-4 mRNA were detected in most of the peripheral organs.

ABV-4 genome was detected as score 1, score 2 and score 3 in the heart, liver, kidney, pancreas, adrenal gland, and skin during the whole investigation period 230 dpi. ABV-4 mRNA was only detected as score 1 in the peripheral organs.

The kinetic of ABV-4 genome increased in the heart, liver, pancreas and skin at mid time point (115,116,120 dpi) until late time point at 230 dpi. The kinetic of ABV-4 genome in the kidney was detected as score 1, score 2 and score 3 during the whole investigation period 230 dpi. The kinetic of ABV-4 mRNA neither decreased nor increased in the peripheral organs.

Taking together, the genomic RNA was comparable in the peripheral organs after ABV-2 infection. More viral mRNA was found in the peripheral organs after ABV-2 infection. After ABV-4 infection, more genomic RNA than viral mRNA was found in the peripheral organs after ABV-4 infection.

Table 38: Scores of genomic RNA detection of ABV-2 after ABV-2 infection

dpi	bird ID	CNS			Gastrointestinal organs				Peripheral organs							
		brain	s.cord	eye	crop	gizzard	prov.	intestine	heart	liver	kidney	spleen	pancreas	adrenal .g	skin	muscles
32	39	2	N.A	0	0	2	2	A	2	1	1	N.A	2	N.A	N.A	0
46	32	1	1	1	2	2	1	1	0	0	3	N.A	2	N.A	2	0
50	25	0	0	1	1	1	2	2	2	0	0	0	N.A	N.A	2	0
68	24	1	0	1	1	1	1	1	2	1	3	N.A	2	N.A	2	0
76	34	0	N.A	1	1	1	1	1	2	2	0	N.A	0	N.A	2	0
84	47	1	N.A	N.A	1	2	2	2	0	2	0	2	2	N.A	1	0
86	27	1	N.A	N.A	2	2	1	1	2	1	3	N.A	1	N.A	N.A	0
88	45	0	N.A	2	1	2	1	1	3	2	0	0	2	N.A	2	0
120	19	1	N.A	3	1	1	1	1	2	2	3	N.A	1	3	3	0
137	48	0	N.A	1	1	1	1	1	3	1	1	N.A	1	N.A	0	0
172	30	1	N.A	3	1	2	3	1	0	2	3	1	2	2	1	0
231	22	1	N.A	3	2	2	2	1	2	1	2	2	1	N.A	1	1
231	40	0	N.A	1	1	1	1	1	3	2	2	0	1	N.A	2	1
231	49	1	N.A	0	1	1	3	1	2	1	2	N.A	1	N.A	1	0
231	33	0	N.A	2	1	1	1	1	1	2	3	N.A	3	N.A	N.A	0
231	42	2	2	3	1	1	3	1	2	2	1	N.A	3	2	1	0
231	29	1	N.A	A	A	A	A	A	A	A	A	N.A	N.A	N.A	1	0
231	46	1	N.A	3	1	2	1	1	3	1	2	1	2	N.A	1	0

CNS= central nervous system, s.cord= spinal cord, N.A= not available, Prov.= proventriculus, dpi= days post infection, A= autolytic organ, = CNS, = GIT, = peripheral organs

Table 39: Scores of mRNA detection of ABV-2 after ABV-2 infection

dpi	bird ID	CNS			Gastrointestinal organs				Peripheral organs							
		brain	s.cord	eye	crop	gizzard	prov.	intestine	heart	liver	kidney	spleen	pancreas	adrenal .g	skin	muscles
32	39	1	N.A	0	0	0	1	A	2	2	2	N.A	3	N.A	N.A	0
46	32	0	0	0	1	2	2	1	0	0	0	N.A	0	N.A	0	0
50	25	1	1	0	1	1	3	3	1	0	0	0	N.A	N.A	1	0
68	24	0	0	0	2	3	2	2	3	2	1	N.A	1	N.A	1	0
76	34	1	N.A	0	2	3	2	2	3	3	0	N.A	0	N.A	1	0
84	47	0	N.A	N.A	1	2	3	1	0	3	0	0	0	N.A	1	0
86	27	3	N.A	N.A	1	2	2	3	2	3	1	N.A	0	N.A	N.A	0
88	45	1	N.A	0	2	2	2	1	3	3	0	0	0	N.A	1	0
120	19	0	N.A	1	2	3	1	1	3	3	1	N.A	0	1	1	0
137	48	1	N.A	0	3	2	2	1	2	2	0	N.A	0	N.A	0	0
172	30	0	N.A	1	2	2	3	2	0	1	1	0	0	1	1	0
231	22	0	N.A	1	3	2	3	2	3	2	1	0	0	N.A	0	1
231	40	1	N.A	0	3	2	1	1	3	2	0	0	0	N.A	0	1
231	49	0	N.A	0	3	2	3	2	1	1	1	N.A	0	N.A	0	0
231	33	1	N.A	0	1	2	1	1	2	2	0	N.A	1	N.A	N.A	0
231	42	0	0	1	1	2	2	2	3	2	0	N.A	0	0	0	0
231	29	1	N.A	A	A	A	A	A	A	A	A	N.A	N.A	N.A	1	0
231	46	1	N.A	1	1	3	1	2	2	2	0	0	0	N.A	0	0

CNS= central nervous system, s.cord= spinal cord, N.A= not available, Prov.= proventriculus, dpi= days post infection, A= autolytic organ, = CNS, = GIT, = peripheral organs

Table 40: Scores of genomic RNA detection of ABV-4 after ABV-4 infection

dpi	bird ID	CNS			Gastrointestinal organs				Peripheral organs							
		brain	s.cord	eye	crop	gizzard	prov.	intestine	heart	liver	kidney	spleen	pancreas	adrenal .g	skin	muscles
60	15	1	1	N.A	2	2	1	2	2	1	2	N.A	0	N.A	0	0
66	21	2	N.A	0	1	0	3	2	0	0	3	1	0	N.A	0	0
115	16	1	1	1	1	0	1	0	0	0	3	N.A	0	N.A	0	0
115	19	1	1	2	0	0	3	2	3	3	N.A	1	1	N.A	3	0
115	26	2	2	2	0	2	2	2	0	3	1	1	0	1	2	0
116	13	1	N.A	2	1	1	3	1	0	2	0	1	N.A	N.A	1	3
116	18	2	N.A	1	3	A	A	3	2	2	1	1	1	N.A	2	0
116	25	1	1	1	1	0	3	0	1	1	1	1	1	N.A	2	0
120	12	2	N.A	0	N.A	N.A	0	2	3	0	0	1	0	2	0	0
206	11	1	N.A	1	1	1	1	1	2	2	2	1	N.A	N.A	2	2
229	10	2	1	1	N.A	N.A	N.A	N.A	1	1	1	1	0	N.A	1	0
229	22	1	1	0	1	A	2	1	1	1	1	1	N.A	N.A	1	0
229	23	2	1	0	0	0	A	A	3	2	1	N.A	1	N.A	1	0
229	27	1	1	0	0	0	0	2	0	0	2	1	1	N.A	1	0
229	29	1	1	2	1	0	2	0	2	1	1	N.A	N.A	N.A	1	0
230	20	1	1	0	0	0	2	0	0	3	1	1	0	N.A	3	1
230	24	1	1	0	N.A	0	0	0	0	0	3	1	1	N.A	0	0
230	30	1	N.A	N.A	2	N.A	N.A	2	N.A	2	2	N.A	1	N.A	1	N.A

CNS= central nervous system, s.cord= spinal cord, N.A= not available, Prov.= proventriculus, dpi= days post infection, A= autolytic organ, = CNS, = GIT, = peripheral organs

Table 41: Scores of mRNA detection of ABV-4 after ABV-4 infection

dpi	bird ID	CNS			Gastrointestinal organs				Peripheral organs							
		brain	s.cord	eye	crop	gizzard	prov.	intestine	heart	liver	kidney	spleen	pancreas	adrenal .g	skin	muscles
60	15	2	2	N.A	1	1	1	0	1	1	1	N.A	1	N.A	0	0
66	21	3	N.A	0	1	0	1	1	0	0	1	1	0	N.A	0	0
115	16	3	2	0	1	0	0	0	0	0	1	N.A	0	N.A	0	0
115	19	3	2	0	0	0	0	0	1	1	N.A	1	1	N.A	1	0
115	26	3	3	0	0	0	2	0	0	0	1	1	1	1	1	0
116	13	3	N.A	0	1	1	0	0	0	0	0	1	N.A	N.A	1	0
116	18	3	N.A	0	1	A	A	1	0	1	1	2	1	N.A	1	0
116	25	2	3	0	0	0	1	0	0	0	1	1	1	N.A	1	0
120	12	3	N.A	0	N.A	N.A	0	1	0	0	1	2	0	2	1	0
206	11	3	N.A	0	2	1	1	0	0	1	1	1	N.A	N.A	1	1
229	10	2	3	0	N.A	N.A	N.A	N.A	1	0	1	1	0	N.A	2	0
229	22	3	2	0	1	A	1	1	0	0	1	1	N.A	N.A	1	0
229	23	3	2	0	0	0	A	A	1	0	1	N.A	1	N.A	1	0
229	27	2	2	0	0	0	0	1	0	0	1	1	1	N.A	1	0
229	29	3	2	0	1	0	1	0	0	1	1	N.A	N.A	N.A	1	0
230	20	2	2	0	0	0	1	0	0	0	1	2	0	N.A	1	0
230	24	2	2	0	N.A	0	0	0	0	0	1	2	0	N.A	0	0
230	30	3	N.A	N.A	1	N.A	N.A	1	N.A	0	1	N.A	1	N.A	1	N.A

CNS= central nervous system, s.cord= spinal cord, N.A= not available, Prov.= proventriculus, dpi= days post infection, A= autolytic organ, = CNS, = GIT, = peripheral organs

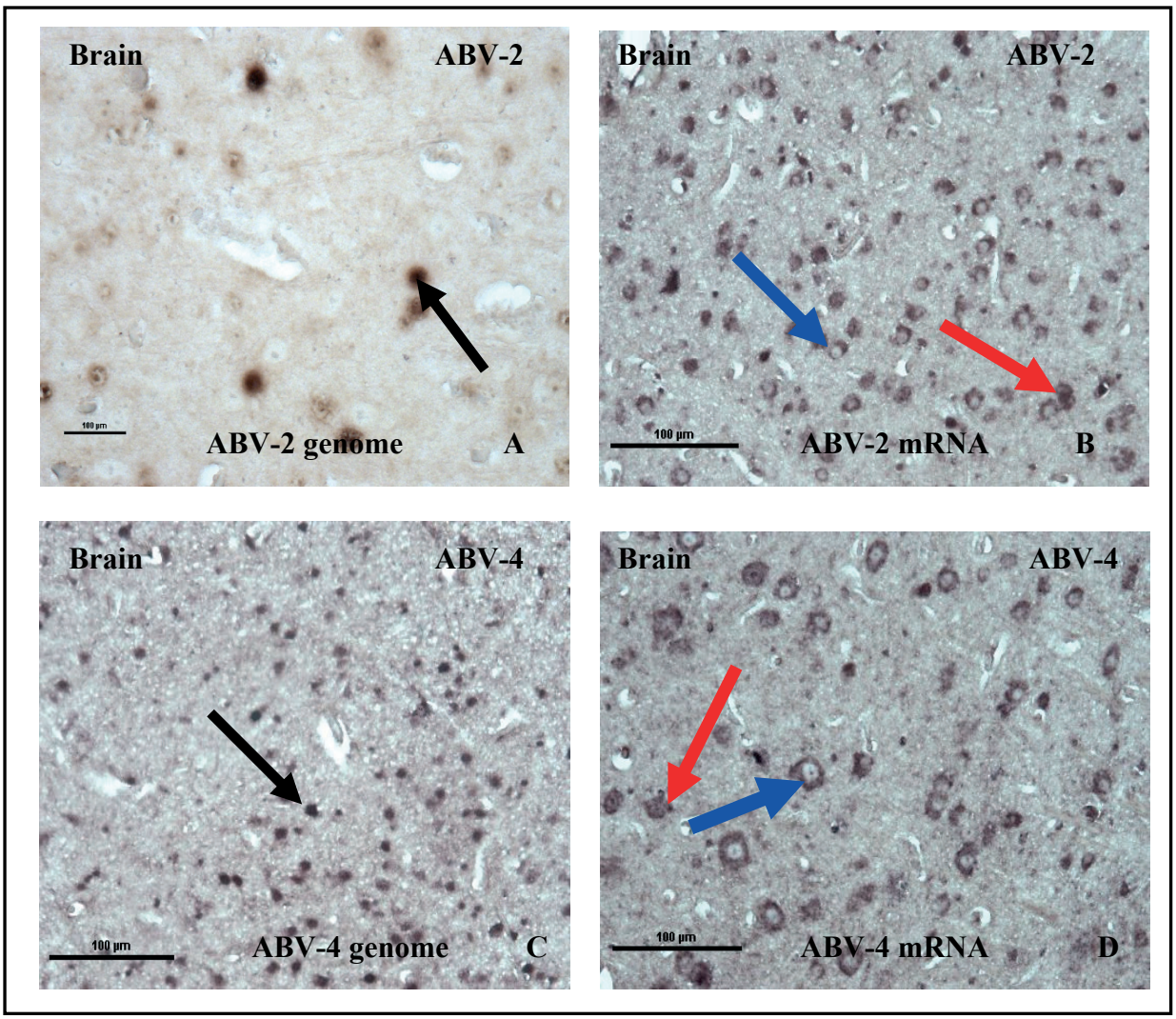

Fig. 20: Demonstration of genomic RNA and mRNA of ABV-2 or of ABV-4 in the CNS by ISH. (A) Brain, genomic RNA of ABV-2 was found in the neurons after ABV-2 infection, ABV-2 genome was found as intranuclear positive signals in the cells (arrow) 86 dpi. (B) Brain, mRNA of ABV-2 found in neurons after ABV-2 infection, ABV-2 mRNA was found as intranuclear positive signals (red arrow) as well as intracytoplasmic positive signals (blue arrow) in the cells, 86 dpi. (C) Brain, genomic RNA of ABV-4 was found in neurons after ABV-4 infection, ABV-4 genome was found as intranuclear positive signals in the cells (arrow), 120 dpi. (D) Brain, mRNA of ABV-4 found in neurons after ABV-4 infection, ABV-4 mRNA was found as intranuclear positive signals (red arrow) as well as intracytoplasmic positive signals (blue arrow) in the cells, 120 dpi. DIG-labelled RNA probes, NBT/X-phosphate staining. Scale bar 100µm.

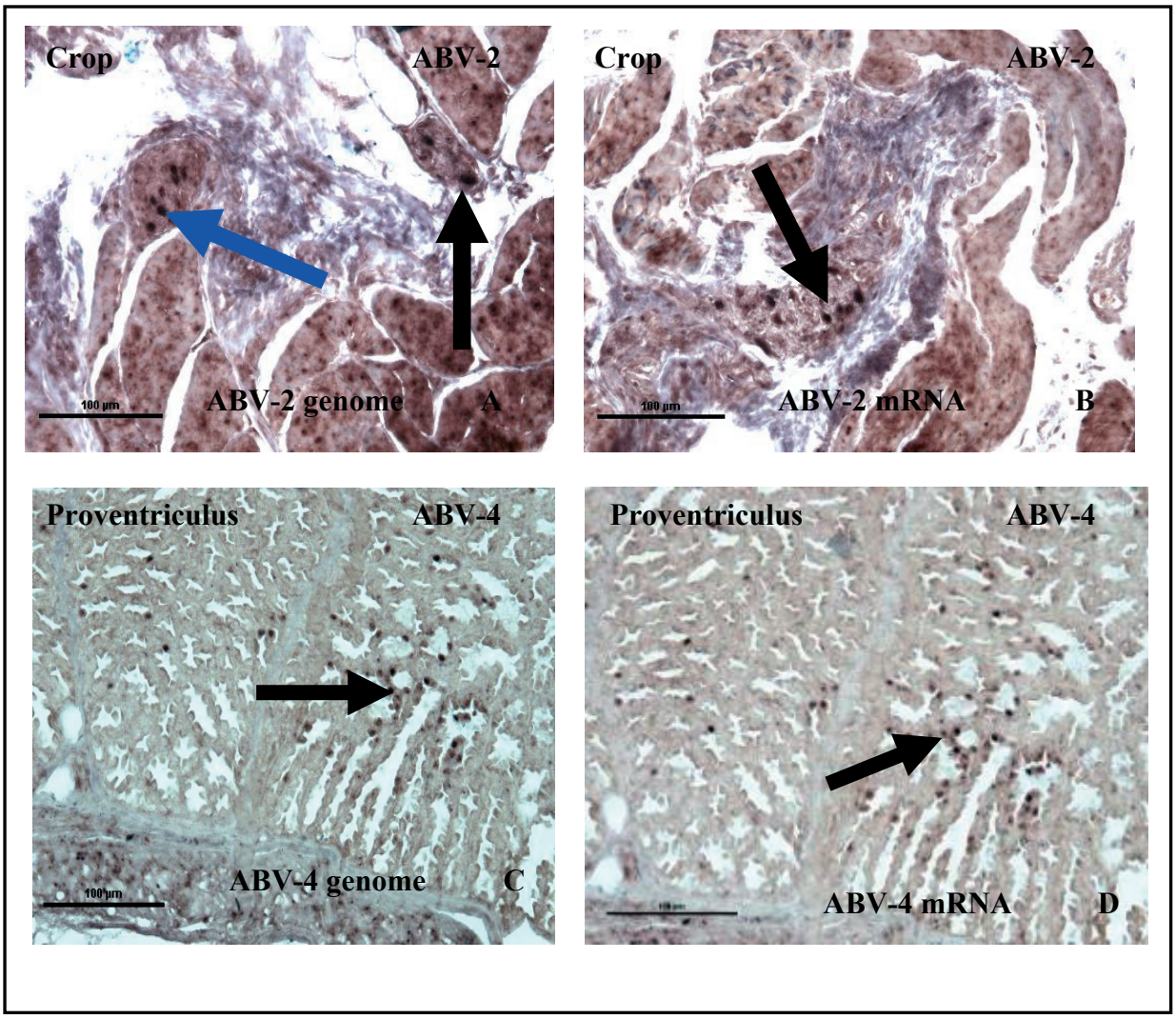

Fig. 21: Demonstration of genomic RNA and mRNA of ABV-2 or of ABV-4 in the GIT by ISH. (A) Crop, genomic RNA of ABV-2 was found in the nuclei of neurons of the enteric ganglia after ABV-2 infection (black arrow), and in smooth muscle nuclei (blue arrow), 137 dpi. (B) Crop, mRNA of ABV-2 was found in the neurons of the enteric ganglia after ABV-2 infection (arrow), 137 dpi. (C) Proventriculus, genomic RNA of ABV-4 was found in the epithelial cells of compound glands in the proventriculus after ABV-4 infection (arrow), 231 dpi. (D) Proventriculus, mRNA of ABV-4 was found in the epithelial cells of compound glands in the proventriculus after ABV-4 infection (arrow), 231 dpi. DIG-labelled RNA probes, NBT/X-phosphate staining. Scale bar 100µm.

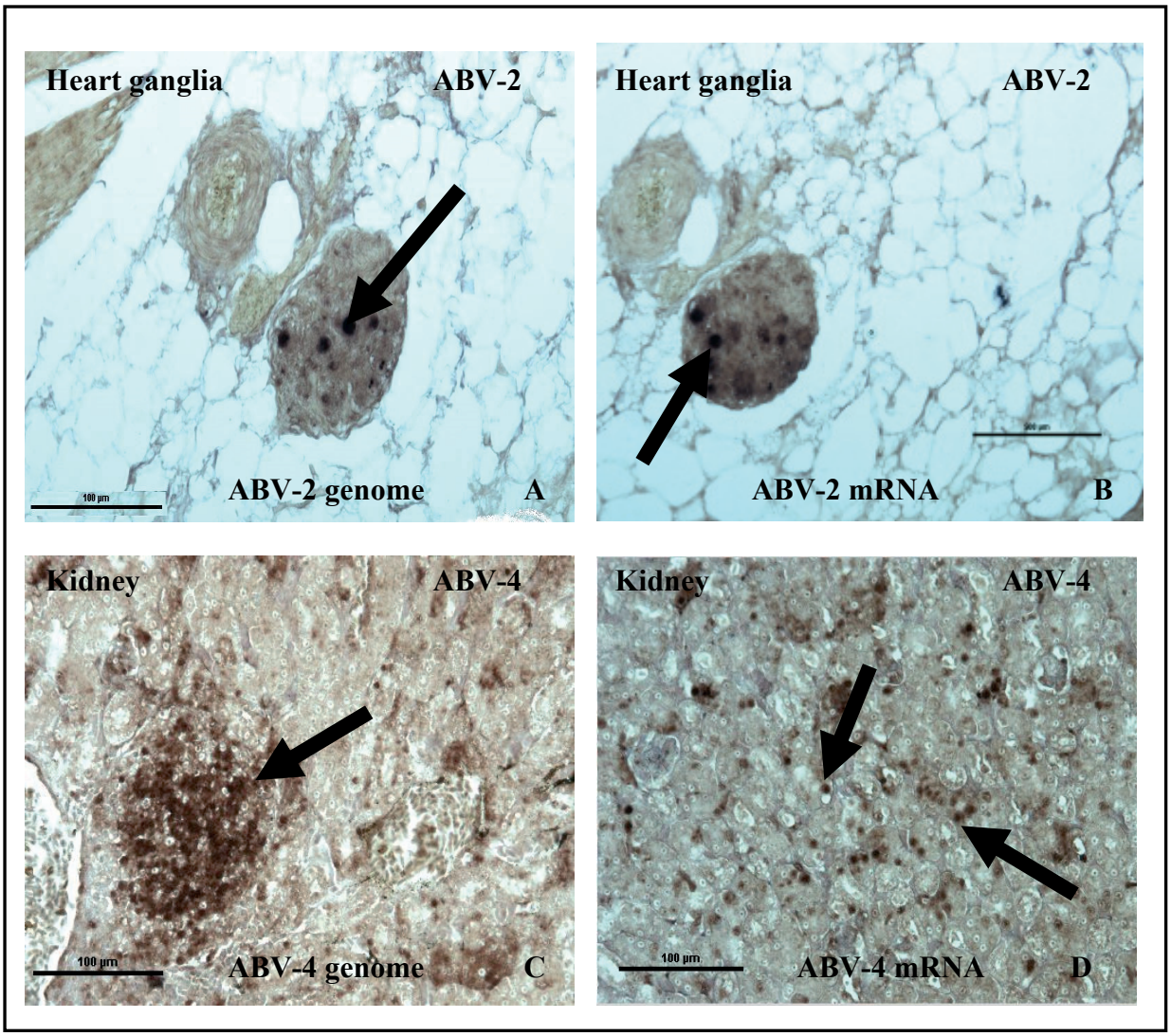

Fig. 22: Demonstration of genomic RNA and mRNA of ABV-2 or of ABV-4 in the peripheral organs by ISH. (A) Heart ganglia, genomic RNA of ABV-2 was found in neurons of the heart ganglia after ABV-2 infection (arrow), 231 dpi. (B) Heart ganglia, mRNA of ABV-2 was found in neurons of the heart ganglia after ABV-2 infection (arrow), 231 dpi. (C) Kidney, genomic RNA of ABV-4 was found in the epithelial cells of renal tubules after ABV-4 infection (arrow), 231 dpi. (D) Kidney, mRNA of ABV-4 was found in the epithelial cells of renal tubules after ABV-4 infection (arrow). DIG-labelled RNA probes, NBT/X-phosphate staining. Scale bar 100µm.

4.10. General comparison between ABV-2 and ABV-4 infection

By analyzing data in tables 30-33, we found statistically significant differences (P<0.05) in the mean scores of inflammatory lesions as well as in the mean scores of viral antigen detection in all organs according to the ABV genotype (**Fig. 23 and 24**).

In the CNS, the mean scores of inflammatory lesions were higher after ABV-4 infection than ABV-2 infection (**Fig. 23**). The mean scores of viral antigen detection were higher in the CNS after ABV-4 infection than ABV-2 infection (**Fig. 24**). In the GIT, the mean scores of inflammatory lesions were the same after ABV-2 and ABV-4 infection (**Fig. 23**). The mean scores of viral antigen detection in the (ic) group were higher in the GIT after ABV-2 infection than in the (iv) group after ABV-2 infection (**Fig. 24**). In the peripheral organs, the mean scores of inflammatory lesions were higher in the (ic) group after ABV-2 infection than in the (ic) group ABV-4 infection (**Fig. 23**) but lower in the (iv) group after ABV-2 infection than in the in the (iv) group after ABV-4 infection. The mean scores of viral antigen detection were higher in the peripheral organs after ABV-4 infection than ABV-2 infection (**Fig. 24**).

Furthermore, our results also showed that there were no significant differences (P<0.05) in the mean scores of inflammatory lesions as well as in the mean scores of ABV antigen detection in all organs according to the route of infection after ABV-2 infection (**Fig. 23 and 24**). The same was true for ABV-4 infection.

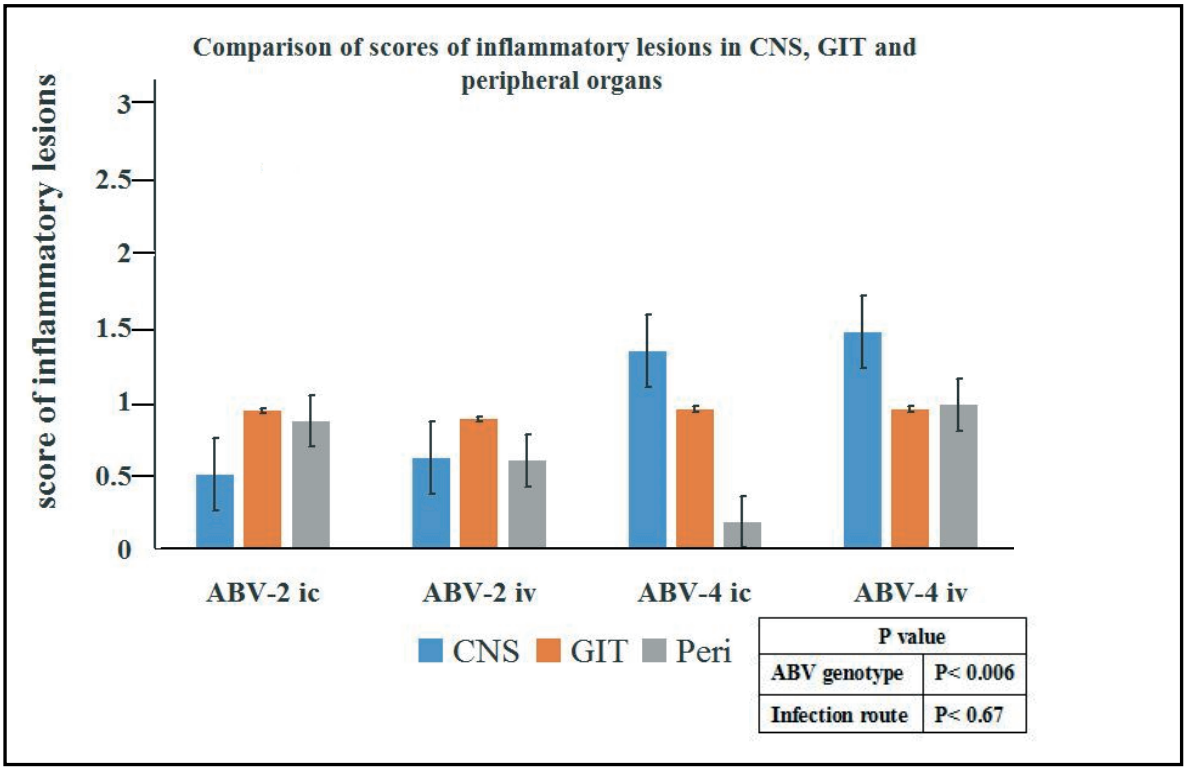

Fig. 23: Comparison of scores of inflammatory lesions in all organs between ABV-2 and ABV-4. (ic) intracerebral, (iv) intravenous, (P) probability, scale bar (standard deviation).

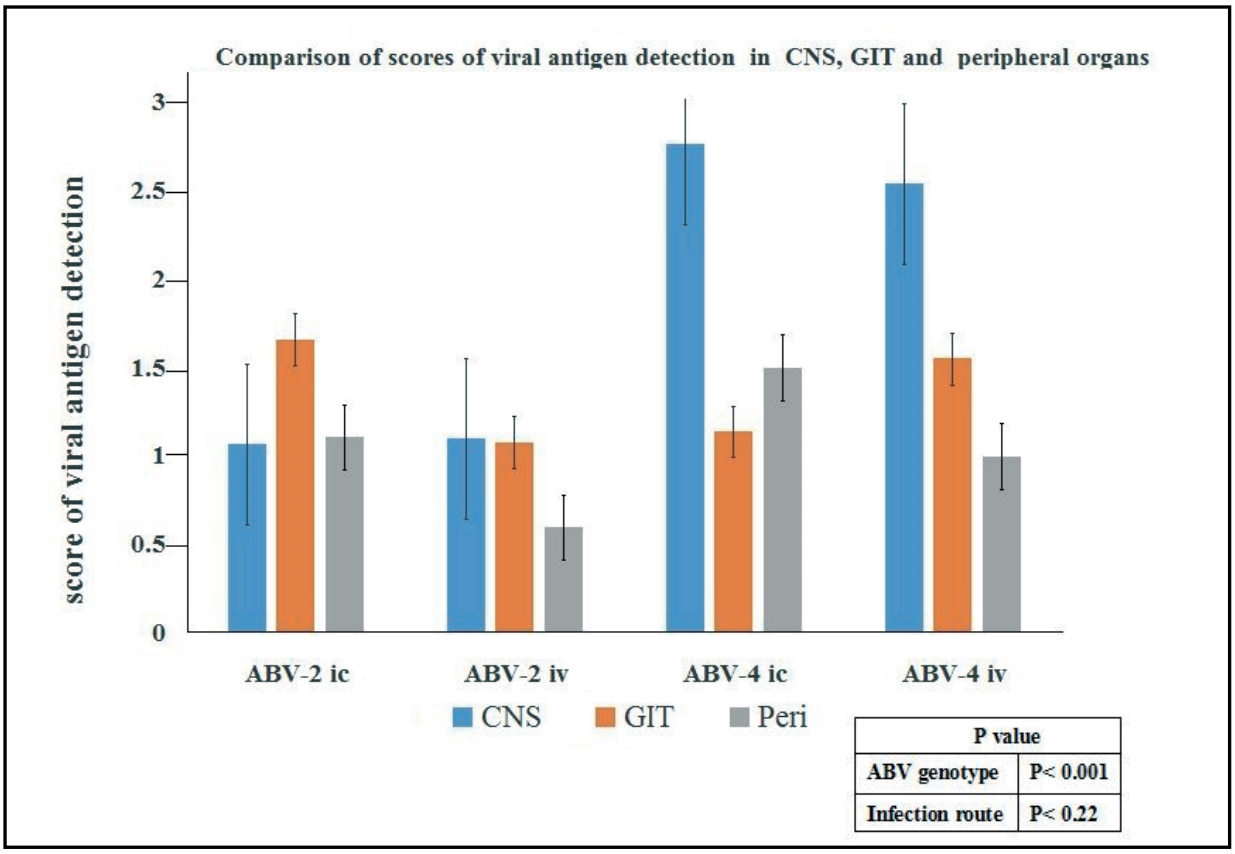

Fig. 24: Comparison of scores of viral antigen detection in all organs between ABV-2 and ABV-4. (ic) intracerebral, (iv) intravenous, (P) probability, scale bar (standard deviation).

4.11. Relationship between inflammatory lesions and viral antigen detection

By analyzing data in tables 30-33, we found that there was a moderate correlation (r= 0.60) between gliosis and viral antigen detection in the CNS after ABV-2 infection. Moreover, there was a moderate correlation (r= 0.60) between inflammatory lesions and viral antigen detection in the CNS after ABV-4 infection but not for ABV-2 infection (**Fig. 25**). The data obtained in tables 30-33, showed no correlation (r = 0.033) between inflammatory lesions and viral antigen detection in the GIT after ABV-2 and ABV-4 infection. The data obtained in tables 30-33, showed a mild correlation (r = 0.38) between inflammatory lesions and viral antigen detection in the peripheral organs after ABV-2 and after ABV-4 infection (**Fig. 26**).

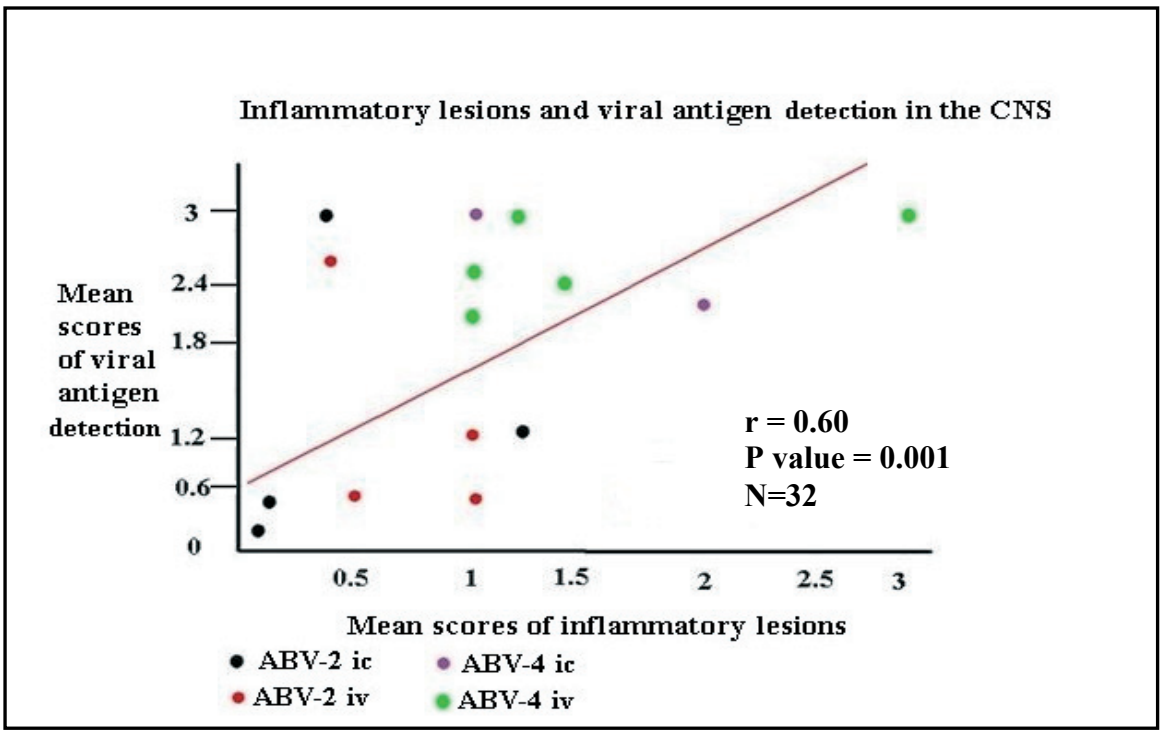

Fig. 25: Correlation between inflammatory lesions and viral antigen detection in the CNS. (P) probability, (r) regression, (N) number of birds. Each dot in the figure represents an intersection of at least two observations of the mean scores of inflammatory lesions and viral antigen detection in the CNS.

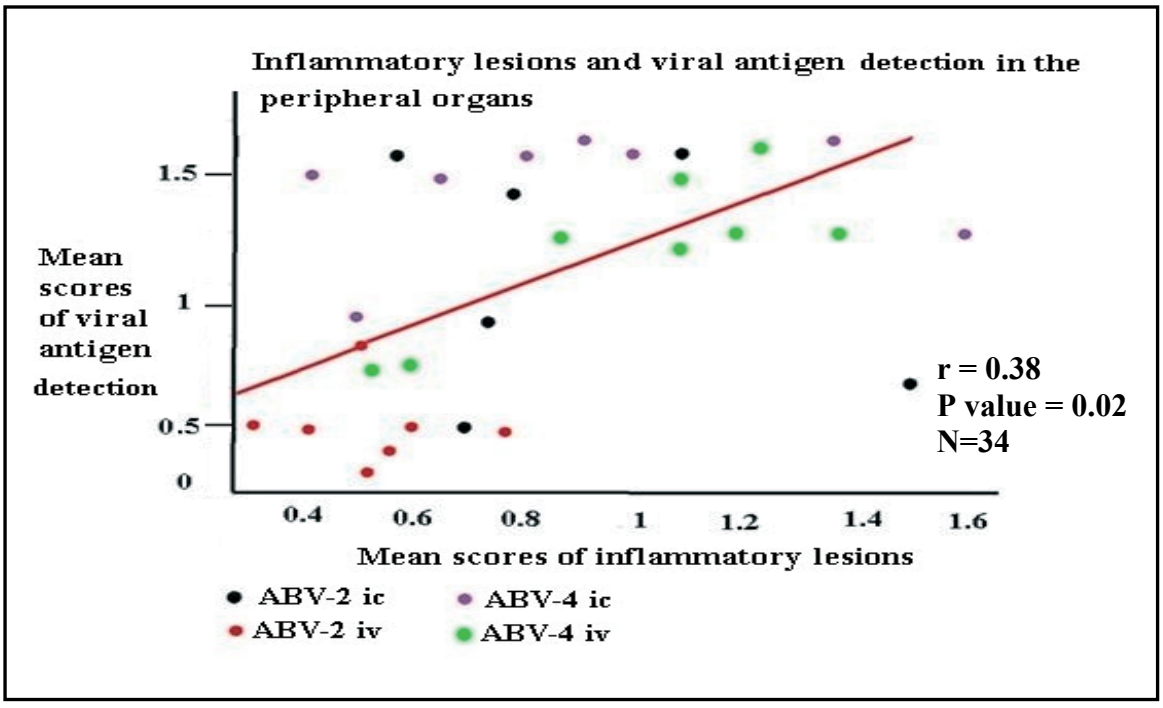

Fig. 26: Correlation between inflammatory lesions and viral antigen detection in the peripheral organs. (P) probability, (r) regression, (N) number of birds. Each dot in the figure represents an intersection of at least two observations of the mean scores of inflammatory lesions and viral antigen detection in the peripheral organs.

4.12. Comparison of histological findings, gross lesions, ABV antigen and ABV-2 RNA after ABV-2 infection

After ABV-2 infection, birds exhibited gastrointestinal and/or neurological signs, had moderate to severe dilatation of proventriculus, they had also viral antigen and ABV-2 RNA in the CNS, GIT and in the peripheral organs. Moreover, birds did not exhibit gastrointestinal or neurological signs, did not display dilatation of proventriculus, they could also have viral antigen and ABV-2 RNA in the CNS, GIT and in the peripheral organs.

Some variability was also detected. No inflammatory lesions were found in the brain but only detected in the GIT and peripheral organs in 1/18 bird which died suddenly at 84 dpi, had gastrointestinal clinical signs, and had not dilatation of proventriculus. Viral antigen and ABV-2 RNA were detected in the CNS, GIT and peripheral organs of this bird.

4.13. Comparison of histological findings, gross lesions, ABV antigen and ABV-4 RNA after ABV-4 infection

After ABV-4 infection, birds exhibited gastrointestinal and/or neurological signs, had moderate to severe dilatation of proventriculus, they had also viral antigen and ABV-4 RNA in the CNS, GIT and in the peripheral organs. Moreover, birds did not exhibit gastrointestinal or neurological signs, did not display dilatation of proventriculus, they could also have viral antigen and ABV-4 RNA in the CNS, GIT and peripheral organs.

Some variability was also detected. Inflammatory lesions, viral antigen and ABV-4 RNA were detected in the CNS, GIT and peripheral organs in 1/18 birds which died suddenly without exhibiting clinical signs, and displayed moderate dilatation of proventriculus. Moreover, inflammatory lesions, viral antigen and ABV-4 RNA were also detected in the CNS, GIT and peripheral organs in 1/18 birds which died suddenly without exhibiting clinical signs, and did not display dilatation of proventriculus.

4.14. Isolation and characterization of cockatiel blood cells

4.14.1. Isolation of cockatiel blood cells

BC cells and MNC were successfully isolated from cockatiels (**Fig. 27**). After optimization of the isolation, the maximum life span of the population of the isolated cells *in vitro* was evaluated. After isolation, buffy coat was found mostly as an incomplete thin layer between red blood cells and plasma. Mononuclear cells were isolated either as a complete or incomplete layer. Number of BC cells ranged 300,000 to 500,000 cells/ml while number of MNC ranged 100,000 to 200,000 cells/ml directly after isolation. Cell viability decreased over time, starting from day 3 until day 15 post isolation (table 42). BC cells were shiny, most predominantly single cells of different types, rounded cells and oval shaped cells (**Fig. 27**) of different sizes (**Fig. 27**). Others remained floating in culture medium for many days. Mononuclear cells looked like small to large single cells, with rounded shape without any aggregates of the cells in culture medium at all.

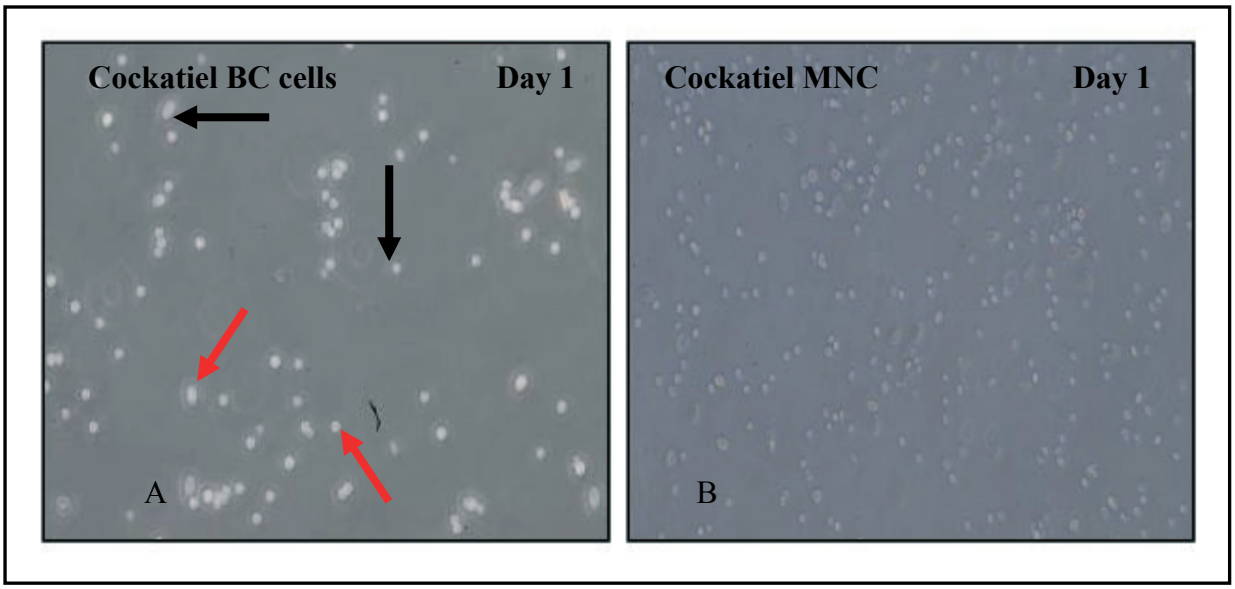

Fig. 27: Isolated blood cells from cockatiels. (A) Buffy coat cells isolated from cockatiel blood by centrifugation. Notice that there are different cell shapes of buffy coat cells (black arrows) and types (red arrows). (B) Peripheral blood mononuclear cells. MNC isolated by Ficoll-Paque™ Premium. Magnification 20x.

Table 42: Viability of BC cells by trypan blue assay

Cell type	Days after isolation	Total number of cells	Viable cells	Cells viability
BC cells	Day 1	500,000 cells	500,000 cells	100 %
	Day 2	500,000 cells	500,000 cells	100 %
	Day 3	490,000 cells	410,000 cells	83 %
	Day 4	460,000 cells	350,000 cells	76 %
	Day 5	410,000 cells	300,000 cells	73 %
	Day 6	390,000 cells	280,000 cells	71 %
	Day 7	350,000 cells	210,000 cells	60 %
	Day 8	310,000 cells	180,000 cells	58 %
	Day 9	290,000 cells	160,000 cells	55 %
	Day 10	230,000 cells	120,000 cells	52 %
	Day 11	180,000 cells	90,000 cells	50 %
	Day 12	140,000 cells	60,000 cells	42 %
	Day 13	90,000 cells	33,000 cells	36 %
	Day 14	30,000 cells	8,000 cells	26 %
	Day 15	10,000 cells	500 cells	5 %

0.4% trypan blue in 1xPBS. IX70 S8F inverted microscope (Olympus, USA)

4.14.2. Characterization of immune cells in cockatiel BC by IIF

Due to lack of specific antibodies that recognize immune cells in psittacine birds, we tested cell surface markers from other species for identifying immune cells in cockatiels. By IIF, we characterized immune cells of cockatiels in BC cells by using cross reactive cell surface markers successfully (**Fig. 28**). IIF results showed that anti-CD3 (rat anti-human CD3), anti-CD4 (mouse anti-chicken CD4), anti-CD8a (mouse anti-chicken CD8a), IgY (mouse anti-duck IgY), anti-thrombocytes (mouse anti-chicken thrombocytes) and anti-monocytes (mouse anti-chicken monocytes) antibodies were cross reactive with cockatiel blood CD3-positive cells, CD4-positive cells, CD8a-positive cells, B cells, thrombocytes and monocytes (**Fig. 28**). Ring-like immunostaining surrounded the targeted cells as a positive plasmamembrane staining (**Fig. 28**). After counting positive and negative cells in each smear under fluorescence microscope manually, our findings showed that the estimated percentage of positive cells for (monocytes 3%, thrombocytes 20%, B cells 9%, CD4-positive cells 36%, CD8a-positive cells 11%, and CD3-positive cells 71%) in cockatiel BC cells at day one after isolation.

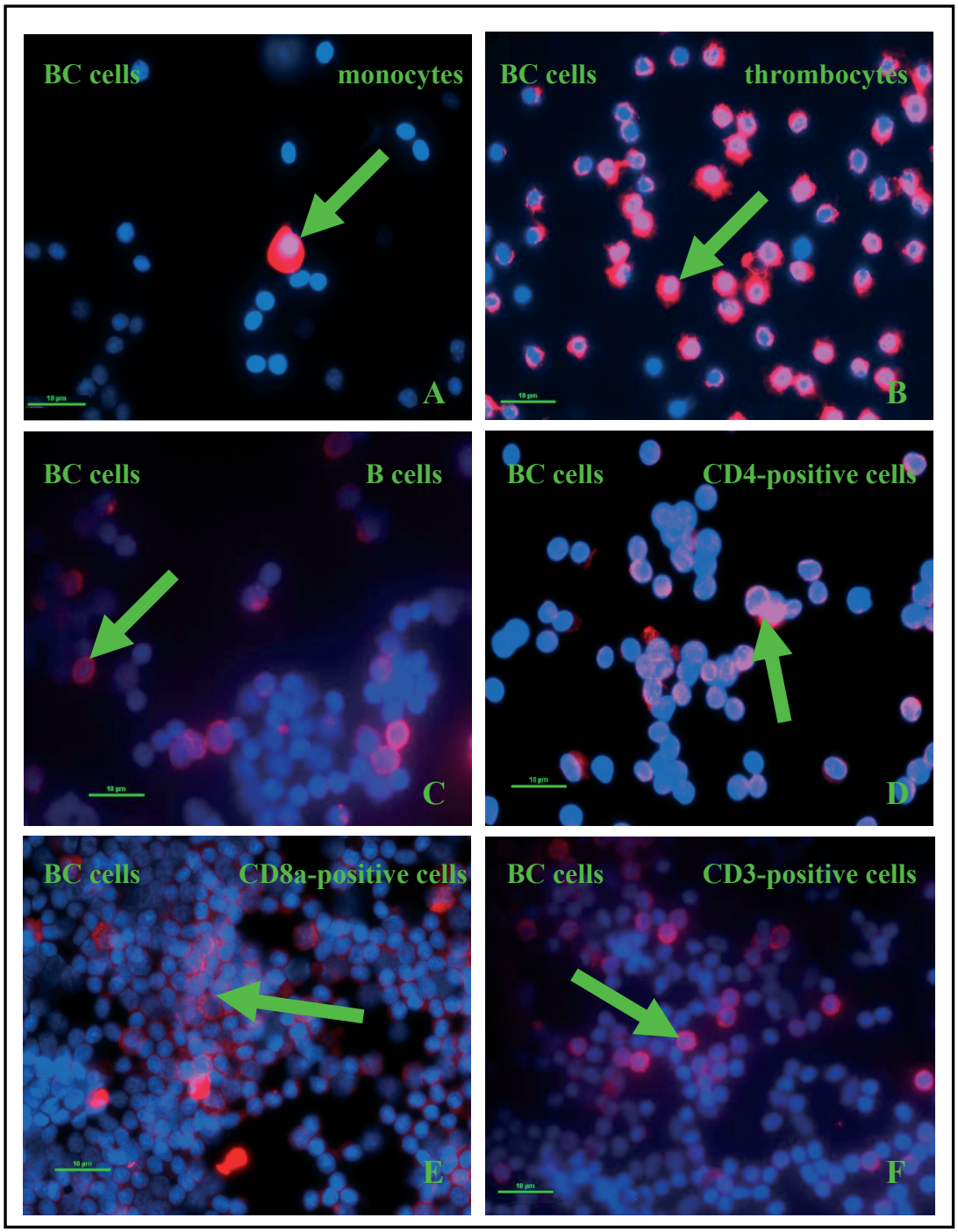

Fig. 28: Indirect immunofluorescence (IIF) for characterization of BC cells from cockatiels. (A) Monocytes in BC, mouse anti chicken monocytes, cy3 conjugate goat anti-mouse. (B) Thrombocytes in BC, mouse anti-chicken thrombocytes, cy3 conjugate goat anti-mouse. (C) B cells in BC, mouse anti-duck IgY, cy3 conjugate goat anti-mouse.(D) CD4-positive cells in BC, mouse anti-chicken CD4, cy3 conjugate goat anti-mouse. (E) CD8a-positive cells in BC, mouse anti-chicken CD8a, cy3 conjugate goat anti-mouse. (F) CD3-positive cells in BC, rat anti-human CD3, cy3 conjugate goat anti-rat. Ring-like form surrounding the cells (green arrow) indicated positive cells. DAPI staining. Scale bar 100µm.

4.14.3. Characterization of immune cells in cockatiel BC by flow cytometry

After optimization of the FC protocol, we tried to characterize the immune cells in cockatiel BC cells also by flow cytometry (**Fig. 29 and 30**). We found cockatiel B cells, CD4-positive cells, CD8a-positive cells, monocytes, thrombocytes only in low percentages but we did not find CD3-positive cells in BC cells. We detected positive immunofluorescence signals in the positive control of every cell surface marker except for the positive control of CD3 cells. Cell counting in each sample was performed by the automated flow cytometer. The obtained results showed that low percentage of positive cells for (monocytes 3.3%, thrombocytes 3.2%, B cells 3.8%, CD4-positive cells 7.3%, CD8a-positive cells 6.2%, CD3-positive cells 0.2%) in cockatiel BC cells at day one after isolation (**Fig. 29 and 30**).

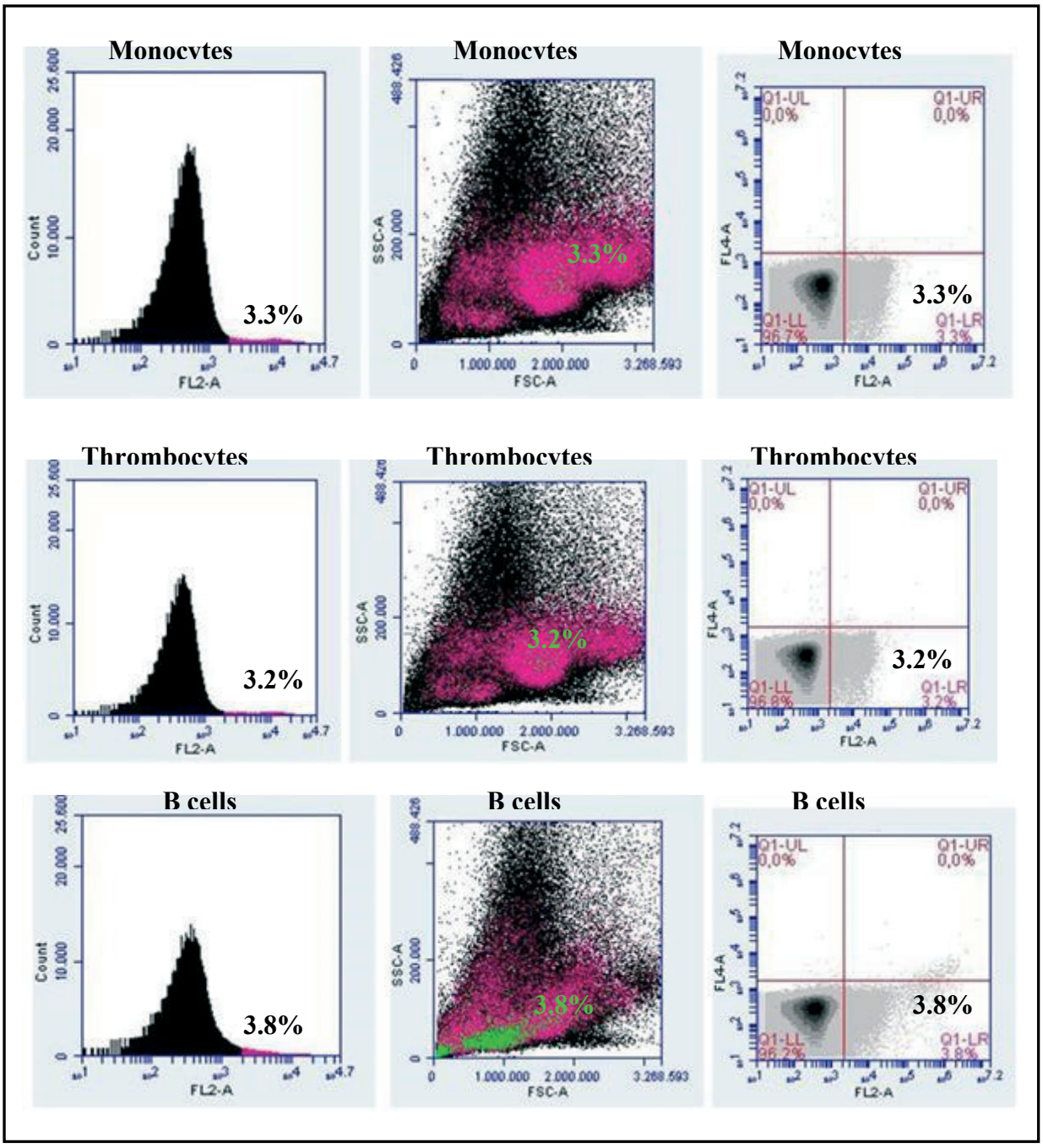

Fig. 29: Characterization of monocytes, thrombocytes and B cells in buffy coat of cockatiels by flow cytometry. Mouse anti-chicken monocytes, mouse anti-chicken thrombocytes and mouse anti-duck IgY antibodies were used as primary antibodies. Phycoerythrin (PE) conjugate goat anti-mouse IgG was used as a secondary antibody. Monocytes, thrombocytes, and B cells were detected in FL2-A channel of the flow cytometer, indicating positive cells. BD accuri C6 software, BD acurri C6 flow cytometer (BD Biosciences, Germany).

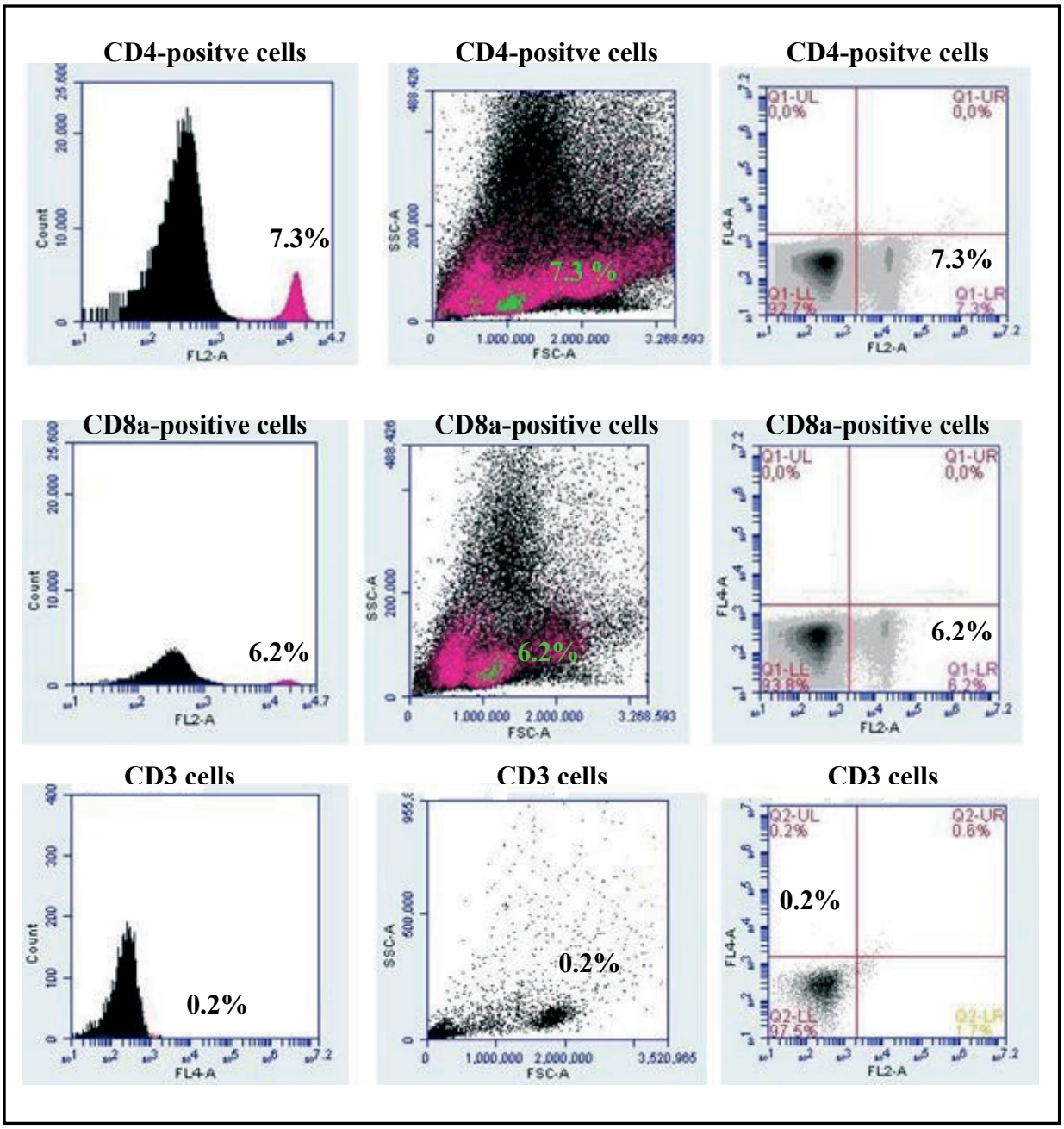

Fig. 30: Characterization of CD4 and CD8a-positive cells in buffy coat of cockatiels by flow cytometry. Mouse anti-chicken CD4, mouse anti-chicken CD8a were used as primary antibodies. Phycoerythrin (PE) conjugate goat anti-mouse IgG was used as secondary antibody for anti-CD4 and anti-CD8a antibodies. CD4 and CD8a were detected in FL2-A channel of the flow cytometer, indicating positive cells. Rat anti-human CD3 was used as primary antibody. Allophycocyanin (APC) conjugate goat anti-rat IgG was used as secondary antibody for anti CD3 antibody. CD3 was not detected in FL4-A channel of the flow cytometer, indicating negative results. BD accuri C6 software, BD acurri C6 flow cytometer (BD Biosciences, Germany).

4.15. Experimental infection of BC cells with ABV-4 and demonstration of ABV antigen and ABV-4 RNA at early time point (3 and 5 dpi)

4.15.1. Demonstration of ABV antigen in BC cells

We examined infected and non infected BC cells every day and investigated the viability. One day p.i, cell viability was 99% (table 40). Two days p.i, 70% of cells were viable and appeared as clumps or cells aggregates. Four days p.i. cell viability was 65%, then declined gradually until 15 days post infection (table 43). ABV antigen was not found in cockatiel BC cells at 3 and 5 dpi by IIF. By IIF, we found intranuclear positive signals in the positive control but not in cockatiel BC cells.

Table 43: Viability of infected and non BC cells after ABV-4 infection

Cell type	Days after isolation	Cells viability of BC cells	
		Non infected	Infected with ABV-4
BC cells	Day 1	100 %	99 %
	Day 2	99 %	70 %
	Day 3	79 %	69 %
	Day 4	73 %	65 %
	Day 5	71 %	63 %
	Day 6	69 %	60 %
	Day 7	63 %	57 %
	Day 8	60 %	51 %
	Day 9	52 %	48 %
	Day 10	49 %	44 %
	Day 11	45 %	39 %
	Day 12	42 %	32 %
	Day 13	30 %	23 %
	Day 14	22 %	12 %
	Day 15	8 %	5 %

0.4% trypan blue in 1xPBS. IX70 S8F inverted microscope (Olympus, USA)

4.15.2. Demonstration of ABV-4 RNA in BC cells

ABV-4 RNA was not detected in cockatiel BC cells after ABV-4 infection. We found ABV-4 RNA only in the positive control (cDNA of the ABV-4 suspension) but not in BC cells after ABV-4 infection.

4.16. Experimental infection of BC cells with ABV-4 and demonstration of ABV antigen and ABV-4 RNA at early time point (9 and 15 dpi)

4.16.1. Demonstration of ABV antigen in BC cells

ABV antigen detection was not positive in BC cells at late time points (9 and 15 dpi) after infection with ABV-4 (**Fig. 31**).

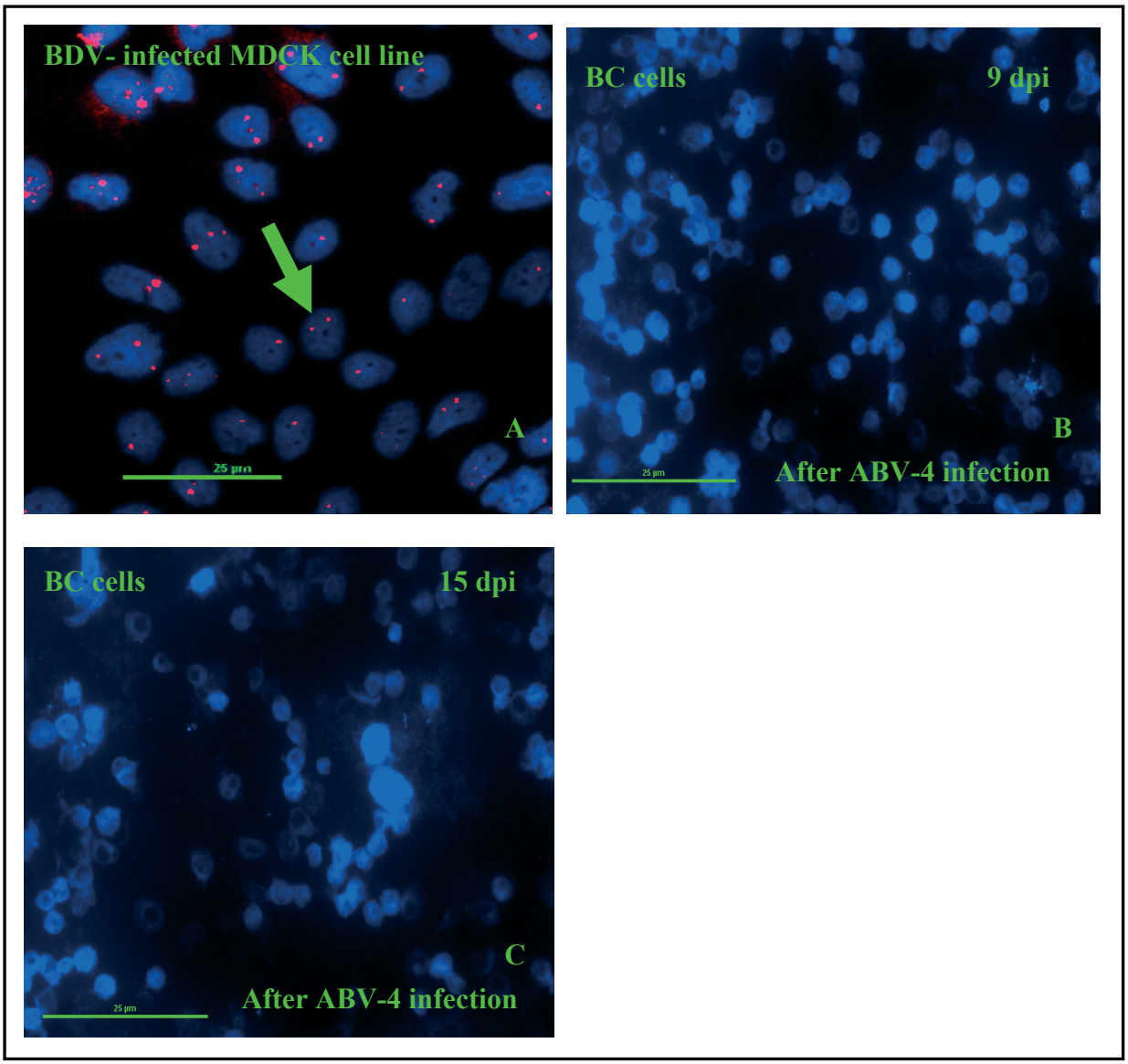

Fig. 31: Indirect immunofluorescence (IIF) for demonstration of ABV antigen in BC cells at day 9 and 15 after ABV-4 infection. (A) BDV infected MDCK H1766 cell line (positive control), red intranuclear inclusions indicate BDV infected cells (green arrow). (B) BC cells, 9 dpi, absence of intranuclear positive signals in BC cells after ABV-4 infection. (C) BC cells, 15 dpi, absence of intranuclear positive signals in BC cells after ABV-4 infection. Polyclonal anti-BoDV rat serum (primary antibody), Cy3 conjugate goat anti-rat (H and L) (secondary antibody). Scale bar 25 µm.

4.16.2. Demonstration of ABV-4 RNA in BC cells

By PCR, ABV-4 RNA was not found in BC cells at day 9 and 15 after ABV-4 infection (**Fig. 32**). ABV-4 RNA could also not be detected in non infected BC cells. However, ABV-4 RNA was amplified in the positive control (ABV-4 suspension). Taking together, ABV-4 RNA was not found in the BC cells after ABV-4 infection.

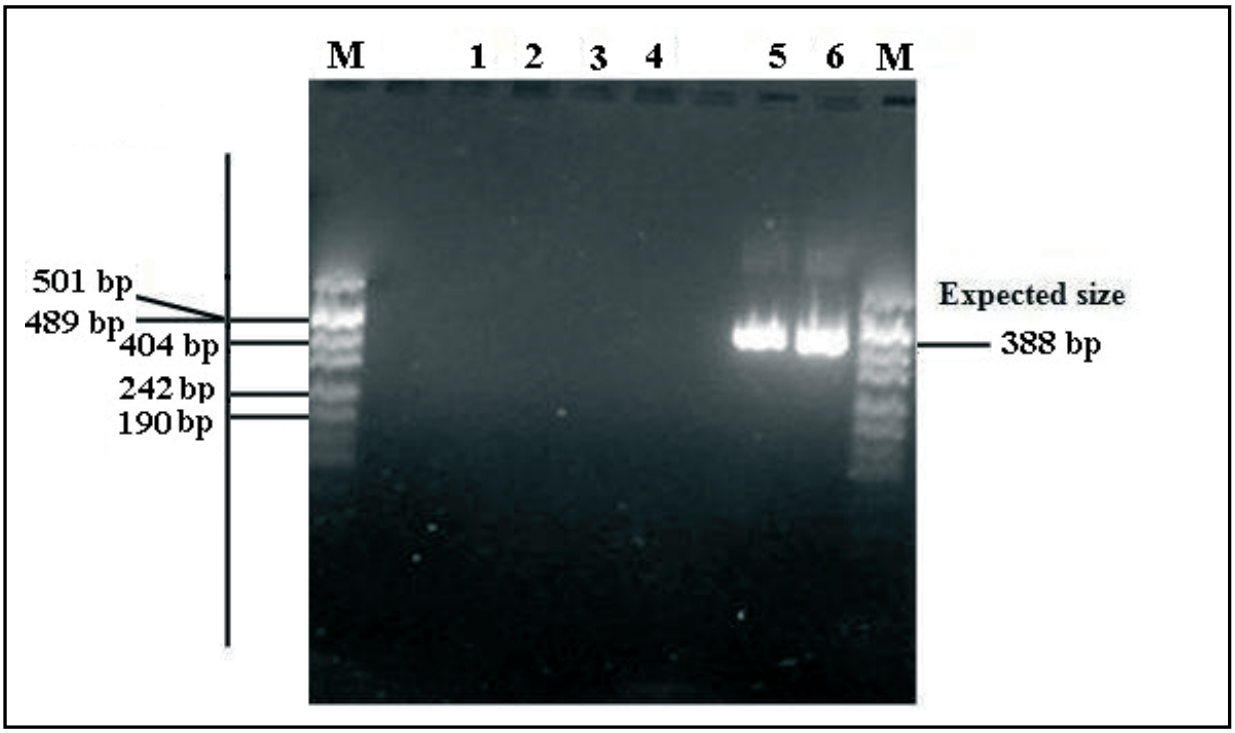

Fig. 32: Polymerase chain reaction (PCR) for detection of ABV-4 in BC cells at day 9 and 15 after ABV-4 infection. (M) pUC19 DNA/MspI (HpaII) Marker, 23 (Thermo Scientific, Germany). Lane 1= PCR products of infected BC cells at day 9 in culture. Lane 2= PCR products of non infected BC cells at day 9 in culture. Lane 3= PCR products of infected BC cells at day 15 in culture. Lane 4= PCR products of non infected BC cells at day 15 in culture. Lane 5 and 6= cDNA amplificated from ABV-4 suspension (positive control). 2% agarose, 6 volt/cm electrodes distance, one hour.

4.17. Experimental infection of BC cells after stimulation with PHA-M mitogen

4.17.1. Stimulation of BC cells with PHA-M

After optimizing the stimulation conditions of BC cells *in vitro*, we stimulated BC cells with phytohemagglutinin M (PH-M) mitogen successfully (**Fig. 33**). Comparison of trypan blue assay and IIF methods to investigate the percentage of stimulated BC cells proved that BC cells were stimulated and the proliferation rate increased over the time (table 44). Both methods showed that stimulated BC cells reached the maximal rate of the proliferative response at day 3 post stimulation with PHA-M mitogen. By IIF, we investigated the

proliferative rate of stimulated BC cells at day 0 post stimulation in order to monitor the starting point of the stimulation. Presence of distinct intranuclear positive signals to anti-bromodeoxyuridine (BrdU) antibodies in the stimulated BC cells was an indicator for the BC cell proliferation (**Fig. 34**). We found that stimulated BC cells started to proliferate 2 hours post stimulation (2 hours= 8 %, 4 hours= 15 %, 6 hours= 19 %, 8 hours= 23 %, and 10 hours= 29 %). At day 0, the maximal percentage of the proliferating BC cells was 10 hour post stimulation. Moreover, we found that the percentage of proliferating BC cells increased over time (day 1= 40%, day 2= 64%, day 3= 88%, day 4= 86%, day 5= 81%, day 6= 74%, day 7= 71%, and day 8= 68%) as shown in table 44. The stimulated BC cells reached the maximal proliferative rate at day 3 post stimulation. The percentage of proliferating BC cells decreased from day 9 until day 15 post stimulation (day 9= 55%, day 10= 51%, day 11= 46%, day 12= 31%, day 13= 19%, day 14= 4%, and day 15= 1%) as shown in table 44. Microscopically, we found that stimulated BC cells agglutinated post stimulation with PHA-M mitogen indicating successful stimulating of BC cells. Most of the stimulated BC cells agglutinated as clumps at day one after stimulation and did not separate anymore over the time of stimulation. Results of counting stimulated BC cells in the IIF corresponded to data of counting of stimulated BC cells by trypan blue assay (table 44).

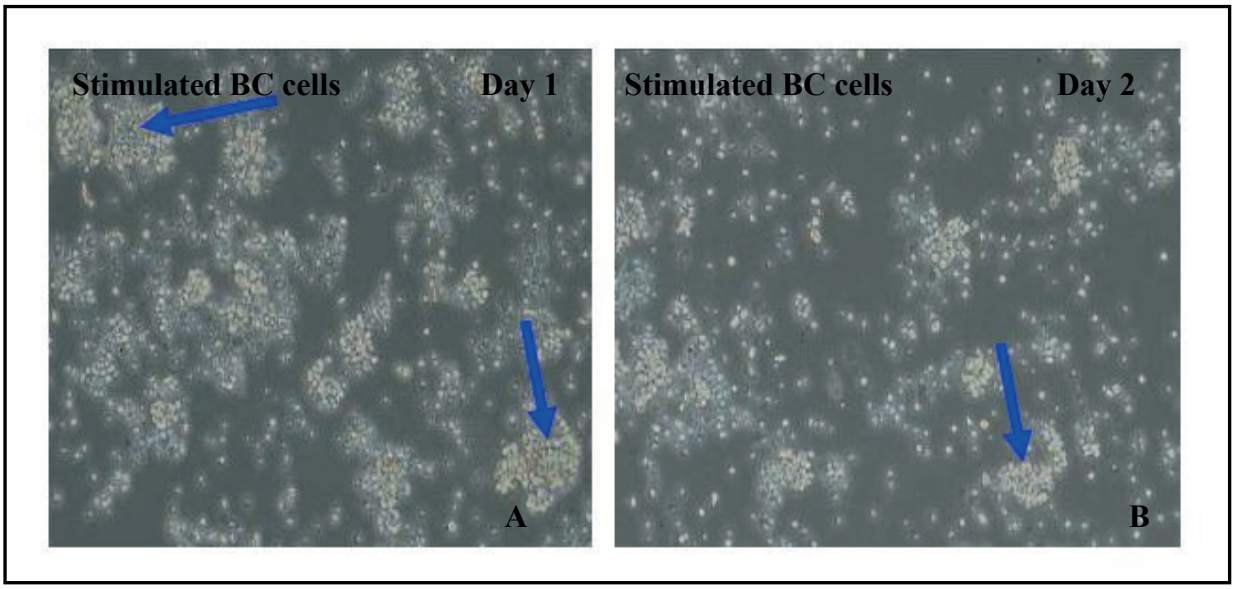

Fig. 33: Buffy coat cells from cockatiels after stimulation with PHA-M mitogen. BC cells agglutinated in culture medium one day post stimulation by PHA-M mitogen (blue arrow). (A) Stimulated BC cells at day one. (B) Stimulated BC cells at day two. Magnification 20x.

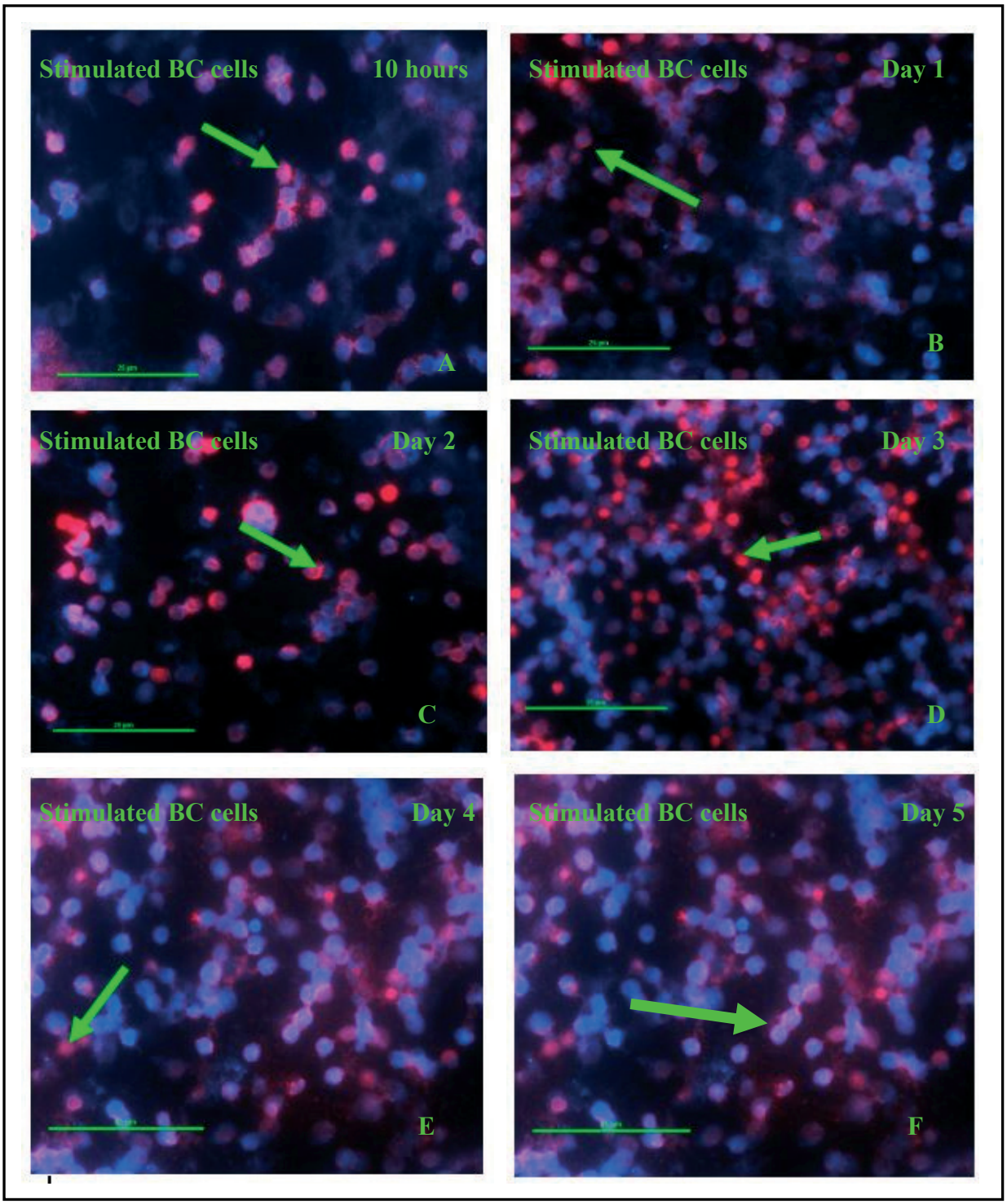

Fig. 34: IIF for demonstration of BrdU in BC cells after stimulating with PHA-M mitogen. Red intranuclear signals indicate BC cells stimulation and proliferation (green arrow). (A) Detection of BrdU 10 hours post stimulation. (B) Detection of BrdU one day post stimulation. (C) Detection of BrdU two days post stimulation. (D) Detection of BrdU three days post stimulation. (E) Detection of BrdU four days post stimulation. (F) Detection of BrdU five days post stimulation. Mouse anti-BrdU antibody (primary antibody), cy3 conjugate goat anti mouse (secondary antibody), scale bar 100µm.

Table 44: Comparison between stimulated and non stimulated BC cells

Days post stimulation	BC cells	Trypan blue assay		IIF (400 cells / smear field)	
		Total count number	Percentage of stimulation	Total count number	Percentage of stimulation
The day of isolation	Stimulated	632,000 cells	29%	120 cells	30%
	Non stimulated	490,000 cells		280 cells	
Day 1	Stimulated cells	686,000 cells	40%	160 cells	40%
	Non stimulated	490,000 cells		240 cells	
Day 2	Stimulated cells	801,000 cells	64%	220 cells	55%
	Non stimulated	489,000 cells		180 cells	
Day 3	Stimulated	885,000 cells	88%	336 cells	84%
	Non stimulated	471,000 cells		64 cells	
Day 4	Stimulated	827,000 cells	86%	340 cells	85%
	Non stimulated	445,000 cells		60 cells	
Day 5	Stimulated	706,000 cells	81%	316 cells	79%
	Non stimulated	390,000 cells		84 cells	
Day 6	Stimulated	643,000 cells	74%	288 cells	72%
	Non stimulated	370,000 cells		112 cells	
Day 7	Stimulated	588,000 cells	71%	280 cells	70%
	Non stimulated	344,000 cells		120 cells	
Day 8	Stimulated	527,000 cells	68%	256 cells	64%
	Non stimulated	314,000 cells		144 cells	
Day 9	Stimulated	465,000 cells	55%	204 cells	51%
	Non stimulated	300,000 cells		196 cells	
Day 10	Stimulated	362,000 cells	51%	152 cells	38%
	Non stimulated	240,000 cells		248 cells	
Day 11	Stimulated	277,000 cells	46%	160 cells	40%
	Non stimulated	190,000 cells		240 cells	
Day 12	Stimulated	209,000 cells	31%	108 cells	27%
	Non stimulated	160,000 cells		292 cells	
Day 13	Stimulated	95,000 cells	19%	44 cells	11%
	Non stimulated	80,000 cells		356 cells	
Day 14	Stimulated	20,800 cells	4%	24 cells	6%
	Non stimulated	20,000 cells		376 cells	
Day 15	Stimulated	4,040 cells	1%	12 cells	3%
	Non stimulated	4,000 cells		388 cells	

0.4% trypan blue in 1xPBS. BC cells= Buffy coat cells, IIF= indirect immunofluorescence

4.17.2. Experimental infection of stimulated BC cells at day 1 post isolation

4.17.2.1. Demonstration of BrdU incorporation from 0 – 5 dpi and stimulation

By IIF, we investigated the BrdU incorporation in stimulated BC cells. We found that BC cells proliferated from day 0 until the end of the observation at day 5 post stimulation with PHA-M (**Fig. 34**). By IIF, percentage of BrdU positive BC cells was 40% at day 1, increased to 64% at day 2, and reached maximal percentage of BrdU positive BC cells (88% and 86%) at day 3 and day 4, respectively. At day 5, percentage of BrdU positive BC cells decreased to 81%. The highest percentage of proliferating BC cells were counted at day 3 and day 4. By comparison between results of IIF and results of trypan blue assay in stimulated BC cells, we did not find a difference between counting the stimulated BC cells by trypan blue assay and the percentage of positive cells which were labelled with anti-BrdU antibody, indicating that both methods were equivalent (table 44).

4.17.2.2. Demonstration of ABV antigen from 0 – 5 days post infection, and stimulation

ABV antigen detection was not found in stimulated and non stimulated BC cells at day 0, 1, 2, 3, 4, and 5 after ABV-4 infection (**Fig. 35**).

4.17.2.3. Demonstration of ABV-4 RNA from 0 – 5 days post infection, and stimulation

We investigated the presence of ABV-4 RNA in stimulated BC cells at 10 hours post stimulation and infection with ABV-4. We also investigated the presence of ABV-4 RNA at day 1, 2, 3, 4 and 5 post stimulation and infection with ABV-4. ABV-4 RNA has not been found in stimulated and in non stimulated BC cells from day 0 until day 5 by RT-PCR (**Fig. 36 and 37**).

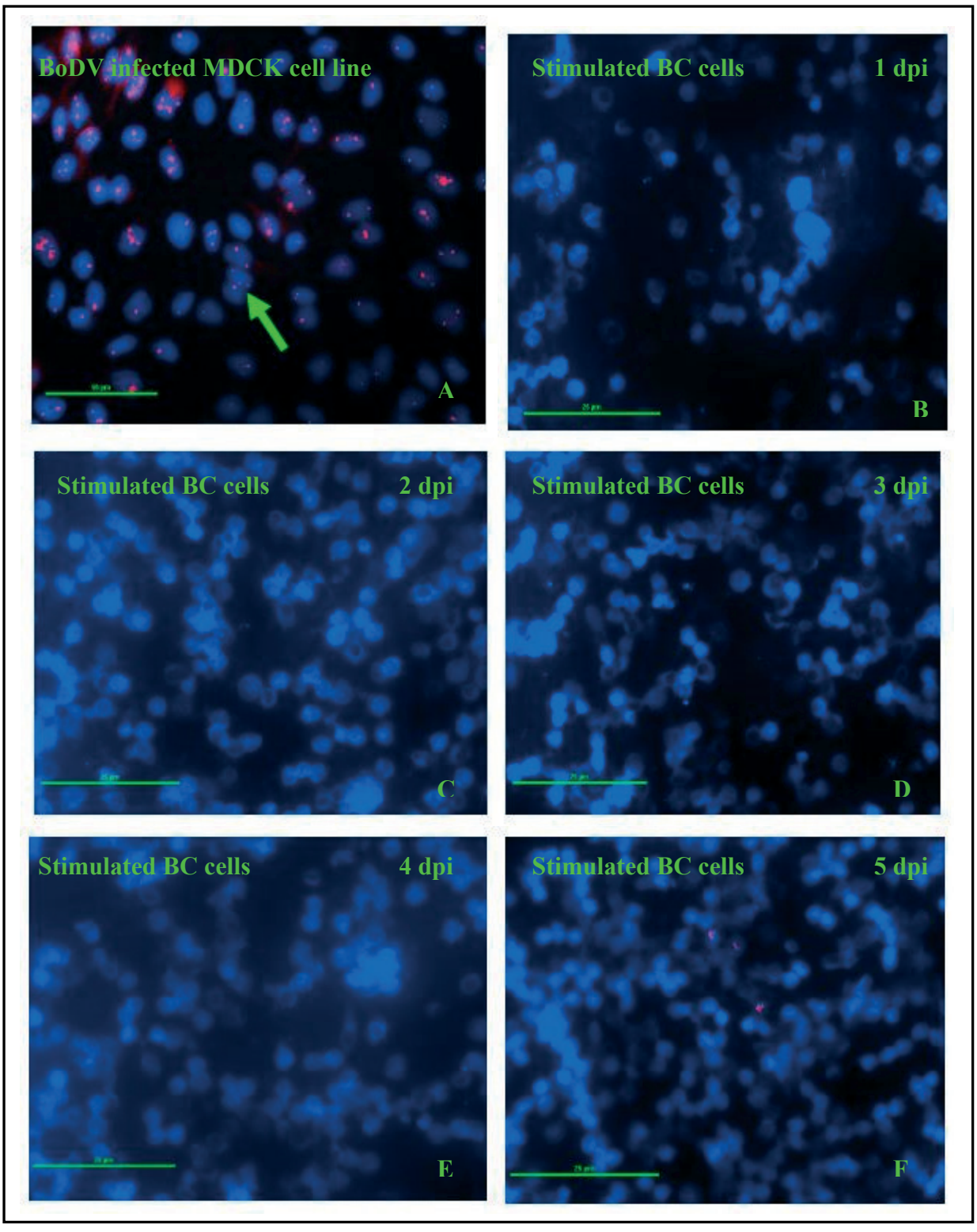

Fig. 35: IIF of stimulated BC cells after ABV-4 infection. BC cells were stimulated with PHA-M at day of isolation. (A) BoDV infected MDCK cell line (positive control), red intranuclear inclusions represent viral antigen (green arrow). (B, C, D, E, and F) Stimulated BC cells after ABV-4 infection, no viral antigen detected. Polyclonal anti-borna disease virus rat serum (primary antibody), cy3 conjugate goat anti-rat (secondary antibody), scale bar 100µm.

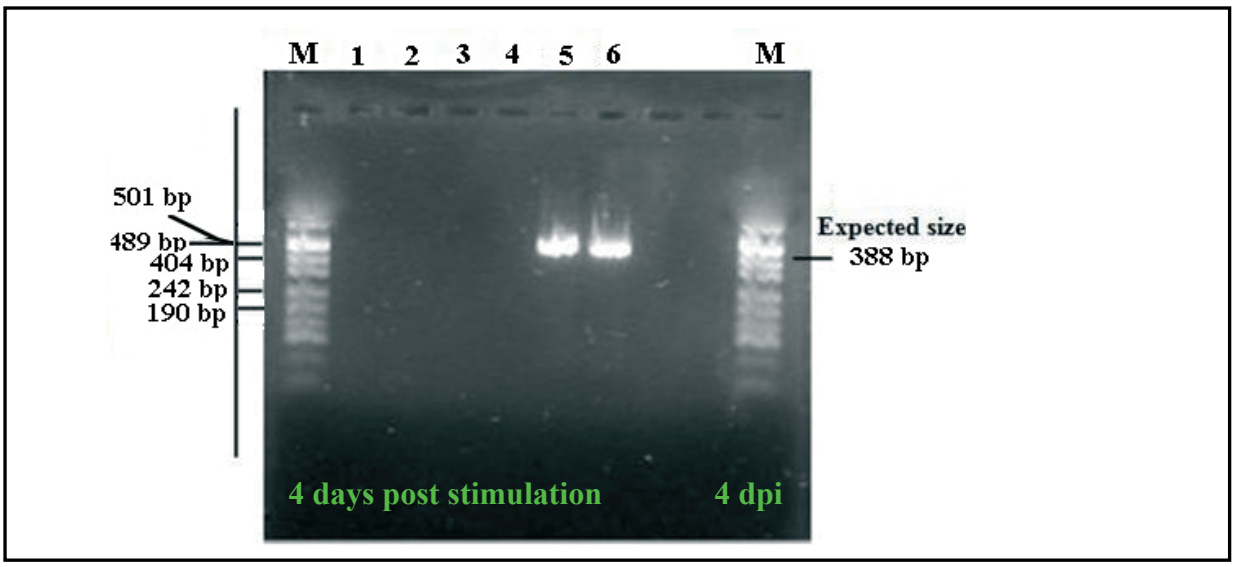

Fig. 36: Amplification of cDNA of stimulated BC cells at day 4 after ABV-4 infection. (M) pUC19 DNA/MspI (HpaII) Marker, 23 (Thermo Scientific, Germany). Lane 1= PCR products of stimulated, infected BC cells (4 days in culture), lane 2= PCR products of non stimulated, infected BC cells (4 days in culture), lane 3= PCR products of stimulated, non infected BC cells, lane 4= PCR products of non stimulated, non infected BC cells. Lane 5 and 6 =ABV-4 suspension (positive control). 2% agarose, 6 volt/cm electrodes distance, one hour.

4.17.3. Experimental infection of stimulated BC cells at day 3 post stimulation

4.17.3.1. Demonstration of BrdU incorporation from 4 – 14 days post stimulation

By IIF, we investigated the synthesis of BrdU in stimulated BC cells from 4-15 days post stimulation. We found that BC cells were stimulated with PHA-M. By counting BrdU positive BC cells, proliferating BC cells increased over time. Proliferating BC cells decreased in their number from day 9 onward. By IIF, we detected few proliferating BC cells (not more than 4%) in the slide smear at day 14 post stimulation. At day 15, we did not detect stimulated BC cells indicating the end of stimulation phase at this time point.

4.17.3.2. Demonstration of ABV-4 RNA from 4 – 14 days post stimulation

By RT-PCR, we investigated the presence of ABV-4 RNA in stimulated BC cells from day 4 until day 14 post stimulation and infection. We infected the stimulated BC cells with ABV-4 where they had high cells proliferation rate at day 3 post stimulation. ABV-4 RNA was not detected in stimulated BC cells at day 4, 6, 8, 10, 12 and 14 post stimulation (**Fig. 37 and 38**).

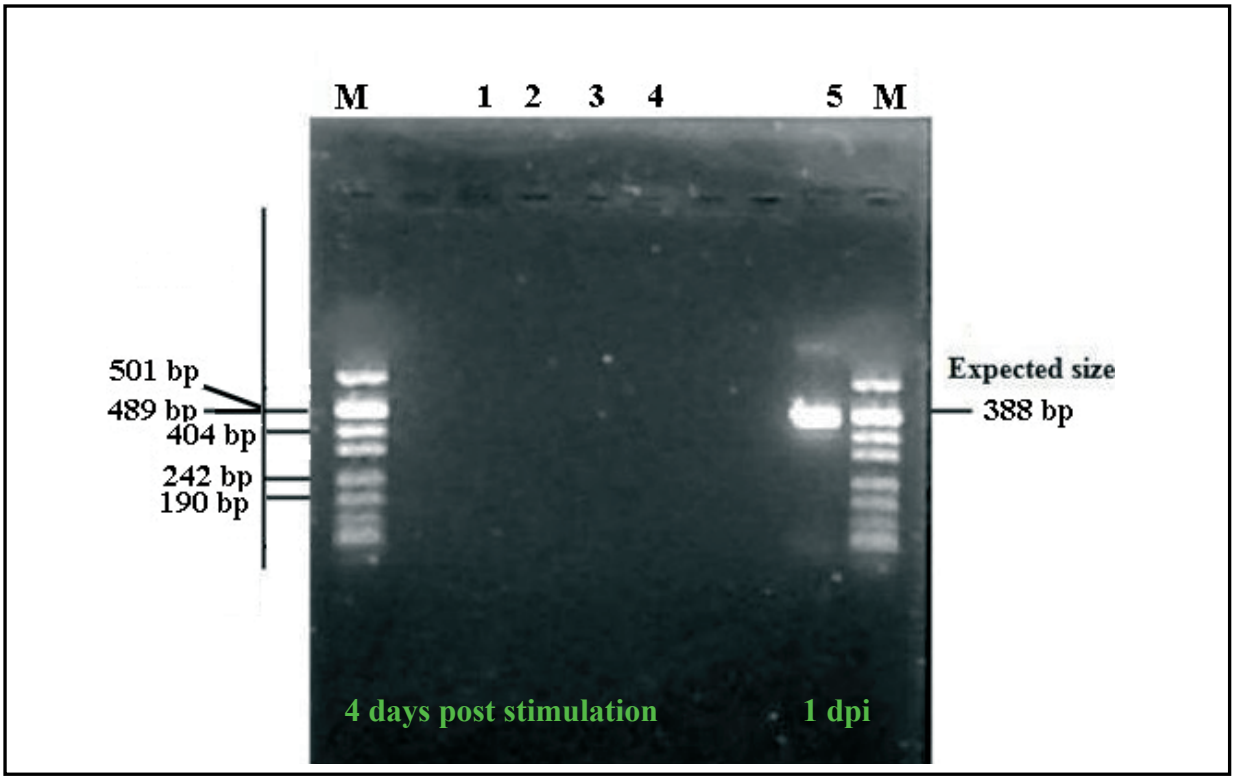

Fig. 37: Amplification of cDNA of stimulated BC cells at day 4 post stimulation, after ABV-4 infection. (M) pUC19 DNA/MspI (HpaII) Marker, 23 (Thermo Scientific, Germany). Lane 1=PCR products of stimulated, infected BC cells (4 days post stimulation, 1 dpi), lane 2= PCR products of non stimulated, infected BC cells, lane 3= PCR products of stimulated, non infected BC cells, lane 4= PCR products of non stimulated, non infected BC cells. Lane 5=ABV-4 suspension (positive control). 2% agarose, 6 volt/cm electrodes distance, one hour.

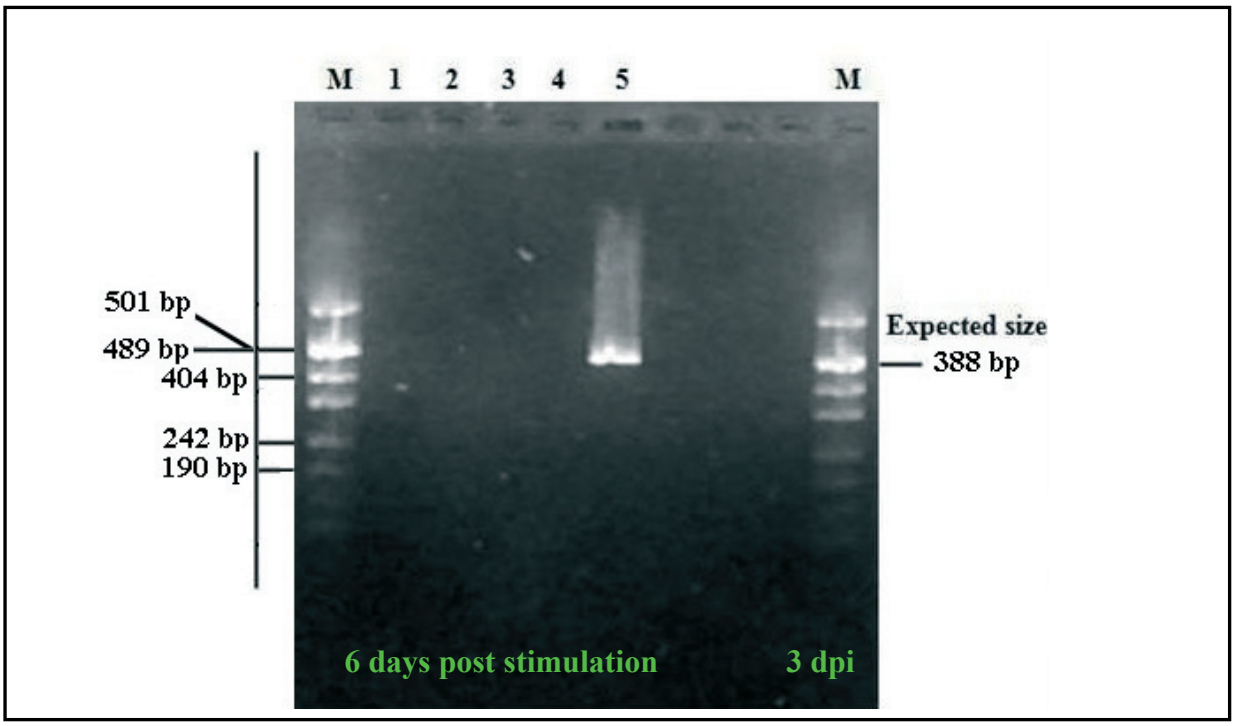

Fig. 38: Amplification of cDNA of stimulated BC cells at day 6 post stimulation, after ABV-4 infection. (M) pUC19 DNA/MspI (HpaII) Marker, 23 (Thermo Scientific, Germany). Lane 1=PCR products of stimulated, infected BC cells (6 days post stimulation, 3 dpi), lane 2= PCR products of non stimulated, infected BC cells, lane 3= PCR products of stimulated, non infected BC cells, lane 4= PCR products of non stimulated, non infected BC cells. Lane 5=ABV-4 suspension (positive control). 2% agarose, 6 volt/cm electrodes distance, one hour.

5. Discussion

PDD is fatal inflammatory disease which affects the central, autonomic, and peripheral nervous system disease mainly in psittacine. PDD is characterized by non purulent ganglioneuritis and encephalitis (Berhane et al., 2001). In 2008, two independent research groups are reported that avian Borna virus (ABV) is the causative agent of PDD (Honkavuori et al., 2008; Kistler et al., 2008). The pathogenesis of ABV infection is still incompletely understood. To date, fourteen ABV genotypes have been detected in both psittacine and non psittacine birds (Kuhn et al., 2015). Whether differences in the pathogenicity among the 14 ABV genotypes exist is largely unknown. Distribution pattern of ABV in naturally PDD affected birds were characterized in many previous studies using immunohistochemistry (IHC), reverse transcription polymerase chain reaction (RT-PCR) and Western blotting assay (Honkavuori et al., 2008; Gancz et al., 2009; Kistler et al., 2010; Lierz et al., 2009; Ouyang et al., 2009; Weissenböck et al., 2009; Lierz et al., 2010; Raghav et al., 2010; Reßmeyer et al., 2010; Wünschmann et al., 2011; Rubbenstroth et al., 2013). We characterized the distribution pattern of inflammatory lesions, ABV antigen, ABV-2 RNA, and ABV-4 RNA in experimentally ABV-2 and ABV-4 infected cockatiels respectively in order to get insight in potential different pathogenicity of the ABV genotypes. ABV-2 and ABV-4 induced a persistent infection via intracerebral and intravenous inoculation after experimental infection with ABV-2 and ABV-4 in cockatiels (Piepenbring et al., in revision). After 22 days post ABV-2 infection, and 33 days post ABV-4 infection, the infected animals developed typical clinical symptoms for PDD via different routes of infection especially when inoculated via the intravenous route. This finding payed attention that blood cells might be a target for ABV in psittacine birds and let us to hypothesize that blood cells might have a role for the spread of the ABV infection within organs. ABV belongs phylogenetically to *Bornaviridae* but for the mammalian Borna disease virus, the intravenous route of infection was not successful. Carbone and colleagues, (1987) mentioned that Borna disease virus (BoDV) failed to induce infection in experimentally infected rats via intravenous and oral route of infection. Findings of this study (Carbone et al., 1987) showed that inoculated rats developed clinical Borna disease via the intraceberal, intranasal, intramuscular and subcutaneous inoculation. It is unclear whether ABV and mammalian borna disease virus have the same biological properties to invade the body cells and spread throughout the body. The mode of dissemination of ABV to all organs after ABV infection is still debated and need further investigations. To investigate the potential role of blood cells after ABV infection, therefore, another aim of the study was to analyze whether blood cells could be infected with ABV.

5.1. Comparison of the clinical observations

After experimental infection with ABV-2 and ABV-4 in cockatiels, 5/18 birds of the ABV-4 infected groups exhibited symptoms on day 33 dpi consistent with PDD, mostly neurological signs in contrast to 12/18 birds of the ABV-2 infected groups (Piepenbring et al., 2012). Within the ABV-2 infected groups, clinical signs occurred on day 22 dpi and consisted of mostly gastrointestinal clinical signs. This is in line with (Kistler et al., 2008; Honkavouri et al., 2008) and many subsequent studies where ABV was identified as the aetiological agent for PDD in psittacines since 2008. The onset of clinical signs appeared earlier in the experimentally infected birds after ABV-2 infection than ABV-4 infection. That means, ABV-2 could have more rapid onset of clinical signs (22 dpi) in comparison to experimentally ABV-4 infected birds (33 dpi) and more gastrointestinal signs were induced. This might indicate that ABV-2 has more tropism to the GIT. In contrast, ABV-4 seems to have more tropism toward the CNS.

5.2. Comparison of gross lesions

Proventriculi were enlarged in 10/18 birds after ABV-2 infection and in 7/18 birds after ABV-4 infection. In the ABV-2 group, 5 birds had a severely dilated proventriculus in contrast to one bird in the ABV-4 group. This might indicate that gross lesions were more severe in the experimentally ABV-2 infected cockatiels than after experimental infection with ABV-4 (Piepenbring et al., 2012). It was reported that the clinical presentation of gastrointestinal dysfunction is secondary within the enteric nervous system (Shivaprasad et al., 1995; Berhane et al., 2001; Schmidt et al., 2003; Kistler et al., 2008; Ouyang et al., 2009; Gray et al., 2010).

5.3. Histological findings

Since the discovery of ABV as the etiological agent for PDD, histopathological lesions associated with ABV infection were described in many previous studies in naturally ABV-infected psittacines which suffered from PDD (Kistler et al., 2008; Lierz et al., 2009; Ouyang et al., 2009; Raghav et al., 2010; Wünschmann et al. 2011; Delnatte et al., 2013).

5.3.1. Histological findings after ABV-2 infection

In the CNS, mild and moderate gliosis was detected in the brain in 13/18 experimentally ABV-2 infected birds. No obvious inflammatory infiltrates were found in the brain in 18/18 birds. The kinetic of gliosis decreased at mid time point (86-172 dpi) until late time point 231 dpi in the 13/18 birds. This might indicate that ABV-2 is less pathogenic to the CNS and the gliosis could represent a reaction pattern of the CNS which can also been seen after ABV-4 infection.

In the GIT, inflammatory lesions were detected in all GIT organs most severely in intestine and proventriculus, indicating that these organs were the most affected GIT organs after ABV-2 infection. Inflammatory lesions in the GIT consisted of mononuclear cells infiltrates in the intestinal mucosa, lamina muscularis as well as around nerves and ganglia of gizzard proventriculus, and intestine or in the ganglia and nerve fibers of crop. These findings are in line with previous reports (Ouyang et al., 2009: Raghav et al., 2010; Staeheli et al., 2010: Delnatte et al., 2013) where the lymphoplasmacytic myenteric ganglioneuritis was detected in the GIT organs in psittacines suffering from PDD. An independent study has also shown that lymphoplasmacytic infiltrates in the gizzard and proventriculus are highly characteristic for PDD (reviewed in Staeheli et al., 2010). The kinetic of inflammatory lesions in the GIT showed variability. It showed a consistency in severity of the inflammatory lesions in the crop and gizzard during the whole investigation period 231 dpi. In the proventriculus, it decreased at mid time point (88-172 dpi) but it increased late time point at 231 dpi. In the intestine, it was variable during the whole investigation period. We still do not know the reasons behind the variability of inflammatory lesions in the GIT after ABV-2 infection.

In the peripheral organs, inflammatory lesions were mainly found in the kidney, liver, spleen and skin. Inflammatory lesions in the peripheral organs were found as infiltration of mononuclear cells, sometimes with follicular shape-like appearance. This could be normal activation reaction of the immune system as also present in the mock and sentinel birds. Periganglionitis and/or perineuritis were also detected in the peripheral organs. This is typical lesion and this lesion was already detected in many previous studies (Kistler et al., 2008; Honkavouri et al., 2008; Gray et al., 2009). Peripheral neuritis was also detected in most of the peripheral organs in psittacine birds affected with PDD (Shivaprasad et al., 1995; Berhane et al., 2001; Rinder et al., 2009; Raghav et al., 2010). The lymphocytic infiltrates are not restricted to neural tissue of the gastrointestinal tract and may also be seen in conduction fibers of the heart, the adrenal gland in naturally occurring PDD affected psittacines. We also detected mononuclear infiltration in the ganglia adjacent to the heart and kidney after ABV-2

infection. These findings are in accordance with observations of Raghav et al., 2010 in psittacine with PDD. The kinetic of inflammatory lesions did not change markedly in all peripheral organs during the whole investigation period of 231 dpi.

5.3.2. Histological lesions after ABV-4 infection

In the CNS, mild, moderate and severe inflammatory lesions were detected in the brain in 17/18 experimentally ABV-4 infected birds. Inflammatory lesions were also detected in the spinal cord as mild and moderate in 11/18 birds. The perivascular cuffing of mononuclear cells has already been described as typical histopathological lesion in the CNS in naturally ABV infected birds in many of previous studies (Kistler et al., 2008; Honkavouri et al., 2008; Delnatte et al., 2013; Ouyang et al., 2009; Raghav et al., 2010). We detected the mononuclear encephalitis with multifocal perivascular cuffing mainly in the cerebrum after ABV-4 infection. The data presented here were supported by the similar results obtained by Ouyang et al., 2009 where the perivascular cuffing mainly was detected in the cerebrum and brain stem in ABV infected birds. The kinetic of inflammatory lesions in the CNS increased at late time point, indicating an active induction of immune response in the CNS.

In the GIT, inflammatory lesions were detected in all GIT organs most severely in gizzard and proventriculus, indicating that these organs were the most affected GIT organs after ABV-4 infection. The kinetic of inflammatory lesions in the GIT revealed that inflammatory lesions decreased in all GIT organs at 230 dpi in experimentally ABV-4 infected birds. This might indicate a resolution of inflammation in the GIT started at late time point 230 dpi after ABV-4 infection.

In the peripheral organs, inflammatory lesions were mainly found in the liver, kidney, heart, spleen, and pancreas. Infiltrations of mononuclear cells were also detected as follicular shape-like aggregations in the liver, kidney, and pancreas. Such infiltrates were also detected in the mock and sentinel birds. These findings are in line with (Gray et al., 2009). Periganglionitis and/or perineuritis were also detected as typical lesion in the peripheral organs. Our results are in accordance with findings of Raghav et al., 2010 who detected characteristic lymphoplasmacytic infiltrates in the ganglia adjacent to the adrenal gland, heart, liver, kidney, CNS and also in the GIT organs in 16 psittacine birds suffered from PDD. Last and colleagues (2012) detected ABV-4 in PDD affected captive bred blue and gold macaws (*Araara rauna*) in South Africa. Findings of the study showed that lymphoplasmacytic encephalitis, gastrointestinal myenteric gangioneuritis and leiomyositis were detected in the PDD affected birds. Our results are also in accordance with this study (Last et al., 2012). The kinetic of

inflammatory lesion in the peripheral organs was variable. We do not know why the kinetic inflammatory lesions in the peripheral organs showed variability after ABV-4 infection.

5.3.3. Comparison of histological lesions after ABV-2 and ABV-4 infection

In the CNS, gliosis was detected but no obvious inflammatory lesions in the brain in 13/18 experimentally ABV-2 infected birds. After ABV-4 infection, perivascular cuffings was detected in the brain in 17/18 experimentally ABV-4 infected birds. This could be explained that induction the immune response in the brain differs after ABV-2 and ABV-4 infection. The kinetic of gliosis decreased at mid time point (86-172 dpi) until 231 dpi after ABV-2 infection while the kinetic of inflammatory lesions in the brain showed consistency as mild and moderate during the whole investigation period 230 dpi after ABV-4 infection. The variability between gliosis and inflammatory lesions remained unclear. The reason for that has to be investigated in future studies. It might indicate a different induction of immune response after ABV-2 and ABV-4 infection.

In the GIT, inflammatory lesions were detected in the crop as mild in 14/18 experimentally ABV-2 infected birds. After ABV-4 infection, inflammatory lesions were detected in the crop as mild and moderate in 9/18 experimentally ABV-4 infected birds. This means that the severity of inflammatory lesions in the crop after ABV-4 infection were higher than after ABV-2 infection. Inflammatory lesions were detected in the gizzard as mild and moderate in 15/18 experimentally ABV-2 infected birds. Inflammatory lesions were detected in the gizzard as mild and moderate in 3/18 experimentally ABV-4 infected birds. This means that inflammatory lesions in the gizzard after ABV-2 infection were more severe than after ABV-4 infection. Inflammatory lesions have been detected as mild, moderate and severe in the proventriculus and intestine after ABV-2 and after ABV-4 infection. This means that inflammatory lesions in the proventriculus and intestine after ABV-2 infection were comparable severity. The kinetic of inflammatory lesions in the GIT showed variability after ABV-2 infection but it decreased in all GIT organs at 230 dpi after ABV-4 infection. It is still unclear why the kinetic of inflammatory lesions in the GIT was variable after ABV-2 and decreased in the GIT after ABV-4 infection. This might indicate that induction of immune response is different and infection with both genotypes needs to be further studied.

In the peripheral organs, inflammatory lesions were predominantly detected in the liver, kidney, spleen and skin after ABV-2 infection while inflammatory lesions were mainly detected in the, liver, kidney, heart, spleen, pancreas and skin after ABV-4 infection. These data indicate that inflammatory lesions were found in more peripheral organs after ABV-4 than after ABV-2 infection but can occur in principle in all peripheral organs. These findings

are in line with (Rinder et al., 2009; Weissenböck et al., 2009; Wünschmann et al., 2011). We found that the kinetic of inflammatory lesion in the peripheral organs after ABV-2 infection was not the same as after ABV-4 infection. The kinetic of inflammatory lesion in the peripheral organs was more severe after ABV-4 infection than after ABV-2 infection. These data indicate that there is variability in the severity of inflammatory lesions in the peripheral organs after ABV-2 and ABV-4 infection. It might indicate to a different induction of immune response. The statistical analysis showed significant differences ($P<0.05$) in the mean scores of inflammatory lesions in the CNS, GIT and in the peripheral organs according to the ABV genotype. Our results showed no significant differences ($P<0.05$) in the mean scores of inflammatory lesions in the CNS, GIT and peripheral organs according to the route of inoculation. That means that ABV-2 and ABV-4 initiated infection in cockatiels regardless to the route of inoculation and differences in inflammatory lesions are rather due to the used ABV genotype than due to the route of infection.

5.4. Characterization of the infiltrating immune cells after ABV infection

Characterization of the immune cell infiltration in the experimentally ABV-2 and ABV-4 infected cockatiels was hampered due to unavailability of specific cell surface markers that recognize cockatiel immune cells. By immunohistochemistry, only CD3-positive cells could be stained but not B cells or macrophages in the cellular infiltrates after ABV-2 and ABV-4 infection. We detected CD3-positive cell in the CNS (in the brain) and other organs such as liver, kidney, skin, gizzard, proventriculus, intestine and spleen as it known for the mammalian BoDV infection (reviewed in Herden et al., 2013). This is the first report of characterization of the immune cell infiltrations in organs after ABV-2 and ABV-4 infection. Our findings are in accordance with Stitz et al., 2002 that T cells mediated the immune response in mammalian BoDV infection. Whether ABV infection induced a comparable delayed type hypersensitivity reaction (Richt et al., 1994; Stitz et al., 2002; reviewed in Herden., 2013). This needs to be further investigated. ABV genotype, genetic host factors, and immune response might play a role in the outcome of the ABV infection. The immunopathogenesis of ABV genotypes is still unknown. Further investigations about whether immunopathologic mechanisms that are based on a T cell–mediated immune reaction, as known for BoDV infection are needed for ABV infection.

5.5. Distribution patterns of ABV antigen

Immunohistochemistry (IHC) has already been performed to study the tissue distribution and localization of ABV in PDD affected psittacines (Rinder et al., 2009; Weissenböck et al., 2009; Ouyang et al., 2009). In the present study, it was shown that polyclonal rabbit anti-Borna disease virus antibody was cross reactive antibody with ABV as described by Herzog et al., 2010 and Piepenbring et al., 2012. We found that the distribution patterns of ABV-2 in experimentally ABV-2 infected cockatiels was similar to the distribution patterns of naturally ABV-infected psittacines (Rinder et al., 2009; Gancz et al., 2009; Lierz et al., 2009; Ouyang et al., 2009; Weissenböck et al., 2009; Lierz et al., 2010; Raghav et al., 2010; Wünschmann et al., 2011; Rubbenstroth et al., 2013). We found that ABV-2 was mainly localized in the GIT and peripheral organs. That is in accordance with findings of a previous study (Kistler et al., 2010) in which ABV-2 distribution pattern was predominately restricted to the GIT organs in naturally ABV-infected psittacines. We also found that ABV-4 has a strong tropism towards the CNS and peripheral organs. This is in line with (Payne et al., 2011) where ABV-4 was not only detected in the cells of the central and autonomic nervous systems, but also within the mononuclear cells infiltrating the various organs such as adrenal gland, heart, spleen, liver, kidney, lungs, pancreas, testes and ovary in apparently healthy cockatiels (*Nymphicus hollandicus*). ABV antigen was found primarily in the nuclei and cytoplasm of neurons including Purkinje cells and in glial cells through out the brain as described in naturally ABV-infected psittacines suffering from PDD by (Gancz et al., 2009; Weissenböck et al., 2009; Wünschmann et al., 2011). We detected ABV antigen in neurons of the brain, glial cells of the spinal cord, liver cells, neurons of adjacent ganglia in the heart, epithelial cells around feather follicles in the skin, and epithelial cells in the renal tubules of the kidney, neurons of the enteric ganglia in the lamina muscularis of gizzard, proventriculus and intestine, nerve fibers, epithelial cells in the crop, gizzard and proventriculus, and smooth muscle fibers in the lamina muscularis of all GIT organs after ABV-2 and ABV-4 infection. This indicates that the virus was disseminated in neural and non neural cells as previously described in naturally ABV-infected birds (Weissenböck et al., 2009; Kistler et al., 2010; Payne et al., 2011; Wünschmann et al., 2011).

5.5.1. Distribution pattern of ABV antigen after ABV-2 infection

In the CNS, viral antigen detection was detected in the as score 1, score 2 and score 3 in the CNS after ABV-2 infection. We found viral antigen in neurons and glial cells in the cerebrum and brain stem after ABV-2 infection. Our results are in line with (Kistler et al., 2008; Staeheli et al., 2010) where ABV P was detected in the nucleus and cytoplasm of neurons in

the brain in natural cases of PDD. ABV antigen was also found in Purkinje neurons suggesting that ABV could play a role in the control of motor activity. Viral antigen in the brain was detected as score 1 and score 2 during the whole investigation period. These data indicate viral persistence in the CNS as known for the mammalian borna viruses.

In the GIT, viral antigen was detected in all GIT organs over the entire investigation period. ABV antigen was mainly localized in the GIT organs after ABV-2 infection. These findings are in line with Rinder et al., 2009; Weissenböck et al., 2009 where ABV antigen was found in the nucleus and the cytoplasm not only of neural tissues but also in other cell types including GI epithelium, and cells in the lamina propria of the intestine psittacine birds with PDD (Rinder et al., 2009; Weissenböck et al., 2009). Viral antigen in the GIT was detected as score 1 and score 2 in all GIT organs during the whole investigation period of 231 dpi. This indicates a viral persistence in the GIT after ABV-2 infection. However, some variability in viral antigen detection was also found in the GIT after ABV-2 infection. Viral antigen was not found in the crop in 1/18 birds but it was detected as score 3 in the gizzard in 1/18 bird and in the proventriculus in 2/18 birds. It might indicate that so far unknown host factors played a role in such variability.

In the peripheral organs, viral antigen was mainly detected in the heart, liver, kidney, pancreas, and skin. Thus, the virus has tropism to these peripheral organs. In previous studies, ABV-P was not only found in the cells of the central and autonomic nervous systems, but was also present in the other organs such as heart, liver, spleen and pancreas after natural ABV-2 and ABV-4 infection in cockatiels (Rinder et al., 2009; Payne et al., 2011a; Kistler et al. 2010; Wünschmann et al., 2011). Our results are in line with Rinder et al., 2009; Payne et al., 2011a; Kistler et al. 2010; Wünschmann et al., 2011. Viral antigen was detected in liver cells, neurons of adjacent ganglia in the heart, epithelium of renal tubules, around ducts in the pancreas, around feather follicles in the skin. Thus, viral antigen was found in neural and non neural cells. This is in agreement with previous studies (Weissenböck et al., 2009; Rinder et al., 2009; Payne et al., 2011a; Kistler et al. 2010; Wünschmann et al., 2011). Viral antigen in the peripheral organs revealed variability among the peripheral organs. It increased in the liver and kidney at 231 dpi but it was consistent as score 1 and score 2 in the heart and pancreas during the whole investigation period. We do not know why such variability occurs. This requires further investigations. Our findings showed that viral antigen increased in the peripheral organs at late time point at 231 after ABV-2 infection, indicating a broad distribution of ABV-2 in the late stages of the infection. This is in line with Lierz et al., 2009.

In birds that lacked signs of PDD, viral antigen and ABV-2 RNA could also show a broad distribution pattern. This is in line with Wünschmann et al., 2011.

5.5.2. Distribution pattern of ABV antigen after ABV-4 infection

In the CNS, viral antigen was detected in the brain as score 1, score 2 and score 3 in 18/18, in the spinal cord as score 1 and score 2 in 11/18 and in the eye as score 1, score 2 and score 3 in 9/18 experimentally ABV-4 infected birds. This showed that ABV-4 has strong tropism to the CNS. Our results are consistent with findings of Ouyang et al., 2009. The kinetic of viral antigen detection in the CNS showed consistency as score 1 and score 2 during the whole investigation period in experimentally ABV-4 infected birds. This indicates a persistence infection of the CNS during the entire investigation period of 230 dpi. The kinetic of viral antigen detection in the eye decreased at late time point. It might be possible that viral antigen in at least certain cells in the eye was not found at early time points 60 and 66 dpi or could be cleared from the eye at late time points 230 dpi.

In the GIT, we detected viral antigen in all GIT mainly in intestine and proventriculus. Our results are in line with Weissenböck et al., 2009 where ABV antigen was detected in the gastrointestinal tract in 31 psittacine birds suffering with PDD in Europe. Our results are also in accordance with Kistler et al, 2010 where ABV-P was detected in tissues of the gastrointestinal tract in naturally ABV-infected psittacine birds suffering from PDD. We detected viral antigen in neurons of the enteric ganglia in the lamina muscularis of gizzard and proventriculus and intestine, epithelium and smooth muscle fibers of the GIT, and blood vessels. These findings are in line with Rinder et al., 2009; Weissenböck et al., 2009; Last et al., 2012 in naturally ABV-infected psittacines. The kinetic of viral antigen in the GIT decreased in all GIT organs and was negative at late time point in experimentally ABV-4 infected birds. This might indicate clearance of the virus from the GIT by the immune response at late time points. However, this needs to be confirmed in further studies.

In the peripheral organs, viral antigen detection was mainly detected in the heart, liver, kidney and spleen. Thus, ABV-4 has tropism to these peripheral organs. It was described that ABV antigen was distributed broadly in the peripheral organs in naturally ABV-infected psittacines which suffered from PDD (Rinder et al., 2009; Kistler et al., 2010; Wünschmann et al., 2011). This is in agreement with Rinder et al., 2009; Kistler et al., 2010; Wünschmann et al., 2011. Viral antigen in the peripheral organs was detected in the liver, kidney, pancreas and spleen as score 1, score 2, and score 3 during the whole investigation period of 230 dpi. This indicates viral persistence in the peripheral organs after ABV-4 infection.

5.5.3. Comparison of ABV antigen distribution after ABV-2 and ABV-4 infection

In the CNS, viral antigen was not detected in the brain in 4/18 birds after ABV-2 infection but it was detected as score 1, score 2 and score 3 in 17/18 birds after ABV-4 infection. This indicates that ABV-4 has a strong tropism toward the CNS than ABV-2. Viral antigen was not detected in the brain in 2/18 birds at early time points 46-86 dpi, in 1/18 birds at mid time points at 88-137 dpi, and in 1/18 birds at late time points at 231 dpi after ABV-2 infection. However, viral antigen was detected in all GIT organs and in all the peripheral organs of these birds. It might be possible that the virus was cleared from the CNS in these birds, substantiating the role of host factors such as variation in the individual immune status among birds. Viral antigen in the CNS revealed that viral antigen was detected as score 1 and score 2 during the whole investigation period after ABV-2 and after ABV-4 infection. This indicates that ABV-2 and ABV-4 exhibited viral persistence in the CNS.

In the GIT, viral antigen was detected in all GIT organs mainly in gizzard and proventriculus in all birds after ABV-2 infection. It was also detected all GIT organs mainly in intestine and proventriculus but not in all birds after ABV-4 infection. This means that there is individual variation in distribution of viral antigen in the GIT among birds according to the genotype. This also means that ABV-2 has a strong tropism to the GIT than ABV-4. Viral antigen was detected as score 1 and score 2 in all GIT organs during the whole investigation period after ABV-2 infection, indicating viral persistence in the GIT after ABV-2 infection. Viral antigen decreased in all GIT organs at late time point 230 dpi after ABV-4 infection, probably indicating that the virus could be eliminated from the GIT by the immune response at late time points. This also might support that ABV-4 has less tropism to the GIT in comparison to ABV-2.

In the peripheral organs, viral antigen was predominantly detected in the heart, liver, kidney, pancreas, spleen and skin after ABV-2 infection while viral antigen was mainly detected in the heart, liver, kidney and spleen after ABV-4 infection. This indicates that ABV-2 and ABV-4 have broad tissue tropism in the peripheral organs as reported for naturally ABV-infected captive psittacines which suffer from PDD (Rinder et al., 2009; Wünschmann et al., 2011). However we also found some variability in detection of viral antigen in the liver and heart after ABV-2 infection and after ABV-4 infection. In the liver, viral antigen was not found at early time points but it was detected as score 1 in most of experimentally ABV-2 infected birds and also as score 2 in one bird at mid time points and late time points after ABV-2 infection. In contrast, viral antigen was detected in the liver as score 1, score 2 and score 3 during the whole investigation period after ABV-4 infection. In the heart, viral antigen

was detected in neurons of the adjacent ganglia but not in the heart itself after ABV-2 infection. In comparison, it was not only found in neurons of the pericardial ganglia but also in muscle fibers of the heart, smooth muscle layer, myocardial fibers and Purkinje fibers after ABV-4 infection. We do not know why such variability in detection of viral antigen in the liver and heart occurs. It might indicate that ABV-4 has a stronge tropism to the liver and heart than ABV-2. The kinetic of viral antigen detection in the peripheral organs decreased in all the peripheral organs at late time point 231 dpi after ABV-2 infection but it increased in all the peripheral organs at mid time points until late time points after ABV-4 infection. This might indicate that ABV-2 could be cleared from the peripheral organs at late time points while ABV-4 exhibited viral persistence in the peripheral organs during the whole investigation period. This also indicate that induction of immune response differ according to the genotype.

The statistical analysis showed significant differences ($P<0.05$) in the mean scores of viral antigen detection in the CNS, GIT and in the peripheral organs according to the ABV genotype (**Fig.23** and **Fig.24**). This means that viral antigen detection in the CNS, GIT and peripheral organs after ABV-2 infection was not the same after ABV-4 infection. Our results showed no significant differences ($P<0.05$) in the mean scores of viral antigen detection in the CNS, GIT and peripheral organs according to the route of inoculation. This means that ABV-2 and ABV-4 initiated ABV infection in cockatiels regardless to the route of inoculation.

5.6. Demonstration of ABV RNA

Distribution pattern of ABV-2 and ABV-4 genomic RNA as well as viral mRNA of these genotypes were described in naturally ABV-infected psittacines suffering from PDD by in situ hybridization (Weissenböck et al., 2010). However, this is the first report describing the detection of ABV-2 and ABV-4 RNA as well as viral mRNA of these genotypes in experimentally ABV-2 and ABV-4 infected cockatiels by in situ hybridization. We found that ISH could be used as a tool for localizing ABV RNA in tissues of birds with PDD to detect viral replication and transcription in affected tissues. Our results showed that ABV-2 genome and ABV-2 mRNA were mainly distributed in the GIT and in the peripheral organs. However, ABV-2 genome and ABV-2 mRNA were also detected in the CNS but with low scores. This indicates that ABV-2 has higher tropism to the GIT and peripheral organs. Our results showed that ABV-4 genome and ABV-4 mRNA were mainly distributed in the CNS and in the peripheral organs. However, ABV-4 genome and ABV-4 mRNA were also detected in the GIT but with low scores and not in all birds. This indicates that ABV-4 has tropism for CNS and peripheral organs. We found that ABV-2 and ABV-4 RNA were detected in the same cells

type in the CNS, in the GIT, and in the peripheral organs. ABV-2 genome or ABV-4 genome were only detected intranuclearly within affected cells. In the proventriculus, ABV-4 genome and ABV-4 mRNA were detected mostly in the nucleus of epithelial cells. ABV-2 mRNA or ABV-4 mRNA were detected intranuclearly and intracytoplasmically within the affected cells. These data are also in line with Weissenböck et al., 2010.

5.6.1. Distribution pattern of ABV-2 RNA after ABV-2 infection

In the CNS, ABV-2 genome and/or ABV-2 mRNA were detected in the CNS in experimentally ABV-2 infected birds. This indicates an active replication and transcription of ABV-2 in the CNS. That is in consistency with findings of (Piepenbring et al., in revision) where total viral RNA was detected in the brain in all experimentally ABV-2 infected birds. Now, a question presents itself, why we detected either ABV-2 genome or ABV-2 mRNA or both in the brain after ABV-2 infection. An interpretation for this finding is that ABV-2 RNA might not be evenly distributed in the brain, and we had investigated the viral RNA in an area where ABV-2 genome or ABV-2 mRNA was not present as in BoDV infected horses. This means that ABV-2 genome or ABV-2 mRNA were below of ISH detection in some birds. BoDV RNA could be restricted to a certain regions in the brain. ABV-2 genome and ABV-2 mRNA were detected in the cerebrum only. ABV-2 genome was not detected in the brain in 6/18 birds. Moreover, ABV-2 mRNA was not detected in the brain in 8/18 birds. This indicates that ABV-2 has a weaker tropism in the CNS. The kinetic of ABV-2 RNA detection in the brain revealed that ABV-2 genome and ABV-2 mRNA were detected as score 1 during the whole investigation period. This could be explained that there is viral persistence but with low amounts of infected animals in the CNS. ABV-2 genome was detected in the brain as score 2 only in 1/18 bird at early time points 46-86 dpi and also in 1/18 bird at late time point 231 dpi. It might be that these two birds were more susceptible.

In the GIT, ABV-2 genome and ABV-2 mRNA were detected in all GIT organs during the whole investigation period of 230 dpi in 18/18 birds. This indicates that ABV-2 can successfully replicate and transcribe in the GIT organs during the whole period investigated and can persist in these organs. Presence of ABV-2 RNA in all the GIT organs during the whole investigation period indicated viral persistence in the GIT organs and the higher amount of the positive cells indicate a high tropism to the GIT organs. ABV-2 genome was detected in the GIT as score 1 and score 2 while ABV-2 mRNA was detected in the GIT as score 1, score 2 and score 3 during the whole investigation period 231 dpi. This means that there was abundance of ABV-2 mRNA in the GIT and ABV-2 transcription is efficient in the GIT. Weissenböck and colleagues (2010) also detected ABV-2 genome and ABV-2 mRNA

mainly in the GIT organs in naturally ABV-infected psittacine suffering from PDD. These results are also in accordance with findings of Kistler et al., 2010 who found that ABV-2 is broadly distributed in the GIT organs in the naturally occurring PDD psittacine birds.

In the peripheral organs, ABV-2 genome and viral mRNA were detected in all the peripheral organs in 18/18 experimentally ABV-2 infected birds over the entire investigation period. Weissenböck and colleagues (2010) detected ABV-2 RNA in the central and peripheral nervous system in naturally ABV-infected psittacines suffering from PDD. Our results are in agreement with Weissenböck et al., 2010. Thus, ABV-2 can replicate and transcribe in the peripheral organs. ABV-2 genome was detected as score 1, score 2, and score 3 in all the peripheral organs while ABV-2 mRNA was detected as score 1, score 2 and score 3 in the heart and liver but not in the kidney and skin during the whole investigation period 231 dpi. That means that there was abundance in the genomic RNA of ABV-2 in the peripheral organs. The kinetic of ABV-2 genome neither decreased nor increased in the heart, liver, kidney and was detected as score 1, score 2 and score 3 during the whole investigation period 231 dpi. This indicates viral persistence in the peripheral organs. The kinetic of ABV-2 mRNA in the liver, pancreas, and skin decreased at late time points 231 dpi. This could be explained that ABV-2 transcription decreased in these organs at late time points and is not needed in huge amount to maintain viral persistence.

5.6.2. Distribution pattern of the ABV-4 RNA after ABV-4 infection

In the CNS, ABV-4 genome and viral mRNA were detected in the CNS in 18/18 experimentally ABV-4 infected birds. Thus, ABV-4 replication and transcription was effective in the CNS. ABV-4 genome and ABV-4 mRNA were detected in the cerebrum and cerebellum, indicating to a broad distribution pattern of ABV-4 RNA in the CNS. This also indicates that ABV-4 has strong tropism to the CNS. Weissenböck and colleagues (2010) detected ABV-4 genome and ABV-4 mRNA in brain in naturally ABV-infected psittacines suffering from PDD (Weissenböck et al., 2010). Our data are in line with (Weissenböck et al, 2010). The kinetic of ABV-4 genome neither increased nor decreased in the brain and was detected as score 1 and score 2 during the whole investigation period of 230 dpi. Moreover, ABV-4 mRNA neither increased nor decreased in the brain and was detected as score 2 and score 3 during the whole investigation period of 230 dpi and was therefore of higher scores. This might indicate active transcription until the end of the investigation period. This also indicates viral persistence in the CNS. These findings are in discrepancy with Weissenböck et al., 2010 in which ABV-4 genome was detected much more than ABV-4 mRNA in the CNS in naturally ABV-infected birds. The authors explained that ABV-4 transcription was not well

developed in naturally ABV-infected birds and this might be due to a more efficient host defense mechanism which also could explain the generally chronic course of the disease. We used semiquantitaive scores to evaluate and discriminate between ABV-2 and ABV-4 genome and their mRNA in experimentally ABV-2 and ABV-4 infected birds but we do not know how Weissenböck et al., 2010 evaluated the ABV-4 genome and ABV-4 mRNA in the various tissues of psittacine birds suffering from PDD. Moreover, the time point of detection of ABV-2 RNA or ABV-4 RNA was known in all experimentally ABV-2 and ABV-4 infected birds but it was unknown to Weissenböck et al., 2010. The preferential transcription of ABV-4 in the CNS during the whole period of 231 dpi provides a strong tropism of ABV-4 to the CNS and an ideal mechanism for ABV persistence. Our findings are in accordance with observations from natural or experimental BoDV infections in mammals, where viral mRNAs are usually more abundant than genomic RNAs (Ikuta et al., 2002; Werner-Keiss et al., 2008).

In the GIT, ABV-4 genome and viral mRNA were detected in all GIT organs in experimentally ABV-4 infected birds, indicating an active replication and transcription of the virus in the GIT. Weissenböck and colleagues (2009) mentioned that ABV-4 also replicated in the CNS and in the visceral organs in naturally ABV-infected birds suffering from PDD. Our results are therefore in line with Weissenböck et al., 2009. ABV-4 genome was detected in all GIT organs as score 1, score 2 and score 3 while ABV-4 mRNA was detected in the GIT organs as only score 1 and score 2 during the whole investigation period. This indicates that there was more ABV-4 genome in the GIT in comparison with ABV-4 mRNA. Thus, transcription of ABV-4 in the GIT seems to be less active and more replication might take place than in the CNS and ABV-4 might have a weak tropism in the GIT. Weissenböck and colleagues (2010) detected an abundance of ABV-4 genome in the GIT in comparison with viral mRNA in naturally ABV-infected psittacine suffering from PDD. Our results for the GIT are therefore in line with Weissenböck et al., 2010 but not for the CNS. Many experimentally ABV-4 infected birds did not expressed ABV-4 mRNA in the GIT. We can not rule out that there was no ABV-4 mRNA in the GIT organs in these birds after ABV-4 infection. It might be possible that there are small amount of the viral mRNA in the GIT organs after ABV-4 infection which were under the detection level of the ISH and therefore could not be detected.

The kinetic of ABV-4 genome and ABV-4 mRNA decreased in all GIT organs at late time points 230 dpi. It might be possible that ABV-4 was diminished from the GIT at late time points and also means that ABV-4 has less tropism to the GIT.

In the peripheral organs, ABV-4 genome was detected in all the peripheral organs in experimentally ABV-4 infected birds. ABV-4 mRNA was found but not in all the peripheral

organs. This indicates that ABV-4 replicates effectively in the peripheral organs but ABV-4 transcription seems to be less effective. Our results for the peripheral organs are in discrepancy with Weissenböck et al., 2010 where ABV-4 mRNA was much more than ABV-4 genome in naturally ABV-infected psittacines suffering from PDD. Thus, the time point was not known for the naturally ABV-infected psittacines suffering from PDD which were investigated by Weissenböck. It might also be possible that there was indeed ABV-4 mRNA in all peripheral organs of all experimentally ABV-4 infected birds but it was below our detection by ISH. The kinetic of ABV-4 genome increased in the heart, liver, pancreas and skin at mid time points 115,116,120 dpi until late time points at 230 dpi, indicating the active viral replication in the peripheral organs at mid time points and late time points. The kinetic of ABV-4 mRNA neither decreased nor increased in all peripheral organs, indicates viral persistence.

5.6.3. Comparison of ABV RNA distribution after ABV-2 and ABV-4 infection

In the CNS, we detected ABV-2 genome and/or ABV-2 mRNA in the CNS after ABV-2 infection. ABV-4 genome and ABV-4 mRNA were detected in the CNS in 18/18 experimentally ABV-4 infected birds. This indicates that ABV-4 replicates and transcribes more actively in the CNS in comparison with ABV-2. The kinetic of ABV-2 genome was detected as score 1 and score 2 while the kinetic of ABV-2 mRNA was detected as score 1 during the whole investigation period. We detected the ABV-4 genome in the CNS as score 1 and score 2 during the whole investigation period 230 dpi while we detected ABV-4 mRNA as score 2 and score 3 during the whole investigation period of 230 dpi. Thus, ABV-4 mRNA was more abundant than ABV-2 mRNA indicating more transcription of ABV-4 in the CNS than ABV-2. This also indicates viral persistence and also means that ABV-4 transcription was efficient in the CNS.

In the GIT, we found that ABV-2 genome and ABV-2 mRNA in all GIT organs and in all experimentally ABV-2 infected birds, indicating active ABV-2 replication and transcription in the GIT. Moreover, the ABV-2 transcription was efficient in the GIT. In only 1/18 birds, ABV-2 mRNA was not found in the gizzard. It might be possible that there was ABV-2 transcript in this bird but it was below of our detection by ISH. After ABV-4 infection, we detected ABV-4 genome and ABV-4 mRNA in the GIT but not in all birds. Moreover, we found more positive cells harbouring ABV-4 genome in the GIT in comparison with ABV-4 mRNA. This means that ABV-4 transcription was less active in the GIT than for ABV-2. We found that kinetic of ABV-4 genome and ABV-4 mRNA decreased in all GIT organs at late time points 230 dpi which might indicate that ABV-4 diminished from the GIT at late time points and also means

that ABV-4 has less tropism to the GIT. The kinetic of ABV-2 RNA was variable. ABV-2 genome increased in the proventriculus, and decreased in the intestine at late time points at 231 dpi.

In the peripheral organs, ABV-2 genome and ABV-2 mRNA were detected as score 1, score 2, and score 3 in all the peripheral organs during the whole investigation period of 231 dpi, indicating active replication and transcription in the peripheral organs. ABV-4 genome and ABV-4 mRNA were detected in most but not all of the peripheral organs after ABV-4 infection. ABV-4 genome was detected as score 1, score 2 and score 3 in the peripheral organs while ABV-4 mRNA was detected as score 1 in the peripheral organs. This means that abundant ABV-4 genome was found in the peripheral organs. In some birds, we detected ABV-4 genome but we did not detect ABV-4 mRNA in some of the peripheral organs after ABV-4 infection. We can not rule out that ABV-4 mRNA was not found in the peripheral organs after ABV-4 infection. There are at least two possible explanations for this observation. **(1)** Degradation of ABV-4 mRNA might have occurred during methodology. **(2)** It might also be possible that there were small amounts of viral mRNA in the peripheral organs but these amounts were bellow of detection in the peripheral organs after ABV-4 infection by ISH. Nevertheless, this also means that ABV-4 transcription was not as effective as ABV-2 transcription in the peripheral organs.

The kinetic of ABV-2 RNA neither decreased nor increased in the peripheral organs, indicating viral persistence. ABV-2 mRNA decreased in the liver, pancreas, and skin at late time point 231 dpi, which might be diminished in these organs at late time points. However, we still do not know why there was a variation in the kinetic of ABV-2 genome and ABV-2 mRNA in the peripheral organs.

The kinetic of ABV-4 genome increased in the heart, liver, pancreas and skin at mid time points 115,116,120 dpi until late time point at 230 dpi, indicating active replication of the virus at mid time points and late time points 230 dpi. The kinetic of ABV-4 mRNA neither decreased nor increased in the peripheral organs. However, we also still do not know why there was a variation in the kinetic of ABV-4 genome and ABV-4 mRNA in the peripheral organs.

5.7. Comparison of histological findings, detection of ABV antigen and ABV RNA and clinical observation

Our results showed a moderate correlation (r= 0.60) between inflammatory lesions and viral antigen detection in the CNS after ABV-2 and after ABV-4 infection. That means, any change in inflammatory lesions in the CNS after ABV-2 or ABV-4 infection leads to change in viral antigen detection in the CNS after ABV-2 or ABV-4 infection. Our results also showed a mild correlation (r = 0.38) between inflammatory lesions and viral antigen detection in the peripheral organs after ABV-2 and after ABV-4 infection. That means, any change in inflammatory lesions in the peripheral organs after ABV-2 or ABV-4 infection leads to change in viral antigen detection in the peripheral organs after ABV-2 or ABV-4 infection. After ABV-2 infection, we detected variability in the course of ABV-2 infection in experimentally ABV-2 infected birds as previously described (acute, intermittent, abortive, and inapparent infection) in naturally ABV infected psittacines (Heffels-Redmann et al., 2011). We found that birds which exhibited gastrointestinal and/or neurological signs, had dilatation of proventriculus, they had also viral antigen and ABV-2 RNA in the CNS, GIT and in the peripheral organs. These findings might represent an acute form of the infection but not when this occur at mid time points or late time points. However, some variability was found i.e bird 25 exhibited gastrointestinal signs, had dilatation of proventriculus, mild inflammatory lesions in the brain, viral antigen detection, ABV-2 mRNA were detected but ABV-2 genome was not detected in the brain of this bird. By RT-PCR, Piepenbring detected low total ABV-2 RNA load (Ct value=28) in the brain in bird 25. It might be possible that such small amount of ABV-2 genome in the brain of this bird was below of detection by ISH. Moreover, Piepenbring detected ABV-2 RNA as total RNA in the brain of bird 25 by RT-PCR. By ISH, we discriminated between ABV-2 genome and ABV-2 mRNA and we detected ABV-2 mRNA in the brain of bird 25. Another example for variability, bird 34 exhibited gastrointestinal signs, had dilatation of proventriculus, mild inflammatory lesions in the brain, and ABV-2 mRNA were detected. However, we could not be able to detect viral antigen and ABV-2 genome in the brain of bird 34. By RT-PCR, Piepenbring detected low total ABV-2 RNA load (Ct value=29) in the brain in bird 34. It might be possible that such small amount of ABV-2 genome in the brain of this bird was below of detection by ISH. Moreover, birds could not exhibit gastrointestinal or neurological signs, did not displayed dilatation of proventriculus but they could also have viral antigen and ABV-2 RNA in the CNS, GIT and in the peripheral organs. This indicates to asymptomatic ABV infection. That is in line with (Lierz et al., 2009; Payne et al., 2011; Encinas-Nagel et al., 2014) where the ABV RNA and

viral antigen were detected in healthy birds which exposed to ABV infection. The reasons for the differences in the clinical outcome have to be further investigated.

After ABV-4 infection, we detected variability in the course of ABV-4 infection in experimentally ABV-4 infected birds as previously described (acute, intermittent, abortive, and inapparent infection) in naturally ABV infected psittacines (Heffels-Redmann et al., 2011). Birds exhibited gastrointestinal and/or neurological signs, had dilatation of proventriculus and they had also viral antigen and ABV-4 RNA in the CNS, GIT and in the peripheral organs. These findings might represent an acute form of the infection but not when this occur at mid time points or late time points. However, some variability was found i.e bird 15 exhibited gastrointestinal and neurological signs, had dilatation of proventriculus, inflammatory lesions in all organs, viral antigen detection in all organs except in skin, ABV-4 genome was detected in all organs especially in the peripheral organs but ABV-4 mRNA was not detected in all peripheral organs of this bird. By RT-PCR, Piepenbring detected low total ABV-4 RNA load in all the peripheral organs of bird 15. Birds did not exhibit gastrointestinal or neurological signs, did not display dilatation of proventriculus, they could also have viral antigen and ABV-4 RNA in the CNS, GIT and in the peripheral organs. This indicates to asymptomatic ABV infection. That is in line with (Lierz et al., 2009; Payne et al., 2011; Encinas-Nagel et al., 2014) where the ABV RNA and viral antigen were detected in healthy birds which exposed to ABV infection.

5.8. Isolation of cockatiels blood cells

Piepenbring and colleagues (2012) demonstrated successful experimental infection via intracereberal and intravenous route of infection with ABV-2 and ABV-4 in cockatiels. However, the potential infection of blood cells was still unclear. In the current study, we investigated the potential role of blood cells for dissemination of ABV infection. Boyum (1968) was the first researcher who isolated peripheral blood mononuclear cells from human blood. Carlson and Kaneko (1973) isolated leukocytes from bovine peripheral blood. Boyum (1976) also isolated macrophages from human blood. Lee and colleagues (1996) described isolation of blood cells in a wide range of species of animals. Lavoie and Grasman (2005) described the optimal conditions for isolation, cryopreservation, and mitogenesis of peripheral blood lymphocytes from chickens (*Gallus domesticus*) and wild herring gulls (*Larus argentatus*). In this study, we provided for the first time an optimized protocol for isolation of cockatiel BC cells from small amount of blood volume. After successful isolation of BC cells, we determined the life span of BC cells in culture (15 days).

5.9. Characterization of the immune cells in cockatiel BC cells by IIF

Characterization of BC cells is very important to know which cells were exactly in culture. However, by morphological analysis it is difficult to differentiate between BC cells. It is difficult to differentiate thrombocytes from erythrocytes in chicken (Lavoie and Grasman, 2005). Likewise, scanning electron microscopy (SEM) is not an appropriate approach and helpful technique to distinguish peripheral blood mononuclear cells of chickens according to their morphology (Burkhardt, 1979). IIF is a useful approach to identify blood cells and cell surface markers using different cross reactive antibodies. Due to the lack of specific cell surface markers that identify immune cells of cockatiel blood, we tested the cross reactivity of antibodies directed against other species blood cells. Many previous studies have already demonstrated the homology between cell surface markers of chicken and other species of mammals. For instance, there is homology between chicken and mammalian B cell (Batten et al., 2000; Rolink and Melchers, 2002, Schneider et al., 2004). Findings of previous studies (Chen et al., 1996; Cooper et al., 1991) described a highly similarity between chicken T cell from *Gallus gallus domesticus* and mammalian T cells. The same was true with duck CD4 cells and CD25 cells when compared to mammalian T cells (Revathi et al., 2012). Another study (Luhtala, 1998) substantiated the homology between CD4 cells, CD8 cells and T cell receptor (TCR) in chicken to CD4 cells, CD8 cells and TCR in mammals. Tregaskes and colleagues (1995) described an appropriate conservation between chicken and mammalian CD8 genes. Avian TCR1 and TCR2 have recently been shown large proportion of homology to mammalian TCR receptors (Chen et al., 1986; Bucy et al., 1988; Josef et al., 1988). Michael and colleagues (2012) mentioned that chicken thrombocytes have great homology to mammalian thrombocytes. Mast and colleagues (1997) described conservation between chicken mononuclear phagocytes and mammalian mononuclear phagocytes. Characterization of blood cells has been described in many different species of mammals, birds and man but not in cockatiels. We provided the first detailed report for characterization of the immune cells in cockatiel blood by using reliable cross reactive cell surface markers by IIF. The normal percentage of CD3 cells in avian blood is 76% (Kushima et al., 2004). Our findings also show a high percentage of CD3 positive cells (estimated 71%) in cockatiel BC by IIF (not by FC). Bounus and Stedman (2000) also mentioned that T lymphocytes are the most circulatory leukocytes in avian blood. Heterophils are regarded as the most predominant leukocytes population in the blood of most avian species (Fudge, 2000; Latimer and Bienzle, 2000). The normal percentage of CD4 cells in avian blood is 41% (Kushima et al., 2004). Our findings show a comparable percentage of CD4 positive cells (estimated 36%) in cockatiel BC. The

normal percentage of CD8 cells (alpha and beta) in avian blood are not exceeding 20% (Kushima et al 2004). Our findings also show a low percentage of CD8a positive cells (estimated 11% by IIF) in cockatiel BC. We detected 71% CD3-positive cells in the BC cells population. Moreover, we detected 36% CD4-positive cells, and 11% CD8a-positive cells. CD3 is a pan-T cell marker and it bounds to the membranes of all mature T cells. The estimated percentages of CD4-positive cells, and CD8a-positive cells (47%) did not match to the 71% of CD3-positive cells in the BC cells population. It means that 24% positive cells that were detected in the 71% CD3-positive cells of the BC cells population were lacking. It might be possible that these cells were other peripheral blood T-lymphocytes such as suppressor T cells, natural killer T cells, or even other subtypes of CD8 or CD4 cells (beta or gamma but not alpha). The normal percentage of B cells in avian blood ranged between 10-14% (Domingo et al., 1986). Our results show a low percentage of peripheral blood B positive cells (estimated 9% by IIF) in cockatiel BC and are therefore in agreement with Domingo et al., 1986. The normal percentage of monocytes in blood range between 0-5%. We found few countable monocytes (1-10 positive cells) in the whole smear. We found low percentage of thrombocytes in cockatiels buffy coat cells (estimated 20% by IIF) and that is in agreement with a previous study (Lavoie and Grasman, 2005) who demonstrated that percentage of thrombocytes in buffy coat cells from herring gulls is 20% whereas proportion of thrombocytes in the isolated mononuclear cells are ranged 40-77 %.

5.10. Characterization of the immune cells in cockatiel BC cells by FC

Mack Fulwyler was the inventor of the flow cytometer particularly the cell sorter in 1965 (Fulwyler, 1965). Characteristics that can be measured by flow cytometry include cell size, cytoplasmic complexity, nucleic acid content, membrane-bound and intracellular proteins (Recktenwald, 1993; Keren et al., 1994; Shaprio, 1995; Watson, 1999). Characterization of the immune cells in birds has been described in many of previous studies in different species of birds by flow cytometry. In chicken, it was used to characterize chicken monocytes (Mast *et al.,* 1997), chicken thrombocytes (Lacoste et al., 1994) and chicken bone marrow-derived professional antigen-presenting cells (Zhiguang et al., 2010). In turkey, it was used to identify turkey CD4 and CD8 cells (Li, et al., 1999). In owls, it was used to identify the CD3 cells in great horned owl (*Bubo virginianus*) (Malka et al., 2008). In duck, it was used to recognize B lymphocytes proportion, T lymphocytes, T helper and T cytotoxic (Kothlow et al., 2005). Flow cytometric findings of other studies showed a homology between human and chicken immune cells. Marko and colleagues (1993) found the functional and biochemical conservation of chicken and human CD4 molecule by flow cytometry. Revathi and

colleagues, (2012) described the suppressive properties of chicken CD4 and CD25 positive cells similar to that of mammalian regulatory T cells by flow cytometry. Rodenberg and colleagues (2012) analyzed lymphocytes obtained from the blood, spleen, and bursa of normal chickens and of chickens infected with infectious bursal disease virus (IBDV) for phenotypic expression of CD4, CD8, and immunoglobulin cell surface markers by IIF and flow cytometry. Many recent studies have also investigated the expression of the chicken CD8 and CD4-positive cells after infection with Marek's disease virus (MDV) (Toshifumi et al., 1995) or after adenovirus infection (Chun et al., 2012) in chicken spleen, thymus, and blood by FC. We tested the cross reactivity of chicken cells surface markers to recognize cockatiel immune cells in FC. However, despite a broad range of methological approaches, it was not possible to reproduce and obtain results of IIF in the FC. We obtained low percentages of CD4-positive cells, CD8a-positive cells, monocytes, thrombocytes and B cells in cockatiel BC cells in the FC. We did not obtain positive results with CD3 marker in the FC. The results obtained by flow cytometry were in discrepancy with the data by IIF. Therefore, we believe the obtained results in the IIF that fit with the literature data but we do not believe the results which were obtained in the FC for characterization the immune cells in the BC. It is still unknown why we did not obtain similar positive results in the FC as in the IIF. It might be possible that cell surface markers that we used them in the IIF were not cross reactive in the FC or antigen were shed from the cells during the procedure. It might also possible that the FC protocol needs a further optimization. Another possibility that there are major differences in the sensitivity and quantification between flow cytometry and IIF (Uehlinger et al., 2008). That means, differences in the duration of laser excitation and detector sensitivity, the way the data is displayed, and what constitutes a signal between IIF and FC would make a difference to limit the detection of signals.

5.11. ABV-4 infection of cockatiel BC cells

5.11.1. ABV antigen and ABV-4 RNA in cockatiel BC cells

IIF and PCR findings showed that neither ABV antigen nor ABV-4 RNA was detected in stimulated or non stimulated BC cells after experimental infection with ABV-4. Thus, blood cells could not be infected with ABV-4 by using the approaches of this study. By IHC, we found slight positive reactions of ABV antigen in endothelium of blood vessels of the heart, liver, and kidney in experimentally ABV-2 and ABV-4 infected birds. We still do not know whether such positive immunostaining in the endothelium was unspecific reaction when using polyclonal antibodies (anti-p24 antibodies) or indeed associated with ABV infection. This should be therefore tested in the future. It might be possible that vascular or lymphatic

endothelium of blood vessels contribute to disseminate ABV within peripheral organs after experimental infection with ABV-2 and after ABV-4 in cockatiels. This needs to be further investigated. By IHC, we have also found positive reactions of ABV antigen in some cells that located in the center of the follicular shape-like aggregations of the cellular infiltrates in the skin, pancreas, kidney, and liver. We do not know whether these are macrophage or dendritic cells presenting viral antigen. This requires more investigations. If so, this could be explained by the fact that these antigen presenting cells (APCs) have processed the ABV antigen, engulfed it and eventually present it on the cell surface to the T cells of the immune system in order to induce a primary immune response (Kaspers and Kaiser, 2014). Our data suggest that blood cells can not be infected with ABV-4 by using the applied techniques.

5.12. ABV-4 infection of stimulated BC cells

5.12.1. Stimulation of BC cells with PHA-M mitogen

PHA-M mitogen is a T cell mitogen (Mills et al., 1985), however, other studies suggesting that PHA also has some effect on B lymphocytes (Chess et al., 1974, Knuutila and Kovanen, 1987, Weksler and Kuntz, 1976). PHA-M mitogen was used to activate B and T lymphocytes in human as well as in different species of animals in vitro in many previous studies, in mice (Doenhoff et al., 1976), chicken (Tapani et al., 1978) and for human peripheral blood lymphocytes (Mire-Sluis et al., 1978). IIF results showed that BC cells started to proliferate in culture 2 hours after incubation with PHA-M mitogen until day 14 post stimulation with PHA-M mitogen. For the first time, we investigated the stimulation of cockatiel BC cells after 2 hours post stimulation with PHA-M mitogen. Our results also showed that stimulated BC cells reached the maximal rate of cells proliferation at day 3 post stimulation with PHA-M mitogen. We detected high percentage (86%) of stimulated BC positive cells at day 3 post stimulation. These results are in line with findings of a previous study (Thiel and Burkhardt, 1984) who suggested that chicken peripheral blood lymphocytes have high mitogenic response to PHA-M at day 2 and day 3 post stimulation with PHA-M mitogen. In the current study, best stimulation results were obtained when PHA-M mitogen in a dilution of 1:15. These results are in accordance with that reported by (Thiel and Burkhardt, 1984). With this work, we also provided for the first time how to stimulate cockatiel BC cells.

5.12.2 Assessment of the proliferative state in cockatiel BC cells

Detection of bromodeoxyuridine incorporation was used as an indicator for proliferation of cells in many previous studies by using different methods, i.e., immunohishtochemistry (Green et al., 1992; Wesley et al., 1998), flow cytometry (Harry and John, 1992), and immunofluorescence (Gratzner et al., 1975; Petersen et al., 2012). With this work, we provided for the first time an optimized protocol for detection of the proliferating cells in cockatiels after stimulation with PHA-M mitogen by investigation of BrdU incorporation.

5.12.3. ABV antigen and ABV-4 RNA in stimulated BC cells

We investigated whether stimulated BC cells could be infected with ABV-4 at a certain stage of differentiation. By IIF and PCR, we did not find ABV antigen and ABV-RNA in stimulated BC cells by IIF and by PCR respectively. Burkhardt and Müller (1987) found that lymphocytes could be infected with IBD virus at a certain stage of cells differentiation after stimulation with PHA-M mitogen. Burkhardt and Müller, (1987) demonstrated that the proliferating lymphoid cells isolated from chicken are the target cells for infectious bursal disease (IBD) virus indicating that IBD needs a rather immature target cells than mature cells for viral replication and infection. The study was suggested that IBD virus can replicate in lymphoblasts but not in lymphocytes obtained from phytohaemagglutinin (PHA-M) stimulated cultures and not in unstimulated lymphoid cells. Another study already (Müller, 1986) suggested that infectious bursal disease virus prefers to replicate in the in a population of proliferating cells characterized by increased thymidine uptake and by blast cell formation. Our results did not show viral antigen and ABV-4 RNA in stimulated or unstimulated BC cells after ABV-4 infection. The stimulated BC cells could also not be infected with ABV-4.

In the end, we still asking ourselves many open questions, we found slight positive reactions of ABV antigen in endothelium of blood vessels of the heart, liver, and kidney in experimentally ABV-2 and ABV-4 infected birds by IHC. We still do not know whether such positive immunostaining in the endothelium was unspecific reaction when using polyclonal antibodies (anti-p24 antibodies) or indeed associated with ABV infection. By IHC, we also found positive reactions of ABV antigen in some cells that located in the center of the follicular shape-like aggregations of the cellular infiltrates in the skin, pancreas, kidney, and liver. We do not know whether these are macrophage or dendritic cells presenting viral antigen. This requires more investigations. A question is presents itself, why the kinetic of inflammatory lesions, viral antigen, and viral RNA was variable among organs according to the genotype after ABV-2 and ABV-4 infection. Further investigations are needed to understand the pathogenesis of ABV and the different ABV genotypes. Another question

remains unclear how ABV-2 and ABV-4 reached to the GIT and peripheral organs when both genotypes were inoculated intravenously. Mode of transmission by which ABV spread within central and peripheral nervous systems and organs after ABV-2 and ABV-4 infection remains unclear. It might be possible that ABV infection was generalized within organs via infected macrophages or endothelial cells or may be transmitted via transient viremia. Further research into details of ABV widespread within organs will be essential to understand the pathogenesis of ABV after infection.

6. Summary

Avian Borna viruses (ABV) are the etiological agents for proventricular dilatation disease (PDD). Distribution patterns of ABV-2 and ABV-4 in experimentally ABV-2 and ABV-4 infected cockatiels were similar to distribution patterns of ABV in naturally PDD affected psittacines. ABV-2 and ABV-4 exhibited broad tissue distribution patterns in all organs in experimentally ABV-2 and ABV-4 infected cockatiels. Inflammatory lesions, ABV antigen, ABV-2 genome and ABV-2 mRNA were mainly detected in the gastrointestinal tract (GIT) and peripheral organs after ABV-2 infection. Inflammatory lesions, ABV antigen, ABV-4 genome and ABV-4 mRNA were predominantly detected in the central nervous system (CNS) and peripheral organs after ABV-4 infection. ABV-2 transcription was effective in the GIT organs after ABV-2 infection. ABV-4 transcription was operative in the CNS after ABV-4 infection. These findings indicate distinct differences in biological behaviour between the used ABV-2 and ABV-4 isolates. By immunohistochemistry, CD3-positive cells were detected in cellular infiltrations in all organs after ABV-2 and ABV-4 infection. Isolation of buffy coat (BC) cells of cockatiels and stimulation with phytohaemagglutinin (PHA-M) were successfully established. Characterization of CD3-positive cells, CD4-positive cells, CD8a-positive cells, monocytes, B cells, and thrombocytes was successful in cockatiel BC by indirect immunofluorescence. Characterization of CD4-positive cells, CD8-positive cells, monocytes, B cells, thrombocytes cells but not CD3-positive cells was possible in cockatiel BC by flow cytometry. ABV antigen and ABV-4 RNA were not found in BC cells of cockatiels from day 0 until day 15 post infection with ABV-4. Moreover, ABV antigen and ABV-4 RNA were not found in stimulated BC cells from day 0 until day 15 after stimulation and ABV-4 infection. These results providing first evidence that cockatiel blood cells could not directly be infected with ABV-4.

Further investigations on the role of macrophages or endothelial cells for the dissemination of ABV infection within an infection are therefore required.

6. Zusammenfassung

Aviäre Bornaviren (ABV) sind Auslöser der neuropathischen Drüsenmagendilatation (proventricular dilatation disease, PDD). Die Verteilungsmuster von ABV-2 und ABV-4 in experimentell ABV-2 und ABV-4 infizierten Nymphensittichen stimmten mit dem Verteilungsmuster des Virus in natürlich an PDD erkrankten Psittaziden überein. Die beiden Genotypen ABV-2 und ABV-4 nach experimenteller Infektion von Nymphensittichen ein breites Verteilungsmuster in allen Organen auf. Entzündliche Läsionen, ABV-Antigen, ABV-2-Genom und ABV-2-mRNA wurde hauptsächlich im Gastrointestinaltrakt (GIT) und in peripheren Organen nach ABV-2-Infektion festgestellt. Im Vergleich dazu wurden nach Infektion mit ABV-4 entzündliche Läsionen, ABV-Antigen, ABV-4-Genom und ABV-4-mRNA vorherrschend im zentralen Nervensystem (ZNS) und in peripheren Organen festgestellt. Nach ABV-2-Infektion läuft eine effektive Transkription des Virus vor allem im GIT ab, während es nach ABV-4-Infektion zu einer deutliche Transkription im ZNS kommt. Diese Ergebnisse zeigen, dass es deutliche unterschiede im biologische Verhalten zwischen den verwendung ABV-2 und ABV-4 Isolaten gibt. Mittels Immunhistochemie konnten nach ABV-2- und ABV-4-Infektion CD3-positive Zellen in den zellulären Infiltrationen in allen Organen festgestellt werden. Die Isolierung von Buffy-Coat (BC) Zellen von Nymphensittichen und ihre Stimulation mit Phytohämagglutinin (PHA-M) wurden in dieser Arbeit erfolgreich. Mit Hilfe von indirekter Immunfluoreszenz konnten CD3-positive Zellen, CD4-positive Zellen, CD8-positive Zellen, Monozyten, B-Zellen und Thrombozyten in BC Zellen Charakterisierung von Nymphensittichen werden.

In der Durchflusszytometrie war die Charakterisierung von CD4-positive Zellen, CD8-positive Zellen, Monozyten, B-Zellen, und Thrombozyten, aber nicht von CD3-positive Zellen aus Nymphensittich BC möglich. Unsere Untersuchung zeigt weiterhin, dass kein ABV-Antigen und keine ABV-4-RNA in Buffy-Coat (BC) Zellen von Nymphensittichen im Zeitraum von 0 Tagen bis zu 15 Tagen nach einer Infektion mit ABV-4 gefunden wurden. Außerdem waren kein ABV-Antigen und keine ABV-4 RNA in stimulierten BC-Zellen von Tag 0 bis Tag 15 nach der Stimulation und ABV-4-Infektion nachweisbar.

Diese Ergebnisse zeigt dass Nymphensittichblutzellen nicht direkt mit ABV-4 infiziert werden.

Weitere Untersuchungen über die Rolle von Makrophagen oder Endothelzellen in der Verbreitung der ABV-Infektion innerhalb des infection wird erforderlich.

8. References

Antinoff, N., 2001. It isn't always PDD: Three cases with proventricular enlargement. In: Proceedings of the Annual Conference of the Association of Avian Veterinarians: Bergman E (Ed.), 35–37.

Berhane, Y., 2004. Studies on the etiology and pathology of proventricular dilatation disease. Doctoral thesis. University of Guelph, Canada. 150 pages.

Berhane, Y., Smith, D., Newman, S., Taylor, M., Nagy, E., Binnington, B. and Hunter, B. 2001. Peripheral neuritis in psittacine birds with proventricular dilatation disease. Avian Pathology: 30**,** 563-70.

Bond M., Down, D., and Wolf, S., 1993. Screening for psittacine proventricular dilatation syndrome. In: Proceedings of the Annual Conference of the Association of Avian Veterinarians; Jackson G (Ed.), 92–97.

Boyum, A., 1968. Isolation of mononuclear cells and granulocytes from human blood. Scandinavian Journal of Clinical & Laboratory Investigation: 21:77-89.

Boyum, A., 1976. Isolation of lymphocytes, granulocytes and macrophages. Scandinavian Journal of Immunology: 5, issue 5, 9–5.

Brady, M., and Finlan, M., 1990. Radioactive labels: autoradiography and choice of emulsions for in situ hybridization. In: in situ hybridization: principle and practice (J. M. Polak & J. O'D. McGee Ed.) Oxford: Oxford University Press.

Briese., T., de la Torre J., Lewis., A., Ludwig., H., Lipkin., W., 1992. Proceedings of the National Academy of Sciences of the United States of America: 89*,* 11486–11489.

Briese., T., Schneemann, A., Lewis., A., Park., Y., Kim., S., Ludwig., H., and Lipkin., W.,1994. Genomic organization of Borna disease virus. Proceedings of the National Academy of Sciences of the United States of America: 91: 4362-4366.

Buongiorno-Nardelli M., and Amaldi F. 1969. Nature: 225, 946-7.

Burkhardt, E., and Müller, H., 1987. Susceptibility of chicken blood lymphoblast and monocytes to infectious Bursal disease virus (IBD). Archives of Virology: 94, 297-303.

Carbone, K., Duchala, C., Griffin, J., Kincaid, L., and Narayan, O., 1987. Pathogenesis of Borna Disease in Rats: Evidence that intra-axonal spread is the major route for virus dissemination and the determinants for disease incubation. Journal of Virology: 61, issue 11, 3431-3440.

Carlson, G., and Kaneko, J., 1973. Isolation of Leukocytes from Bovine peripheral blood. Experimental Biology and Medicine (Maywood): 142, issue 3, 853-856.

Chan, V., and McGee, J., 1990. Non-radioactive probes: preparation characterization, and detection. In: In Situ Hybridization: Principle and Practice (J. M. Polak & J. O'D. McGee Ed.) Oxford: Oxford University Press.

Chase, G., Mayer, D., Hildebrand, A., Frank, R., Hayashi, Y., Tomonaga, K., and Schwemmle, M., 2007. Borna disease virus matrix protein is an integral component of the viral ribonucleoprotein complex that does not interfere with polymerase activity. Journal of Virology: 81, 743-9.

Chess, L., Macdermotc, R., and Schlossman, S., 1974. Immunologic functions of isolated human lymphocyte subpopulation. Journal of Immunology: 113, 1113-1121.

Chomczynski, P., and Sacchi, N., 1987. Single-step method of RNA isolation by acid guanidinium thiocyanate-phenol-chloroform extraction. Analytical Biochemistry: 162, issue 1, 156-9.

Clark, F.D., 1984. Proventricular dilatation syndrome in large psittacine birds. Avian Disease: 28, 813–815.

Clemente, R., and de la Torre., J., 2007. Cell-to-cell spread of Borna disease virus proceeds in the absence of the virus primary receptor and furin-mediated processing of the virus surface glycoprotein. Journal of Virology: 81**,** 5968-5977.

Clubb, S.L., 2009. Proventricular dilation disease. In: Proceedings of the 81st Western Veterinary Conference: 707, 4.

Chun-jie, W., Siriguleng, Y., Ao-ri-ge-le, De-gang J, Hong-qiang, Y., Huai-ping, Lillehoj, H., Si-mu-ji, D., Andrew, C., and Si-ri-gu-leng, X., 2012. Regulation of T lymphocytes subpopulations in specific pathogen free chickens following experimental fowl adeno virus VIII infection. Brazilian Journal of Microbiology: 1281-1290.

Compans, W., Melsen, R., de la Torre, C., 1994. Virus-like particles in MDCK cells persistently infected with Borna disease virus. Virus research: 33, 261-268.

Cros, J. F., and Palese, P., 2003. Trafficking of viral genomic RNA into and out of the nucleus: influenza, Thogoto and Borna disease viruses. Virus Research: 95**,** 3-12.

Cubitt, B., Oldstone, C., and de la Torre, J., 1994. Sequence and genome organization of Borna disease virus. Journal Virology: 68**,** 1382-96.

Cytel Studio StatXact Vers. 9.0.0, 2010. Statistical Software for exact nonparametric inference, user manual. CYTEL Inc., Cambridge, MA 02139, U.S.A.

Dahlhausen, B., Aldred, S., and Colaizzi E., 2002. Resolution of clinical proventricular dilation disease by cyclooxygenase 2 inhibition. In: Proceedings of the Annual Conference of the Association of Avian Veterinarians: 9–12.

Daoust, P., Julian, R., Yason, C., and Artsob, H., 1991. Proventricular impaction associated with nonsuppurative encephalomyelitis and ganglioneuritis in two Canada geese. Journal of Wildlife Diseases: 27, 513–517.

De Kloet, S., and Dorrestein, G., 2009. Presence of avian bornavirus RNA and anti-avian bornavirus antibodies in apparently healthy macaws. Avian Disease: 53, 568 – 573.

De Kloet A., Kerski, A., and de Kloet, S., 2011. Diagnosis of avian bornavirus infection in psittaciformes by serum antibody detection and reverse transcription polymerase chain reaction assay using feather calami. Journal of Veterinary Diagnostic Investigations: 23, 421–429.

De la Torre, J., 1994. Molecular biology of borna disease virus: prototype of a new group of animal viruses. Journal of Virology: 68 (12): 7669–7675.

De la Torre, J., 2002. Molecular biology of Borna disease virus and persistence. Frontiers in Bioscience: 7, 569-579.

Delnatte, P., Berkvens, C., Kummrow, M., Smith, D.A., Campbell, D., Crawshaw, G., Ojkic, D. and DeLay, J., 2011. New genotype of avian bornavirus in wild geese and trumpeter swans in Canada. Veterinary Record: 169: 108.

Delnatte, P., Ojkic, D., DeLay, J., Campbell, D., Crawshaw, G., and Smith, D., 2013. Pathology and diagnosis of avian bornavirus infection in wild Canada geese (*Branta canadensis*), trumpeter swans (*Cygnus buccinator*) and mute swans (*Cygnus olor*) in Canada: a retrospective study. Avian Pathology: 42, 114-128.

Dixon, W., 1993. BMDP Statistical Software Manual, Volume 1 and 2. University of California Press, Berkeley, Los Angeles, London.

Doenhoff, M., Janossy, G., and Kerbel, R., 1976. Enumeration of polyclonal mitogen-responsive cells in different lymphoid tissues of the mouse. Immunology: 30, 367.

Doneley, R., Miller, R., and Fanning, T., 2007. Proventricular dilatation disease: an emerging exotic disease of parrots in Australia. Australian Veterinary Journal: 85**,** issue 3, 119-123.

Dorrestein, G., Honkavuori, K., Briese, T., Tizard, I., Bastiaansen, P., Verschuren, M., Lipkin, W., and de Kloet, S., 2010. Overview of the role and diagnosis of avian bornavirus related to PDD in psittacines. In: Proceedings of the 7th International Congress on Wild and Exotic Animals; Paris, France; 8 pages.

Dürrwald, R., Kolodziejek, J., Muluneh, A., Herzog, S., and Nowotny, N., 2006. Epidemiological pattern of classical Borna disease and regional genetic clustering of Borna disease viruses point towards the existence of to-date unknown endemic reservoir host populations. Microbes and Infection: 8, 917–929.

Dürrwald, R., Kolodziejek, J., Weissenböck, H., and Nowotny, N., 2014. The bicolored white-toothed shrew crocidura leucodon (HERMANN 1780) is an indigenous host of mammalian Borna disease virus. PLoS One: 9, issue 4, e93659.

Eickmann., M., Kiermayer., S., Kraus., I., Gössl., M, Richt JA, Garten W., 2005. Maturation of Borna disease virus glycoprotein. Federation of European Biochemical Societies, letter: 579(21):4751-6.

Enderlein, D., Piepenbring, A., Herzog, S., Herden, C., Crosta, L., Oberhäuser, K., Muller, H., Hebel, C., Hammer, S., Kaleta, E., Gerlach, H., Heffels-Redmann, U., and Lierz, M., 2011. The situation of ABV in endangered psittacines like the Spix's macaw. In: Proceedings of the 11th European Association of Avian Veterinians; Samour J (Ed.): 228-229.

Fulwyler, M., 1965. Electronic separation of biological cells by volume. Science: 150, 698.

Fujino, K., Horie, M., Honda, T., Nakamura, S., Matsumoto, Y., Francischetti, M., and Tomonaga K., 2012. Evolutionarily conserved interaction between the phosphoproteins and X proteins of bornaviruses from different vertebrate species. PLoS One: 7:e51161.

Gancz, A., Kistler, A., Greninger, A., Farnoushi, Y., Mechani, S., Perl, S., Berkowitz, A., Perez, N., Clubb, S., and DeRisi, J., 2009. Experimental induction of proventricular dilatation disease in cockatiels (*Nymphicus hollandicus*) inoculated with brain homogenates containing avian bornavirus 4. Journal of Virology: 6, 100.

Gancz, A., Clubb, S., and Shivaprasad, H., 2010. Advanced diagnostic approaches and current management of proventricular dilatation disease. Veterinary clinics of North America exotic animal practice: 13, 471–494.

Gerlach, H., 1991. Macaw wasting disease, a 4 year study on clinical case history, epizootiology, analysis of species, diagnosis and virological results. Proc. European Association Avian Veterinarians. 273-281.

Gerlach, H., 1994. Viruses. In: Avian medicine: principles and application; Ritchie BW, Harrison GJ, Harrison IR (Eds.); Wingers, Lake Worth, FL, USA; 862–948.

Graham, D., 1984. Infiltrative splanchnic neuropathy, a component of the "wasting macaw" complex. Proc: Association Avian Veterinarians. 275.

Graham, D., 1991. Wasting proventricular dilatation disease: a pathologist's view. In: Proceedings of the Annual Conference of the Association of Avian veterinarians: 43–44.

Gratzner, H., Leif, R., Ingram, D., and Castro, A., 1975. The use of antibody specific for bromodeoxyuridine for the immunofluorescent determination of DNA replication in single cells and chromosomes. Experimental Cell Research: 95, issue 1, 88–94.

Gray, P., Villanueva, I., Mirhosseini, N., Hoppes, S., Payne, S., and Tizard, I., 2009. Experimental infection of ducks (*Anas platyrhynchos*) with avian bornavirus. Proceedings of the Association Avian Veterinarians. 7.

Gray, P., Hoppes, S., Suchodolski, P., Mirhosseini, N., Payne, S., Villanueva, I., Shivaprasad, H., Honkavuori, K., Lipkin, W., and Briese, T., 2010. Use of avian bornavirus isolates to induce proventricular dilatation disease in Conures. Emerging infectious diseases: 16, 473– 479.

Green, J., Edward, R., and Manson, M., 1992. Immunohistochemical detection of bromodeoxyuridine-labelled nuclei for *in vitro* cell kinetic studies. Methods in Molecular Biology: 80, 131-135.

Gregory, C., Latimer, K., Niagro, F., Ritchie, B., Campagnoli, R., Norton, T., McManamon, R., and Greenacre, C., 1994. A review of proventricular dilatation syndrome. Association of Avian Veterinarians: 8, 69-75.

Gregory, C., 1995. Proventricular dilatation disease. In: Ritchie, B. W. (Ed.): Avian Viruses Function and Control. Wingers Pub Lake Worth, Florida, 444-445.

Gregory, M., Smoyer, W., Sedman, A., Kershaw, D., Valentini, R., Johnson, K., and Bunchman., T., 1996. Long-term cyclosporine therapy for pediatric nephrotic syndrome: a clinical and histologic analysis. Clinical Journal of the American Society of Nephrology: 7, 543-549.

Gregory, C., Branson, W., Latimer, K., Campagnoli, R., Pesti, D., and Lukert, P., 1997. Proventricular dilatation disease: In: Proceedings of the Annual Conference of the Association of Avian Veterinary; Doolen M (Ed.): 43–52.

Gregory, C., Ritchie, B., Latimer, K., Steffens, W., Pesti, D., Campagnoli, R. and Lukert, P., 1998. Progress in understanding proventricular dilatation disease, Proceed: International Aviculture Society, Orlando, Florida: 1-6.

Gonzalez-Dunia, D., Cubitt, B., and de la Torre, J. C., 1998. Mechanism of Borna disease virus entry into cells. Journal of Virology: 72**,** 783-800.

Gregory, C.R., Branson, W., Latimer, K., Steffens, W., Pesti, D., Campagnoli, R., and Lukert, P., 2000. Progress in understanding proventricular dilatation disease. In: Proceedings of the Annual Conference of the Association of AvianVeterinians, Bergman E (Ed.): 269–275.

Grund, C. H., Werner, O., Gelderblom, H., Grimm, F., and Kosters, J. 2002. Avian paramyxovirus serotype 1 isolates from the spinal cord of parrots display a very low virulence. Journal of Veterinary Medicine. B Infectious Diseases and Veterinary Public Health: 49, 445-451.

Guo, J., Covaleda, L., Heatley, J., Baroch, J., Tizard, I., and Payne, S., 2012. Widespread avian bornavirus infection in mute swans in the Northeastern United States. Veterinary Medicine, Research and Reports: 3: 49–52.

Guo, J., Shivaprasad, L., Rech, R., Heatley, J., Tizard, I., and Payne, S., 2014. Characterization of a new genotype of avian bornavirus from wild ducks. Journal of Virology: 11: issue 197, 2-7.

Harry, A., and John, A., 1990. Detection of bromodeoxyuridine-labeled cells by differential fluorescence analysis of DNA fluorochromes. Methods in Cell Biology: 33, 199–206.

Heatley, J., and Villalobos, A., 2012. Avian bornavirus in the urine of infected birds. Veterinary Medicine: Research and Reports: 3, 19–23.

Heffels-Redmann, U., Enderlein, D., Herzog, S., Herden, C., Piepenbring, A. , Neumann, D., Müller, H., Capelli, S., Oberhäuser, K., Gerlach, H., Kaleta, E.F., and Lierz, M., 2011. Occurrence of avian bornavirus infection in captive psittacines in various European countries and its association with proventricular dilatation disease. Avian Pathology: 40, 419-426.

Hagiwara K., Momiyama N., Taniyama H., Nakaya T., Tsunoda N., Ishihara C., and Ikuta K., 1997. Demonstration of Borna disease virus (BDV) in specific regions of the brain from horses positive for serum antibodies to BDV but negative for BDV RNA in the blood and internal organs. Medical Microbiology and Immunology: 186, issue 1, 19-24.

Heffels-Redmann, U., Enderlein, D., Herzog, S., Piepenbring, A., Bürkle, M., Neumann D., Müller, H., Capelli, S., Müller H, and Oberhäuser K., 2012. Follow-up investigations on different courses of natural avian bornavirus infections in psittacines. Avian Diseases: 56, 153–159.

Herden, C., Herzog, S., Wehner, C., Zink, J., Richt, A., and Frese, K., 1999. Comparison of different methods of diagnosing Borna disease in horses post mortem. In: Equine Infectious Diseases, 8. International Conference, Dubai, 1998, 286290

Herden, C., Briese., T., Lipkin., W., and Richt., J., 2013. Fields of Virology. Chapter 39, 1124-1150.

Herzog, S., Enderlein, D., Heffels-Redmann, U., Piepenbring, A., Neumann, D., Kaleta, E.F., Müller, H., Lierz, M., and Herden, C., 2010. Indirect immunofluorescence assay for intra vitam diagnostic of avian bornavirus infection in psittacine birds. Journal of Clinical Microbiology: 48, 2282–2284.

Honkavuori, K., Shivaprasad, H., Williams, B., Quan, P., Hornig, M., Street, C., Palacios, G., Hutchison, S., Franca, M., and Egholm, M., 2008. Novel bornavirus in psittacine birds with proventricular dilatation disease. Emerging infectious diseases: 14, 1883–1886.

Hoppes, S., Gray, P., Payne, S., Shivaprasad, H., and Tizard, I., 2010. The isolation, pathogenesis, diagnosis, transmission, and control of avian bornavirus and proventricular dilatation disease. Veterinary Clinics of North America: Exotic Animal Practice: 13: 495–508.

Hoppes, S., Tizard, I., Shivaprasad, H., Guo, J., and Heatley, J., 2012. Treatment of avian bornavirus-infected cockatiels (*Nymphicus hollandicus*) with oral meloxicam and cyclosporine. In: Proceedings of the 33rd Annual Conference of the Association of AvianVeterinians; Bergman E (Ed.), Louisville, KY, USA: 27.

Hoppes, S., Tizard, I., and Shivaprasad, H., 2013. Avian bornavirus and proventricular dilatation disease: diagnostics, pathology, prevalence and control. Veterinary clinics of North America exotic animal practice: 16, 339–355.

Horie, M., Honda, T., Suzuki, Y., Kobayashi, Y., Daito, T., Oshida, T., Ikuta, K., Jern, P., Gojobori, T., Coffin, M., and Tomonaga, K. 2010. Endogenous non-retroviral RNA virus elements in mammalian genomes. Nature: 463, 84–87.

Horie, M., Kobayashi, Y., Suzuki, Y., and Tomonaga, K., 2013. Comprehensive analysis of endogenous bornavirus-like elements in eukaryote genomes. Philosophical Transactions of the Royal Society of London: 368, 1626.

Horie, M., Ueda, K., Ueda, A., Honda, T., and Tomonaga, K., 2012. Detection of avian bornavirus 5 RNA in *Eclectus roratus* with feather picking disorder. Microbiology and Immunology: 56, 346–349.

Hughes, E., 1984. The pathology of myenteric ganglioneuritis, psittacine encephalomyelitis, proventricular dilatation of psittacines, and macaw wasting syndrome. Proc: 33rd Western poultry disease Conference. 85-87.

Ikuta, K., Hagiwara., K., Taniyama., H., Nowotny., N., 2002. Epidemiology and infection of natural animal hosts. In: Carbone, K.M. (Ed.), Borna disease virus and its role in neurobehavioral disease. American Society for Microbiology, Washington, DC, 87–123.

Kaspers., B., Kaiser., P., 2014. Avian Immunology (Second Edition): 169–188.

Kerski, A., de Kloet A., and de Kloet S., 2012. Vertical transmission of avian bornavirus in psittaciformes: avian bornavirus RNA and anti-avian bornavirus antibodies in eggs, embryos, and hatchlings obtained from infected Sun Conures (*aratinga solstitialis*). Avian Diseases: 56, 471–478.

Keren, D., Hanson, C., and Hurtubise, P., 1994. Flow cytometry and clinical diagnosis. Chicago: American Society of Clinical Pathology Press: 664.

Kerski, A., de Kloet, A., and de Kloet, S., 2012. Vertical transmission of avian bornavirus in psittaciformes: avian bornavirus RNA and anti-avian bornavirus antibodies in eggs, embryos, and hatchlings obtained from infected Sun Conures (*aratinga solstitialis*). Avian Disease: 56, 471–478.

Kiermayer., S., Kraus., I., Richt., J., Garten., W., Eickmann., M., 2002. Identification of the amino terminal subunit of the glycoprotein of Borna disease virus. Federation of European Biochemical Societies: 6, 531(2): 255-258.

Kistler A.L., Gancz, A., Clubb, S., Skewes-Cox, P., Fischer, K., Sorber, K., Chiu, C.Y., Lublin, A., Mechani, S., and Farnoushi, Y., 2008. Recovery of divergent avian bornaviruses from cases of proventricular dilatation disease: identification of a candidate etiologic agent. Journal of Virology: 5, 88.

Kistler, A., Smith, J., Greninger, A., DeRisi, J., and Ganem, D., 2010. Analysis of naturally occurring avian bornavirus infection and transmission during an outbreak of proventricular dilatation disease among captive psittacine birds. Journal of Virology: 84, 2176– 2179.

Knuutila, A., and Kovanen, P., 1987. Relative proportions of mitotic T and B cells in PHA-hulated lymphocyte cultures. Cancer Genetic Cytogenet: 29, 151-1 54.

Kobayashi, T., Kamitani, W., Zhang, G., Watanabe, M. Tomonaga, K. and Ikuta., K., 2001. Borna disease virus nucleoprotein requires both nuclear localization and export activities for viral nucleocytoplasmic shuttling. Journal of Virology: 75**,** 3404-12.

Kobayashi., T., Shoya., Y., Koda., T., Takashima., I., Lai., P., Ikuta., K., Kakinuma., M., Kishi., M., 1998. Nuclear targeting activity associated with the amino terminal region of the Borna disease virus nucleoprotein. Journal of Virology: 243, issue 1, 188-197.

Kohno, T., Goto1, T., Takasaki, T., Morita1, C., Nakaya, T., Ikuta, K., Kurane, I., Sano, K., and Nakai M., 1999. Fine structure and morphogenesis of Borna disease virus. Journal of Virology: 73, 760-6.

Korbel, R., and Rinder, M., 2011. Ophtalmological findings in birds affected with PDD. In: Proceedings of the 11th European Association of Avian Veterinians Conference; Samour J (Ed.); 193.

Kothlow, S., Mannes, N., Schaerer, B., Rebeski, D., Kaspers, B., and Schultz, U., 2005. Characterization of duck leucocytes by monoclonal antibodies. Developmental & Comparative Immunology: 29, issue 8, 733–748.

Kuhn, J., Dürrwald, R., Bào, Y, Briese, T., Carbone, K., Clawson, A., Joseph L., deRisi, J., Garten, W., Jahrling, P., Kolodziejek, J., Rubbenstroth, D., Schwemmle, M., Stenglein., M., Tomonaga, K., Weissenböck, H., and Nowotny, N., 2015. Taxonomic reorganization of the family *Bornaviridae*. Archives of Virology: 160, issue 2, 621-32.

Lacoste-Eleaume, A., Bleux, C., Quéré, P., Coudert, F., Corbel, C., and Kanellopoulos-Langevin, C., 1994. Biochemical and functional characterization of an avian homolog of the integrin GPIIb-IIIa present on chicken thrombocytes. Experimental Cell Research: 213, issue 1, 198-209.

Last, R., Weissenböck, H., Nedorost, N., and Shivaprasad, H., 2012. Avian bornavirus genotype 4 recovered from naturally infected psittacine birds with proventricular dilatation disease in South Africa. Journal of the South African Veterinary Association: 83, issue 1, 938-941.

Lavoie, E., and Grasman, K., 2005. Isolation, cryopreservation, and mitogenesis of peripheral blood lymphocytes from chickens (*Gallus domesticus*) and wild herring gulls (*Larus argentatus*). Archives of Environmental Contamination and Toxicology: 48, issue 4, 552-558.

Li, Z., Nestor, K., Saif Y., Fan, Z., Luhtala, M., and Vainio, O., 1999. Cross-reactive anti-chicken CD4 and CD8 monoclonal antibodies suggest polymorphism of the Turkey CD8α molecule. Poultry science: 78, 1526-1531.

Lierz, M., Hafez, H., Honkavuori, K., Gruber, A., Olias, P., Abdelwhab, E., Kohls, A., Lipkin, I., Briese, T., and Hauck, R., 2009. Anatomical distribution of avian bornavirus in parrots, its occurrence in clinically healthy birds and ABV-antibody detection. Avian Pathology: 38, 491–496.

Lierz, M., Herden, C., Herzog, S., and Piepenbring, A., 2010. Proventricular dilatation disease and avian bornavirus as a possible cause. Tierarztl Prax Ausg Kleintiere Heimtiere: 38, 87–94.

Lierz, M., Piepenbring, A., Herden, C., Oberhäuser, K., Heffels-Redmann, U., and Enderlein, D., 2011. Vertical transmission of avian Bornavirus in psittacines. Emerging Infectious Diseases: 17, 12.

Lierz, M., Piepenbring, A., Heffels-Redmann, U., Herzog, S., Herden, C., and Enderlein, D., 2012. Experimental infection of cockatiels with different avian bornavirus genotypes. In: Proceedings of the 33rd Annual Conference of the Association of Avian Veterinarians; Bergman E (Ed.); Louisville, KY, USA; 9–10.

Lipkin, W. I., and Briese, T., 2007. *Bornaviridae*, 5th ed, vol. 2. Lippincott Williams & Wilkins, Philadelphia.

Levine, B., and Practice, C., 2003. Common disorders of amazons, Australian Parakeets, and African Grey Parrots. Seminars in Avian and Exotic Pet Medicine 12**:**125-130.

Lublin, A., Mechani, I.S., Perl, S., and Bendheim, U., 2006. An outbreak of proventricular dilatation disease in psittacine breeding farm in Israel. Israel Journal of Veterinary Medicine: 61, 16–19.

Malik., T., Kobayashi., T., Ghosh., M., Kishi., M., Lai., P., 1999. Nuclear localization of the protein from the open reading frame x1 of the Borna disease virus was through interactions with the viral nucleoprotein. Journal of Virology: 258, issue 1, 65-72.

Malka, S., Crabbs, T., Mitchell, E., Zehnder, A., Kent, M., Lowenstine, L., and Hawkins, M., 2008. Disseminated lymphoma of presumptive T-cell origin in a great horned owl (*Bubo virginianus*). Avian Medcine and Surgery: 22, issue 3, 226-33.

Mannl, A., Gerlach, H., and Leipold, R., 1987. Neuropathic gastric dilatation in psittaciformes. Avian Diseases: 31, 214–221.

Marko, L., Jan, S., Yoshikazu, H., Takashi, O., Paavo, T., and Olli, V., 1993. Analysis of Chicken CD4 by Monoclonal Antibodies Indicates Evolutionary Conservation Between Avian and Mammalian Species. Hybridoma: 12, 6.

Marietto-Goncalves, G., Troncarelli M., and Sequeira J., 2009. Proventricular dilatation disease (PDD) and megaesophagus in a blue-fronted Amazon parrot (*Amazona aestiva*) - Case report. Veterinary Zootec*:* 16, 69–73.

Mast, J., Goddeeris, B., Peeters, K., Vandesande, F., and Berghman, L., 1997. Characterization of chicken monocytes, macrophages and interdigitating cells by the monoclonal antibody KUL01. Veterinary Immunology and Immunopathology: 61, 343–357.

Mayer, A., and Danner, K., 1974. Persistent infections caused by Borna virus. Infection: 2, issue 2, 64-69.

Mills, G., Lee, J., Cheung, R., and Gelfande, W., 1985. Characterization of the requirements for human T cell mitogenesis by using suboptimal concentrations of phytohemagglutinin. Immunology: 135, 3087-3093.

Mirhosseini, N., 2011. Molecular detection and characterization of avian bornavirus. Doctoral thesis. Texas A&M University, United States of America.

Mirhosseini, N., Gray, P., Tizard, I., Payne, S., 2012. Complete genome sequence of avian bornavirus genotype 1 from a Macaw with proventricular dilatation disease. Journal of Virology, 86: 7023.

Mire-Sluis, A., Wickremansighe, R., Hoffbrand, A., Timms, A., and Gillian E., 1987. Human T lymphocytes stimulated by phytohaemagglutinin undergo a single round of cell division without a requirement for interleukin-2 or accessory cells. Immunology: 607-12.

Monaco, E., Hoppes, S., Guo, J., and Tizard I., 2012. The detection of avian bornavirus within psittacine eggs. Avian Medicine and Surgery: 26:144–148.

Müller, H., 1986. Replication of infectious bursal disease virus in lymphoid cells. Archives of Virology: 87, issue 3, 191-203.

Nakamura, Y., Kishi, M., Nakaya, T., Asahi, S., Tanaka, H., Sentsui, H., Ikeda, K., and Ikuta K., 1995. Demonstration of Borna disease virus RNA in peripheral blood mononuclear cells from healthy horses in Japan. Vaccine: 13, issue 12, 1076-1079.

Naspitz, C., and Richter, M., 1968. The action of phytohemagglutinin *in vivo* and *in vitro,* a review. Progress in Allergy: 12, 1-85.

Nowotny, N., Kolodziejek, J., Jehle, O., Suchy, A., Staeheli, P., and Schwemmle, M. 2000. Isolation and characterization of a new subtype of Borna disease virus. Journal of Virology: 74: 5655–5658.

Olias., P., Adam., I., Meyer., A., Scharff., C., Gruber., A., 2014. Reference genes for quantitative gene expression studies in multiple avian species. PLoS ONE: 9, issue 6, e99678.

Ogawa, H., Sanada, Y., Sanada, N., Kudo, M., Tuchiya, K., Kodama, T., and Uetsuka, K., 2011. Proventricular dilatation disease associated with avian bornavirus infection in acitron-crested cockatoo that was born and hand-reared in Japan. The Journal of Veterinary Medical Science: 73, 837–840.

Ouyang, N., Storts, R., Tian, Y., Wigle, W., Villanueva, I., Mirhosseini, N., Payne, S., Gray, N., and Tizard., I., 2009. Histopathology and the detection of avian bornavirus in the nervous system of birds diagnosed with proventricular dilatation disease. Avian Pathology: 38, 393-401.

Payne, S., Shivaprasad, H., Mirhosseini, N., Gray, P., Hoppes, S., Weissenbock, H. and Tizard, I., 2011a. Unusual and severe lesions of proventricular dilatation disease in cockatiels (*Nymphicus hollandicus*) acting as healthy carriers of avian Bornavirus (ABV) and subsequently infected with a virulent strain of ABV. Avian Pathology: 40, 15–22.

Payne, S., Covaleda, L., Jianhua, G., Swafford, S., Baroch, J., Ferro, P., Lupiani, B., Heatley, J., and Tizard, I., 2011b. Detection and Characterization of a Distinct Bornavirus Lineage from Healthy Canada Geese (*Branta canadensis*). Journal of Virology: 85, issue 22, 12053–12056.

Payne, S.L., Guo, J., and Tizard, I., 2012a. Bornaviruses in North American waterfowl. In: Hambrick J and Gammon LT (eds) Ducks, Habitat, Behavior and Diseases. New York: Nova Scientific Publishers.

Payne, S., Delnatte., D., Guo, J., Heatley, J., Tizard, I., and Smith, D., 2012b. Birds and Bornavirus. Animal Health Research Reviews: 13, 145–156.

Perpinan, D., Fernandez-Bellon, H., Lopez, C., and Ramis, A., 2007. Lymphocytic myenteric, subepicardial and pulmonary ganglioneuritis in four nonpsittacine birds. Avian Medicine and Surgery: 21, 210–214.

Petersen, M., Davids, L., and Kidson, S., 2012. Simultaneous immunofluorescent labeling using anti-BrdU monoclonal antibody and a melanocyte-specific marker in formalin-fixed paraffin-embedded human skin samples. Applied Immunohistochemistry & Molecular Morphology: 20, issue 6, 614-7

Piepenbring, A., Enderlein, D., Herzog, S., Kaleta, E., Redmann, U., Ressmeyer, S., Herden, C., and Lierz, M., 2012. Pathogenesis of avian bornavirus in experimentally infected cockatiels. Emerging Infectious Diseases: 18, 2.

Piepenbring., A., Enderlein., D., Herzog., S., Al-Ibadi., B., Heffels-Redmann., U., Heckmann., J., Lange-Herbst., H., Herden., C., Lierz., M., 2015. ABV-2 isolate causes different disease patterns in cockatiels than ABV-4. Avian Pathology. In revision.

Planz, O., and L. Stitz, L., 1999. Borna disease virus nucleoprotein (p40) is a major target for CD8 T-cell-mediated immune response. Journal of Virology: 73, 1715-8.

Poenisch, M., Unterstab, G., Wolff, T., Staeheli, P., and Schneider., U., 2004. The X protein of Borna disease virus regulates viral polymerase activity through interaction with the P protein. Journal of General Virology: 85**,** 1895-1898.

Poenisch, M., Burger, N., Staeheli, P., Bauer, G., and Schneider, U., 2009. Protein X of Borna disease virus inhibits apoptosis and promotes viral persistence in the central nervous systems of newborn-infected rats. Journal of Virology: 83, 4297-4307.

Pyper., M., and Gartner., A., 1997. Molecular basis for the differential subcellular localization of the 38- and 39 kilodalton structural proteins of Borna disease virus. Journal of Virology: 71, 5133-5139.

Pyper M., Clements, J., and Zink, C., 1998. The nucleolus is the site of Borna disease virus RNA transcription and replication. Journal of Virology: 72, issue 9, 7697-7702.

Raghav, R., Taylor, M., DeLay, J., Ojkic, D., Pearl, D., Kistler, A., DeRisi, J., Ganem, D., and Smith, D., 2010. Avian bornavirus is present in many tissues of psittacine birds with histopathologic evidence of proventricular dilatation disease. Journal of Veterinary Diagnostic Investigation: 22, 495–508.

Reavill, D., 2007. Lesions of the proventriculus/ventriculus of pet birds: 1640 cases. In: Proceedings of the Annual Conference of the Association of AvianVeterinians; 89-93.

Recktenwald, D., 1993. Introduction to flow cytometry: principles, fluo-rochromes, instrument set-up, calibration. Journal of Hematotherapy: 2, 387–394.

Reßmeyer, S., Herzog, S., Enderlein, D., Heffels-Redmann, U., Lierz, M., Herden, C., and Buchinder, A., 2010. Distribution patterns of avian bornavirus in psittacine birds suffering from proventricular dilatation disease. In: Proceedings of the Annual Conference of the European College of Veterinary Pathology: 9, 324.

Revathi, S., Ramesh, K., and Selvaraj, A., 2012. Regulatory T cell properties of thymic CD4-positive CD25-positive cells in ducks. Veterinary Immunology and Immunopathology: 149, 20– 27.

Richt., J., Fürbringer., T., Koch., A., Pfeuffer., I., Herden., C., Bause-Niedrig., I., Garten., W., 1998. Processing of the Borna disease virus glycoprotein gp94 by the subtilisin-like endoprotease furin. Journal of Virology: 72, issue 5, 4528-4533.

Richt., J., Schmeel., A., Frese., K., Carbone., K., Narayan., O., and Rott., R., 1994. Borna disease virus-specific T cells protect against or cause immunpathological Borna disease. Journal of Experimental Medicine: 179, 1467.

Ridgway, R., and Gallerstein, G., 1983. Proventricular dilatation in psittacines.In: Proceedings of the Annual Conference of the Association of Avian Veterinians: 228–230.

Rinder, M., Ackermann, A., Kempf, H., Kaspers, B., Korbel, R., and Staeheli, P., 2009. Broad tissue and cell tropism of avian bornavirus in parrots with proventricular dilatation disease. Journal of Virology: 83, 5401-5407.

Rinder, M., Kronthaler, F., Hufen, H., and Korbel, R., 2012. Avian bornavirus infections in canaries (*Serinus canaria*). Proceedings of the Association of Avian Veterinians.

Rodenberg, J., Sharma, J., Belzer, S., Nordgren, R., and Naqi, S., 1994. Flow cytometric analysis of B cell and T cell subpopulations in specific-pathogen-free chickens infected with infectious bursal disease virus. Avian Diseases: 38, issue 1, 16-21.

Rubbenstroth, D., Rinder, M., Kaspers, B., and Staeheli, P., 2012. Efficient isolation of avian bornaviruses (ABV) from naturally infected psittacine birds and identification of a new ABV genotype from a salmon-crested cockatoo (*Cacatua moluccensis*). Veterinary Microbiology: 161, 36–42.

Rubbenstroth, D., Rinder, M., Stein, M., Höperc, D., Kaspersd, B., Brosinskib, K., Horiea, M., Schmidte, V., Leglerf, M., Korbelb, R., and Staeheli, P., 2013. Avian bornaviruses are widely distributed in canary birds (*Serinus canaria domestica*). Veterinary Microbiology: 165, 287-295.

Rubbenstroth, D., Brosinski, K., Rinder, M., Olbert, M., Kaspers, B., Korbel, R., and Staeheli, P., 2014a. No contact transmission of avian bornavirus in experimentally infected cockatiels (*Nymphicus hollandicus*) and domestic canaries (*Serinus canaria forma domestica*). Veterinary Microbiology: 172, issue 1-2, 146-156.

Rubbenstroth, D., Schmidt, V., Rinder, M., Legler, M., Corman, M., Staeheli, P. 2014b. Discovery of a new avian bornavirus genotype in estrildid finches (*Estrildidae*) in Germany. Veterinary Microbiology: 168, 318–323.

Schmidt, R.E., Reavill, D.R., and Phalen, D.N., 2003. Pathology of pet and aviary birds. Iowa State Press, Ames, IA, USA.

Schneemann., A., Schneider., P., Lamb., R., Lipkin., W., 1995. The Remarkable Coding Strategy of Borna Disease Virus: A New Member of the Nonsegmented Negative Strand RNA Viruses. Journal of Virology: 210, 1-8.

Schneider, U., Naegele, M., Staeheli, P., and Schwemmle, M., 2003. Active Borna disease virus polymerase complex requires a distinct nucleoprotein-to-phosphoprotein ratio but no viral X protein. Journal of Virology: 77, 11781-11789.

Schneider, U., 2005. Novel insights into the regulation of the viral polymerase complex of neurotropic Borna disease virus. Virus Research: 111, 148-160.

Schwemmle., M., Jehle., C., Shoemaker., T., Lipkin., W., 1999. Characterization of the major nuclear localization signal of the Borna disease virus phosphoprotein. Journal of General Virology: 80, issue 1, 97-100.

Shapiro, H., 1995. Practical flow cytometry, 3rd edition. New York: Wiley-Liss, 542.

Shivaprasad, H., Barr, B., Woods, L., Moore, J., Kinde, H., Anderson, M., and Droual, R., 1995. Spectrum of lesions (pathology) of proventricular dilatation syndrome of psittacines. In: Proceedings of the Annual Conference of the Association of Avian Veterinians: 505–506.

Shivaprasad, H., 2005. Proventricular dilation disease in peregrine falcon (*Falco peregrinus*) .Proceedings annual Conference association of Avian Veterinians: 107–108.

Shivaprasad, H., Weissenböck, H., Hoppes, S., Gray, P., Payne, S., and Tizard, I., 2010. Pathology of experimental avian bornavirus infection in psittacines and chickens. In: Proceedings of the American association of Veterinary laboratory diagnosticians; Minneapolis, MN, USA: 97.

Shuman, S., 1991. Recombination mediated by Vaccinia virus DNA topoisomerase I in Escherichia coli is Sequence Specific. Proceedings of the National Academy of Sciences: 88, 10104-10108.

Shuman, S., 1994. Novel approach to molecular cloning and polynucleotide synthesis using vaccinia DNA topoisomerase. The Journal of Biological Chemistry: 269, 32678-32684.

Smith, D., Berkvens, C., Kummrow, M., Campbell, D., Ojkic, D., and DeLay, J., 2010. Identification of an avian bornavirus in the brains of Canada geese (*Branta canadensis*) and trumpeter swans (*Cygnus buccinator*) with non-suppurative encephalitis. In: Proceedings of the 59th Wildlife disease association annual meeting; Cholatal CS, Ferreyra H, Chirife A (Eds.); Iguazù, Argentina: 58.

Staeheli, P., Rinder, M., and Kaspers, B., 2010. Avian bornavirus associated with fatal disease in psittacine birds. Journal of Virology: 84, 6269–6275.

Staeheli, P., Sauder, C., Hausmann, J., Ehrensperger, F., and Schwemmle, M., 2000. Epidemiology of Borna disease virus. Journal of General Virology: 81, 2123–2135.

Steinmetz, A., Pees, M., Schmidt, V., Weber, M., Krautwald-Junghanns, M., and Oechtering G., 2008. Blindness as a sign of proventricular dilatation disease in a grey parrot (*Psittacus erithacus erithacus*). Journal of Small Animal Practice: 49, 660–662.

Stenglein, D., Leavitt, E., Abramovitch, M., McGuire, A., and DeRisi, L., 2014. Complete genome sequence of a reptile bornavirus recovered from a wild caught Elapsoidea loveridgei. Genome Announcements: 2, issue 5:e00779-14

Stitz, L., Soeder, D., Deschl, U., Frese, K., and Rott, R., 1989. Inhibition of immune-mediated encephalitis in persistently Borna disease virus-infected rats. Journal of Immunology: 143, 4250–4256.

Stitz, L., Noske, K., Planz, O., Furrer, E., Lipkin, W., and Bilzer T., 1998. A functional role for neutralizing antibodies in Borna disease: influence on virus tropism outside the central nervous system. Journal of Virology: 72, 8884–8892.

Stitz, L., Bilzer, T., and Planz, O., 2002. The immunpathogenesis of Borna disease virus infection. Frontiers in Bioscience: 7, 541-555.

Suedmeyer, W., 1992. Diagnosis and clinical progression of three cases of proventricular dilatation syndrome. Avian Medicine and Surgery: 6, 159–163.

Sullivan, N., Mackie, J., and Miller, R., 1997. First case of proventricular dilatation syndrome (macaw wasting disease) in Australia. Australian Veterinary Journal: 75, 674.

Tapani, H., Jukka, S., Lars, H., and Antti, V., 1978. Stimulation of Chicken Lymphocytes by T- and B-Cell Mitogens. Cellular Immunology: 39, 70-77.

Taylor, M., Dobson, H., Hunter, B., and Atkinson, R., 1997. New research in gastrointestinal motility in normal and disease states. In: Proceedings of the Annual Conference of the Association of Avian Veterinians; Doolen M (Ed.): 131–134.

Thiel, H. and Burkhardt, E., 1984. Development of optimal conditions for the stimulation of chicken peripheral blood lymphocytes by phytohaemagglutinin (PHA) in the microculture system. Veterinary Immunology and Immunopathology: 6, 327-340.

Tomonaga, K., Kobayashi, T., and Ikuta, K., 2002. Molecular and cellular biology of Borna disease virus infection. Microbes and Infection: 4**,** 491-500.

Toshifumi, M., Masakazu, H., Kazuhiko, O., Chihiro, S., and Misao, O., 1995. Immunomodulation of peripheral T cells in chickens infected with Marek's disease virus: involvement in immunosuppression. Journal of General Virology: 76, 2979-2985.

Vahlenkamp T., Enbergs H., and Müller H., 2000. Experimental and natural borna disease virus infections: presence of viral RNA in cells of the peripheral blood**.** Veterinary Microbiology; 76, issue 3, 229-244.

Vice., C., 1992. Myocarditis as a component of psittacine proven-tricular dilatation syndrome in a Patagonian conure. Avian Diseases: 36, 1117–1119.

Uehlinger., D., Barkema., H., O'Handley., R., Parenteau., M., Parrington., L.,VanLeeuwen, J., Dixon., B., 2008. Comparison of flow cytometry and immunofluorescence microscopy for the detection of *Giardia duodenalis* in bovine faecal samples. Journal of Veterinary Diagnostic Investigation; 20, 178–185.

Villanueva, I., Gray, P., Mirhosseini, N., Payne, S., Hoppes, S., Honkavuori, K., Briese, T., Turner, D., and Tizard, I., 2010. The diagnosis of proventricular dilatation disease: use of a western blot assay to detect antibodies against avian bornavirus. Veterinary Microbiology: 143,196–201.

Walker., M., Jordan., I., Briese., T., Fischer., N., and Lipkin., W., 2000. Expression and Characterization of the Borna Disease Virus Polymerase. Journal of Virology: 74, issue 9, 4425–4428.

Watson, J.V., 1999. The early fluidic and optical physics of cytometry. Cytometry: 38, 1–14.

Wehner., T., Ruppert., A., Herden., C., Frese., K., Becht., H., Richt., J., 1997. Detection of a novel Borna disease virus-encoded 10 kDa protein in infected cells and tissues. Journal of General Virology: 8, 2459–2466.

Weissenböck, H., Bakonyi, T., Sekulin, K., Ehrensperger, F., Doneley, R., Dürrwald, R., Hoop, R., Erdélyi, K., Gál, J., and Kolodziejek, J., 2009a. Avian bornaviruses in psittacine birds from Europe and Australia with proventricular dilatation disease. Emergency Infectious Diseases: 15, 1453–1459.

Weissenbock, H., Sekulin, K., Bakonyi, T., Högler, S, and Nowotny, N., 2009b. Novel avian bornavirus in a nonpsittacine species (canary; *Serinus canaria*) with enteric ganglioneuritis and encephalitis. Journal of Virology: 83, 11367–11371.

Weksler, M., and Kuntz, M., 1976. Synergy between human T and B lymphocytes in their response to phytohaemagglutinin and pokeweed mitogen. Immunology: 31, 273-281.

Wensman., J., Munir., M., Thaduri., S., Hörnaeus., K., Rizwan., M., Blomström., A., Briese., L., Lipkin., W., and Berg., M., 2013. The X proteins of bornaviruses interfere with type I interferon signalling. Journal of General Virology: 94, 263–269.

Werner-Keiss., N., Garten., W., Richt., J., Porombka., D., Algermissen., D., Herzog., S., Baumgärtner., W., Herden., C., 2008. Restricted expression of Borna disease virus glycoprotein in brains of experimentally infected Lewis rats. Neuropathology and Applied Neurobiology: 34, 590–602.

Wesley M., Garret H., and Guthrie, H., 1998. Detection of Bromodeoxyuridine in Paraffin-embedded Tissue Sections Using Microwave Antigen Retrieval is Dependent on the Mode of Tissue Fixation. Biochemica: 1.

Woerpel, R., Rosskopf, W., and Hugues, E., 1984. Proventricular dilatation and wasting syndrome: myenteric ganglioneuritis and encephalomyelitis of psittacines; an update. In: Proceedings of the Annual Conference of the Association of Avian Veterinians; Groskin R (Ed.): 25–28.

Wünschmann, A., Honkavuori, K., Briese, T, Lipkin W., Shivers, J., and Armien, A., 2011. Antigen tissue distribution of avian bornavirus (ABV) in psittacine birds with natural spontaneous proventricular dilatation disease and ABV genotype 1 infection. Journal of Veterinary Diagnostic Investigation: 23, 716–726.

Wyss, F., Deb, A., Watson, R., and Hammer, S., 2009. Radiographic measurements for PDD diagnosis in Spix's macaws (*Cyanospitta spixii*) at Al-Wabra Wildlife Preservation (AWWP), Qatar. In: Proceedings of the International Conference on diseases of zoo and wild animals: 349–354.

Zimmermann, V., Rinder, M., Kaspers, B., Staeheli, P., Rubbenstroth, D. 2014. Impact of antigenic diversity on laboratory diagnosis of avian bornavirus infections in birds. Journal of Veterinary Diagnostic Investigation: 26, 769– 777

Zhiguang, W., Lisa, R., John, R., Jim, K., Colin, B., and Pete, K., 2010. Generation and characterization of chicken bone marrow-derived dendritic cells. Immunology: 129, issue 1, 133–145.

9. Annexes

9.1. Dyes

4' 6-diamidino-2-phenylindole (DAPI) (Thermo scientific, Germany)

1 mg (DAPI) 4', 6-diamidino-2-phenylindole (MW 350.2 g/mol)

1 ml sterile water

3 3'-diaminobenzidine tetrahydrochloride dihydrate (DAB) (Fluka, Germany)

To prepare a staining solution of the DAB, add:

100 mg DAB (final concentration 0.05%)

200 ml 0.1M imidazol, adjusted with HCl to pH 7.08 (final concentration 0.1M)

70 µl hydrogen peroxidase (H_2O_2) (final concentration 0.01%)

Papanicolaou

Diluted 1:10 in bi-distilled water, mixed and then infiltrated.

Midori-green dye (Nippon Genetics Europe GmbH, Germany)

Diluted 1:10 in sterile water, mixed and then stored in the refrigerator until use.

6X orange DNA loading dye (Thermo Scientific, Germany)

Ready to use

9.2. Sera

5 % goat serum in sterile 1xPBS

5 ml goat serum (Sigma Aldrich, Germany)

95 ml sterile 1x PBS

20% pigs serum / TBS

20 ml pig serum (PAA, Austria)

80 ml TBS

10 % rat serum / TBS

10 ml Rat serum (PAA, Austria)

90 ml TBS

Horse serum (Dako, Germany)

9.3. Kits

Avidin biotin complex Vectastain kit® (Vector laboratories Inc, USA)

Elite ABC complex (Vector laboratories Inc, USA)

Digoxigenin (DIG) RNA labeling (SP6/T7) kit (Roche, Germany)

TOPO TA cloning kit (Life technologies, Germany)

QIAGEN Multiplex PCR Kit (Qiagen, Germany)

RNasey Mini kit (Qiagen, Germany)

Qiamp viral RNA mini kit (Qiagen, Germany)

QuantiTect Reverse Transcription kit (Qiagen, Germany)

9.4. Primary antibodies

Polyclonal rabbit anti Borna disease virus (BoDV) antibody

Mouse anti-duck IgY (Biorad, Germany)

Mouse anti-human CD20 (DCS ImmunoLine, Germany)

Rat anti-feline CD45, clone B220 (Cedarlane, USA)

Mouse anti-dog IgG (Dianova, USA)

Mouse anti-human MUM1 protein (Dako, Germany)

Mouse anti CD79 cy, clone JBC117 (Dako, Germany)

Mouse anti CD79 cy, clone HM 57 (Acris, Germany)

Rabbit anti-human CD3 (Dako, Germany)

Myeloid histiocyte antigen, clone MAC 378 (Dako, Germany)

Rabbit anti-human lysosome (Dako, Germany)

Mouse anti-chicken monocytes, KUL01 (Biorad, Germany)

Alkaline phosphatase (AP) conjugated anti-digoxigenin antibody (Roche, Germany)

Rabbit anti-human CD3 (Dako, Germany)

Mouse anti-human CD3, clone PC3 (Dako, Germany)

Mouse anti-human CD3, clone F7.2.38 (Dako, Germany)

Rat anti-human CD45R, clone B220 (Dako, Germany)

Rabbit anti-dog IgG2a (Dako, Germany)

Mouse anti-human CD79αcy, clone HM 57 (Dako, Germany)

Mouse anti-human CD79αcy, clone JBB117 (Dako, Germany)

Mouse anti-chicken CD4, clone2-35 (Biorad, Germany)

Rat anti-human CD3, clone CD3-12 (Biorad, Germany)

Mouse anti-chicken CD8a, clone 11-39 (Biorad, Germany)

Mouse anti-duck IgY, clone14A3 (Biorad, Germany)

Mouse anti-chicken thrombocytes, clone 11C3 (Biorad, Germany)

Mouse anti-chicken monocytes, clone KUL01 (Biorad, Germany)

9.5. Secondary antibodies

Biotinylated pig anti-rabbit IgG antibody (Vector laboratories Inc, USA)

Biotinlynated goat anti-mouse IgG (Vector lab, USA)

Biotinlynated horse anti-mouse IgG (Vector lab, USA)

Biotinlynated rabbit anti-rat IgG (H+L) (Vector, USA)

Pig anti rabbit IgG1 (Dako, Germany)

Rat anti-mouse IgG (Dianova, USA)

Pig anti-rabbit IgG (Dako, Germany)

Cy3 conjugate goat anti-rabbit IgG (H+L) (Dianaova, USA)

Cy3 conjugate goat anti-rat IgG (H+L) (Dianaova, USA)

Cy3 conjugate goat anti-mouse IgG (H+L) (Dianaova, USA)

Allophycocyanin (APC) conjugated goat anti-rat IgG1 (BD Bioscience, Germany)

Phycoerythrin (PE) conjugated goat anti-mouse (BD Bioscience, Germany)

Mouse anti-BrdU antibody (Santa Cruz Biotechnology, Germany)

9.6. Solutions and Buffers

Washing buffer, to prepare 15 ml washing buffer (WP): add

14, 910 µl 1 % BSA / 1x PBS

15 µl 10 % NaN3

75 µl 5% goat serum

0.1M imidazol /HCL buffer (pH 7.1)

Dissolve:

6.81 g imidazol in 500 ml distilled water

Adjust with 1N HCl to pH 7.1, then fill it to 1 liter.

Endogenous hydrogen peroxidase (H_2O_2) solution, add:

177 ml of pure methanol

3 ml hydrogen peroxidase (H_2O_2) (final concentration 0.05%)

Tris-buffered Saline (TBS), pH 7.6

60.57 g Tris (MW 121.14) (Carlroth, Germany)

600 ml bi-distilled H_2O

400 ml 1 M HCl, Adjust pH with 1 M HCl

5 x TBE electrophoresis Buffer

54 g Tris (MW 121.14)

27.5 g Boric acid (MW 61.83)

20 ml 0.5M EDTA (MW 372.24)

1 l bi-distilled H_2O, Autoclave at 121 ºC, 80 minutes, stored at 4- 8 ºC

0.5 x TBE electrophoresis Buffer

100 ml 5 x TBE

900 ml bi-distilled H_2O

2% agarose gel

0.6 g agarose

30 ml 0.5x TBE buffer

Citrate Buffer (pH 6.5)

9 ml 0.1M citric acid

41 ml 0.1M Na_2- Citrate

500 ml bi-distilled H_2O

5M NaOH

20 g NaOH (MW 40 g/mol)

100 ml bi-distilled H_2O

0.2M Disodium Ethylenediaminetetraacetate (EDTA)

7.44 g EDTA-Na_2

100 ml bi-distilled H_2O, Adjust volume with 5N NaOH pH to 8

4M Lithium chloride

25.4 g LiCl (MW 49.39 g/mol)

250 ml bi-distilled H_2O

1x phosphate buffered saline (PBS)

8 g NaCl (MW 58.44)

0.2 g KCl (MW 74.56)

1.44 g Na2-HPO4 2 H_2O (MW 177.99)

0.24 g KH2PO4 (MW 136.09)

700 ml bi-distilled H_2O, adjust pH with 1 M NaOH to 7.4 and then, adjust volume to 1 liter with distilled H_2O. Autoclave it at 121 ºC, 80 minutes

10 x PBS, pH 7.4

80 g NaCl (MW 58.44)

2 g KCl (MW 74.56)

14.4 g Na_2-HPO4 2 H_2O (MW 177.99 g/mol)

2.4 g KH_2PO_4 (MW 136.09)

700 ml bi-distilled H_2O, adjust pH with 1 M NaOH to pH7.4, then, adjust volume to 1 l with distilled H_2O, Autoclave it at 121 ºC, 80 minutes

DEPC-H_2O RNAse free water

1 ml of Diethylpyrocarbonat (DEPC)

1 l of bi-distilled H_2O

Mix overnight, autoclave at 120 ºC, one hour and 15 minutes

0.5 M EDTA-Na_2 pH 8

18.6 g Di-Nitrium-EDTA-di-hydrate (MW 372.13 g/mol)

60 ml of bi-distilled H_2O with DEPC

Adjust solution with 5N NaOH to pH 8

20 x SSC (standard saline citrate) pH7

175.3 g NaCl (MW 58.44)

88.2 g Tri-Na-Citrate x 2 H_2O (MW 294.1)

800 ml bi-distilled H_2O

Adjust pH to 7.0 with 1 M HCl

Adjust volume to 1 l with bi-distilled H_2O, Autoclave at 121 ºC, 80 minutes

2 x SSC (standard saline citrate)

50 ml 20 x SSC

500 ml bi-distilled H_2O

0.2 x SSC (standard saline citrate)

1.2 ml 20 x SSC

120 ml bi-distilled H_2O

2 x SSC + 5 mM EDTA-Na2

50 ml 20 x SSC pH 7.0

5 ml 0.5 M EDTA-Na_2

Adjust volume to 500 ml with bi-distilled H_2O, autoclave it at 121 ºC, 80 minutes

0.2M HCl

50 ml 2N HCL

450 of bi-distilled H_2O

1 M Tris pH 8.0

12.11 g Tris (MW 121.14)

50 ml bi-distilled H_2O

Adjust pH with 1 M HCl to 8.0, Adjust volume with bi-distilled H_2O to 100 ml. Autoclave it at 121 ºC, 80 minutes

Proteinase K

16.2 mg Proteinase K (Boehringer Mannheim, Germany)

1 ml 10 mM Tris-HCL pH7.5

0.1M $CaCl_2$

1.47 g $CaCl_2$ (MW 147.02 g/mol)

100 ml of bi-distilled H_2O

Proteinase K solution

1 ml 1 M Tris pH 8.0

1 ml 0.1 $CaCl_2$

Adjust volume to 60 ml with DEPC-H_2O, mix

1M $MgCl_2$

20.33 g $MgCl_2$ (Hexanhydrate MW 203.3 g/mol)

100 ml of bi-distilled H_2O

5M NaCl

29.22 g NaCl (MW 58.44 g/mol)

100 ml of bi-distilled H_2O

3M NaCl

87.66 g NaCl (MW 121.14 g/mol)

500 ml of bi-distilled H_2O

0.2 % Glycine-PBS

1 g Glycine (MW 75.07)

450 ml PBS pH 7.4, Adjust pH with 1M HCl to 7.4

Adjust volume to 500 ml with PBS pH 7.4, Autoclave at 121 ºC, 80 minutes

4 % Paraformaldehyde, pH 7.4

40 g Paraformaldehyde

900 ml PBS pH 7.4

Dissolve at 60 °C on a magnetic stirrer

Adjust pH with 1M NaOH to 7.4

0.25 % Acetanhydride in 0.1 M Triethanolamine-DEPC-H_2O (pH 7.5)

894 mg Triethanolamine (Merck, Germany)

50 ml DEPC-H_2O

Adjust pH with 1 M HCl to 7.5

Add 150 µ l Acetanhydride (Fluka, Germany)

Adjust volume to 60 ml with DEPC-H_2O

PBS + 5 mM MgCl2

10 ml 10 x PBS

5 µl 1 M $MgCl_2$

Adjust volume up to 100 ml with bi-distilled H_2O

Prehybridization mix (PHB-Mix)

450 ml 20 x SSC

675 ml 100 % Formamid

150 ml 50 x Denhardts

210 ml bi-distilled H_2O, Mix and aliquot as 49 ml volume in tubes, store at - 20 °C.

50 x Denhardts

5 g Ficoll

5 g polyvinylpyrrolidone

5g bovine serum albumin

Fill up to 500 ml with bi-distilled H_2O, autoclave at 121 ºC, 80 minutes.

Sodium salt Deoxyribonucleic acid (ssDNA)

10 mg ssDNA (Sigma Aldrich, Germany)

1 ml buffer 4, final concentration (10 mg/ml)

RNA stocks solution (Ribonucleic acid from calf liver type IV)

10 mg RNA (Sigma Aldrich, Germany)

1 ml bi-distilled H_2O treated with DEPC

Final concentration 250µg/ml

0.5M Piprazin (Pipes)

8.65 g PIPES

50 ml of bi-distilled H_2O

20x hybridization salts

10 ml 0.5M EDTA (pH 8)

10 ml 0.5M Pipes (pH 7)

30 ml 5M NaCl

Aliquot and store at - 20 °C

Hybridization mixture (HM)

16 ml 100 % Formamid, deionised

8 ml 20x hybridization salts

3.2 ml 50 x Denhardts

320 µl Heparin (10 mg Heparin 16,000 IU in 1 ml 10% iges Triton X-100)

320 µl 10% iges Triton X-100

Mix and aliquot as 696 µl volume in eppendorfs , store at - 20 °C

6 x SSC (standard saline citrate) with 45 % formamide

36 ml 20 x SSC

54 ml 100 %iges Formamid

50 ml bi-distilled H_2O

RNAse solution

10 ml 3M NaCl

600 µl 1M Tris (pH 8)

120 µl 0.5M EDTA (pH 8)

49 ml bi-distilled H_2O (prewarm it in the water bath at 37 ºC)

2.5 µl RNAse A (5000 U/ml)

100 µl RNase T (100,000 U/ml) (Roche GmbH, Mannheim, Germany)

Buffer 1, pH 7.5

12.11 g Tris (MW 121.14)

8.77 g NaCl (MW 58.44)

500 ml bi-distilled H_2O

Adjust pH with 1 M HCl to 7.5

Adjust volume to 1 l with bi-distilled H_2O

Autoclave at 121 ºC, 80 minutes

Buffer 2 (Blocking solution)

1.2 ml Neutral sheep serum (Sigma Aldrich, Germany)

1.8 ml 10 % Triton X-100

Adjust volume to 60 ml with buffer 1

Buffer 3 (pH 9.5)

12.11 g Tris

5.84 g NaCl

10.17 g $MgCl_2$ X $6H_2O$ (MW 203.3 g/mol)

Fill up to 1000 ml with bi-distilled H_2O, adjust it with 1N HCL to pH 9.5. Autoclave at 121 ºC, 80 minutes

Buffer 4 (pH8)

1.21 g Tris

0.37 g EDTA (MW 372.3 g/mol)

Fill up to 600 ml with bi-distilled H_2O, adjust volume with 2N HCL to pH 8, fill up to liter, autoclave at 121 ºC, 80 minutes

Anti- digoxigenin antibody solution,

For each 3 ml with buffer 1, add

15µl anti-DIG antibody (150 Unit), (Roche GmbH, Germany) , dilution 1:300

31µl sterile Neutral sheep serum (NSS)

94 µl 10% Triton X-100

50 mg/ml 5-bromo-4-chloro-3-indolyl phosphate (BCIP) stock solution

Dissolve:

500 mg BCIP in 10 ml 100% dimethylformamide (DMF).

BCIP stock solutions were stored at -20 °C.

75mg/ml Nitroblueteterazolium (NBT) Stock Solution, dissolve:

1g NBT in 13.3 ml of 70% dimethylformamide in water.

The NBT stock solutions were stored at -20 °C.

NBT/ BCIP staining solution

250 µl Nitroblueteterazolium (NBT) (75 mg / ml NBT Stock Solution)

210 µl X-Phosphate (BCIP) (50 mg / ml BCIP stock solution)

15 mg Levamisol (Sigma Aldrich, Germany)

60 ml Buffer 3

0.1M sodium borate Buffer (Na_2B4O7) (pH 8.5)

380 mg Sodium teteraborate (Carlroth, Germany)

10 ml bi-distilled H_2O

Use 0.2 micron filter membrane to filter.

Adjust volume with 1N HCL to pH 8.5

0.3% Triton X-100

300 µl Triton X-100 (Serva, Germany)

100 ml sterile bi-distilled H_2O

2M HCL

167 ml concentrated HCl (MW 36 g / mol)

1 Liter bi-distilled H_2O

1% BSA / TBS

1 g Bovine serum albumin

100 ml TBS

9.7. Equipments

1. Automatic Tissue Tek VIP® machine (Sakura, Germany)
2. Automatic Tissue-Tek® TEC ™ (Sakura, Germany)
3. Fully automated Leica RM2255 rotary microtome (Leica, Germany)
4. Automatic HMS740 Microm robot-stainer (Microm GmbH, Germany)
5. Automated Tissue Tek® coverslipper machine (Sakura, Germany)
6. PTC-200 Peltier thermal cycler (Biorad, Germany)
7. UV light with a transilluminator (Bachhofer Laboratories, Germany)
8. Scale (Ohaus, Germany)
9. Mettler Balance Scale Model PN1210 (Mettler-Toledo GmbH, Germany)
10. Mettler Toledo PM4600 DeltaRange Balance (Mettler-Toledo GmbH, Germany)
11. Heating Magnetic Stirrer (Heidolph instruments GmbH, Germany)
12. Vortex mixerer (Heidolph instruments GmbH, Germany)
13. Vortex mixerer (MAGV instruments GmbH, Germany)
14. Centrifuge 5415C (Eppendorf, Germany)
15. Universal 32 centrifuge (Hettich, Germany) for FC
16. Rotina 48RC Centrifuge (Hettich, Germany)
17. Microcentrifuge Rotor (Thermo Scientific, Germany)
18. Laboratory water bath (Labortechnik, Germany)

19. Laboratory water bath (Memmert, Germany)
20. Water bath at the cell culture lab (Kottermann laboratories GmbH, Germany)
21. Incubator (Memmert, Germany)
22. Heraeus® BBD6220 CO2-Incubator (Thermo Scientific, Germany)
23. IX70 S8F inverted microscope (Olympus, USA)
24. Eclipse E200 microscope (Nikon, Germany)
25. Nikon fluorescence microscope (Nikon, Germany)
26. Accu Block™ Mini heat block (Labnet International Inc, Germany).
27. BD flow cytometer machine (BD Bioscience, Germany).
28. Sterilizer (Memmert, Germany)
29. Medizintechnik sterilisator (Melag, Germany)
30. Vertical floor-standing autoclave (Systec, Germany)
31. pH meter (Blue line, Germany)
32. Heraues laminiair instrument (Thermo scientific, Germany)
33. Laminar flow hood (Weiss GWE GmbH, Germany)
34. Laminar flow (Captair, Germany)
35. Airflow control DIN EN 14175 (Vinitex GmbH, Germany)
36. UVC/TM-AR DNA/RNA UV-cleaner box (LTF Labortechnik GmbH, Germany)
37. BMP51 Label maker (Brady, Germany)
38. Nanodrop®2000 spectrophotometer (Thermo scientific GmbH, Germany).

ACKNOWLEDGEMENT

First and above all, I praise Allah (the God). I am thankful to Almighty Allah, most Gracious, who in His infinite mercy has guided me, providing me this opportunity and granting me the capability to complete this PhD work successfully. I would like to thank Allah who giving me Patience, health, wisdom, and blessing to accomplish this thesis. Without all these things, I can't finish this Ph.D thesis.

With deep sense of gratitude, I acknowledge **my loving parents** for their immeasurable love for education and support me all the time. I am also deeply thankful to **my siblings**, for their support and encourage. Special thanks to **my sweetheart wife** who has always been my side and my inspiration during the difficult times of this project. My deepest gratitude to my children **(Teeba, Abdurrahman** and **Tooqa)** who have also acknowledged for giving me the strength and courage during doing this study in Germany.

I would like to thank my promoter **Professor Dr. habil Christiane Herden** who had faith in me and providing me with the opportunity to pursue my Ph.D study under her supervision. Professor Dr. habil Christiane Herden has been the ideal thesis supervisor. Her sage advice, insightful criticisms, correction of the thesis, patient and warm encouragement aided the writing of this thesis in innumerable ways.

I would also like to thank **Professor Dr. Eberhard.H.Burkhardt** for his advices in each step of way during doing the Ph.D at the institute. Thank you for always having your door open to answer my questions and for your useful advices on my project.

I am grateful to **Professor Carsten Staszyk** for allowing me to use the flow cytometer in his laboratory. I would also like to thank **Carmen Schrock** for her significant contribution in analyzing the FACS data. A very special thanks goes out to **Dr.Sibylle Herzog** for providing the virus and Borna disease virus infected cell lines. I would also like to express my gratitude to **Dr. Werner Hecht** for his guidness and his assistance to me side by side to generate the ISH riboprobes. **Dr.Klaus Failing** is also appreciated for helping with the statistical analysis.

Special thanks to the team of tissue sectioning at our institute representing by **Sabina Wack, Alexandra Luh and Anette Arttelt** for their technical efforts in preparation of the tissue slices. **Anne Piepenbring, Helena Schneider, Sara.Malberg,** and **Julia Heckmann** are also acknowledged for assisting me during collection of blood samples. Thank you all !!!!!

Fund of this study is from German Academic exchange service. I would like to acknowledge the financial support of DAAD and MOHER Iraq.

DEDICATION

To honor the memory of my late father, I gratefully dedicated my Ph.D thesis posthumously to my beloved father. My father would have been happy to see me getting the Ph.D from Germany before passing away. My father taught me that even the largest task can be accomplished if it is done one step at a time. My father is supported me throughout the entire doctorate program in Germany. Without his kindness and extensive support to me, I could not finish this study. This thesis is appreciatively dedicated to my mother, who taught me that the best kind of knowledge to have is that which is learned for its own sake. My mother, you are profoundly appreciated. I have also dedicate this thesis to my brilliant and outrageously loving wife for her endless love, encouragement and support to me since the beginning of my Ph.D study in Germany. My wife has been a constant source of support and encouragement during the challenges in my study. Also, this thesis is dedicated to my daughter (Teeba), my son (Abdulrahman) and my daughter the kind-hearted little girl (Tooqa) who have been a great source of motivation and inspiration. I would like to sincerely thank them. I would not have been able to achieve my goals including this Ph.D degree without their love and support.

Finally, this thesis is dedicated to all those who believe in the richness of learning.

Basim 2015

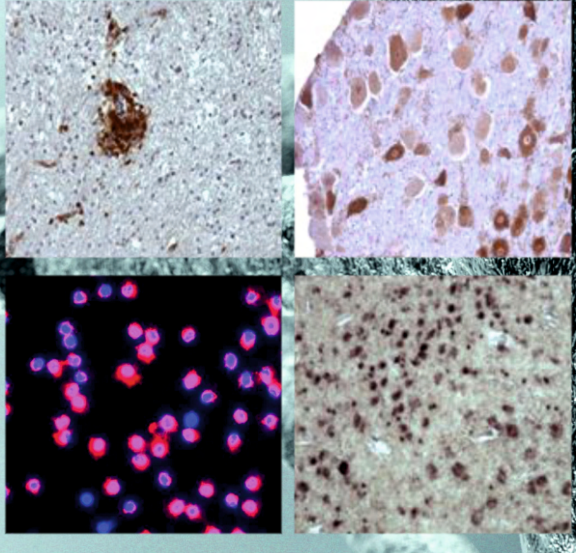

édition scientifique
VVB LAUFERSWEILER VERLAG

VVB LAUFERSWEILER VERLAG
STAUFENBERGRING 15
D-35396 GIESSEN

Tel: 0641-5599888 Fax: -5599890
redaktion@doktorverlag.de
www.doktorverlag.de

ISBN: 978-3-8359-6313-9

Photo front cover: Fotolia.de